



Wood-Based Panels

An Introduction for Specialists



cost

Edited by
Heiko Thoemen
Mark Irle
Milan Sernek

Wood-Based Panels

An Introduction for Specialists

Edited by

**Heiko Thoemen
Mark Irle
Milan Sernek**

Brunel University Press

Contents

List of Contributors.....	ix
Preface.....	xiii
1 Wood-Based Panel Technology	1
<i>Chapter Summary</i>	<i>1</i>
1.1 Introduction.....	1
1.2 Why Make Wood-Based Panels?	3
1.3 The Manufacture of Particleboards: A Short Overview	5
1.3.1 Defining Particleboard.....	5
1.3.2 Wood as a Raw Material.....	5
1.3.3 Particle Production.....	12
1.3.4 Particle Drying.....	18
1.3.5 Particle Sorting	22
1.3.6 Resin Metering and Blending	25
1.3.7 Common Adhesives.....	31
1.3.8 Mattress Forming.....	33
1.3.9 Mattress Pre-Pressing and Pre-Heating	36
1.3.10 Pressing.....	38
1.3.11 Processing Steps Immediately after Pressing	47
1.4 The Manufacture of Oriented Strand Board: A Short Overview .	55
1.4.1 Introduction	55
1.4.2 Manufacture of OSB.....	56
1.5 The Manufacture of Medium Density Fibreboard: A Short Overview.....	61
1.5.1 Introduction	61
1.5.2 Manufacture of MDF.....	62
1.6 The Manufacturing of Plywood: A Short Overview.....	74
1.6.1 Introduction	74
1.6.2 The Manufacturing Steps.....	75
1.6.3 Peeling	78
1.6.4 Dryers	82

This publication is supported by COST

Published by Brunel University Press, London, UB8 3PH. England

This book may be cited as: Wood-Based Panels - An Introduction for Specialists

ISBN 978-1-902316-82-6

No permission to reproduce or utilise the contents of this book by any means is necessary, other than in the case of images, diagrammes or other material from other copyright holders. In such cases, permission of the copyright holders is required.

Neither the COST Office nor any person acting on its behalf is responsible for the use which might be made of the information contained in this publication. The COST Office is not responsible for the external websites referred to in this publication.

© COST Office, 2010

Cover photos: Courtesy of Dieffenbacher GmbH, Eppingen, Germany

Layout: Henrik Schmidt, Wentorf, Germany

1.6.5	Veneer Preparation.....	82
1.6.6	Board Layup.....	83
1.6.7	Pressing.....	84
1.6.8	Finishing.....	85
1.7	A Potted History of Wood-Based Composites.....	85
1.8	References.....	90
2	Water Absorption of Wood and Wood-Based Panels – Significant Influencing Factors.....	95
	<i>Chapter Summary</i>	95
2.1	Introduction.....	95
2.2	Sorption Behaviour and Capillary Water Absorption.....	98
2.2.1	Ultimate State of Wood-Water.....	98
2.2.2	Sorption Behaviour.....	99
2.2.3	Water Absorption by Capillary Forces.....	102
2.2.4	Swelling and Shrinkage.....	103
2.2.5	Influence of Wood Moisture on the Surface Roughness of Wood-Based Materials.....	108
2.3	The Relationship between Moisture Content and Properties.....	110
2.4	References.....	114
2.5	Annex: Tables Listing Selected Properties of Wood and Wooden Materials.....	116
3	Transport Phenomena.....	123
	<i>Chapter Summary</i>	123
3.1	Heat and Mass Transfer Mechanisms in Porous Media.....	123
3.1.1	Introduction.....	123
3.1.2	The Heat Transfer Mechanisms.....	124
3.1.3	The Mass Transfer Mechanisms.....	126
3.2	Heat and Moisture Transfer in the Drying of Particles/Fibres... ..	129
3.2.1	Introduction.....	129
3.2.2	Drying Regimes in Convective Drying.....	131
3.2.3	Heat Transfer.....	132
3.2.4	Moisture Movement.....	133
3.2.5	Effects of Wood Chip Properties.....	136

3.3	Heat and Mass Transfer Mechanisms in Hot Pressing.....	138
3.3.1	Introduction.....	138
3.3.2	Heat Transfer.....	140
3.3.3	Mass Transfer.....	142
3.3.4	Internal Mat Conditions.....	144
3.3.5	Transport Properties.....	150
3.4	Heat and Moisture Transfer in Conditioning.....	160
3.4.1	Introduction.....	160
3.4.2	Internal Conditions during Conditioning.....	160
3.4.3	Relevant Heat and Mass Transfer Mechanisms.....	162
3.5	Diffusion of chemicals.....	163
3.5.1	Introduction.....	163
3.5.2	Diffusion of Resins.....	163
3.5.3	Diffusion of Wax and Other Additives.....	164
3.6	References.....	167
4	Advanced Imaging Techniques in Wood-Based Panels Research.....	177
	<i>Chapter Summary</i>	177
4.1	Introduction.....	177
4.2	Virtual Prototyping: Opportunities and Challenges.....	180
4.2.1	Levels of Complexity in the Internal Microstructure of the Composites.....	180
4.2.2	Compatibility between Testing Approaches and Numerical Models.....	181
4.3	The Advanced Imaging Techniques.....	182
4.3.1	Digital Image Analysis.....	183
4.3.2	Multi-Scale and Multi-Modal Correlation.....	189
4.3.3	Optical Measurement of Deformations and Strains.....	191
4.3.4	Inverse Problem Approach.....	191
4.3.5	New Developments in Modeling.....	193
4.4	References.....	194

5 Adhesive Bond Strength Development	203
<i>Chapter Summary</i>	203
5.1 Introduction.....	203
5.2 Fundamentals	204
5.3 Monitoring the Development of Adhesive Bond Strength.....	208
5.3.1 Thermomechanical Analysis (TMA)	209
5.3.2 Dynamic Mechanical Analysis (DMA)	210
5.3.3 Torsional Braid Analysis (TBA).....	211
5.3.4 Automated Bonding Evaluation System (ABES)	213
5.3.5 Integrated Pressing and Testing System (IPATES)	216
5.3.6 Other Techniques	217
5.4 Open Questions	219
5.5 References	221
6 Innovative Methods for Quality Control in the Wood-Based Panel Industry	225
<i>Chapter Summary</i>	225
6.1 Introduction.....	225
6.2 Infrared Thermography	226
6.2.1 Principles of Infrared Thermography.....	226
6.2.2 Infrared Cameras.....	228
6.2.3 Thermography for Non-Destructive Testing.....	229
6.2.4 Application and Examples	231
6.3 Near Infrared Reflectometry	236
6.3.1 Origin of NIR Spectra.....	236
6.3.2 NIR Reflectometry.....	237
6.3.3 Panel Properties and NIR Spectra.....	238
6.3.4 Multivariate Techniques for Data Analysis	239
6.3.5 Technical Aspects	239
6.3.6 Applications and Examples.....	240
6.4 Nuclear Magnetic Resonance.....	244
6.4.1 Nuclear Spin.....	244
6.4.2 Panel Properties and Nuclear Spin.....	245

6.4.3 Applications of NMR in the Wood Based Panel Industry	245
6.5 References.....	248
7 Carbon Materials and SiC-Ceramics made from Wood-Based Panels	251
<i>Chapter Summary</i>	251
7.1 Introduction.....	251
7.2 Specific Wood Based Materials.....	252
7.2.1 Raw Materials and the Manufacturing Process	253
7.2.2 Characterisation	253
7.3 Carbon Materials.....	254
7.3.1 Carbonization.....	255
7.3.2 Characterisation	256
7.3.3 Potential Applications.....	256
7.4 SiC-Ceramics.....	257
7.4.1 Siliconisation	258
7.4.2 Characterisation	259
7.4.3 Potential Applications.....	259
7.5 References.....	261
8 Thermally and Chemically Modified Wood-Based Panels	265
<i>Chapter Summary</i>	265
8.1 Introduction.....	265
8.2 Chemical Modification	267
8.3 Thermal Modification	271
8.4 Modification of Panels.....	275
8.5 Conclusion	276
8.6 References.....	278

List of Contributors

Chapter 1 Wood-Based Panel Technology

Mark Irle

Ecole Supérieure du Bois
BP 10605 - Rue Christian PAUC
44306 Nantes
France
mark.irle@ecoledubois.fr

Marius C. Barbu

Faculty of Wood Industry
University "Transilvania" Brasov
Str. Colina Universitatu nr. 1
500084 Brasov
Romania
cmbarbu@unitbv.ro

Chapter 2 Wood-Water-Interaction

Peter Niemz

Institute for Building Materials (IfB), Wood Physics
ETH Zurich,
Schafmattstr. 6
8093 Zurich
Switzerland
niemzp@ethz.ch

Chapter 3 Transport Phenomena

Luisa Carvalho

Department of Wood Engineering
Polytechnic Institute of Viseu
Campus Politécnico de Repeses
3504 510 Viseu
Portugal
lhcarvalho@demad.estv.ipv.pt

Jorge M. S. Martins

Department of Wood Engineering
Polytechnic Institute of Viseu
Campus Politécnico de Repeses
3504 510 Viseu
Portugal
jmmartins@demad.estv.ipv.pt

Carlos A.V. Costa

Laboratory of Process, Environment and Energy Engineering
 Faculty of Engineering
 University of Porto
 Rua Dr. Roberto Frias s/n
 4200-465 Porto
 Portugal
 ccosta@fe.up.pt

Chapter 4 Imaging Techniques**Lech Muszyński**

Department of Wood Science and Engineering
 Oregon State University
 119 Richardson Hall
 Corvallis, OR 97331
 USA
 lech.muszynski@oregonstate.edu

Maximilien E. Launey

Lawrence Berkeley National Laboratory Materials Sciences Division
 University of California Berkeley
 1 Cyclotron Road, MS 62-203
 Berkeley, CA 94720
 USA
 melauney@lbl.gov

Chapter 5 Bond Strength Development**Milan Sernek**

Biotechnical Faculty
 University of Ljubljana
 Rozna Dolina, Cesta VIII/34
 1000 Ljubljana
 Slovenia
 milan.sernek@bf.uni-lj.si

Manfred Dunky

Institute of Wood Science and Technology
 BOKU-Vienna
 Peter Jordan Strasse 82
 1190 Vienna
 Austria
 manfred.dunky@boku.ac.at

Chapter 6 Quality Control**Jochen Aderhold**

Fraunhofer Institute for Wood Research
 Wilhelm-Klauditz-Institut, WKI
 Bienroder Weg 54E
 38108 Braunschweig
 Germany
 jochen.aderhold@wki.fraunhofer.de

Burkhard Plinke

Fraunhofer Institute for Wood Research
 Wilhelm-Klauditz-Institut, WKI
 Bienroder Weg 54E
 38108 Braunschweig
 Germany
 burkhard.plinke@wki.fraunhofer.de

Chapter 7 Wood Panel-Based Ceramics**Olaf Treusch**

Wessling Group
 Forstenrieder Str. 8-14,
 82061 Neuried
 Germany
 olaf.treusch@wessling.de

Chapter 8 Modified Wood-Based Panels**Martin Ohlmeyer**

Institute of Wood Technology and Wood Biology (HTB)
 Johann Heinrich von Thuenen-Institute (vTI)
 Leuschnerstrasse 91
 21031 Hamburg
 Germany
 martin.ohlmeyer@vti.bund.de

Wulf Paul

Sonae Industria (UK) Ltd
 Moss Lane, Knowsley Industrial Park
 L33 7XQ Knowsley
 United Kingdom
 w.paul@sonae.co.uk

Preface

Wood-based panels is a general term for a variety of different board products, which have an impressive range of engineering properties. While some panel types are relatively new on the market, others have been developed and successfully introduced more than hundred years ago. However, even those panel types having a long history of continuous optimization are still a long way from being fully developed and they probably never will be. Technological developments on the one hand and new market and regulative requirements, combined with a steadily changing raw material situation, drive continuous improvements of wood-based panels and their manufacturing processes.

Advances particularly in the fields of adhesive formulations, production technology, as well as online measuring and control techniques, have triggered a technology push. The adaptation of these technologies to the wood-based panels industry has been motivated by the requirement to improve product quality and reduce manufacturing costs at the same time, or, in other words, to secure the competitiveness of the wood-based panel producers. But there is also a continuous market pull that drives the panel manufacturers and research institutes towards product innovations. Examples of such developments are the increasing demand for light furniture, or the need to adapt panel properties so that new coating technologies can be applied.

Considerable endeavours have been made to ensure that wood-based panels have no negative effects on human health. In particular, panel product formaldehyde emissions have been dramatically reduced over the last decades, and further reduction is still the subject of huge efforts applied by panel manufacturers, adhesive suppliers and researchers. In addition, a relatively new issue which is the detection and reduction of volatile organic compounds (VOCs) emitted from wood-based panels has come to the agenda. Again, product and process adaptations are needed to meet the new challenges.

The third major driving force for the permanent further development of wood-based panels and the respective production processes is the continuously changing raw material situation. The raw material used in an individual production line usually depends on what is available in a relatively small catchment area, and therefore may vary considerably between different sites. However, there are not only regional variations of the raw material supply, but also changes over time caused by several factors. For example, forest management schemes have altered and will continue to do so. Moreover, the demand from other industries and of the

energy sector for wood previously used mainly for panel manufacturing has dramatically increased in many regions. These changes force the panel producers to shift towards alternative sources, including recovered wood, and permanently push the panel industries to modify and optimize their processes in order to maintain a consistent quality level. Clearly, the high variability of the wood raw material constitutes a challenge not known by many other industries.

The challenges listed here are considerable. On the other hand, a fibre- or particleboard is a hierarchically organized product, with quite elaborate structures on the different size scales from the molecular to the macroscopic level. Improving the engineering properties of panels requires several of these hierarchical levels to be considered simultaneously. This complexity of the material structure is what makes it so challenging to manipulate the panel properties. Or in other words, innovations are difficult without understanding the fundamental mechanisms at each of the hierarchical levels.

The intention of this book is to give a general description of modern panel manufacture, but to also provide some state of the art information on a selected list of fundamental topics. Of course, it is not possible to include all important aspects of panel manufacture into such a book. Therefore, it is our intent to give examples and to stimulate the interested reader to continue his studies by means of the respective technical literature. This book may be used as a textbook for undergraduate and graduate students, as assistance for practitioners, and as reference work for scientists working in the field. It is an introduction into wood-based panel manufacture, but hopefully provides new insights into the fundamentals of the production technology even for specialists.

Heiko Thoemen

Professor at Bern University of Applied Sciences (BFH)

Biel/Bienne, Switzerland, in June 2010

A Word from the Chairman

COST Actions are initiatives funded by the European Commission. An Action is essentially a network of scientists and industrialists who are interested in a particular topic. The principal aim of an Action is to provide coordination at the European level of research funded at a national level with a view to avoid repetition and encourage synergies between existing and future research projects.

COST Action E49 is entitled **Processes and Performance of Wood-Based Panels** and is concerned with all aspects of the wood-based panel (WBP) sector including: raw materials (wood, adhesives, coatings, coverings, etc.) manufacture of all panel types, their end-use and properties.

To differentiate WBP products from other wood composite materials, E49 defines a panel product as one in which the thickness of the product is considerably smaller than either its width or length and its manufacture includes a flat-pressing step. The broad categories of products covered are: particleboards; oriented strand boards (OSB); fibreboards, particularly hardboards and medium density boards (MDF); and the veneer-based products including plywood and laminated veneer lumber (LVL).

E49 has three Working Groups: 1. Process optimisation and process innovation; 2. Fundamentals and modelling; and 3. Performance in use and new products. This state of the art report has been prepared by both WG1 and 2.

This state of the art report has been written by a number of experts who have freely given up their time to write a range of interesting and informative chapters. These experts are to be applauded as the main beneficiaries of this work are the scientific community and the WBP sector. Certainly, this report may enhance the reputations and notoriety of its contributors, but, this is not what drives them; I truly believe that the authors of this report genuinely wish to help the WBP sector and for people to better understand WBP products. None of the authors will receive any financial reward for their contribution and so I hope that, like me, you will appreciate their efforts.

The principal editor of this report is Heiko Thoemen, who is also the leader of WG2. He has been the driving force behind this work from the beginning and his dedication has finally borne fruit with the publication of this report. Heiko Thoemen has been assisted by the leader of WG1, Marius Barbu. The first chapter aims to set the scene for the chapters that

follow by providing an overview of WBP manufacturing technology and this is the main contribution from WG1; the other chapters have come from members of WG2.

All members of E49 have contributed to this report in some way and I thank each and every one of them for their efforts. Special mention must go to the members of the core group: the two leaders mentioned above, Mizi Fan (WG3) and vice chair of E49, Eleftheria Athanasiadou.

I wish to acknowledge the magnificent support E49 has received from the COST Office in Brussels. In particular, E49 has been successfully guided by Günter Siegel and Melae Langbein and their assistants – many thanks to you all.

Mark Irle

Chairman of E49 and

Deputy Director of Ecole Supérieure du Bois

Nantes, France, in June 2010

Chapter 1

Wood-Based Panel Technology

Mark Irle and Marius C. Barbu

CHAPTER SUMMARY

This chapter provides an overview of the manufacture of particleboards, oriented strand boards, dry process fibreboards and plywood. The main aim of this chapter is to provide enough background information so that the reader may more readily understand the chapters that follow. It is further hoped that this chapter encourages researchers to contribute research effort to the WBP sector.

1.1 INTRODUCTION

The principal aim of this chapter is to provide the reader with a brief overview of the manufacturing technologies used to wood-based panel (WBP) products so that they may better understand the more in-depth chapters that follow.

There are some excellent English reviews on WBP manufacture for example Maloney (1993), Moslemi (1974), Schniewind et al (1989), Walker (1993 and 2006) and Youngquist (1999). Unfortunately, the most recent of these is over 10 years old and technology moves fast in response to ever changing markets. Consequently, it is hoped that this chapter will serve as a supplement to existing reviews.

WBP products are made with fibres, particles or veneers, see Figure 1.1. Each of these three raw materials is discussed in the following chapters on particleboard, fibreboard and plywood manufacture.

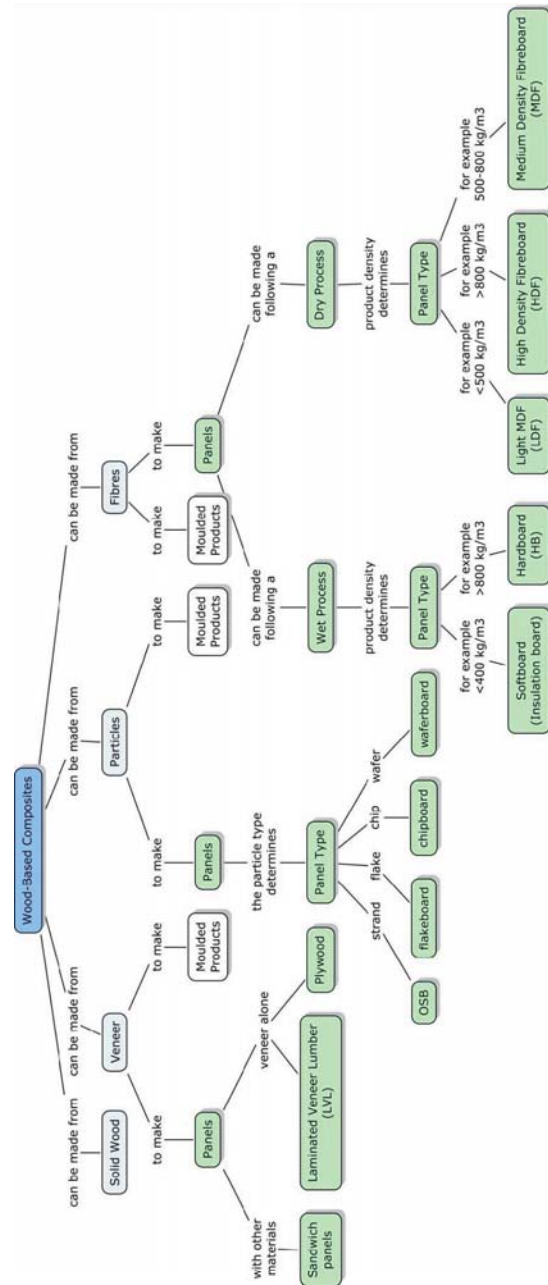


Figure 1.1: A map summarising the wide range of wood composites that can be made. This chapter is concerned with the panel products in the dark boxes.

1.2 WHY MAKE WOOD-BASED PANELS?

It is often quoted that the manufacture of WBP products has been brought about by the ever increasing cost of logs and lumber, which in turn, has caused the managers of the world's forest resource to investigate ways and means of using trees more efficiently. This is certainly true, as many wood composites can utilise low grade logs such as thinnings, bowed and twisted logs. They can also use wood by-products and recycled materials. All sawmills produce large quantities of residues in the form of chips, sawdust, and slabs. Even the most efficient sawmiller is unlikely to convert more than 65% of each log in his yard. These residues can be used to manufacture some of the many kinds of particleboards and fibreboards that are made today.

Even disregarding the economic advantages, panel products would still be manufactured because of man's general desire for better building materials. As a building material, wood has a great number of advantages but also some disadvantages; the main one being its variability. Wood is a very variable material both between and within species, and not just in appearance but, more importantly, in density, strength, and durability. Table 1.1 and Table 1.2 show that wood composites can be manufactured to have very much more uniform properties.

Table 1.1: Dimensional stability of timber and boards. Change in dimensions from 30% to 90% relative humidity (Dinwoodie 1981).

	Direction to grain or board length		
	Parallel (%)	Perpendicular (%)	Thickness (%)
Solid Timber			
Douglas fir	negligible	2.0-2.4	2.0-2.4
Beech	negligible	2.6-5.2	2.6-5.2
Plywood			
Douglas fir	0.24	0.24	2.0
Particleboard			
UF bonded	0.33	0.33	4.7
PF bonded	0.25	0.25	3.9
MF/UF bonded	0.21	0.21	3.3
Fibre-building board			
Tempered	0.21	0.27	7-11
Standard	0.28	0.31	4-9
MDF	0.24	0.25	4-8

Although the strength properties of wood composites are generally lower than solid timber they are more consistent. This means that they can

support loads with smaller safety margins, which in effect reduces the apparent difference in strength between solid wood and composites.

Bacteria, fungi and insects, readily decay wood, especially when it is wet. Some panel products are better in this respect, particularly in the case of insect attack. Cement bonded composites have been found to be extremely resistant to degradation by fungi and even termites.

Other benefits of wood composites come from the fact that their properties can be engineered. Lumber is limited to a large extent by size, width in particular. It is difficult to obtain wood wider than 225 mm and thicker than 100 mm. The dimensions of typical panels vary from market to market but are usually 2 – 2.5 m long and 1 – 1.5 m wide, but it is possible to buy panels in much larger sizes if necessary. The majority of houses built today have particleboard floors because wooden floors are more expensive to buy and lay. The comparatively large size of a tongue and grooved particleboard floor panel (2440 x 660 mm in the UK) enables a floor to be laid down far faster and produces a less "creaky" and flatter result than a traditional timber floor. Wood composites can be made to have special properties such low thermal conductivity, fire resistance, better bio-resistance or have their surfaces improved for decorative purposes.

Table 1.2: Strength properties of timber and boards (Dinwoodie 1981).

	Thickness (mm)	Density (kg/m ³)	Bending Strength (MPa)		Bending Stiffness (MPa)	
			Par.	Perp.	Par.	Perp.
Solid Timber						
Douglas fir	20	500	80	2.2	12700	800
Plywood						
Douglas fir	4.8	520	73	16	12090	890
Douglas fir	19	600	60	33	10750	3310
Chipboard						
UF bonded	18.6	720	11.5	11.5	1930	1930
PF bonded	19.2	680	18.0	18.0	2830	2830
MF/UF bonded	18.1	660	27.1	27.1	3460	3460
Fibre-building board						
Tempered	3.2	1030	69	65	4600	4600
Standard	3.2	1000	54	52	---	---
MDF	9-10	680	18.7	19.2	---	---

1.3 THE MANUFACTURE OF PARTICLEBOARDS: A SHORT OVERVIEW

1.3.1 Defining Particleboard

Particleboard is used as a generic term for any panel product that is made with wood particles. Of course, there is a great range of particle shapes and size used to make particleboards. The type of particle is therefore used to define the type of particleboard product. For example, following English terminology, **chipboard** is made with chips, a flakeboard with flakes, oriented strand board (OSB) with strands and so on (see Figure 1.1 for examples). Most European countries use the term particle rather than chip and therefore particleboard as a term for chipboard. To avoid confusion over whether the text is referring to particleboard in the generic sense or particleboard in the specific product sense, the name chipboard is being used in this text for the specific product.

Another aspect of particleboards is that the wood particles are bonded together by adding a synthetic adhesive and then pressing them at high pressures and temperatures. This is important as the manufacture of these panel products has a marked influence on their subsequent properties.

1.3.2 Wood as a Raw Material

Approximately 95 % of the ligno-cellulosic material used for particleboard production is wood. The rest consists mainly of seasonal crops such as flax, bagasse, and cereal straw. A discussion of these various seasonal crops is beyond the scope of this chapter.

Some wood species are more suitable for particleboard production than others.

1.3.2.1 Workability

A material that is difficult and costly to break into particles is not suitable. Once produced, the chips should have smooth surfaces and a minimum of end grain otherwise the particle will absorb too much adhesive to be cost effective. The characteristics of a chip are, to a certain extent, dependent on the anatomy of the wood. Softwoods are preferred to hardwoods because they tend to be easier to cut and the vessels present in hardwoods cause the chip to have a rough surface.

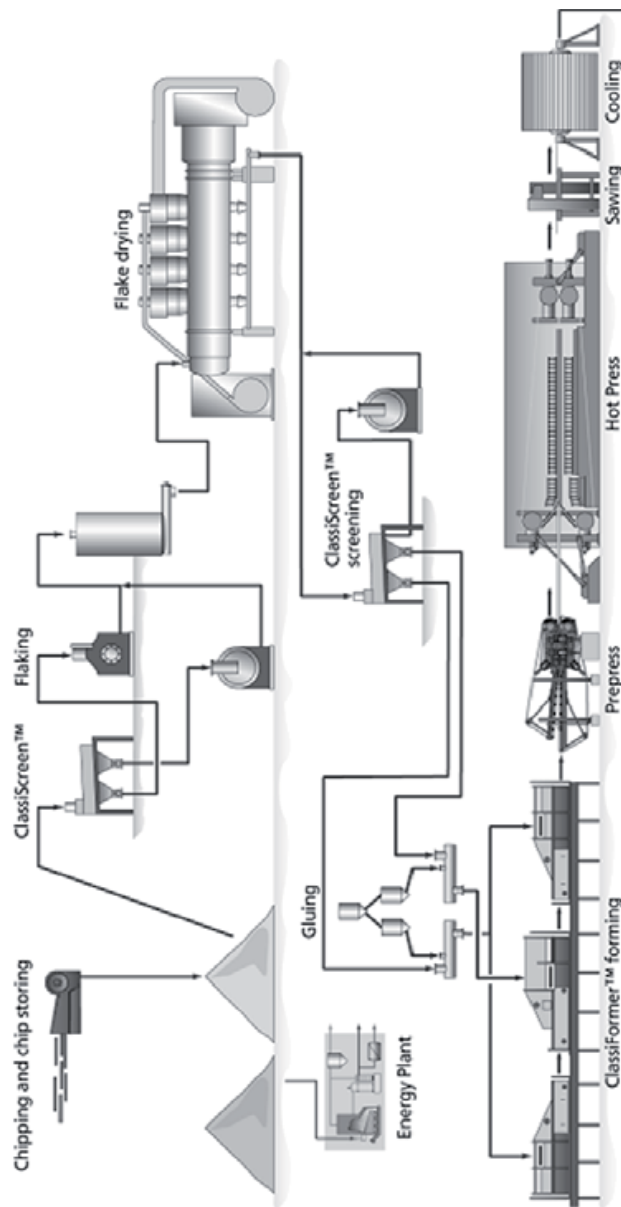


Figure 1.2: The main process stations in a Particleboard production line (Metso Panelboard).

1.3.2.2 Density

In order to manufacture a board of adequate strength the particles must be compressed to at least 5 % above their natural density. In practice the raw material is usually compressed to nearer 50 % of its natural density; so if a raw material of about 400 kg/m³ is used then the finished board will have a density of approximately 600 kg/m³. This degree of compression is needed to achieve good chip-to-chip contact.

Figure 1.3 shows the relationship between raw material density and particleboard physical properties. From this graph it is clear that for a single specie bending strength increases with compaction ratio. This is as expected because the more the particles are squashed the greater the contact between them. The graph also shows that for a specific bending strength the required particleboard density increases with the density of the raw material. Most regulations specify minimum strengths, consequently a manufacturer using say Birch (*Betula spp*) will have to produce boards of much higher density than another using Spruce (*Picea spp*) to attain these minimums. The heavy boards will require a larger press for manufacture, incur greater transport costs, and be more difficult to cut and handle. Therefore, it is not surprising that low density woods are preferred.

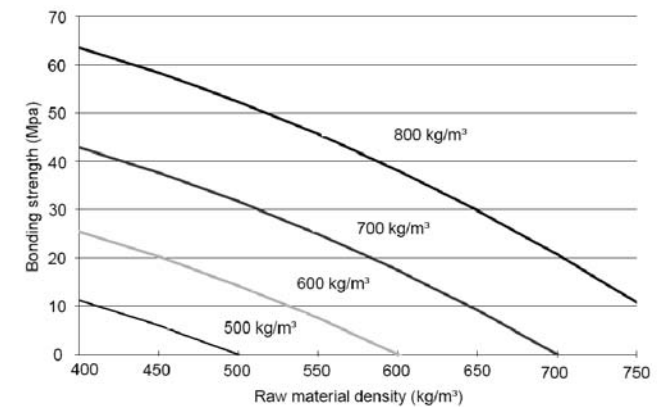


Figure 1.3: Relationship between raw material density and particleboard bending strength, as predicted by a computer model.

Practically all the physical and mechanical properties of particleboards are related to density. A manufacturer who attempts to use a number of different density species over a production period, will produce boards

with inconsistent properties unless he mixes the chips of the different species to form a uniform **furnish** for the press.

1.3.2.3 pH of wood

The curing rates of formaldehyde-based resins, e.g. urea formaldehyde (UF) which is used to make most of the world's particleboard production, are very dependent on the pH of the environment in which they cure. All wood species have a pH, if a near neutral species is used then a resin may not cure sufficiently, or if an acidic species is used then precure may result. When adhesive precure occurs the board's surface layer is weak and flaky. This is because the adhesive cures before the particles have been compressed and so when the press closes the precured resin bonds are broken. The pH of the raw material is not usually a problem if it remains fairly constant, but if it fluctuates then the quantities of hardeners and buffers added to the adhesives would have to be continually altered to suit the wood in use. Differences occur between species, within species depending on where the tree grew, and within the tree (principally a difference between heart and sapwood). In addition, the pH and buffer capacity of wood can change with storage time and conditions (Elias and Irle, 1996).

1.3.2.4 Permeability

It is postulated that very permeable species of wood will produce poor quality particleboard because chips from such wood will absorb the adhesive applied to it thus creating starved joints. The way a wood breaks down is probably more important than its permeability as this will determine the amount of exposed end grain. The amount and type of extractives present might be even more important still as these will influence the contact angle that the adhesive makes with the wood after blending. It is practically impossible to show the effect of wood permeability on particleboard properties, because when two boards made with different species are compared many more factors other than just wood permeability will be different. For example, anatomy will affect surface roughness and possibly the geometry of the particles and these two factors could be more important than particle permeability.

1.3.2.5 Wood sources

In addition to having the physical characteristics described above the raw material should also be inexpensive and available in sufficient quantities to support sustained production over many years. Conventional

particleboards generally compete with each other on price, because there are many manufacturers producing very similar products. Therefore, to be competitive cheap low grade raw materials must be used. Other forms of particleboard such as oriented strand board (OSB) require much higher quality raw materials because they need **engineered particles** (strands). The extra cost involved in manufacturing these chips is offset by the greater selling price of the finished product. The seasonal availability of agricultural crops has to a large extent prevented the wide spread exploitation of the enormous volume of suitable ligno-cellulosic material produced on farms around the world.

It has already been said that the vast majority of particleboards are made from wood. Wood is obtainable in three forms; as round wood, which is being used less due to costs, as residues from other processes and as recovered wood (normally processed in the form of large chips).

Round wood

The best particleboard furnish can be produced from round wood. A particleboard manufacturer has as much control over particle size, shape, and surface quality as is possible. This situation also allows the decision as to leave the bark on the wood prior to chipping or not.

The disadvantage with this raw material is cost. In addition, there is the cost of actually chipping the wood. The cost of this is split between the capital cost of the equipment together with running costs. On top of this there is the cost of drying the particles.

Wood residues

The success of the particleboard industry stems from its ability to utilise wood residues. **Forest residues** may take the form of treetops and branches, or particles from chipped stumps. The former have not proved popular because they contain a high quantity of bark and needles.

Sawmill residues are preferred since the slabs, edge trimmings, or chips, if a chipping head rig is used, are usually debarked. The larger residues have to be chipped, so they have some of the advantages and disadvantages of the round wood described above. However, sawmill residues are likely to have a lower moisture content than round wood, so the chips produced should require less drying. Further downstream there are the joinery manufacturers who produce vast amounts of **shavings** and **sawdust**. Of the two, shavings are preferred, however, since they are used for pellet manufacture and animal bedding the demand for them is high, so the cost of shavings is usually prohibitive. The prime advantage of sawdust is that it is cheap. Joinery mill residues are usually dry and in a

particulate form so only secondary break down is needed to produce particleboard furnish. However, much less control over particle geometry is possible and the residue is likely to contain a range of different wood species.

Sawdust, which many particleboard manufacturers buy and use, is increasing in cost rapidly as it is being used for pellet manufacture. When used as a surface layer furnish it helps to produce a hard smooth dense surface which many furniture manufacturers prefer. **Tensile strength perpendicular to plane of board**, often called **internal bond (IB)** strength, is improved by the addition of sawdust. This is probably due to increased inter-particle contact. Other physical properties are lowered by sawdust addition.

Plywood mill veneer cores are an excellent raw material for particleboard manufacture. They are all the same size, inexpensive, and of course bark free. Of course, the volumes available are limited.

Recovered wood

Competition is very fierce in most sectors of the panels industry and so many manufacturers concentrate on reducing manufacturing costs as much as possible. Most manufacturers of particleboard use recovered wood to reduce their manufacturing costs because it is often a cheap alternative to other sources of wood and it is generally drier than other sources and so there is a considerable saving in energy during the drying stage of panel production.

Using recovered wood seems to be an environmentally friendly thing to do and makes economic sense, but it does not come without its own problems. The particleboard industry has always used a lot of “wastes” as raw materials for its products. These have included using trimmings, sanding dust and reject boards within the production line, sawmill wastes, secondary processing residues, e.g. off-cuts, shavings and sawdust, and forest residues. Many of these are classified as being **pre-consumer** sources of recovered wood. In other words, they are residues generated as a result of making a product, e.g. wooden furniture, and have not been used for a particular purpose prior to being used as a raw material for another product, in this case, particleboard.

The trend of greater use of recovered wood has come from a greater use of **post-consumer** sources of recovered wood such as demolition timbers, old furniture and pallets and packaging.

Many sources of recovered wood, but especially post-consumer sources, contain **contaminants** that must be removed. These include: minerals,

e.g. stones, concrete, soil, etc.; ferrous metals, e.g. iron and steel; non-ferrous metals, e.g. aluminium, lead, brass, etc.; and organic materials such as plastics, paints, rubber, and fabrics. Sophisticated cleaning systems are available but these require significant capital expenditure. Generally, the economic benefits of using recovered wood justify the investment required and so a considerable increase in the use of recovered wood is anticipated for particleboard manufacture over the next couple of years.

The limitation in the use of recovered wood in many countries is the lack of infrastructure to collect, process and deliver it. Another potential limitation is competition for this resource from the new **bioenergy generation plants**, which are often established with the help of state grants and subsequently supported through the receipt of higher than market prices for each unit of energy produced.

The use of recovered wood in particleboard provides manufacturers with an opportunity to market their products as being environmentally friendly; in much the same way as the paper industry has successfully promoted recycled paper products.

Bark

Ideally bark should not be included in a particleboard furnish as it reduces board strength properties and increases resin demand. Bark is most often removed from small diameter logs with a **drum debarker** (Figure 1.4). The inclination and the dimensions of the drum (length 6 to 60 m and diameter 3 to 4.5 m) ensure the out-feed but also the retention time of the logs. Keeping a ratio of 0.7 between the log length and drum diameter this debarker can process up to 350 m³/h with a bark removal efficiency of up to 99 %.

During wood chipping, and subsequent drying and sorting operations, the bark is reduced to a fine dust. It is thought that the adhesive is absorbed by the dust, because of its high surface area to volume ratio, thus lowering the amount of adhesive available for inter-particle bonding. Including bark also tends to increase thickness swelling, linear expansion and decrease IB strength.

Some people regard the darker board colour which results from including bark depreciates its marketability. Despite these disadvantages most manufacturers do not debark their logs before further processing for cost reasons. About half of the bark is removed from the wood furnish, however, at two stages: primary chipping, where large pieces of bark fall off and are removed; after drying where bark dust makes up a high

proportion of the dust collected at the air-cleaning cyclones. The bark is usually burnt in the factory's boilers as it has a high calorific value; often providing up to 30 % of a factory's thermal energy need.

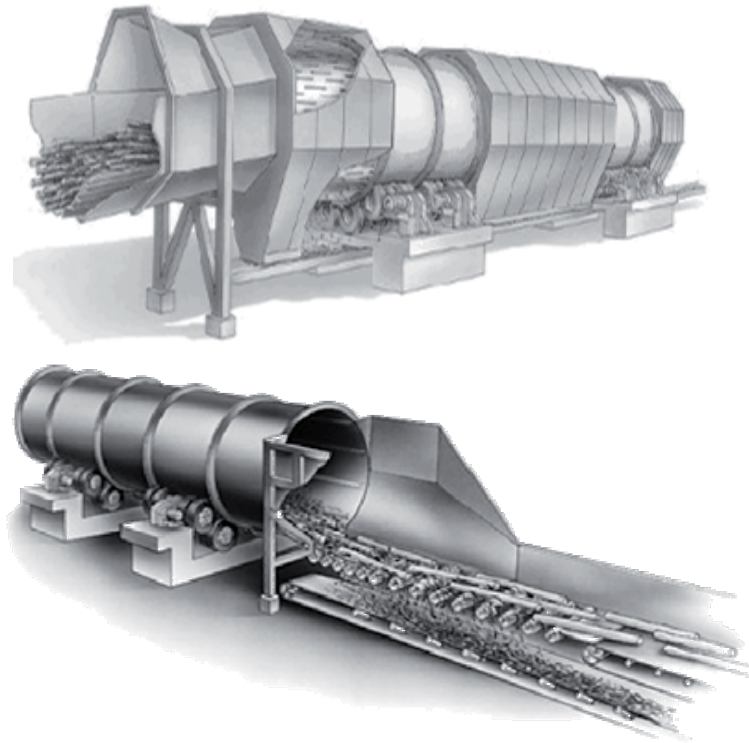


Figure 1.4: Drum debarker for thin logs, thinnings and branches (Metso Panelboard).

1.3.3 Particle Production

The way particleboard furnish is produced is dependent on the raw material. Figure 1.5 illustrates some of the many routes which are possible. Details of the machines themselves are shown in Figure 1.6 through to Figure 1.11. Fischer (1972) covers the main operational aspects of many of the wood reductionisers used in modern particleboard

mills. Although this reference is rather old the general principles are still relevant in today's factories.

There are many different ways to generate particleboard furnish. For example, if the raw material were round wood a manufacturer may decide to use a drum flaker only, sort the produced flakes and sending those that are too small to a boiler. Alternatively he may decide to use a hacker to initially break the wood down, and then use a knife ring flaker to reduce the hacker chips to particles.

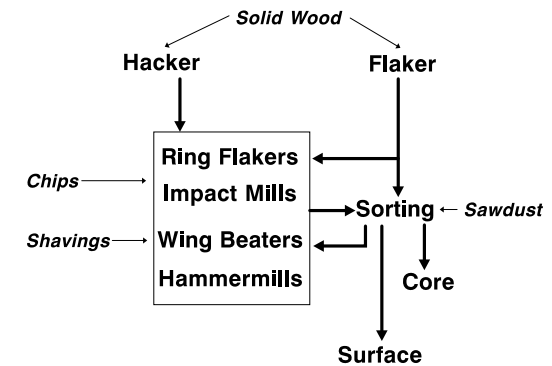


Figure 1.5: Different methods of producing particleboard furnish.

1.3.3.1 Primary Breakdown Machines

Hackers tend to be large and robust with drum diameters up to 2.4 m. They can chip logs of random length and diameter; the logs can even be twisted or bent. The logs are fed end on to the drum so chip size is largely controlled by adjusting the feed speed (20-36 m/min). However, large particles are held in the cutting zone by a heavy breaker screen, which typically has square meshes twice the chip length (<100 mm) and are therefore broken down by subsequent passes of the knives. The particles produced are thick (<10 mm) and long (<40-80 mm) with a wide size distribution: 15 % fine (<5 mm) and 10 % oversize (>50 mm). The two to five knives large and are spring loaded into the drum so that if a large stone enters the cutting zone then damage to the knife is minimised, see Figure 1.6. Particle surfaces tend to be rough and fractured since they are produced more by a splitting than a cutting action. They must be broken down further and this is often done with knife ring flakers, see below, the resultant furnish tends to be splinter like.

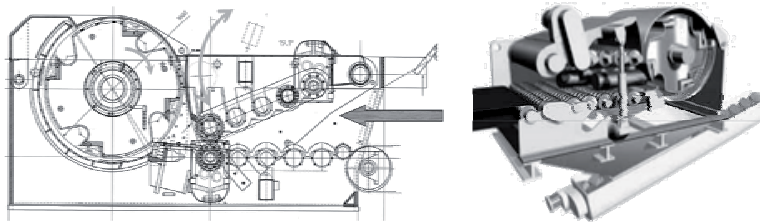


Figure 1.6: The inside of a large drum hacker (Bruks-Klöckner and Pallmann).

A hacker with a 1 MW motor and a shaft rotating at 300-400 rpm is capable of converting logs up to 1 m in diameter. It can produce around 150 tons wet (or 70 tons o.d.) of chips 35-50 mm long per hour. A hacker provides versatility as it can process a wide range of woods in various forms. Not all chipboard manufacturers have chosen not to install hacker/knife ring combinations because the quality of furnish produced is not as good as that possible with flakers. In addition, recent developments in flaking technology which now allow some versions of both **disc and drum flakers** to utilise random length and diameter logs, has reduced the versatility gap between hackers and flakers.

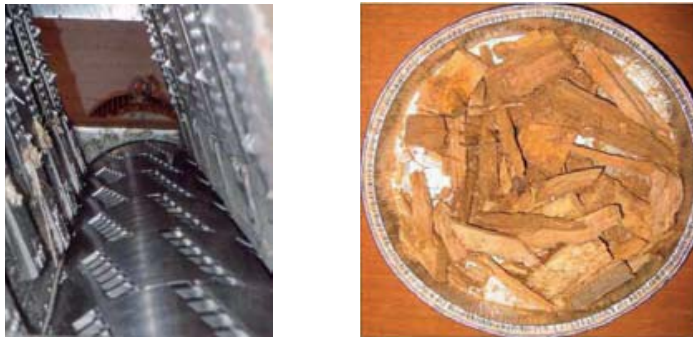


Figure 1.7: Vertical drum flaker capable of cutting fixed length, random diameter logs and softwood chips, (Pallmann)

Round wood can also be chipped with drum or disc flakers. Early **drum flakers** were limited to logs that were cut to length (dependent on length of drum, see Figure 1.7) and fairly straight. Current drum and disc flakers can use random length logs of poorer quality. In all drum flakers, regardless of the type, the knives are set at an oblique angle to the axis of the drum. This is to reduce vibration and strain applied to the drum bearing as the knife impacts the log; it also causes a slicing action.

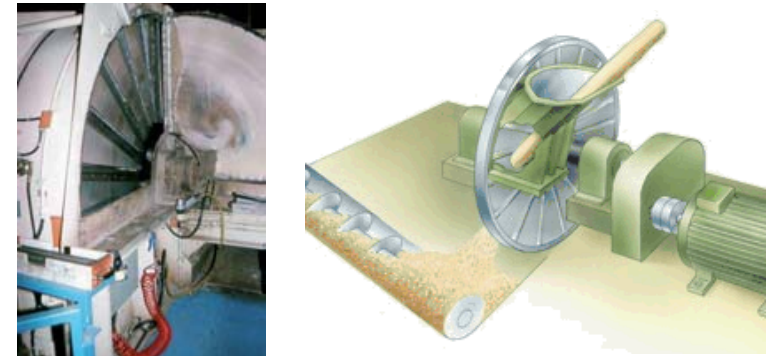


Figure 1.8: Vertical disc flakers that can cut random length logs (Metso Panelboard).

The development of **disc flakers** has followed a similar line to that of drum flakers in that early versions were limited to logs of a specific length. For example, the first flaking system installed at the OSB factory in Inverness in 1986, used horizontal disc flakers which accepted logs cut to approximately 1 m in length. Cutting the logs into short lengths reduces the problems associated with bent and twisted logs. In 1994 the horizontal disc flakers were replaced with vertical disc flakers similar to that shown in Figure 1.8. These flakers can convert logs of mixed lengths and diameters to flakes of predefined lengths and thicknesses. The installed power of 500 kW allows using a 2 m diameter disc with six knives an output of 50 tons wood/hour at a belt conveyer in feed speed of 76 m/min.

1.3.3.2 Secondary breakdown machines

A **knife ring flaker** is so called because of its outer ring of knives (Figure 1.9). Two versions of this machine exist: one with a stationary outer ring and the other with a counter rotating ring (Figure 1.9 left). The latter machine has a higher throughput and is more appropriate for wet material. The outer rings (10-55 kW) can be replaced in 5 to 25 minutes which significantly reduces down time. The diagram to the right illustrates how the inner impeller (100-630 kW) forces the wood particles against the outer ring of knives. The thickness of the resultant chip is determined by the protrusion of the blades. Ring diameter can be between 600 to 2000 mm including 28 to 92 knives and ring width from 140 to 600 mm, depending on the throughput required. The circulated air by the impeller varies between 4000 and 18000 m³/h allowing the processing of 2 to 30 tons/hour o.d. chips.



Figure 1.9: Knife ring flaker (Pallmann).

The machines of the type shown in Figure 1.9 are known as **impact mills** because the particles are reduced by them striking against the solid “anvil” in the centre of the outer ring. The larger and heavier a particle is the greater the moment it accumulates from the spinning inner propeller, therefore, the greater chance that it will strike the anvil with sufficient force to break it.

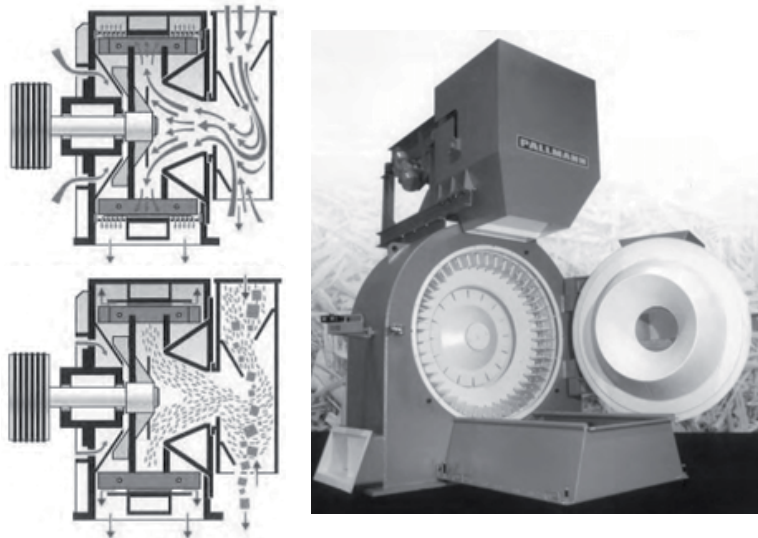


Figure 1.10: An impact mill double stream (Pallmann).

Small particles will not accumulate much momentum from the spinning propeller and are much more likely to follow the air flow (100 m/s)

through the holes of the mesh and not be reduced further. These machines are efficient as in general only those particles which require reducing are broken down. Such machines are often used for the preparation of surface particles. Typically, these machines are 800 to 1800 mm in diameter, have a grinding track width of 150 to 500 mm, powered by motors of 100 to 1000 kW, creating an airflow of 6000 to 30000 m³/h and have an output of 1 to 10 tons chips o.d./hour.

Wing beaters are similar to impact mills except that the outer screen does not have a solid region. Particles which are too large to pass through the screen are ground down to the appropriate size by successive strikes from the rotating impellor. Again larger particles will accumulate more moment and strike the outer mesh ring with more force.



Figure 1.11: A hammer mill (Maier and Pallmann).

The hammers of a **hammer mill** (see Figure 1.11) are attached to the central shaft by hinges which allow the hammers to swing back if they collide with a large particle. Large particles are therefore broken down by a series of blows. Particle size is determined by the size and shape of the holes in the screen. The robust construction of these machines enables them to break down solid wood into splinter like particles. Hammer mills are available in a very wide range of sizes from laboratory-scale to huge machines like that shown in Figure 1.11, which are used to produce particles from recovered wood. Consequently, rotor diameter can vary between 230 to 1800 mm, rotor lengths from 250 to 2000 mm, motor size from 160 to 500 kW, producing 30-80 m³ o.d. chips/h.

1.3.3.3 Particle geometry

Wood composite properties can be engineered, to a certain extent, by adjusting particle geometry. Unfortunately there is a lot of contradictory evidence in this area. The clearest patterns emerge when board properties are compared to the slenderness ratio of particles. Slenderness ratio is calculated by dividing the particle's length by its thickness:

$$\text{slenderness ratio} = \frac{\text{length}}{\text{thickness}}$$

For the majority of properties long thin chips seem best. However, surface quality (smoothness and hardness) and IB strength are enhanced small particles. This is why most manufactures attempt to classify their furnish using the fine particles for the surface layers and the larger particles for the core.

1.3.4 Particle Drying

Once the particles have been cut their moisture content must be reduced to between 2 and 8 %, depending on the adhesive system to be used to make the WBP. Such low moisture contents are required because residual moisture is converted to steam in the hot pressing stage, if too much steam is generated then, when the press opens, the board is likely to be delaminated by the sudden release of steam pressure.

There are a number of different dryer types on the market as shown in Figure 1.12. However, chapter will just consider the two of the most common, the **three pass** and **single pass dryers**.

Figure 1.13 illustrates the basics of a **three pass dryer**. The particles are introduced into the central tube which will often be heated by a direct flame fuelled by gas, oil or wood residue. The majority of dryers are capable of being heated by more than one heat source thus ensuring that particle drying can occur all year round. The conditions in the central tube are quite harsh; temperatures range from 250 to 850 °C (700 °C is typical) and the air speeds are often as high as 8 m/s. In the second tube the air flow is reversed. A combination of water evaporation and greater tube volume causes the air temperature and speed to fall. In the final outer tube the air flow is again reversed and the air temperature will have fallen to between 60 and 100 °C.







Dryer type	Scheme	Temp. range	Drying time	Drying capacity
Rotary bundle dryer		up to 200°C	≤ 20 min	1 ... 9 t/h
Tube bundle dryer		up to 160°C	n.a.	10 ... 18 t/h
Single-pass drum dryer		up to 450°C	20 - 30 min	≤ 40 t/h
Three-pass dryer		up to 400°C	5 - 7 min	≤ 25 t/h
Flash tube pre-dryer		up to 500°C	≈ 20 s	2 ... 14 t/h
Jet tube dryer		approx. 500°C	≈ 0,5 - 3 min	≤ 10 t/h

Figure 1.12: The characteristics of different chip dryer types (from Ressel 2008, acc. to Deppe and Ernst 2000).

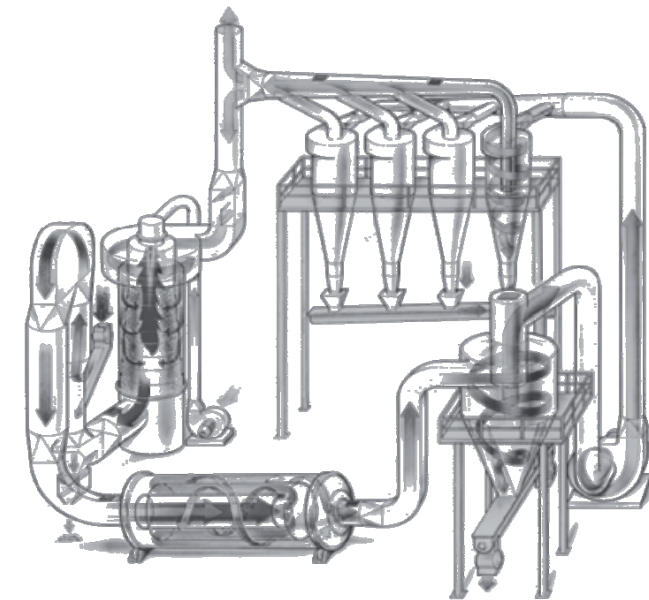


Figure 1.13: A three pass dryer (Metso Panelboard).

The outer tube rotates, typically at 8 rpm, thus causing the particles to tumble, which aids their passage through the dryer. These dryers are good in that they are compact for a given evaporation rate. Typical dryers of this type maybe 30 m long, 4.5 m in diameter and have evaporation rates of 7 tons per hour, reaching a drying capacity of 25 tons furnish per hour.

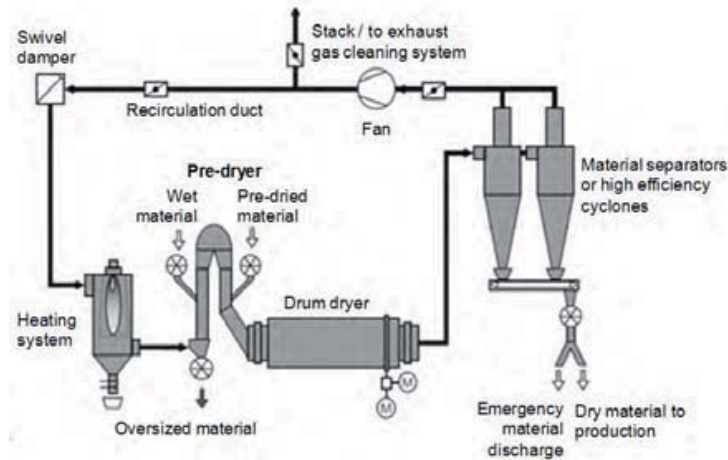


Figure 1.14: A single-pass dryer with dust extraction system (from Ressel 2008, acc. to Buettner2003).

The conditions inside a **single pass dryer** (see Figure 1.14) tend to be moderate in comparison to the three-pass dryer. For example the inlet temperature will usually be around 500 °C and the average particle dwell time is increased to compensate for the lower temperatures. The dwell time can range from 20 minutes to as much as 60 minutes. The particles are helped through the dryer by heated paddles and the rotation of the drum itself.

An increase in demand for particleboard has caused many factories to expand which, in turn, has created the need for higher throughputs. The current trend is towards the installation of a single large dryer including a flash tube pre-dryer (500 °C) with a high evaporation rate of maybe 50 tons/hour whereas previously 5-10 tons/hour would have been the norm. In recent years, most new dryers that have been installed are of the single pass type with a predrying step and all are large with drying capacity rates around the 70 tons of furnish or more per hour.

The amount of energy required to evaporate a unit of water from a wood chip is dependent on the way the chip is heated, the particle geometry and

the moisture content of the wood. Heat transfer by conduction is more rapid than by convection, so those dryers that heat the particles mainly by conduction, i.e. by touching the dryer sides or plates in the dryer, are likely to use less energy, see Table 1.3. Water evaporates more readily at high wood moisture contents, particularly above fibre saturation point (FSP). Below FSP the water is physically bound to the wood cell wall thus increasing the energy required to evaporate it.

Table 1.3: The specific energy required to evaporate 1 kg of water by different dryer types.

Dryer Type	Specific Heat Requirement (kJ/kg H ₂ O evaporated)
Three pass	3350 to 3675
Single pass	3255 to 3550
Contact dryer	3150

Operational particleboard factories are often easy to find because there is usually a large white cloud coming from the dryer exhaust stack. Many people incorrectly assume this to be smoke but in fact it is mainly made up of steam. Small dust particles and **Volatile Organic Compounds (VOCs)** are also present in the cloud and the emission of these is restricted. The VOCs can have a strong smell and can be irritating. They emanate from the wood, e.g. terpenes, waxes, other organic extractives, etc. and also from the sander-dust if this is used as a fuel.

Emissions from dryers are limited by regulation. In general, manufacturers are not permitted to achieve these limits by dilution, instead they must limit the production of emissions or install a treatment process, e.g. a scrubber (WESP –wet electrostatic precipitator). These restrictions may cause a move toward lower drying temperatures (inlet temperatures of <400°C) coupled with additional exhaust cleaning.

Drying small particles of wood to very low moisture contents is obviously a hazardous operation. Consequently all modern dryers have sophisticated fire detection and extinguishing systems. Many dryers also have **spark detectors** and automatic controlled **sprinkler nozzles** that are designed to detect a potential fire or explosion hazard before either occurs.

For efficient drying it is very important to determine the moisture content of the furnish as it enters and exits the dryer. The moisture content of the input material is likely to vary between 12-150 %. If dry material were to be allowed to enter the dryer without appropriate control (lowering temperature and increasing gas circulation) an explosion may result. Consequently, moisture meters for the input need to be accurate at

estimating moisture contents above FSP. The output meters, on the other hand, should accurate in the range of 0-20 % ± 0.2 %. In addition, the meters should be capable of measuring the moisture content of moving material from different species, having different bulk densities and geometries. Most systems rely on the use of infrared light or microwaves to measure moisture content.

1.3.5 Particle Sorting

Some manufacturers sort their particles before drying, so those outside the desired range are not dried, which saves energy. Another goal of wet screening in the particleboard lines is to adjust the ratio between face and core particle before drying. The drying of particles process can be controlled more accurately when particle size distribution is known before. But wet particles are difficult to sort efficiently as they tend to stick together. Consequently, in most particleboard factories the particles are classified after drying.

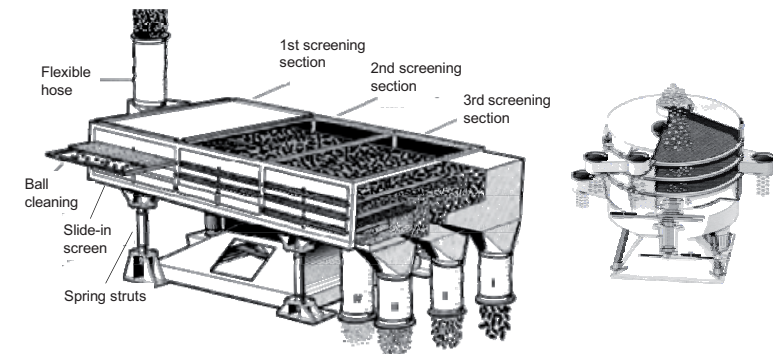


Figure 1.15: Gyratory rectangular and tumbling screen sieve (Allgaier).

There are two methods of sorting particles: **mechanical sieves** and **air classifiers**. There are three types of the mechanical sieves found in industry: **vibrating inclined screen**, **vibrating horizontal screen**, and **gyratory screen**, which are readily recognisable from their housings. All of these work on the same principle in that the particles are fed over a series of wire meshes, the particles either fall through or are passed to a collecting bin, see Figure 1.15.

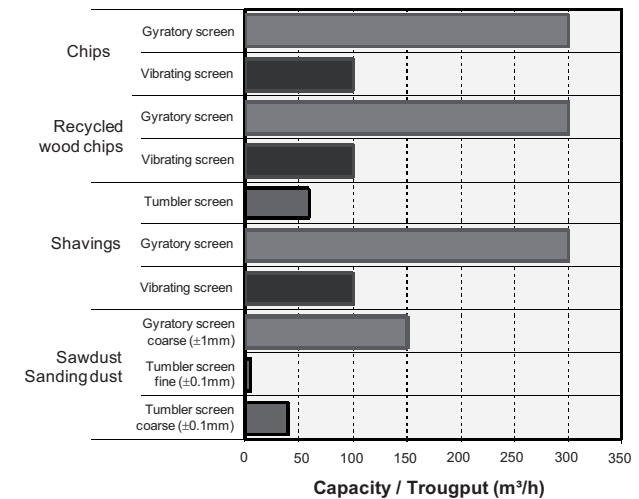


Figure 1.16: Performances of different screening systems (from Ressel, 2008, acc. to Allgaier).

Air classifiers sort particles by air flow. Particles are introduced into a counter flowing air stream so that the small particles are taken away by the air flow and the heavier particles fall to the bottom where they are removed by mechanical means, see Figure 1.17. A number of these may be joined together in series, each with a different air flow calculated to sift out a particular size. These are most commonly used in conjunction with a sieve system.

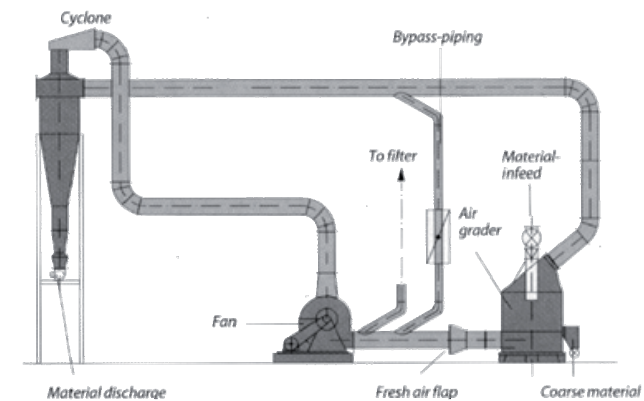


Figure 1.17: An air classifier, wind sifter (Metso Panelboard).

For the forming of the particle mattress consisting of face and core layers the sorting of dried particles into size and shape categories (fractions) like dust, fines, coarse, over-size is necessary. The efficiency of the separation and number of fractions depend on the number of screens. This equipment needs additional cleaning, maintenance and noise reduction measures.

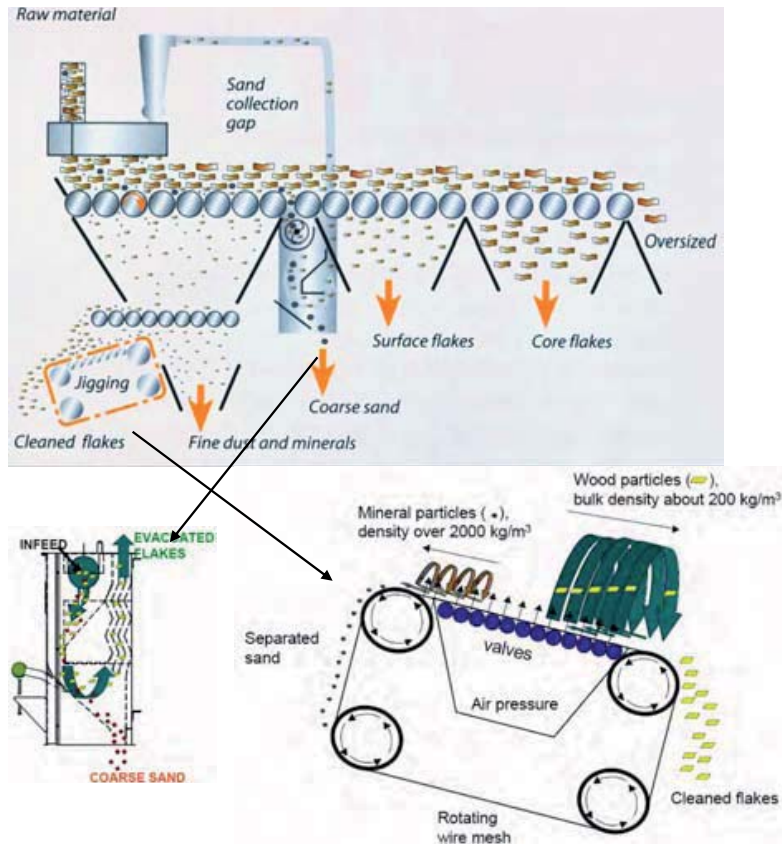


Figure 1.18: Compact cleaning system for particle screening and foreign matter separation (Metso Panelboard).

The combination of a screening conveyer, air sifter, magnetic drum and heavy particle separators in one machine provides a compact cleaning system that is particularly effective when recovered wood is used as raw material for the particleboard production. This system separates oversize,

heavy particles, ferrous and partially non-ferrous matter and mineral impurities and dust (Figure 1.18).

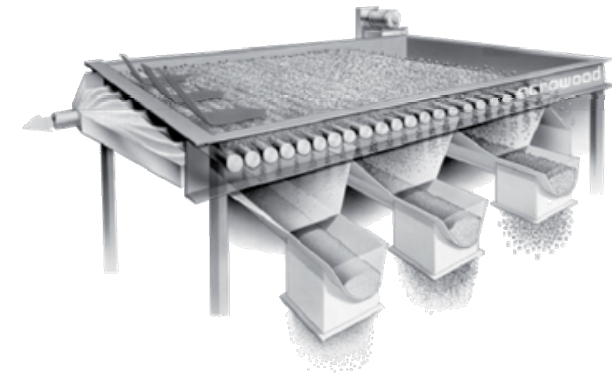


Figure 1.19: A roller system for sorting particles generated from recovered raw material (Acrowood).

Particle size classification can also be achieved using **dynamic screens of rotating rollers** as shown in Figure 1.19. The advantage of this method is that the screens are largely self-cleaning. The texture of the roller surface and the distance in-between them permits highly accurate separation of particles into face and core fractions and also the elimination of sand, soil and foreign particles.

1.3.6 Resin Metering and Blending

(A significant part of this section is taken from Ressel 2008)

Liquid raw adhesives are often purchased as water-based solutions, containing approximately 50% (PF) to 65% (UF) solids. These are thermosetting adhesives in which the curing process (condensation reaction) has been interrupted before delivery of the solution, thus storage duration is limited to several weeks depending on season, transportation and storage temperature. Adhesives can be purchased in powder form for longer storage, but, this rarely used in Europe

Before application on the dried furnish the adhesive solution must be blended, according to proven recipes, with water and additional additives, e.g. hardeners, colours, fire retardants, preservatives, etc.. Different adhesive formulations may be used for the surface and core layers. The amount of adhesive mix to be added is calculated on a solid adhesive substance to oven dry wood basis.

The hardener solution, which is added to catalyse the resin curing reaction is introduced as a percentage of solid hardener substance to solid resin basis, is added as late as possible to avoid premature curing due to production line stoppages. The surface and core layers experience different curing conditions during hot pressing and so different adhesive mixes are used for surface and core layer furnishes.

Resination of the furnish is a continuous process, which requires constant and continuous mass and/or volume flow control (furnish weight, resin weight/volume) to guarantee accurate blending and uniform panel properties. The mixing of the adhesive recipe on the other hand before application to the furnish fractions, is done either continuously or batch wise. The type and amount of adhesive depends on panel type (interior or exterior application), particle size, hot pressing conditions etc. The data in Table 1.4 are just for general information and may vary.

Table 1.4: Typical resin addition levels for different panel types (Ressel, 2008).

Particle board	UF	4 % - 10 %	→ surface layer	8 % - 14 %
			→ core layer	4 % - 8 %
	PF	6 % - 8 %	→ surface layer	8 % - 12 %
			→ core layer	6 % - 9 %
	MDI	2 % - 6 %	→ surface layer	6 % - 8 %
			→ core layer	2 % - 4 %
OSB	PF	6 % - 8 %		
	MDI	2 % - 6 %		
MDF	UF	8 % - 14 %	→ in blow-line resin application	
	UF	6 % - 10 %	→ resin application to dry fibres	
	MUF	8 % - 12 %	→ for HDF as flooring quality	
	MDI	≈ 4 % - 10 %		
all panel types	wax	0,3 % - 2 %	applied as micro-crystalline wax emulsion or liquid paraffin	

UF bonded particleboard for interior application

UF resin (66 % solid content)	100 kg	Hardener solution
Hardener (15 %)	10 kg	SL 5 % (NH ₄) ₂ SO ₄
Paraffin emulsion (50%)	10 kg	10 % NH ₃
Water	12 kg	85 % H ₂ O
Adhesive solution	132 kg	CL 10 % (NH ₄) ₂ SO ₄
		5 % NH ₃
		85 % H ₂ O

Table 1.4: continued

PF bonded particleboard for exterior application		
PF resin (45 % solid content)	100 kg	Hardener solution
Hardener (50 %)	5 kg	SL none
Paraffin emulsion (50%)	15 kg	CL 50 % K ₂ CO ₃
Water	0 kg	50 % H ₂ O
Adhesive solution	120 kg	

Batch-wise adhesive blending is used for small and medium-capacity particleboard plants, operating with long production series without changing the adhesive formulation. During batch-wise adhesive blending all of the adhesive formulation components, with exception of the hardener, are mixed in a tank. Hardener solution is first added to the furnish in the particle blender

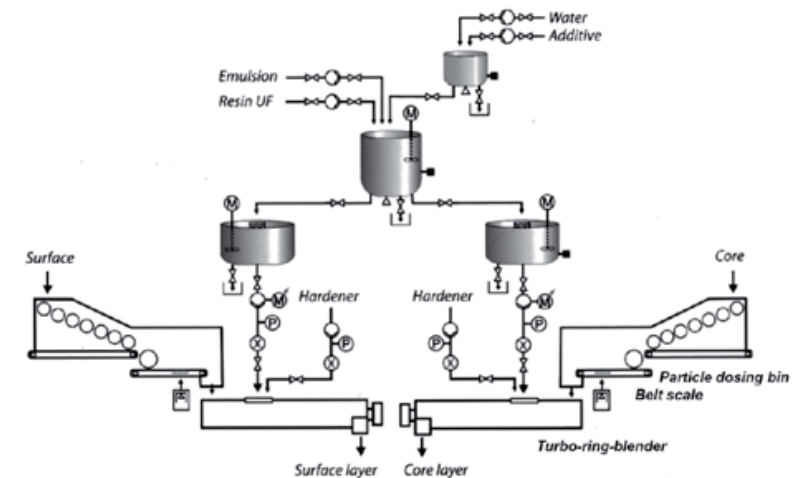


Figure 1.20: Batch wise adhesive blending of particle (Metso Panelboard).

Continuous or in-line adhesive blending is used for large capacity particleboard plants (Figure 1.21). Adhesive blending and the recipes are normally controlled and managed by a computer system. Facilities that use MDI are required to take special precautions. With in-line blending all components are added simultaneously into the particle blender. Pre-conditions for reliable adhesive blending and thus uniform product quality, but also high flexibility in changing the production programme, are reliable and accurate measurement and metering. The benefits of such highly sophisticated systems are: significant raw material savings of up to

5%, optimum adjustment to any type of raw material and requirements through integrated metering on the basis of flow meters and metering scales, high flexibility due to individual simultaneous metering.

Different **methods for measuring and metering** of the adhesive components:

- Mass flow measurement according to the Coriolis-principle, which is suitable for all media with variable density, viscosity or conductivity. The system measures the real mass flow.
- Magneto-inductive flow measurement uses the electric conductivity of the medium as its measuring method and therefore is applicable to aqueous solutions with constant conductivity.
- Mass flow measurement with differential metering scales is a proven and highly accurate measuring and metering method. It is equally suitable for liquid and powdery adhesives and additives. It is easy to calibrate and to check as well as a uniform technology, suitable for all media and flow rates

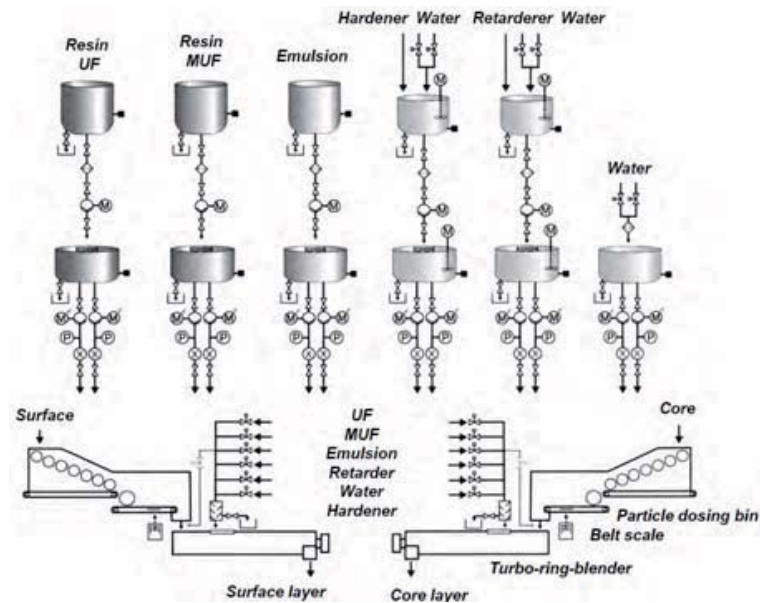


Figure 1.21: Continuous adhesive blending of particle (Metso Panelboard).

Blending is the mixing of dried wood particles and adhesive formulation with the aim of achieving a uniform distribution of drops of resin on each

and every particle. The additives may be atomised by either hydraulic or air spraying nozzles. For the former, the droplet size is dependent on nozzle design, liquid viscosity and liquid pressure (5-17 MPa). The disadvantages of these sprayers are the high pressures required and nozzle clogging. The droplet size for air atomising spraying nozzles is also affected by the above factors (although the liquid pressures are very much lower). In addition, the pressure of the air impacting the liquid jet also influences droplet size. The ideal droplet size is reported to be less than 35 μm in diameter (Moslemi, 1974). In practice the size varies in the range of 30-100 μm . The main reason for this is that formaldehyde adhesives are colloidal suspensions, and suspensions do not atomise readily.

Viscosity and ambient temperature affect resin penetration in wood. Ideally, the resin formulation should remain on the particle surface so that it is available for bonding. The smallest particles absorb five times more resin than the largest on a weight for weight basis. Some mills add the finest particles just at the end of the blender in order to minimize resin absorption

Particle dosing is required to ensure a controlled furnish flow into the blender and to achieve reliable constant resination. Particle dosing bins are built with either one or two belt tables. Additionally they are equipped with dust suction nozzles and belts with scrapers to keep the dosing bin belt clean. The weight scale controls furnish discharge volume. If two separate belt tables operate, the bin itself is separated from the metering belt to allow high bin volume and to ensure high measuring accuracy. On the first belt table, the level of the bin is measured and furnish flow adjusted. The second belt conveys the flakes via online weight scale, controlling the furnish discharge mass (Figure 1.22).

Most modern mills use continuous blenders to add resin and other additives such as wax to the furnish. The spraying of adhesives onto dried particles is often termed blending. Blenders are classified in two types: **short and long retention time**.

From 1950s onwards, the short retention time (2-3 seconds) blenders have been preferred. These are 2-3 m long and 600 mm diameter. They have a short concentrated spraying area, so some particles inevitably receive more resin than others. Resin redistribution is improved in the rest of the blender by violent tumbling (600-1000 rpm) in the bulk of the blender (Figure 1.23).

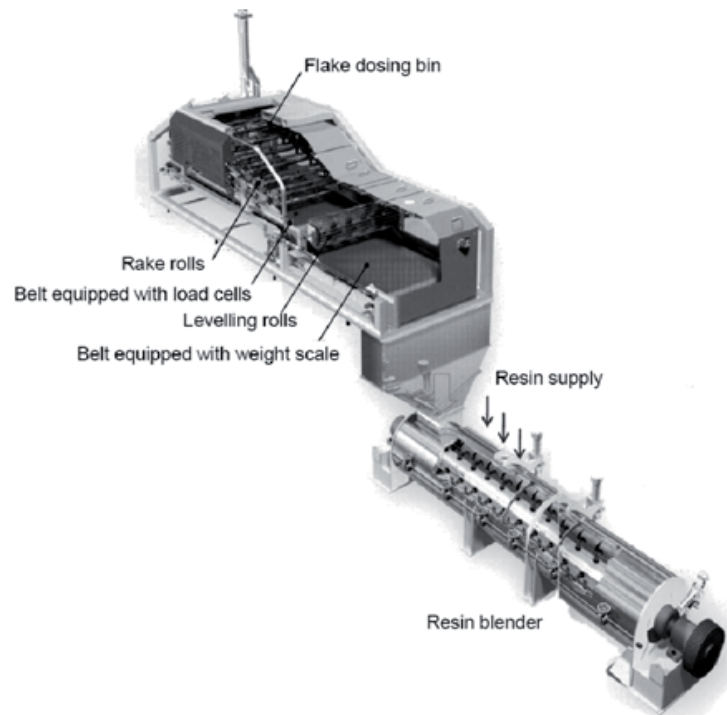


Figure 1.22: Furnish dosing bin and blender (Metso Panelboard).

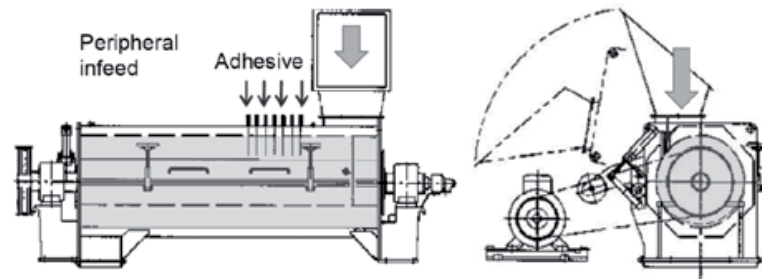


Figure 1.23: A short retention time blender (from Ressel 2008, acc. to Binós).

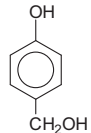
A **long retention blender** is a large drum ($L < 5m$) requiring minutes for the same throughput and job as the short one. It treats the furnish gently and reach an efficient resin distribution for inhomogeneous one.

Manufacturers of single layer and graduated density boards, see section 3.8, will often use a single blender. Two blenders will be used for the production of multi-layered boards; one for the core and one for the surface furnish. This allows the possibility of optimising the additive levels for the different layers. For example, more hardener may be added to the core layer to increase cure rate or more water for the faces to cause a steam shock effect during hot pressing.

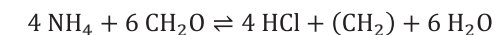
1.3.7 Common Adhesives

For economic production of particleboards the adhesive must cure in the press very quickly, say within 1-5 minutes, but it must also have a potlife of something in excess of 20-30 minutes so that the adhesive does not cure before entering the press. Longer potlives are desired, and achieved by many, to allow for line stoppages.

The most commonly used particleboard adhesive is **UF**, this is followed by **melamine formaldehyde (MF)** and then **phenol formaldehyde (PF)**. Other adhesives have only minor importance in the global view.

Urea	Melamine	Phenol	Formaldehyde
Mono methylol urea $\text{H}-\text{N}(\text{CH}_2\text{OH})-\text{C}(\text{O})-\text{N}-\text{H}$	Mono methylol melamine $\text{HOCH}_2\text{CHN}-\text{C}(\text{N})_2-\text{C}(\text{NH}_2)_2$	Mono methylol phenol 	$\text{H}-\text{C}(\text{O})-\text{H}$

The advantages of **UF** are that it is relatively cheap, cures to a clear or white glueline, provides good dry strength, and there is much production experience with this resin system. In order to achieve a high ratio of potlife to high temperature gel time latent hardeners are used (Meyer, 1981). The most popular of these used to be ammonium chloride (NH_4Cl). When added to UF resin it produces hydrochloric acid by two different mechanisms. In one, it reacts with free formaldehyde and chain end methylol groups thus:



Like similar chemical reactions the reaction rate increases with temperature. So when the ammonium chloride is first added there is a sudden drop in pH, as result of the high availability of free formaldehyde, but then the pH falls at a much slower rate until heat is applied. The

additional source of acid arises from the dissociation of ammonium chloride to ammonia (NH₃) and hydrochloric acid on heating.

A fast transition from liquid to solid in the press can be obtained by adding 1 g of ammonium chloride to 100 g of resin (solids basis). Such addition levels, however, can cause precure, so NH₃ or hexamine are added. The former is better in that it reduces formaldehyde release. The use of ammonium chloride and other halogen containing compounds has fallen. This is because many mills burn the dust from their sanding operations to help heat the chip dryers. Chlorides are therefore released when the dust is burnt because it contains adhesive and the chlorides attack the metal components of the dryers leading to severe corrosion.

Ammonium chloride has been largely replaced with ammonium sulphates and ammonium nitrates; both of which avoid corrosion problems in the dryer.

Using UF resins is not without its disadvantages. UF is not weather resistant, which precludes exterior uses. It also releases formaldehyde and since there are regulations which limit the maximum concentration of formaldehyde in the air, this can restrict the number of interior uses for boards bonded with this resin.

The moisture resistance of UF can be improved by fortifying it with melamine to form a **melamine-urea formaldehyde resin** (MUF). These adhesives are clear and strong, but they are more expensive. The price difference between a fortified and pure UF resin depends on the amount of melamine added, but a pure MF resin is about three times more expensive than pure UF. Although not quite such a problem, MF and MUF resins still emit formaldehyde.

Phenol formaldehyde resins on the other hand are much more weather resistant and do not have a formaldehyde problem. Admittedly, they are more expensive, being approximately twice the price of UF resins. Some people consider the characteristic dark red colour of cured PF resin detracts from the board's appearance, but since most boards are covered in use, e.g. melamine or veneer coverings, this is probably not a major disadvantage. However, in use some additional production problems are encountered with this adhesive. Higher temperatures and longer time periods are required to cure PF. Not only does this reduce productivity but it can also lead to significant penetration of the adhesive into the wood chip; if the glue has been absorbed by the particles then it is not available to bond them together and poor board strength results.

Isocyanate-based adhesives (MDI) have been used for commercial production of particleboards, MDF and OSB. Relative to the volumes of UF adhesives used, however, the isocyanate adhesives are small. These adhesives have become known as MDI, which stands for methylene diphenyl diisocyanate. In actual fact the isocyanates used consist of polymeric forms of MDI. Although more expensive than formaldehyde based adhesives, MDI performs so well that a particleboard with adequate properties can be made with much less resin than is possible with formaldehyde resins. The first isocyanates caused production problems as they tended to cause the board to stick to the metal platens. This has largely been solved using release agents, see Galbraith et al (1983). There are versions of isocyanates that can be mixed with water to form an emulsion which considerably eases the difficulty of spraying very small quantities of resin onto the furnish.

The binder cost as a proportion of total manufacturing costs is around 15-25 % of total. When the amount used is considered (2-10 % of wood weight), then it can be seen that a small change in use or cost can have a significant effect on profit. A great deal of work has been done on wood adhesives. Much of this information has been coherently reviewed by Pizzi (1983) and in the two state of the art reports written by members of COST Action E31 (Dunky et al, 2002 and Johansson et al, 2002).

1.3.8 Mattress Forming

It is vital that this stage is carried out properly. Board density directly affects properties, consequently, the preparation of a consistent mattress is critical in producing a board with suitable properties. The mattress must be laid down uniformly across its length and width, but not necessarily through its thickness. Instead the density profile through the board's thickness must be symmetrical about the board's centre. If this is not achieved then the board will probably warp in service.

Mattress formers are either segregating or non-segregating. They may operate as either batch or continuous formers, the latter are preferred in modern mills. In some small and old mills the mattress is laid onto caul plates, which are metal plates 4 to 6 mm in thickness and the size of the press platens. The caul plate is used to transfer the mattress to other process stages, including pressing. The high capacity mills of today do not use caul plates because of the capacity limitations they impose, capital outlay, maintenance costs, and additional handling equipment required e.g. caul separators and return lines. Instead, in these mills the mattress is laid directly onto a conveyor belt.

Non-segregating formers tend to be used in the production of single or multi-layered boards. There are many different designs from various manufacturers but they all aim to randomly orientate the particles so that the board strength properties are similar with and across the machine direction. The motion of the conveyor belt, or the forming machine, does, however, tend to cause some particle orientation in favour of the machine direction.

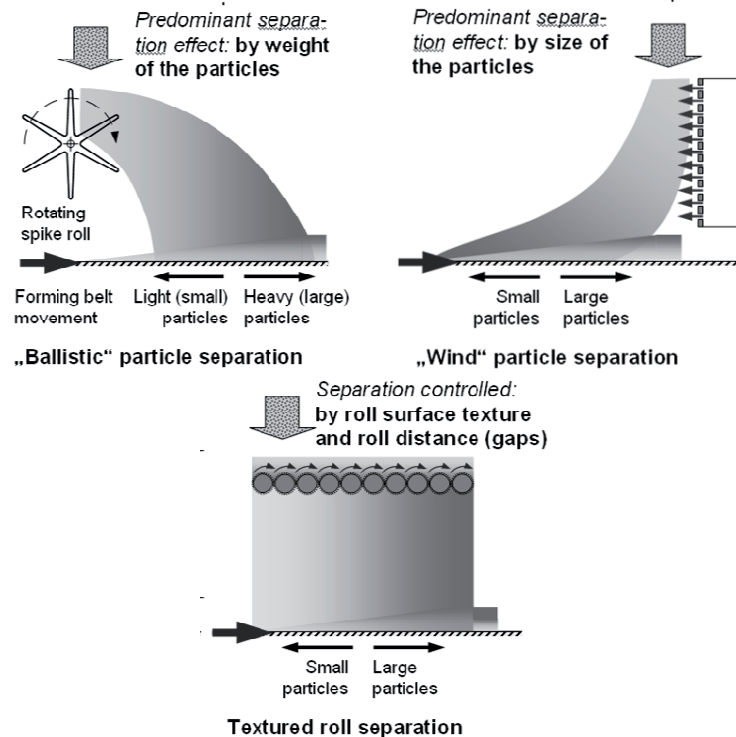


Figure 1.24: Principle of classifying and forming of particle mattresses (Ressel 2008).

Segregating formers work by one of three principles: air jets; throwing rollers and textured separating rolls (see Figure 1.24). In the first machine, particles are dropped in front of a column of air jets. The horizontal air flow created by the air jets causes the small light particles to land on the conveyor belt away from the column; heavier particles tend to settle at the column base. The other former classifies the particles by dropping them onto a spinning ribbed roller. The chips are thrown off the

roller; the heavy particles having more momentum than the small, tend to travel further. The overall effect of both machines is to produce a board with small fine particles on the surfaces (good for smoothness and hardness) and larger chips in the middle (good for bending and impact strength).

Figure 1.25 shows an example of the relatively **new textured roller system** that uses a **bed of rollers** to classify particles. The roller surfaces have a range of patterned surfaces, of which there are many designs with new patterns appearing with further development. The regular patterns have 3D shapes like diamonds/pyramids of 0.5 to 3.0 mm height which facilitate separation whilst minimising further particle size reduction. The diameter of the rollers is around 80 mm and some rotate rapidly (80 rpm) and have a coarse pattern whereas others rotate more slowly (30 rpm) and have a fine pattern. This helps to uniformly distribute the furnish across the whole machine width. The gap between the rollers at one end of the bed is about 0.1 mm and this increases to 2 mm along the length of the bed. Consequently, fine particles are able to pass through at the start of the bed and the larger particles are transported down the bed where the gap increases thus allowing more particles to fall through. Therefore, one bed of rollers is able to lay one half of a panel or one layer if the panel is of a 3-layer structure. A significant advantage is that with proper adjustment of the beds there are no abrupt changes in particle size and densities between layers and this leads to better IB values.

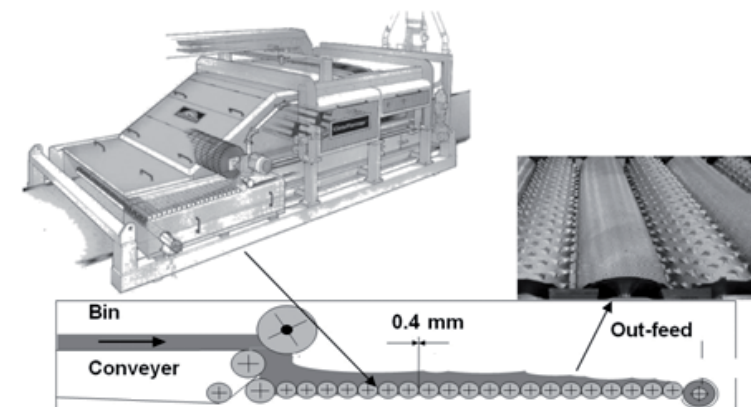


Figure 1.25: Roller (crown) former line for high production rate 3,100 m³/day (Metso Panelboard).

The roller system is very compact compared to traditional formers. This is most obvious when a roller system is retro-fitted to an existing line where,

because it requires less space than previous former, there are large gaps around the new former. The roller system does not require air flow and so there is less dust emission and particle drying so trimmings from mattress can be recirculated back in to the former and still have similar properties to fresh particles. Also it is more able to form low density mattresses and fine and uniform surfaces.

A significant advantage is that, unlike sieve-based systems, the roller system is largely self cleaning. Compared to conventional former the investment is low because the building height is lower, the platforms and supportive structure are simple and no fans and exhausting pipe are necessary. The equipment can eliminate oversize foreign matter and particles and thus protect the steel belts of the continuous press.

1.3.9 Mattress Pre-Pressing and Pre-Heating

The press is the most expensive single piece of equipment in a particleboard factory (approximately 15% of investment) so it must be operated as efficiently as possible. Many presses produce boards in batches whereas the rest of the mill, such as flakers, dryers and formers, operate continuously. As a result, most modern mills have cold pre-presses that compress the mattress to about 50-70% of its formed height (see Figure 1.26).

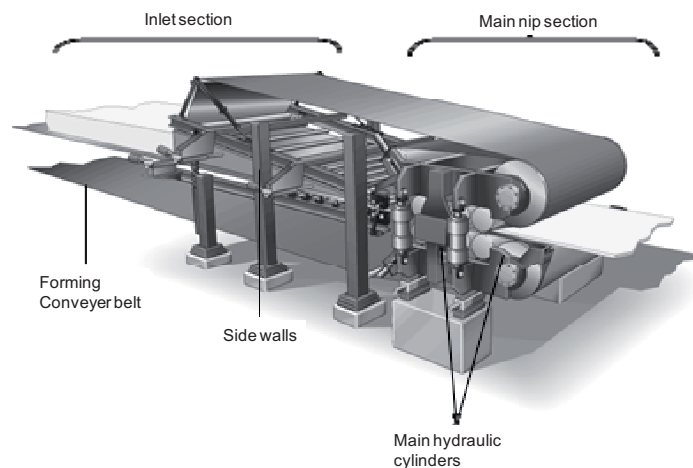


Figure 1.26: A pre-press (Metso Panelboard).

Since a **pre-pressed mattress** is thinner the press does not have to open so much in order to accommodate it. It therefore follows that the press

does not have to close so much to compress the mattress to the desired thickness, which also helps to reduce the chance of pre-cure. A press can compress a pre-pressed mattress far quicker than one that has not been pre-pressed because the prepress squeezes out much of the air in the mattress. This air can sometimes cause particles to be blown out of the side of the mattress if it is pressed too quickly. Consequently, the overall press cycle is reduced. A good example of how pre-presses may increase production was shown by Kronospan who raised their production from 180,000 m³/annum to 216,000 m³, a 20% increase, just by adding pre-presses to their manufacturing lines at the end of the 1970s. All modern lines include a pre-press.

Pre-presses are also used on production lines that have continuous presses. Many of the benefits given above are also of relevance to continuous presses.

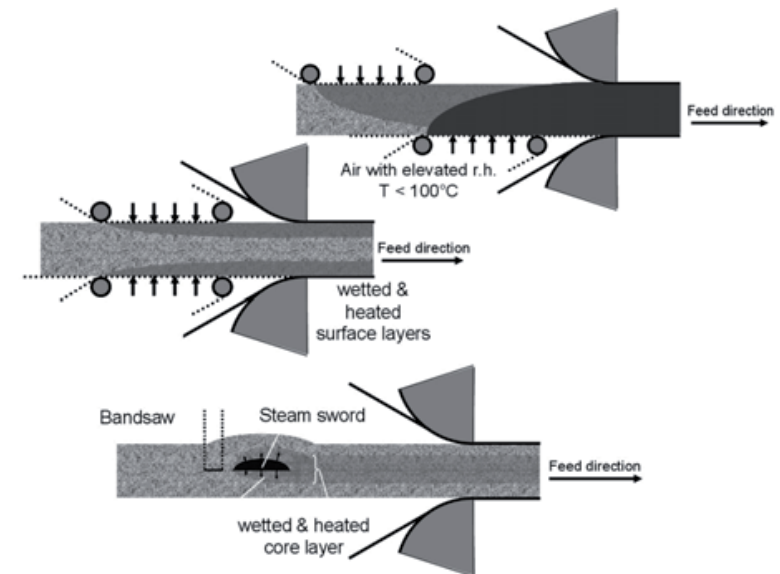


Figure 1.27: Preheating of mattresses using steam or hot air via surface or (only for MDF) via core (Courtesy of M. Gruchot).

After cold pre-pressing, and especially for thicker mattresses, mattress **pre-heating** is used to increase mat temperature (ideally the core) is sometimes used. The most appropriate choice of heating method is dependent on furnish type, moisture content, energy price and board type. Mattress preheating methods include: **electro-magnetic energy** (high

frequency <45 MHz and microwave >2,000 MHz), **heat of condensation** (saturated steam, supersaturated steam, high humid hot air) and **hot dry air**. The high costs of power today largely preclude the use of electromagnetic energy for WBP, but it is still used for the preheating for veneer based products (moulded plywood, LVL, PSL etc.) and for heating during pressing of GLT. For particleboard and especially for dry process fibreboard, preheating typically uses steam or hot air (see Figure 1.27).

1.3.10 Pressing

Particleboard can be made with **batch** or **continuous presses**. Batch presses are available in single or multi-daylight forms. A **single daylight press** (up to 52 m) makes a single board at a time, whereas a **multi-daylight press** produces more than one board per cycle (typical 6-10 for particleboard, but, much larger numbers can also be found).

The majority of commercial size presses are heated by steam, hot water or hot oil, the latter two being preferred because consistent platen wide temperatures are easier to obtain. The use of electric heating elements is restricted to laboratory scale presses because of the high cost and large temperature variations likely in large platens. Other heating systems have been proposed (Moslemi, 1974; Axer, 1975).

Typical **platen temperatures** range from 200 to 220°C. Such high temperatures are required to achieve rapid cure of the adhesive. The specific pressing pressure ranges from 2 to 4 MPa, principally depending on final panel density, but, raw material density and panel thickness also have an impact.

1.3.10.1 Batch Presses

Single Daylight Presses

In order to attain economic capacities and to maximise the advantages of **single daylight**, these presses tend to be designed to manufacture large boards. Most presses installed today are 25 m or longer. Egger (UK) Ltd. had until 2009 a 52 m press, which has now been replaced by a continuous press. Although long, the width of the boards that these presses are invariably no more than 2.8 m. This is to allow steam to escape from the mattress during pressing. Similar widths are found in multi-daylight presses for the same reason.

The main advantage of single daylight type presses is related to the size of product produced. All densified wood composites must be trimmed after pressing, this is not just to provide a straight edge, but also to remove, or

reduce the amount of, edge effects. These edge effects are caused by the inherent temperature and pressure variations experienced by particles in the outer edges of a mattress. As a result the outer portions tend to have inferior physical properties to the bulk of the board, see section 0. The amount of "waste" removed as a proportion of board size is much smaller for large boards than for small ones. A similar reduction in waste tends to occur when non-standard sizes are being cut from large production panels.

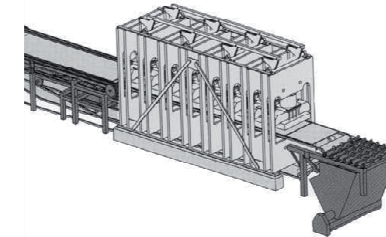


Figure 1.28: A single daylight press (Dieffenbacher).

Better thickness tolerances and shorter pressureless waiting time have contributed to improved sanding allowances of 0.7 – 1.4 mm. The steam injection press is a special single daylight press that can make very thick panels (>50 mm).

Multidaylight Presses

Some **multi-daylight presses** make as many as 48 boards per cycle. Typical multi-daylight presses produce between 4 and 8 boards, 5 to 7 m long and 2.5 m wide. It can be seen that multi-daylight presses have much higher capacities than single daylight presses; for example, a multi-daylight press producing 4 boards 5 m long per cycle will produce the equivalent of a single daylight press 20 m long.

An essential part of using a multi-daylight press efficiently is that all the boards of a press load must enter and exit the press at the same time. Whilst in the press they must also be subjected to the same temperature and pressure regimes. If this is not done then there will be significant variation between the boards of a single press load. Multi-daylight presses therefore have loading and unloading cages attached to them which introduce and extract the boards. Figure 1.29 illustrates the system of arms and levers employed to ensure the simultaneous closing and opening of all daylight. This equipment is not required for single daylight presses.



Figure 1.29: The simultaneous opening and closing mechanism of a multi-daylight press.

A major disadvantage of multi-daylight pressing is the large sanding allowance of 1.0 - 2.5 mm depending on thickness and product type. Low thickness tolerances and softer surfaces due to some pressureless closing time are the main causes of this.

Recent OSB projects have been based on multi-daylight systems, have reached a design capacity of 700,000 m³/a with 12 daylight of 3.66 x 10.37 m. The main reason for the re-gained success of multi-daylight presses for OSB manufacture is that these presses are less affected by glue spots and mat inaccuracies. When continuous presses are used they tend to require significant steel belt repair when used for OSB.

Continuous Presses

Single and multi-daylight presses make boards in batches and yet the rest of production line operates continuously, i.e. blending, forming, pre-pressing. Consequently, equipment is required to transfer mats from the continuous to the batch pressing stages. **Continuous presses**, on the other hand, do not require such equipment and so simplify production flow, see Figure 1.30.

The popularity of continuous presses can be seen in the statistics published in Wood Based Panels International (Wadsworth, 2001 and Natus, 2008) on particleboard production. These show that continuous presses account for 36 % of the manufacturing lines in Europe and around about 50 % of the production volume and these figures will increase over the next few years.

A continuous press can be used to make a wide range of product thicknesses and because the panel leaves the press as one long piece, it can make a wide range of sizes too. Its production capacity is easily

calculated by multiplying its width by the panel exit speed. Thin panels travel through the press much faster (i.e. 3 mm at 120 m/min) than thick ones (i.e. 38 mm at 5 m/min), because there is less material to heat. In theory then, the production capacity of the press is the same regardless of panel thickness. This does not quite happen in practice. They are, however, more efficient than batch presses at making thin panels. A batch press must open, be loaded and then close. This takes a finite amount of time. So when making thin panels, this opening and closing takes a significant proportion of the production time and overall capacity falls.

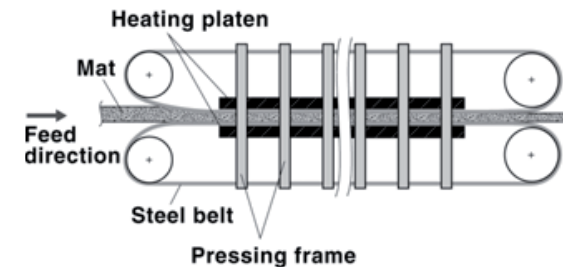


Figure 1.30: A diagram of the principles of a continuous press (Thoemen and Humphrey 1999).

Another advantage caused by the fact that a continuous press remains “closed” the whole time, is that the panels produced have very close thickness tolerances. This in turn, reduces the amount of sanding required. Tremendous amounts of money can be saved by minimising sanding losses.

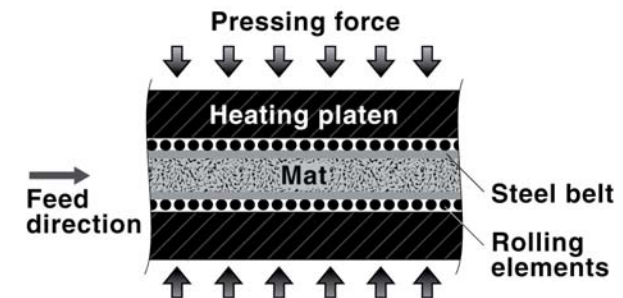


Figure 1.31: A diagram of the mechanism employed to minimise the friction between the stationary hot platens and the moving steel belts that carry the mat through the press (Thoemen and Humphrey 1999).

The use of continuous presses for the production of particleboard, OSB and MDF around the world is a real success story.

Typical press widths are between 1.8 – 3.0 m. Only a few plants exist with widths greater than 3.0 m. Pressure distribution, frame design, and mat de-aeration are the main reasons why presses wider are not made frequently.

There is a continuing trend for greater press lengths and speeds. The longest continuous presses for particleboard and MDF are in the 50 m range and for OSB in the 60 m range (the current record is 77 m). Press line speeds have been increased with the growing demand for thin MDF (< 3 mm) and the ongoing lowering of minimum thickness of this product (<1.5 mm). Line speeds of 120 m/min are now possible. As consequence of these developments, a modern single production line for particleboard can make 2,500 m³/day and 1,500 m³/day for OSB.

The hydraulic systems are characterized by precise pressure control by proportional valve technology. The high line speeds demand fast control systems, which are realized by PLC, local numerical control systems, or by central micro-processor control.

For press gap control, specialized thickness metering systems are needed. Depending on the basic press design these instruments may have to withstand quite high working temperatures. The product thickness profile is fed back to automated control loops to achieve good accuracy.

Continuous presses have controllable heating zones down their length. This adds another variable for manufacturers to use to manipulate board properties so that the product is more suited to a particular end-use, e.g. flooring as opposed to furniture applications, all on the same press. Roll et al. (2001) presented some results from a continuous press that has a cooling zone at the end of the pressing section. It would appear that this helps reduce “blows” and, consequently, the mattress can enter the press with a higher moisture content which helps heat transfer through the mattress and speeds production.

The advantages and disadvantages of continuous presses are summarised as:

Advantage	Disadvantage
Raw Materials: Reduced trimming and sanding losses	High initial cost.
Production: Lower energy requirement per unit volume produced. Similar production capacity at different product thicknesses production capacity of batch presses is reduced when making thin boards. Thickness changes are easy to perform and quick	Steel belt: Need for careful belt tracking control. Belt easily damaged by hard objects on/near mattress surface, so excellent metal detection in mattress required. Extensive wear of belt requires expensive replacement after 3-5 years of operation.
Properties: Reduced density profile that gives a better IB for a given density and reduced tool ware. Reduced precure and no asymmetry so there is scope for resin development	Poor heat transfer from platen to mattress. Not so appropriate for pressing thick (>40 mm) boards. Equipment construction is limited regarding high compression rates nor thin (<2 mm) boards.

The **calendaring presses** were the first systems able to make WBP continuously. They were introduced to the market in 1971. Due to the limited heat transfer and pressure capabilities the calendar presses are limited to thin particleboard and MDF (<4 mm). They often have microwave pre-heaters (Figure 1.32). Around hundred lines of this type are still operating. Limitations in capacity (300 m³/day) caused by the drum diameter (3-4 m) and length (< 2.5 m) and of the density of the product limits development possibilities.

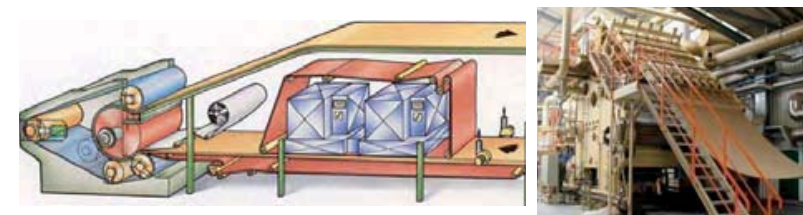


Figure 1.32: Calendar press with microwave pre-heater and simultaneous one face coating, detail with a modern calendar press (Bison and Binos).

1.3.10.2 Mattress conditions during pressing

Prior to pressing a mattress should have the same temperature through out and have a uniform density (symmetrical for multilayer boards). The board's **moisture content** should also be consistent throughout unless a manufacturer is using the **steam shock technique**, more of which later. In addition, there will not be any vapour pressure or internal stresses present in the mattress before pressing. Once pressing starts, however, all of these factors will begin to change at various rates in different parts of the mattress. Consequently, the geographical position of a wood particle will determine the conditions it is subjected to, which in turn will give rise to the board possessing inconsistent physical properties.

The minimum **press time** possible is determined by the time required to heat and cure the adhesive in the core layer. **Heat** is transferred in the mattress is by radiation, conduction and convection (water vapour movement). The latter transfer mechanism is predominant, particularly in the early stages of pressing (Bolton et al, 1989). The main reasons for this are that wood is a good insulator and vapour flow will occur readily as soon as a vapour pressure gradient is created (by surface heating). Note that the surface moisture does not have to turn to steam, which is water above its boiling point, in order to move through mattress since any vapour pressure gradient will induce some flow.

Humphrey and Bolton (1989) and others (see Chapter 3), have developed a **computer model** which predicts changes in mattress environment during pressing. Their model is unlike others in that it is a three dimensional model; predicting conditions across the board's width and length and not just through its thickness like most models. Their model predicts that particles at the edges of a mattress will experience lower vapour pressures and temperatures during the press cycle. These two factors are likely to reduce particle stress relaxation and hence increase the internal stresses remaining in the board after pressing. The effect of this is clearly shown in Figure 1.33, which shows thickness swell across a daylight (2.5 by 4.5 m) of an OSB. Note how the edges swell considerably more than the central region.

The way a board is pressed will determine its density profile, which is the change in density from one surface to the other. A board's density profile can significantly affect its strength properties and therefore its end use.

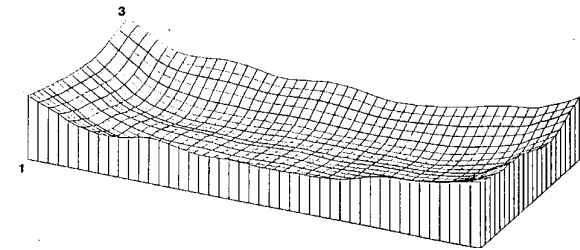


Figure 1.33: Observed thickness swelling across a daylight (4 by 2.5 m) of OSB. Note swelling at lowest point is approximately 10% and 24% at highest point (Bolton, et al 1989)

When a board is first placed into a press its surfaces begin to warm. Since wood temperature is negatively correlated to strength then this surface heating will cause the surface layers to squash more readily than the core. As a result even single layer commercially pressed boards will have higher density surfaces. This is often seen as an advantage because a board with high density surfaces will have a higher bending strength than a board which does not. In addition, the high density makes the surfaces scratch resistant and less prone to absorb paints and adhesives applied to the surface. However, particleboards are usually made to a set thickness and density, so if the surface layers are dense then it follows that the core layers must have a low density. It has already been mentioned that board physical properties are closely related to the density of the product, see section 3.2.2. A low density core will therefore equate to a low IB strength.

Studies have shown that this variation in **density profile** can be reduced by closing the press very slowly e.g. seven or more minutes (Moslemi, 1974). Such long **closing times** inevitably lead to precure in the faces and loss of production. The alternative method would be to close the press extremely quickly, say within a few seconds, so that the surfaces do not have sufficient time to heat up and plasticise, but this would require very large and powerful hydraulic pumps. The relatively new technique of **steam injection** pressing (Geimer, 1982) significantly reduces density variation and, at the same time, greatly reduces total press time. This is achieved by injecting steam through a perforated platen as the board is being pressed. The density variation is reduced by the fact that the board is more uniformly heated through out during compression. Whilst the press cycle may be reduced because the core layer is heated more quickly and so the adhesive starts to cure sooner. Many people see this as steam injection's main advantage, but there are other benefits. Instead of

producing particleboards with conventional properties in half the time, maybe this technique could be used to make much more stable boards using standard press time cycles. Much of the inherent instability of densified wood composites comes from particle densification reversal. When particleboard mattresses are pressed for long enough the stresses induced by compression are relaxed through wood creep, consequently, if stress relaxation is sufficient then spring back through stress reversal becomes much less important. The development of steam injection pressing will also allow the production of much thicker products, 100 mm or more. Such thicknesses cannot be made by conventional means because of the difficulty in heating the core layer.

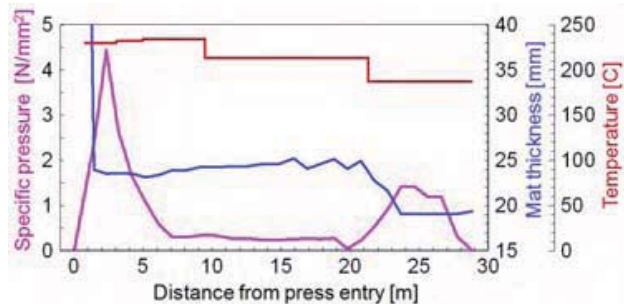


Figure 1.34: The change of parameters during continuous hot pressing, example refers to MDF (Thoemen et al 2006).

Mattress moisture content and distribution will also affect density profile. Some manufacturers apply a fine spray of water to the mattress faces with the idea that during pressing this extra water will evaporate, migrate to the core and therefore heat the centre more quickly. This is known as the steam shock technique. There is evidence that this does indeed happen. The addition of water to the faces has a secondary effect; it plasticises the surface layers so that surface density is increased and density profile variation is enlarged (Maloney, 1993).

As a press closes stresses are induced in the wood particles. These stresses act in opposition to the closing of the press and so the level of stress is often termed counter pressure. A simple press will operate by pumping hydraulic oil into the press rams until a certain pressure is reached. Board thickness is governed by metal stops. When such a press has "closed to stops" the stops will bear the load from the press ram. The stresses in the mattress will begin to fall off with time. Panel thickness can be controlled by using distance transducers and adjusting hydraulic pressure in the rams. Again, the hydraulic pressure will fall during the

cycle. The level of stress remaining in the board once the press opens will be dependent on temperature, moisture content, particle geometry, density of raw material and final product, and total press time.

1.3.11 Processing Steps Immediately after Pressing

All densified wood composites must be **trimmed** after pressing, this is not just to provide a straight edge, but also to remove, or reduce the amount of, edge effects (Figure 1.33). These edge effects are caused by the inherent temperature and pressure variations experienced by particles in the outer edges of a mattress. As a result the outer portions tend to have inferior physical properties to the bulk of the board, see section 3.10.2. The amount of "waste" removed as a proportion of board size is much smaller for large boards than for small ones. A similar reduction in waste tends to occur when non-standard sizes are being cut from large production panels. This explains why, initially large single-daylight presses, and then continuous presses gained in popularity.

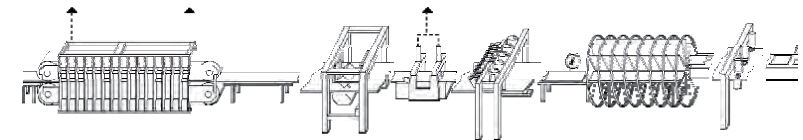


Figure 1.35: Primary board finishing after hot pressing: blister detection, trimming, cutting to length, thickness determination, weighing, and cooling (GreCon).

1.3.11.1 Blister detection

If the internal gas pressure in the mattress at the end of the press time exceeds the internal bond strength in the hot state (at 100°C in core), **blisters** (delaminations) occur. They tend to be concentrated in the middle because this is where gas pressure is highest. Blisters can be found using **ultrasound transmitters** and receivers distributed across the width of the production line immediately after the boards exit the press (Figure 1.36). The earlier this information is available, the easier it is to adapt production parameters. The press operator initially changes the press speed (lowering), then may try reducing the moisture content of the mattress at press entrance or improve the furnish bond by increasing adhesive content; all of which add to production costs. If no blisters are detected and the IB stays within the safety margins, then the operators usually try to gradually increase the line speed to maximise production capacity.

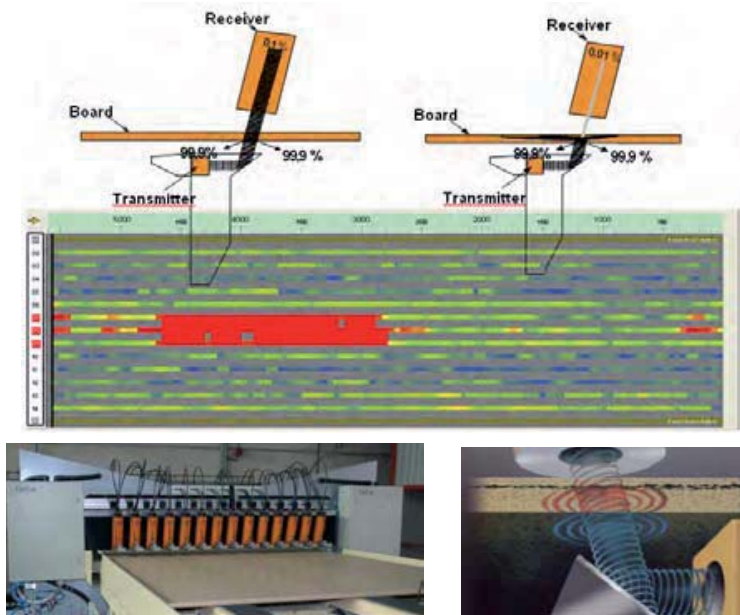


Figure 1.36: Blister detection in the hot panels after press (GreCon).

If the hot panels contain blister they are immediately eliminated from the flow. They may be used as packaging material or rechipped to particles with a hammermill and reused as furnish or as fuel.

1.3.11.2 Trimming and cutting to length

Using a **diagonal or flying saw** composed of two circular saws the continuous press endless hot board is cut to length (normally no more than 6.5 m) to a so called **master panel**. The correlation between the press speed and the traversing circular saws is computer controlled. For thin panels, which are pressed at high speeds, both circular saws operate. Also this sawing equipment has to fulfil high precision for the panel length ± 2 mm, squareness ± 1.5 mm/m and straightness ± 1.5 mm/m.



Figure 1.37: Diagonal saw for cut to length panels after continuous hot pressing (Metso Panelboard).

1.3.11.3 Weighing and panel thickness measurement

Each individual trimmed panel is controlled in terms of thickness and weight. Usually the **thickness** is measured continuously at three or more traces over the whole panel using **roller pair gauges** (Figure 1.38). Between measurements the roller pairs contact each other and calibrate themselves in order to assure a high measurement precision (0.02 mm). For high line speeds (>100 m/min) this type of calibration is not possible and a movable C-frame like that for the ultrasound equipment permits external calibration of the equipment.

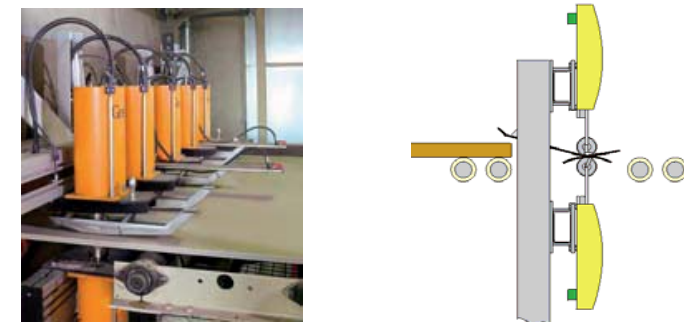


Figure 1.38: Thickness gauge based on contact roller pairs (GreCon and EWS).

Normally, the **weight** of each panel is measured by a **scale** installed under a separate belt conveyor. The weight cells need 2 seconds to obtain an accurate value. For new production lines with high line speeds classic

scales do not have enough time to accurately weigh the panel. Also the accuracy of this weighing system is not very good for thin panels because the weight of the panel is low relative to the weight of the scale itself. Dimensional data from the saws and thickness gauges and the weight of each panel is used to calculate panel density. This can also be achieved using an **X-ray** system, which directly measures the density and can also detect also foreign matters, furnish balls and other defects, but it is relatively expensive.

1.3.11.4 Cooling

Particleboards bonded with UF or MUF must be **cooled** after they have been taken out of the press. If the boards were stacked together immediately, the residual heat would cause thermal **degradation** of the glue. On exiting the press the boards are placed in a star cooler, which looks like a paddle boat wheel (Figure 1.39). The **cooler** is usually large enough to accommodate a sufficient number of boards so that as boards leave the cooler their surface temperature will have fallen to about 40 °C. From the graph shown in Figure 1.40, it can be seen that the internal temperatures are likely to be much higher. Depending on the stack size and season, the temperature in the centre can be more than 55 °C after 3 days of storage.



Figure 1.39: A star cooler.

Phenolic bonded boards can be hot stacked. In fact, hot stacking is recommended for PF bonded boards as their properties are usually seen to improve by this process. It is said that the improvement is due to increased cure of the adhesive, which seems very plausible. However, some of the improvement may also be due to continued internal stress relaxation permitted by the high temperatures in the stack.

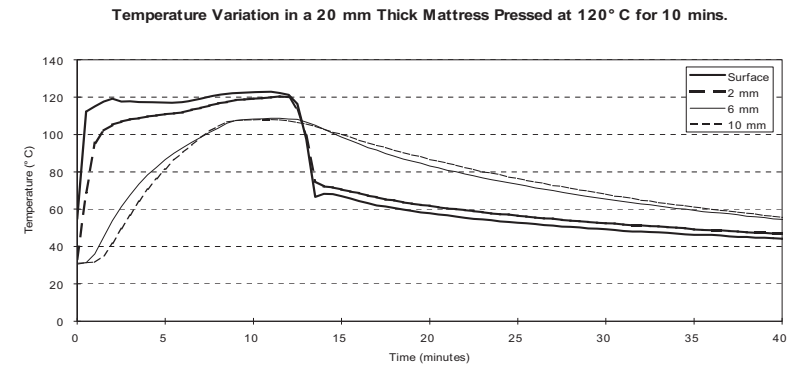


Figure 1.40: Temperature change in a chipboard mattress during and after pressing.

1.3.11.5 Intermediary storage

After **cooling** and **stacking**, the panels are stabilized through additional cooling, curing and rehumidification in an **intermediary storage**. Although transportation based on **fork lift trucks** is still common place, in larger mills it has been replaced with fully automated systems (robots), which are able to handle the big stack sizes with the master formats (press width x 6.5 m x 1.5 m, weighing approximately 20 t) to an intermediary storage of some 0.5 ha or more.

One type of such system is based on **stack care crane bridges**, rolling on overhead rails installed on building frame. Both movements cross- and lengthwise are performed simultaneously, which confer a high transferring rate capacities (transferring speed 3 m/s).

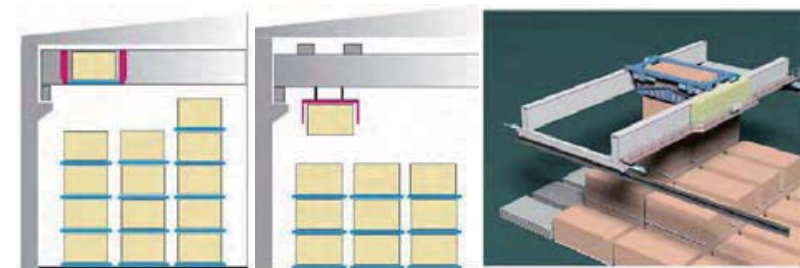


Figure 1.41: Full automatic intermediary crane based storage system (Metso Panelboard).

The systems are keeping the evidence of all piles and towers in a chaotic way. Some advantages of such modern and full automatic intermediary storage system are: the perfect horizontal position of panels in piles, complete protection of edges and surfaces, continuous and precise records of stored volume, minimal energy consumption, low pollution and dust generated relative to the traditional fork lift trucks and no supervision needed by operators. The disadvantages are high investment costs, high skills required for the maintenance team, in case of accidental stop, complete downtime for the whole line.



Figure 1.42: Full automatic intermediary storage system based on chariots (Metso Panelboard).

1.3.11.6 Sanding and Cut-to-Size

There are two reasons why the panels are **sanded** after hot pressing and intermediary storage:

1. To remove procured surfaces that are often weak, fibrous and porous
2. To calibrate panel thickness because the panels springback on release from the press and this varies from panel to panel and also within a panel

The **sanding allowances** depend on panel thickness, press precision and sanding machine (finishing quality). For thin panels (<6 mm), which require a high tolerance, 0.3-0.5 mm sanding allowance for both sides is common. The thicker the panel is, the higher the requested sanding allowance (0.8-1.2 mm). Calculated for the whole panel production (PB and MDF) approximately 3 % of the line output is processed to sanding dust. Generally this dust results from the high densified (600-1000 kg/m³) and high resinated (i.e. 10-12 % UF resin) face layers of the boards. The sanding dust will be air conveyed to a specialised bunker together with trimmings and cut to size off cuts and injected in to the upper part of the

burning chamber of the power plant, generating about one third of the thermal energy.

The **sanding equipment** consists in one **calibration machine** with superposed cylinders and coarse paper grit (60-80) and a **finishing machine** with two or three pairs of oscilating sanding shoes using fine paper grit (100-150) (Figure 1.43).

Panel stacks after 2-3 days intermediary storage have a temperature below 40 °C and their surfaces firm and the resin completely cured. The panel conveyers and rollers feed the panels at 40 to 100 m/min depending on the sanding allowance, thickness and sanding quality target. Generally, the thinner the panels, the higher the in-feed speed. The sanding paper has the same width as the panels for this reason for different width are available different paper sets. The speed of the sanding paper is above 60 m/s. The wear of the sanding paper depends on the resin type and amount, the furnish quality (recycled wood amount), sanding temperature and dust exhaustion performance. The power increase of the sander motors together with surface quality changes (e.g. discoloration) are the first signs of paper wear (in hours). For coating with melamine paper, a **grit** of 120 is sufficient, for lacquering or direct printing 150 grit or even higher is needed. The high in-feed speed makes it impossible to control by eye alone. Typically **defects after sanding** are dark spots (caused by glue balls, foreign matters), light spots (caused by dust agglomeration and non-resinated furnish), longitudinal traces (caused by broken grits or agglomerations on the paper), transverse traces (caused by grit delamination from the paper or deterioration of the paper joint area). Major sanding defects are differences in thickness in the cross sections (caused by cylinder misalignment) and along the panels (caused by the vibration of cylinders due to machine construction or foundations).

The thickness of each panels should be measured on-line in at two points or more before and after sanding in order to allow a continuous machine control and setting. Only big dark spots or major defects can be recognized by the operator. Modern on-line **self learning video control** of both surfaces simultaneously can assure a continuous and reliable check. An important aspect for the process security are the **spark detection** resulting during sanding by the overheating of the grit or contact with metals. The mixture of dry fine dust and air in the exhausting pipes or air filter bags increases the explosion risks. The **dust filtering** from the exhaust air remains an expensive and time intensive maintenance task.

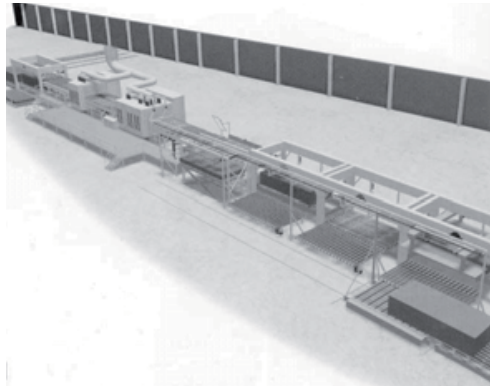


Figure 1.43: Sanding line with calibration (2 heads) and finishing (4 to 6 heads) and grading system (Metso Panelboard).

Cut to size equipment consists of many tables with conveyers and pile positioners, stationary and mobile circular double saws and racks for intermediary storage of small size piles, pilling and packaging units. The theoretical minimum size could be an A4 paper, but in practice, are multiples of doors, furniture size (table, walls or fronts) and flooring elements. The height of a mini pile which can be processed in one cut does not normally exceed 20 cm and needs paired circular saws (under and over the table) so that relatively thin blades can be used to reduce material loss.



Figure 1.44: Cut to size centre (MDF Hallein).

The amount of chips including the panel margins which results by cut to size the master panels in small parts should not exceed 1-3 %. To reach

this target, an optimization of master panel size based on the order of small parts is necessary before production. Small size parts obtain a better price, access an important market segment and allow a flexible use of stored panels. It needs a well prepared production plan, a good organization of the storage areas and many intermediary packet handling zones. The capacity of such a cut to size centre could cover 30 to 50% of the production. Main producers of such systems are Anton, Giben and Schelling.

1.4 THE MANUFACTURE OF ORIENTED STRAND BOARD: A SHORT OVERVIEW

1.4.1 Introduction

Oriented Strand Boards (OSB) are multi-layered panels made from strands of wood of a predetermined shape (typically, 15 - 25 mm wide, 75 - 150 mm long, and 0.3 - 0.7 mm thick) bonded together with a binder (often water resistant) under pressure and heat. The strands in the outer layers are aligned parallel to the long board edge and to the production line. Whereas the strands in the core layer are often smaller and can be randomly oriented, or aligned, generally at right angles to the strands of the face layers. The European specification for OSB is **EN300**.

OSB was first developed in USA based on patents dating from 1935 and later wood panels based on “veneer strips crosswise oriented”. The 1st pilot plant in USA started experimental production in 1963. The 1st plant in Europe operated only in 1978. The growth in demand for OSB is second only to MDF. In only 35 years, the market acceptance is complete and around 100 production lines with a capacity above 40 millions m³/year have been installed around the world. North America is by far the largest producer of OSB; 85 % of the world’s production is concentrated in USA and Canada. Europe operates 15 new factories with a total capacity of 4 millions m³/year.

About 75 % of OSB is used in construction, 20 % for packaging and the rest for decorative and diverse purposes. The standards EN 300 and EN 13986 classify OSB in four classes: OSB/1 is for general purposes in indoor (dry), OSB/2 is load-bearing in dry conditions, OSB/3 is also for load-bearing but in humid conditions and OSB/4 is for heavy duty construction in humid conditions.

OSB is usually made with thicknesses ranging from 10 to 32 mm. Often the most difficult test to pass for OSB/3 and 4 is the IB and MOR after cyclic boiling and so manufacturers use moisture resistant resins like isocyanates (PMDI), phenolic based resins (PF, MUPF) or melamine reinforced UF resins (MUF). The MOR and MOE values observed parallel to the long panel edge are normally double those observed across the panel. This is an effect of the strand orientation in the face layer.

1.4.2 Manufacture of OSB

OSB can be produced only from fresh wood and not recovered wood. Softwoods in form of thinnings, tree tops, cores from veneering etc. are the most common sources of wood. A typical production line (Figure 1.45) is very similar to a particleboard line. The differences being:

- The **stranding** of debarked logs is made in one step via disc flakers (Figure 1.8) or knife ring flaker (Figure 1.9).
- Some manufacturers use two separate **one pass dryers** (Figure 1.12) for the core and faces strands generated with two specialized flakers. This avoids supplementary work and facilitates a precise drying of the different layers (face m.c. > m.c. core), but requires more investment.
- **Strand grading** is achieved in large rotating drums or shacking boxes (Figure 1.46) that rotate at low speeds in order to avoid further strand breakage. Fines and shorts are used in the core whereas long strands kept for the faces, which is the opposite of the particleboard process.
- **Strand blending** is carried out in large separate drums without a central shaft and paddles by atomizing the resins (Figure 1.47)
- The **orientation of the strands** in the faces and core of mattress requires specialized formers (Figure 1.48)
- Generally 80 % of OSB panels are sold unsanded, therefore small capacity sanders are required.

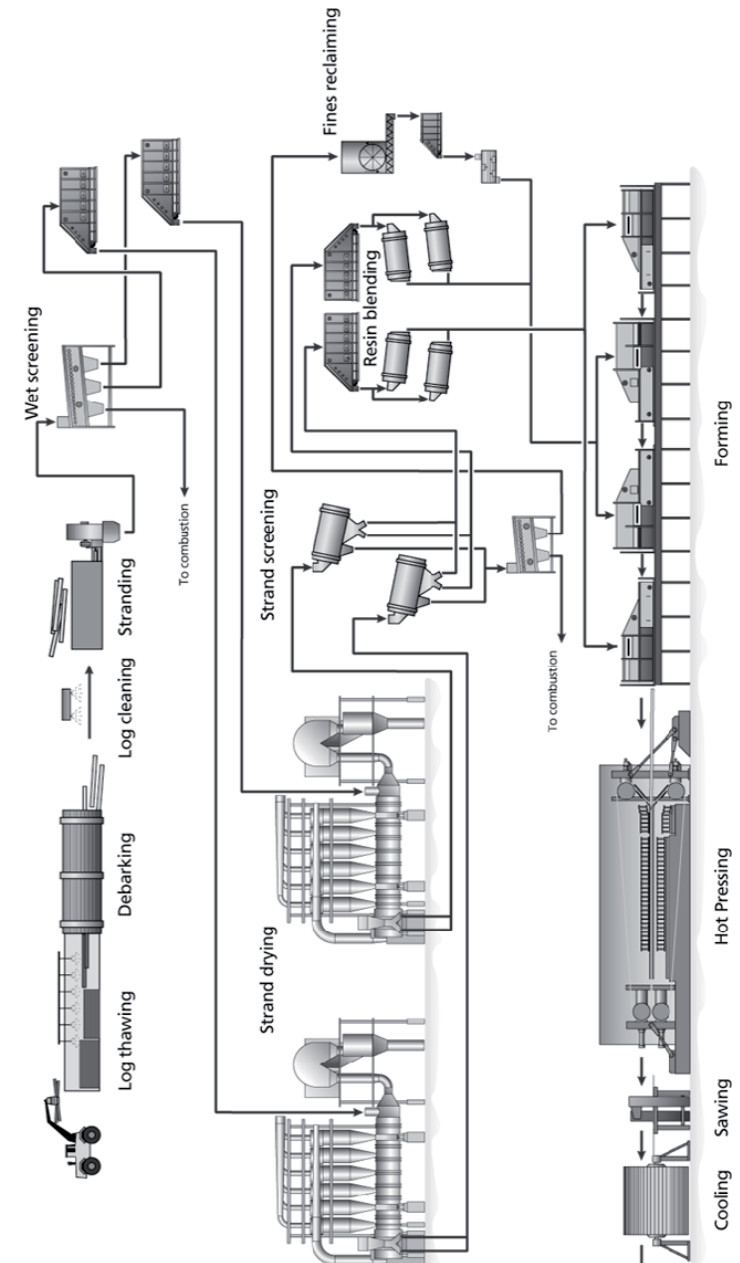


Figure 1.45: The main process stations in an OSB production line (Metso Panelboard).

1.4.2.1 Strand grading

The strands can be graded whilst still wet and fines and dust can also be eliminated before entering the dryer thus saving on energy costs. A **disc screen** is based on interlocked rotating discs which can separate the wet strands into fines (dust), face and core layer fractions (Figure 1.46). Such equipment minimises further strand breakage compared to classical screens, needs no air cleaning and requires less energy but it is relatively expensive.

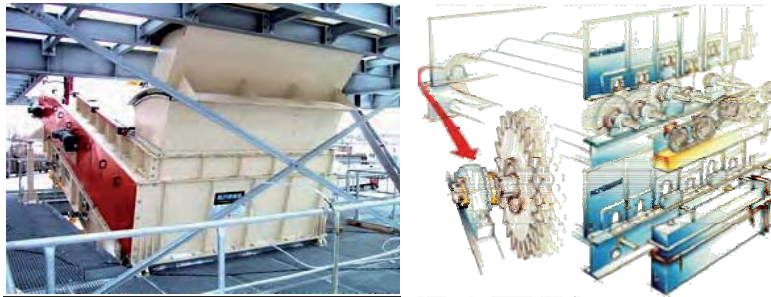


Figure 1.46: Disc screens for the cleaning of wet strands (PAL and Acrowood)

1.4.2.2 Strand resination

Resination of the strands is carried out in large drums (diameter > 2.5 m and length > 8 m) that rotate at low speed (about 100 rpm) without a central shaft (Figure 1.47). The drum filling ratio, rotation speed and retention time (inclination) depends on the production line speed, indirectly on the panel thickness and resin type. Normally, two resination drums (for core and faces) operate in parallel. In place of air nozzles (usually working at high pressure to assure a fog like resin distribution), many atomizing discs (wheels spinning at >10,000 rpm) fixed in two rows on the glue pipes are used. Some years ago the face layers were resinated with MUPF resins and the cores with PMDI, thus avoiding the risk of steel belts sticking and high cyanide emission during hot pressing. The new trend in Europe is to glue the faces and core with 3-6 % and 4-10% PMDI respectively (depending on OSB type). The advantages are: very low formaldehyde emission, good weathering resistance and high line speeds (4-8 s/mm). Whereas the disadvantages are: high costs, the need for permanent application of release agent spraying by nozzles or roller application on the steel belt or mat surface and controlled exhaustion in the press and cooling star area.



Figure 1.47: Drum resination of strands using atomizing discs (Metso Panelboard).

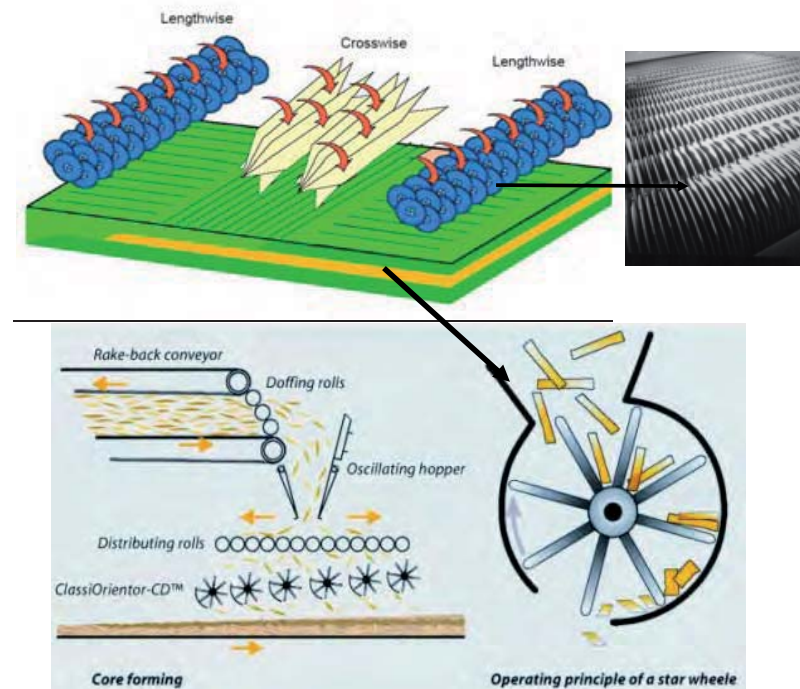


Figure 1.48: The forming principle for OSB face and core layer (Dieffenbacher, Siempelkamp and Metso Panelboard).

1.4.2.3 Strand forming

The **orientation** and **proportion** of long strands in the face layers, particularly at the faces, has a marked effect on parallel bending properties. In the faces, about 80 % of the strands are oriented parallel to forming belt. The space between the discs can be adjusted so that smaller strands can fall between the near the core whereas larger ones fall on to the face (Figure 1.48). In the core the strands are laid across the machine direction, but, the orientation is less well defined and some cases random. The strands are fed in to pockets that rotate and because the strands are long they tend to orientate themselves in the “V” of the pocket. The height of pockets and discs above the mattress can also be used to control the degree of orientation; the higher they are from the mattress the lower the orientation.

1.4.2.4 Strand forming

The **orientation** and **proportion** of long strands in the face layers, particularly at the faces, has a marked effect on parallel bending properties. In the faces, about 80 % of the strands are oriented parallel to forming belt. The space between the discs can be adjusted so that smaller strands can fall between the near the core whereas larger ones fall on to the face (Figure 1.48). In the core the strands are laid across the machine direction, but, the orientation is less well defined and some cases random. The strands are fed in to pockets that rotate and because the strands are long they tend to orientate themselves in the “V” of the pocket. The height of pockets and discs above the mattress can also be used to control the degree of orientation; the higher they are from the mattress the lower the orientation.

1.4.2.5 Strand mattress levelling

Due to the strand shape they tend to naturally lay flat in the mattress and so no prepress is required. A heavy steel drum is enough to **level the mattress** before hot pressing (Figure 1.49). **Trimming** mattress remains are recycled in the core. An electromagnet checked out the ferrous metals before entering the hot press.



Figure 1.49: An OSB levelling roller as prepress unit and trimming/metal detection in the mattress before pressing in a multidays press (Dieffenbacher).

1.5 THE MANUFACTURE OF MEDIUM DENSITY FIBREBOARD: A SHORT OVERVIEW

1.5.1 Introduction

Medium Density Fibreboard (MDF) was first developed in USA from hardboard manufacture. Hardboard is made via a wet process that is similar to paper manufacture and therefore produces a lot of polluted water that requires treatment before disposal. Semi-dry processes were developed in the 1950s and this led to a fully dry-process method. The first dry-process MDF factory was built in Deposit, USA, in 1965 and the first MDF factory in Europe is thought to be that built in the former German Democratic Republic at Ribnitz-Damgarten in 1973 (Williams, 1995).

Since these small beginnings there has been exponential growth in the installed production capacity of MDF across the world. By the early 1990s it was being hailed as a “... one of the most exciting new products to come along over the last 50 years.” (Anon, 1995). There was tremendous optimism in the MDF industry in the early 1990s, which was fuelled by the rapid expansion of both the market and supply. The optimism turned out to be founded and growth continues at an exponential rate.

MDF is an engineered wood product composed of fine **lingo-cellulosic fibres**, combined with a synthetic resin and joined together under heat and pressure to form panels. The most commonly used lingo-cellulosic fibres are wood, but other plant fibres can be used, e.g. bagasse and cereal straws.

MDF is available in a range of thicknesses from 2 to 100 mm and a very wide range of panel sizes. The density of these panels varies from about 500 to 900 kg/m³; panel density tends to increase as panel thickness decreases. Panels have smooth, high density faces and are pink-brown in colour, unless a dye has been added during manufacture.

The European definition of MDF is provided by **EN 316**. The main grades of MDF are: General purpose, dry (MDF), General purpose, humid (MDF.H), Load-bearing, dry (MDF.LA), Load-bearing, humid (MDF.HLS). The minimum requirements for these panels are specified in **EN 622-5**.

1.5.2 Manufacture of MDF

MDF can be produced from a wide range of lingo-cellulosic fibres including agrofibres (Suchsland & Woodson, 1986) and recycled wood (Anon., 1995). MDF fibres are normally made by using a thermo-mechanical pulping (TMP) process. This process uses the combined action of heat and mechanical energy to break the bonds between the cells that make up wood. Wood cells are joined by a region called the middle lamella, which is rich in lignin. **Lignin** is an amorphous polymer that can adsorb small quantities of water, and so, its softening temperature is moisture content dependent. The high temperatures (170-195°C) and humidities (60-120%) used in the TMP process therefore cause significant reductions in the strength of the middle lamella region and this increases the likelihood of failure occurring in the middle lamella when mechanical energy is applied during the refining process.

The main process steps for the production of MDF are described in more detail below:

1.5.2.1 Chipping

Wood is chipped into square particles with sides of approximately 25 mm and 5 mm thick using **drum chipper** (Figure 1.7) or as residues from modern saw-mills using **chipper canter**. Many other sizes are used, including sawdust, depending on the source of the raw material.

The **chips** are screened to remove under- (<2 mm) and over-sized (>50 mm) particles.

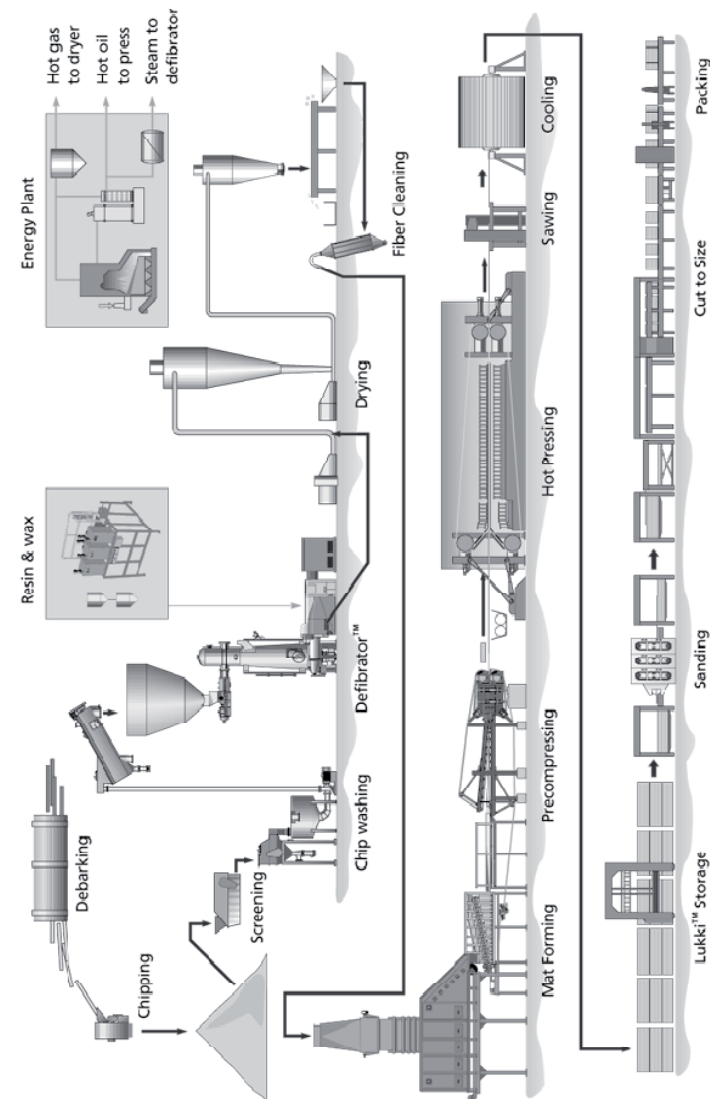


Figure 1.50: The main process stations in an MDF production line (Metso Panelboard).

1.5.2.2 Chip storage

Depending on climate region and availability of raw materials there are many ways to buffer the amount of chips for 2 weeks to 2 months production time, see Figure 1.51. The easiest and cheapest option is to store the chips outdoors on **platforms**, but, this brings the potential of further “contamination” with soil, stones and foreign mater, freezing, or bio-degradation. Another is to use, round steel or concrete **silos** with or without insulation having a volume between 5,000 to 30,000 m³ and diameters of 25 to 42 m. The advantages compared to the out-door platforms are: reliable and uniform line feeding (based on screw reclaimer discharge unit), first in – first out discharge, lower moisture content because the stock is protected from water and snow and no wind blow of the stock.

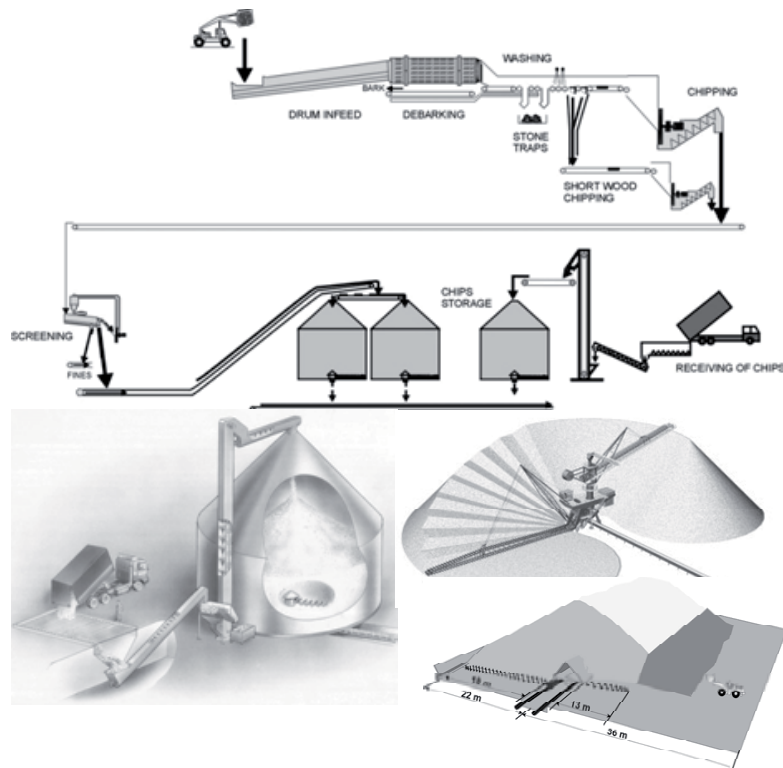


Figure 1.51: Raw material preparation and chips handling/storage for the MDF production (Metso Panelboard).

A **linear storage system** can be closed or open. The closed type is for volumes up to 50,000 m³ (i.e. bark as fuel for energy generation) and open type for volumes up to 200,000 m³. The chips are reclaimed by a conical screw of 10 to 18 m. Also a **boom type stacker** with crane type belt reclaimer and reversible conveyer for in and out feed typical for the paper industry could be used for high capacity plants.

1.5.2.3 Washing

Today **chip washing** is seen as being a compulsory step in order to remove the bark, soil, sand and other abrasive contaminants (Figure 1.52). In this way the life time of the refiner discs is increased and doubled in some cases. The water can be heated to better clean species with high resin or gum content and to defrost chips stored outdoors in winter. In this way also conveyer, screws and dryers are protected and energy saved. The water is kept in a closed loop and cleaned in the same circuit as the water emanating from the chip plug screw. The surface wetting caused by washing is thought to improve steaming and refining.

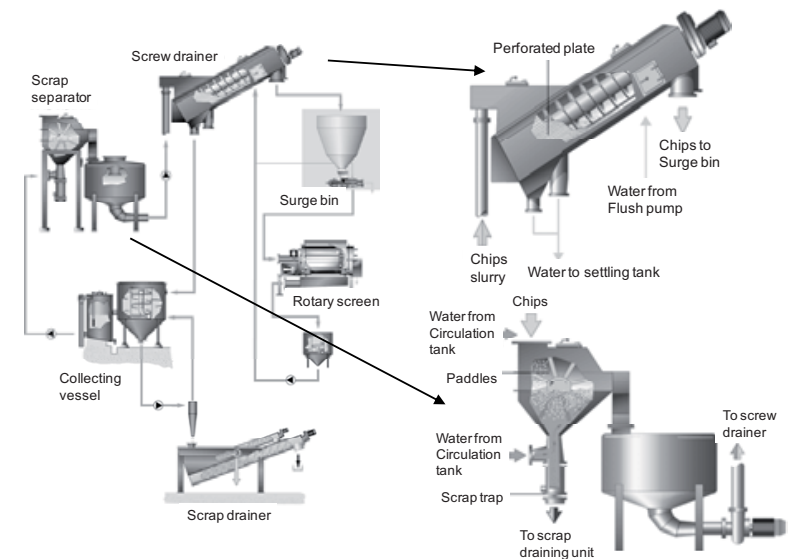


Figure 1.52: Chip washing (Metso Panelboard).

1.5.2.4 Pre-heating

One decade ago was an optional stage where the washed chips are **heated** to 40-60°C at atmospheric pressure in a surge bin (Figure 1.53b). This softens the particles so that a better plug is formed in the **conical screw feeder** (Figure 1.53c), which is a device that allows the continuous compression (2:1 rate) of chips into the main **steaming tube** (Figure 1.53a), which is also known as a **preheater** or **digester**, whilst still maintaining a high pressure in the tube. The plug screw squeezes out some of the free water in the chips. The volume removed can be some m³/h depending on line capacities and raw material. This water and a part of steam condensates must be treated.



Figure 1.53: The main parts of a defibrator: a) tube, b) window, c) plugging screw, d) main engine, e) blow pipe, f) resin injection.

1.5.2.5 Steaming

The compressed and squeezed chips are heated with **saturated steam** at 6 to 10 bar, which creates an internal temperature of 175 – 195 °C for 3 to 7 minutes depending of the **digester** size (5-18 m³), wood species, chip size and required fibre quality. The **retention time** of the chips in the **preheater** influences fibre colour and quality and is determined by the flow rate (screw feeder speed). The **digester level** is controlled by a radio-active measuring device. The discharge is accomplished by ribbon screw unit (Figure 1.55).

Refining

The **refiner** converts steamed chips into fibre bundles. The **refiner housing** is pressurised with saturated steam (8-10 bar). Most refiners have two discs (diameter 44 – 72 inch), one stationary and another that rotate at about 1500 rpm by powerful motors (typically 5-12 MW depending on the diameter of the discs), see Figure 1.55. Wood chips are fed into the gap (about 1 mm) between two discs via a hole in the middle of the stationary disc. The surfaces of the discs have a series of **raised bars**. At the centre of the disc the **breaker bar pattern** is coarse and at the periphery of the disc the bars are much finer (Figure 1.54). Consequently, as the wood is driven across the radius of the disc by centrifugal forces, it is gradually broken down into its constituent fibres and fibre bundles. **Pattern design** depends on wood species and chip size. The **adjustable gap** between the two discs determines the refiner energy consumption (150-400 kWh/ton fibre) and fibre quality. The throughput is typically 15...70 t/h depending on disc and engine size and chip geometry.

The fibres exit via a **discharge opening** positioned in the refiner housing and controlled by a blow valve (Figure 1.53d and e). The purpose of this device is to continuously adjust the flow rate of steam and fibres in to the **blowline** and thereby control the pressure in the refiner housing. A **diverter valve** (Figure 1.53f) after the blow valve can divert the fibre flow to the **start-up cyclone** or to the blowline. The start-up cyclone guarantees a safely start-up and shut-down of the system (under steam pressure). Only if the fibre quality and resination are satisfactory and the process parameters constant (dryer) the valve may be switched to production (blowline).

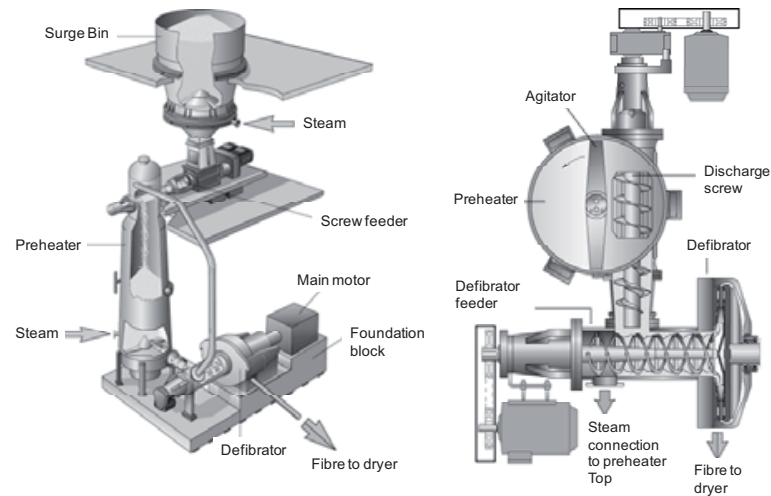


Figure 1.54: A typical pressurised disc refiner based system with preheating unit and digester tube suitable for the production of thermo-mechanical pulp (TMP) (Metso Panelboard).



Figure 1.55: Photographs of the discs and segments found inside of a typical pressurised refiner used to make MDF fibre.

1.5.2.6 Resinating (blowline)

The fibres are discharged from the refiner down a pressurised **blow line**, a pipe of 80 to 120 mm diameter, which conveys the hot, wet fibres and steam to the dryer. **Blending** of the fibre in the blowline under high pressure facilitates a uniform resin distribution due to the steam expansion, which cause high turbulent flow, rapid accelerations (that separate fibres) to high velocities of up to 100 m/s. The adhesive, usually a formaldehyde-based resin (UF), is injected via water cooled 3-5 mm nozzles at high pressure (12-14 bars) in to the blow line with other additives, e.g. water, hardener, repellents, colours, etc. The amount of adhesive added will vary between 8 and 15% (resin solids/oven dry wood basis), depending on grade of panel being made. Disadvantageous of this **blowline blending** is the fact that the resinated fibres have to pass through the flash dryer (110...140°C) which tends to pre-cure some of the resin. To compensate for this a higher resin amount is required (compared to dry resination).

1.5.2.7 Dry blending

A new approach to fibre blending has two stages. In the 1st stage the resin is applied via the blowline at an addition level of only 3-5% adhesive. The wax is applied as usual via refiner discharge screw. The 2nd resination stage takes place (like 30 years ago) in a **separate blender** (Figure 1.56) after fibre drying. Resin is applied by air-nozzles, mounted on a ring in front of the open in-feed (negative air pressure because of exhausting fans) of the **drum blender**. The internal paddles generate a turbulent fibre flow ensuring effective blending. The blender and out-feed pipe are water cooled to avoid resin and fibre deposits. After 2nd dry fibre resination a gentle drying to the target moisture content is recommended by IMAL. It is claimed that resin savings of up to 35 % compared to conventional blowline are possible.



Figure 1.56: Dry fibre blender with open in-feed and spraying nozzles ring (IMAL).

1.5.2.9 Forming

The dry fibre is pneumatically conveyed to **mat formers** via a system of **classifiers** (sifter) and **filters** (Figure 1.58); these latter devices are designed to remove any fibre clumps. The mat formers are designed to distribute an even layer of fibres (no layering) onto a continuously moving belt. The belt speed varies with the panel thickness being made. The fibre mat forming requires a **dosing bin** with integrated weight scale, and a **spreader system**. Due to the fibre consistency, handling and spreading is different to that for particleboards. Only one forming head is used to spread the homogenous fibre mattress. The dosing and metering bin has to assure a constant fibre flow to avoid compressing at the spreader head. A **back-rake conveyor** built on the top of the bin keeps the fibres at a constant height when they reach the doffing rollers.

A typical mat for an 18 mm thick MDF is 680 mm high and has a bulk density of 23 kg/m³.

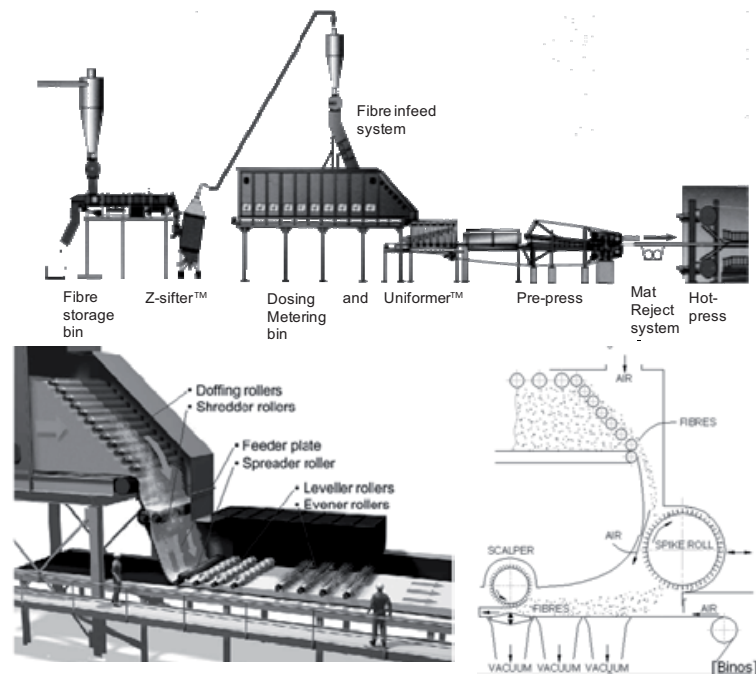


Figure 1.58: Fibre weighing, sifting, mat forming (mechanical) and prepressing until continuous press in-feed and air forming with spike roll (Metso Panelboards and Binos).

1.5.2.10 Pre-pressing

The mat is then passed to a **continuous prepress** (Figure 1.58). Here the mat is squashed to reduce its air content and to increase its density. This reduces the time required for hot pressing and avoids fibre dislocations at the press in-feed. Before pre-pressing a 38 m thick MDF has a mattress height of about 1 m and after the mat height is around 350 mm. Mattresses over 200 mm height (>18 mm panels) are often preheated (section 3.9).

1.5.2.11 Hot-pressing

In principle, the hot-pressing process is similar to that for particleboard described in 1.3.10. The **hot-press** applies a combination of heat (180-210 °C) and pressure (0.5-5.0 MPa) to consolidate the mat and convert it to MDF. The pressing stage can be used to manipulate panel properties by altering the panel's density profile, which is the variation in density through the thickness of the board, see Figure 1.59.

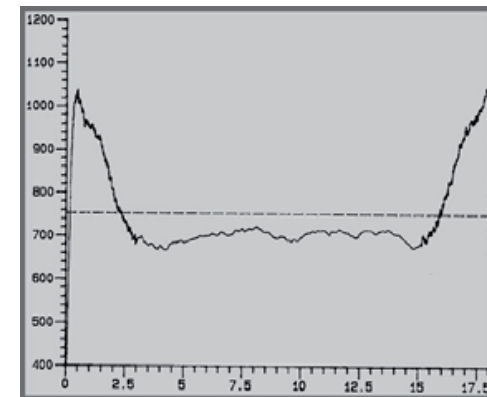


Figure 1.59: A typical density profile for an 18 mm thick MDF panel.

Immediately after pressing the panels are stood on their edges to expose their faces to ambient air to facilitate rapid cooling.

Finishing entails trimming, sanding and cut to size. Various added-value steps such as laminating, profiling and painting may be applied.

1.6 THE MANUFACTURING OF PLYWOOD: A SHORT OVERVIEW

1.6.1 Introduction

Plywood panels usually have an odd number of veneers. The terms 3-ply and 5-ply are commonly used and refer to the number of veneers used to make a panel. Plywoods with seven or more veneers are also made. The need for an **odd number of veneers** is caused by the fact that wood is an anisotropic material, i.e. it has different properties in its three main directions, longitudinal, radial and tangential.

An example of this anisotropic behaviour is the high strength of wood parallel to the grain, e.g. longitudinal compression, compared to strength perpendicular to the grain, e.g. tangential or radial compression. Another is the difference in the dimensional stabilities between the three grain directions. If a dry piece of wood is soaked in water it will swell. It will swell most in the tangential direction and least in the longitudinal direction, with the radial directional movement between the two but nearer the tangential movement. The relative movement between the three directions varies from species to species but is typically around 20:12:1 (tangential:radial:longitudinal). It is this dimensional anisotropy that makes it necessary for plywoods to be made with an odd number of veneers.

Each veneer in a plywood is laid down with its grain at right angles to its neighbour. This is done to minimise the strength anisotropy in the panels. In other words, the longitudinal grain of one veneer reinforces the tangential grain of adjacent veneers. Bonding just two veneers together, so that their grains are at right angles to one another as in a plywood, dramatically reduces strength anisotropy but, such a panel would be dimensionally unstable. To visualise this, imagine the cross-section of a 2-ply panel, with the top veneer showing longitudinal grain and the bottom transverse grain. When placed in water the bottom veneer, in this cross-section, will swell 20 times more than the top veneer, because of the ratio given above, and so the panel will cup.

To make a stable panel, therefore, a third veneer must be added. This creates a panel that is symmetrical through its thickness, i.e. the bottom half is a mirror image of the top half. So when a 3-ply panel is placed in water, the veneers still try to swell, but this time the swelling forces are balanced and the panel remains flat. Plus, the amount of swelling is limited by the longitudinal swelling of adjacent veneers, i.e. generally <1

%, and so plywood panels are very stable. Additional veneers must be added in pairs so as to maintain panel symmetry.

Figure 1.60 shows a cross-section of a 7-ply plywood with the line of symmetry marked. Any dimensional movement in the top half should be counteracted by similar movement in the bottom half.

There are two ways of making **thicker plywood** panels. One is to use thicker veneers and the other is to use more veneers. The advantage of the latter method is that it produces more homogeneous panels. This is because the ratio of veneers in the two directions tends to one as the number of veneers increases. For example, in a 3-ply the ratio is 2:1, in a 5-ply it is 3:2, in a 7-ply 4:3 and so on. Unfortunately, increasing the number of veneers also increases manufacturing costs.

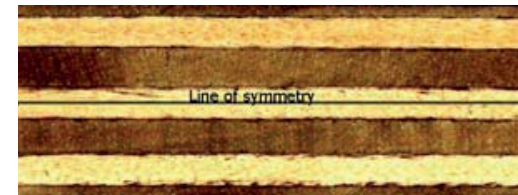


Figure 1.60: The cross-section of a 7-ply plywood with the line of symmetry shown.

1.6.2 The Manufacturing Steps

1.6.2.1 Log preparation

The quality of plywood is largely dependent on the quality of veneer. Cutting smooth-faced veneers requires well maintained equipment and the wood to be as easy to cut as possible. The strength of wood is dependent on its moisture content and so the logs should be kept wet and certainly above their fibre saturation point. Another reason to keep the **logs wet** is to prevent them from cracking as a split in a log will not allow a continuous ribbon of veneer to be produced.

Before veneer can be cut the logs must be prepared so that the wood can be cut efficiently and produce a smooth, even veneer. The peeling step uses a sharp knife that is easily damaged by hard objects like stones, grit, nails, etc. The **bark** often has such hard objects in it as a result of tree felling. Since the bark cannot be cut in to useful veneer it is best to remove the bark before the peeling step so as to protect the knife.

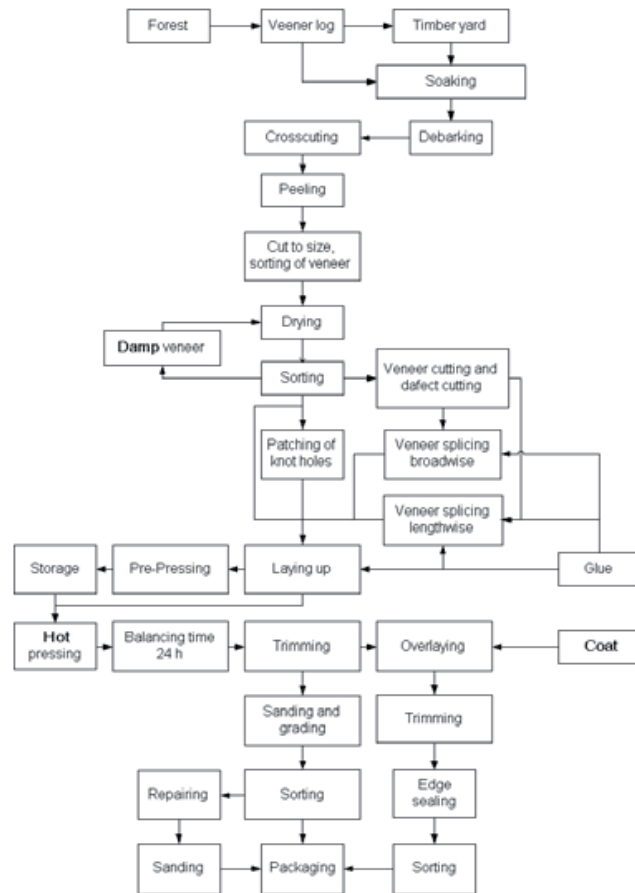


Figure 1.61: An example of a plywood production line flow (Zudrags).

Most plywood factories will cut their logs in to two lengths; a longer one of around 2.7 m and a shorter one of around 1.3 m. The **longer logs** provide veneer for the plywood faces, where the grain direction is normally parallel to the longest edge of the panel, and internal veneers where necessary. Lower quality logs are generally cut to **shorter lengths**, especially if the log is curved, so as to reduce the amount of veneer discarded in forming the perfect cylinder needed to produced full size sheets.

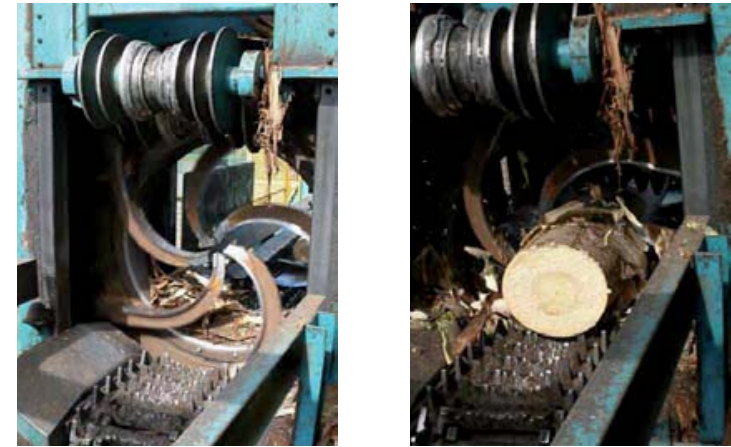


Figure 1.62: Knife ring debarkers are often used to clean logs prior to peeling.

Wood strength can be further reduced by **heating the log** and this can help produce good veneer but the wood should not be heated too much, making it too soft, as fuzzy grain will result in which fibres are pulled out instead of being cut.

The wood is not always heated before peeling, but, it is necessary for high density species, or when cutting thick veneers, and when the logs are frozen. **Warming a log** lowers its strength and reduces wear on knife and especially knots which can cause nicks in knife. As will be shown later, warming the wood also increases its flexibility enabling it to survive some of the strains that are applied to it during peeling.

Logs are **heated** with **steam**, **hot water** or a **combination of the two**. Steaming carries the risk that the log will begin to dry and split, hot water reduces this. The temperature that a log is heated to depends on the species. Generally, the higher a log's specific gravity the higher the temperature. Certainly, low density species, e.g. poplar, do need to be heated. Whereas Okumé, Beech and Oak are heated to 65°C, 80°C and 85°C respectively.

A side effect of heating is **colour change**. Perhaps that most well known is the pink colour that is caused when beech is steamed whereas unsteamed beech has yellow/straw colour. The colour change is associated with chemical changes in the extractives present. Nearly all sapwood of species darken on heating as do many heartwoods and

sometimes the change may not be desirable, especially if it is non-uniform and the veneer is wanted for face veneers.

The heat should be applied carefully. High water temperatures combined with short heating periods cause temperature differentials where the outside and ends of the log are softened but inside is still cold and hard. This situation will cause the veneer to break when the knife hits the cold zone of the log. In extreme cases it can cause chuck spin-out, where the chucks which spin the log at its ends continue to turn when the log stops on the knife edge (see photo).

The **heating time** should be long enough to give an even temperature throughout log, i.e. the temperature differential between the outside and the innermost part of the log should not exceed 6 °C. Clearly the heating time is proportional to the diameter squared of the log, so if the diameter is doubled then heating time is quadrupled.

1.6.3 Peeling

The principal aim of **veneering** is to form continuous sheets. **Veneering knives** tend to have high **rake angles** (typically around 70°) and sharpness angles of around 20°, see Figure 1.63. It goes without saying that the knife should be sharp to ensure that the knife geometry is maintained all the way to the cutting tip.

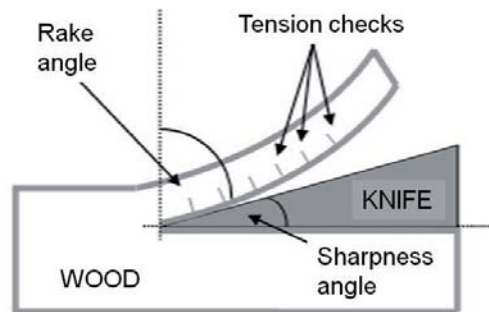


Figure 1.63: A diagram showing the main aspects of veneering.

The veneer is subject to tremendous stresses as it is cut away from the bolt. These stresses cause the veneer to split at regular intervals on the knife side of the veneer. These splits are called **tension** or **lathe checks**. Their presence changes the properties of the surface, particularly in terms of permeability. Consequently, the face without the tension checks is called the “**tight side**” and the face with the checks is the “**loose side**”.

In general, the thicker the veneer, the greater the chance of tension checks being formed. This is because the minimum radius of curvature for a thick veneer is larger than that for a thin veneer or in other words, thin veneer is more pliable than thick veneer. If the checking is very bad, then the veneer can break.

To help minimise tension checks, the wood is kept saturated and often heated to ensure that it is as pliable as possible. A compression force applied just ahead of the knife tip with a nose bar can also reduce tension checking.



Figure 1.64: A magnified view of edge of a plywood showing tension checks (small splits).

The **peeling of veneer** is achieved by rotating a log, or more correctly a **bolt**, against a sharp knife. The bolt is rotated by “**chucks**” inserted in its ends. The chuck teeth, of which there are many designs, provide the torsion resistance needed to rotate the bolt with enough force to cut the veneer from it.



Figure 1.65: Left one of many chuck designs and right the chucks inserted in the log ends.

Profitable plywood manufacture is dependent on maximising the yield of veneer, and preferably in full-size sheet form, from the bolt. Since logs are not perfectly round and often contain defects, simply inserting the chucks that spin the bolt in to the centre might not be the most efficient solution.

Many mills still rely on the trained eye of a skilled operator to **align a log** in the lathe. A **shadow mask** shone on to the log ends is often used to assist decisions (see Figure 1.66). Modern mills tend to use **laser scanning** technology which produces a 3D image of the log that a software optimisation program uses to decide where best to place the chucks.

The size of the chuck also has an effect on yield. On the one hand, a large chuck is needed to avoid chuck spinout and at the start when a log is heavy. On the other, a small chuck diameter allows the log to be peeled to a small spindle. Most modern mills achieve both by using retractable chucks which consist of a central chuck surrounded by an outer ring. Initially, both the ring and chuck are inserted thus providing a large diameter chuck. As the log diameter diminishes the outer ring is retracted thus permitting peeling to a smaller diameter.



Figure 1.66: Two methods of aligning logs: left a shadow mask and right a laser scan of log as it is slowly rotated.

As a bolt's diameter decreases then its resistance to the bending forces exerted by the knife and nose bar falls rapidly because bending resistance is proportional to the diameter cubed. If the log is not supported in some way then the bolt will deflect away from the knife, causing thicker veneer to be cut from the log ends than in the middle. The resultant spindle will be barrel shaped resulting in the loss of veneer.

This situation can be mitigated by supporting the back of the bolt with a **backing roll**. Motorised backing rolls exist that also help to rotate the log permitting even smaller chuck diameters.

Spindless peelers can peel down to 50 mm cores, which can significantly reduce waste when peeling small diameter logs. The technology is not widely used however.

1.6.3.1 Veneer processing

The **veneer ribbon** is often wound on to a bobbin for processing, i.e. clipping to size, dry, etc. at a later date. This method is often known as "**peel and reel**". Although still very common in traditional mills around the world, modern mills tend to favour **processing the veneer ribbon** immediately after it leaves the lathe (Baldwin, 1981).

Mills that tend to peel small diameter logs, e.g. birch in Scandinavia, send the veneer directly to a continuous dryer that is close coupled to the lathe. The advantage of this approach is that the veneer is subject to only one clipping and grading step, whereas, for all other methods there is a clipping and grading step before drying followed by a regrading and possible reclipping step. This approach is not used widely because it is technically difficult to dry a continuous ribbon of veneer. The main difficulty is to ensure that speed of the belt carrying the veneer through the dryer adjusts for the shrinkage that takes place. The shrinkage effectively shortens the length of the veneer and therefore the speed that it should be conveyed through the dryer.

Table 1.5: The three different approaches to veneer processing.

Ribbon Processed Later	Ribbon Processed Immediately	Ribbon Dried Immediately
1. Peel and reel	1. Peel to ribbon	1. Peel to ribbon
2. Clip	2. Clip	2. Dry
3. Sort	3. Sort	3. Clipping
4. Dry	4. Dry	4. Veneer grading
5. Veneer grading	5. Veneer grading	5. Jointing
6. Clipping	6. Clipping	
7. Jointing	7. Jointing	

1.6.3.2 Drying

Whatever the method of veneer, eventually the veneer must be dried. Its moisture content must be reduced to between 6 and 12 %. Considering that the veneer has a moisture content well above FSP, this step requires a lot of energy.

Various drying defects will occur in veneer unless it is dried carefully. Wood is very weak perpendicular to the grain and so veneers often split. It is surprising to learn, perhaps, that splitting is not generally caused by drying but by rough handling as they are splits initiated in green state, perhaps in the tree, or during veneering.

Veneer often has a buckled or wavy appearance. This may be caused by reaction wood or improper cutting. It is undesirable because of the difficulty of laying up a board with veneer that does not lie flat.

Even though veneer is relatively thin collapse and honeycombing defects are still possible if the veneer is dried too fast and at too high a temperature. The rippled surface can sometimes be removed by steam reconditioning. Likewise, case hardening, again caused by drying too fast which generates stresses in the veneer surface.

Drying can also alter the veneer surface so that glue does not wet it so well. For example, extractives can migrate to the surface and alter the contact angle between the glue and veneer surface. Alternatively, the thermal energy can cause cross-linking of cellulose.

1.6.4 Dryers

The two most common dryers are the **roller dryers** and **belt dryers**. The latter allows veneer to be fed in to the dryer with its grain angle perpendicular to the sense of feed. Consequently, they can be used to dry continuous ribbons of veneer. **Roller dryers** are energetically efficient because the rollers are heated and since these carry the veneer through the dryer the direct contact with the dryer permits heating through conduction, which is more efficient than by convection. The rollers are typically 100 mm in diameter.

Very high air speeds of 1000 - 1500 m/min are used in the dryers to minimise the thickness of the boundary layer of air surrounding wood because it is the thickness of this layer that determines drying rate. The air is blown vertically onto the veneer faces facilitating fast drying.

Dryers are split into sections. The temperatures and humidities can be controlled independently and used to help ensure uniform drying. The first stage tends to have the highest temperature of around 150-200 °C. This is acceptable during initial drying because of the high moisture content of the veneer. Subsequent stages are cooler to produce uniform dried veneer.

1.6.5 Veneer Preparation

Veneer grading follows drying. In simple terms, sheets are graded as being best face quality, back face quality and interior quality, i.e. veneers to be used within the panel. Actual grading rules contain many more grades and vary from species to species and type of plywood being made.

Many veneer sheets will require **patching**. This is achieved by stamping out the defect, e.g. a knot, included bark, dark stain, etc, with a standard sized punch. The hole is then filled with a patch with the same shape and size that has been previously punched out of clear veneer. Even more veneer is **jointed together** to form full size sheets. There are many different joint methods: adhesive tape, hot-melt impregnated string, stitching, edge gluing, scarf jointing to name a few. Modern mills use compositors that combine veneer pieces of varying widths in to one long piece that is then cut in to full size sheets.

Many people are surprised to learn that board strength is not significantly affected by the use of veneer sheets that have been joined together. This is because the strength of wood perpendicular to the grain is low and so the presence of a jointed piece is little different to a whole piece.

1.6.6 Board Layup

Despite huge advances in computer technology and automation, plywood panels are still essentially compiled by hand. This is because of the large variation seen in the form and colour of veneers; they are not flat, not particularly flexible and are often split. These factors make it difficult for an automated system to cope with veneer. Humans can recognise veneer defects and can modify the layup accordingly.

The most common method of **applying adhesive** is with a **roller coater** which applies a known amount of adhesive to both faces. Adhesive is applied to both faces of alternate veneers and not every veneer. For example, in a 3-ply panel adhesive is only applied to the middle veneer and for a 5-ply only to veneers 2 and 4. Other adhesive application systems are used including: **curtain coating**, **spraying** and **extrusion**. Discussion of these is beyond the scope of this short review and readers are recommended to read Baldwin (1981).

The **grammage of adhesive** applied varies with grade of panel, type of adhesive, wood species and, in particular, the surface smoothness of the veneer. Less adhesive is necessary for smooth faced veneers. A typical grammage will range from 140 to 240 g/m² per face (or glueline). It is sometimes quoted as a double face measure (and so double the figures given in the previous sentence) because the roller coaters apply adhesive to both faces at once.

When **laying-up plywood**, the veneers placed on the outer faces should be orientated so that their tight faces are exposed. If this is not done, then there is a risk of excessive checking on the surface with time as the veneer moves with changing atmospheric conditions. Some mills have

semi-automatic lay-up lines where surface veneers are handled by machine.

1.6.7 Pressing

Panels are generally **cold prepressed** after lay-up. The aim is to flatten the panels and allow the adhesive to develop tack. Both factors make it easier to feed the panels in to the hot-press. The prepress operates cold and the panels are pressed as a bundle in a single-daylight press.

Prepressing is synchronised with the hot press. Modern mills with large multi-daylight presses often use an automatic loading and unloading cages to minimise dead time between cycles and improve overall production capacity. The **cages** also help to ensure that all panels are subjected to the same temperature histories. The **presses** in such mills also tend to have simultaneous daylight closing mechanisms to ensure that each panel is pressed to the same pressure and for the same time. This results in more consistent panels.

Panels are fed into presses by hand in older mills with smaller presses and these presses tend to close by pressing one day-light against another. So for an upward stroke press, the bottom day-light will close first followed by the second and so on. On opening it is the top daylight that opens first and so it is clear that the panel in the top daylight is pressed for a shorter time than the bottom panel. **Plywood press cycles** are much longer than those for particle- and fibreboards and so the difference in the pressing cycle of the plywood in the top daylight compared to the one in the bottom is relatively small in percentage terms, but, it is different and does not help panel consistency.

The **press temperature** for panels made using amide-based glues, e.g. UF and MF, is between 100 to 120 °C. This is much lower than the temperatures used for particle- and fibreboards using similar adhesives. The lower temperatures are associated with lower internal steam pressures and so less risk of blisters, lower energy costs but also longer press times. The panels are normally cooled briefly before being stacked ready for further processing.

Many types of plywood are made with phenolic-based adhesives, which require more energy to initiate cure. This is achieved using higher press temperatures, typically 160 °C and “hot stacking” immediately after pressing so that the panels remain hot for many hours.

The **length of a cycle** can be calculated using a simple “**rule of thumb**” which is 1 minute plus 30 seconds for each millimetre of panel thickness.

For example, 10 mm thick panel would have a press cycle of around 6 minutes. As mentioned above, this is much longer than for particle and fibreboards, which are pressed between 4 and 10 seconds per millimetre of panel thickness. So a 10 mm thick particleboard may be pressed every 50 s.

The **specific pressure** applied to the panels is around 1 MPa; a little lower for low density plywoods, e.g. poplar and higher for high density plywoods e.g. beech. Once again, this is quite different of particle and fibreboards, which are pressed at around 3 MPa. Pressure is applied in any gluing situation to ensure adequate contact between the bonding surfaces. Since plywood is made of “flat” sheets a low pressure is sufficient to achieve the contact required; particle and fibreboards on the other hand are made of elements with varying sizes and shapes that are randomly orientated so much higher pressure is required to force the elements close enough for the adhesive to bond them together.

The press pressure peaks near the start of the cycle when the wood is cool. The pressure is reduced during the cycle to minimise induced compression and to maintain panel thickness.

1.6.8 Finishing

Boards are **trimmed** so that they have straight edges and 90° corners. Often the panels are **sanded** to ensure panel calibration.

Repairs may be necessary to panel faces and edges. Face repair is most often needed when using a species with dark knots. These can be routed out and the hole filled with a coloured hot-melt plastic. The plastic cools and solidifies very quickly and once sanded it is difficult to see the repair.

Plywood manufacturers have developed a wide range of finishes for their products in order to increase their value and to differentiate themselves from other producers. The **finishes** include: non-slip surfaces, phenolic impregnated paper finishes for concrete form work and various colours.

1.7 A POTTED HISTORY OF WOOD-BASED COMPOSITES

Veneers were initially produced manually, by sawing, and later, mechanized, by means of large diameter rotating saws and special veneer frame saws. It was only in 1818, in France, that the first rotary cutter (lathe) was patented for the production of veneers. The first slicer for decorative veneers was patented somewhat later in 1870. These two inventions have been modernized and upgraded ever since, but they are

still in use today. In 1934 the waterproof synthetic resins (PF glues) were produced, which made possible the production of plywood for exterior applications.

Particleboards originated in Germany. The first mention of the manufacture of such boards dates back to 1887, when Hubbard made a so-called “artificial wood” of wood flour and albumin-based glues, consolidated under high temperature and pressure. In 1889 Kramer obtained a German patent for his method of gluing of wood shavings onto a flax fabric. Then he layered the fabrics in a similar way to plywood (alternatively cross-oriented). In 1905 Watson (USA) developed a method to produce boards of thin square particles (flakes). Today, his patent is still at the centre of flakeboard and OSB manufacturing.

Beckmann (Germany) suggested in 1918 a new technique for the production of a layered board with a core of compressed particles or wood flour and veneer faces; it was the forerunner of the products known at present as Com-Ply, a **veneered particleboard** or plywood with a particle core. Freudenberg (Germany) mentions in 1926 the use of planer shavings glued with resins of the epoch, to produce boards. In 1934 Nevin (USA) recommended the mixing of coarse sawdust and shavings with resins and to harden them by hot-pressing for board manufacturing. Antoni (France) obtained, in the same year, boards from a combination of wood fibres and particles glued with urea- or phenol-formaldehyde resins.

1935 was a very innovative year as researchers in France, Germany, Japan and USA suggested a range of new WBP products. Samsonov (France) suggested the use of **cross-alternating veneer** strips for a particleboard, similar to the present products OSB. Satow (Japan) obtained an American patent for the manufacture of boards made of 75 mm long chips, randomly arranged in order to reduce board warpage. Roher (Germany) outlined the possibility of gluing wood particles onto the surfaces of a plywood core within a single pressing operation.

In 1936 Loetscher (USA) presented a patent concerning the automated manufacturing of particleboards. In 1937 Chappuis (Switzerland) described the manufacture of particleboards from dry particles, by applying powder resins (Bakelite).

Another Swiss, Phol, presented in 1936 his patent for the alternative use of **long veneer strips** (50-200 mm), now used for making load-bearing structures from veneer based composites, i.e. LVL.

During World War II, when the **production of synthetic resins** was improved, the first attempts for the industrial manufacturing of

particleboards were made. Between 1938 and 1940, the German company Torfit obtained two patents for the production of particleboards; liquid resins were used for gluing particles and formed in to a particle mat which was subsequently hot-pressed.

The same company built the first plant for the industrial manufacturing of particleboards in 1941 in Bremen (Germany). Fahrni obtained in 1943 a French patent for the production of particleboards. He later developed equipment (Novopan) for particleboard plants. Kreibaum (Germany) produced between 1947 and 1949 the first extruded, as opposed to flat-pressed, particleboards.

Although the idea of producing **wood fibres** was one and a half century old, it was only in 1844 in Germany that a practical method for producing wood fibres by mechanical processing in the so-called “mills” could be developed. In England, in 1851, a chemical system was invented for wood refining, in order to obtain fibres for paper production. In its competition with other raw materials used to produce paper, wood became the most economically profitable material, due to its low cost and availability. Fibreboard structure is closer to that of paper products than of other wood-based products.

The first **insulation board** plant built in 1898 in England answered the efforts to capitalize the large quantities of oversize fibre bundles removed from pulp.

In 1914 Carl Muench made a **softboard** from wood fibres, which had insulating properties and this explains why this type of product is often called insulation board. “Insulite” is the trade name of this fibreboard, produced in a large plant on the same location since 1916 (USA). A second plant for insulation fibreboards was built in 1931. The manufacturing process is a modified paper making method. A large tank stored the mixture of fibres and water. This mixture was then “dehydrated” on a sloping and continuously moving screen/sieve, thus forming a fibre mat. By drying the wood fibre mat in an oven, porous fibreboards with densities between 160 and 400 kg/m³ could be made. This **wet fibre-board process** has been improved over the years and is an established manufacturing method for fibreboards. It has relatively low production costs because of the relatively small amounts of binders present in the product. Muench investigated alternative sources of fibres and also used agriculture by-products like corn, wheat straw, bagasse, etc. The first plant for insulation fibreboards made with non-wood ligno-cellulose raw materials was built in 1920.

An alternative method for pulping wood using the **steam explosion technique** invented by William Mason was introduced in 1924. Wood chips are introduced in to a vessel called a "gun", which was then pressurised with steam to pressures as high as 8 MPa causing a temperature of around 290 °C. The pressure is suddenly released causing the softened chips to pass rapidly through a grid which breaks up the chips in to coarse fibres. In 1926 in the USA, the Mason Fibre Company started manufacturing the first hardboard using the Masonite process.

Asplund (Sweden) proposed the **thermo-mechanical pulping process** in 1934. This technology has been subsequently widely adopted for making fibres both in the paper and building board industries. The principal steps of this method are described in section 5.2.

The excellent properties of the fibreboards are the result of the bonds created due to lignin reactivation under high pressure, temperature and moisture conditions. In order to improve the fibreboard properties when used in contact with water, additional water-repellent substances (paraffin/wax) or synthetic binders (phenol-formaldehyde resins < 3%) can be added. This technology is widely known as the **wet process** and the fibreboards thus manufactured are internationally known as **hardboard** when panel densities exceed 800 kg/m³ or **softboards** if the density is less than 400 kg/m³. The particularity of this process lies in that water is used to convey fibres and to form the fibre mat. Another specific aspect of the wet process is that a screen is used in the press, at the bottom of the fibre mat, so that water and steam can readily escape during hot pressing. As a result, the screen pattern is embossed on the backside of the finished hardboard. The production of fibreboards using the wet process has decreased drastically during recent decades. The main reason for this is that the process is inefficient for making thick panels (essentially they are limited to panels of 12 mm or less). In addition, the strict environmental requirements imposed on water pollution in highly industrialized countries have significantly increased manufacturing costs. This technology has patent environmental shortcomings regarding the recycling and treatment of waste waters, which contain large amounts of fibres and organic substances (cellulose, lignin, wax, etc.). Nevertheless, softboards still hold an important position in the market of insulation boards (i.e. made of polyurethane foams or of mineral-bonded fibres).

Research dating back to 1945 aimed at replacing the wet forming system with a **dry forming process** using an airflow. Much of the research was conducted in the USA and it ultimately resulted in the development of **Medium-Density Fibreboard** (MDF).

The first two dry-process hardboard plants were built in 1952 in US as an adaptation to industrial production of the semi-dry process. Dry-process hardboards have lower mechanical properties than those made using the wet process, due to the high water absorption capacity of the remaining "unbound" lignin and hemicellulose, but have the advantages of smooth faces on both sides, lower densities, thickness variability and a high workability.

The first MDF plant was built in 1965 in Deposit, USA. The first MDF factory in Europe is thought to be that built in the former German Democratic Republic at Ribnitz-Damgarten in 1973. Other factories were built in Eastern Europe: 1975 Busovaca (today Bosnia-Herzegovina) and 1978 Illirska Bistrica (today Slovenia).

During the last decade, a distinct category of products have appeared, namely the **Low-Density Fibreboards** (400–600 kg/m³).

The use of **multi-opening** and today, **continuous** presses, was the next stage in developing the manufacturing technologies for particleboards, MDF and OSB. These three categories of WBP now dominate the sector in terms of production volume (world 70%, Europe 90%). Equipment production and technology improvement, as well as WBP development, has remained until the late 1990s in German hands, which has fitted out almost the entire WBP factories all over the world. The first continuous press made outside of Germany was produced in China and installed in the Czech Republic.

The field of wood-based composites has dramatic changes ever since the 1950s in terms of production capacities and technological developments. The prospect of producing particles and fibres with various dimensions and shapes, the use of new types of synthetic resins, of modern technologies and specially designed, reliable, partially or completely automated equipment have given a boost to WBP development. It was the beginning of a new age, not only in the production of WBP, but of other wood-based products as well.

1.8 REFERENCES

- Anonymus. (1995). Magic number in sight for world production. Wood Based Panels International 17(October):10-11.
- Anonymus (1997). Wood Based Panels – Transition from British Standards to European Standards. Wood Panel Industries Federation, Edition 3, July 1997.
- Axer, J. (1975). New Concepts for the Production of Particleboard. In Proceedings of the 9th International Particleboard Symposium, W.S.U.
- Balwin, R.F. (1981). Plywood Manufacturing Practices. Miller Freeman Publications Inc., San Francisco.
- Barbu, M.C. (2009): Fibre generation and processing. Presentation during the 4th International Wood Academy, Walailak University, Nakhon Si Thammarat, 05-10.10.09
- Barbu, M.C. (2009): Panel finishing. Presentation during the 4th International Wood Academy, Walailak University, Nakhon Si Thammarat, 05-10.10.09
- Behrens, J. (2009): Pressing of thin panels. Presentation during the 4th International Wood Academy, Walailak University, Nakhon Si Thammarat, 05-10.10.09
- Bolton, A.J., Humphrey, P.E. & Kavvouras, P.K. (1989). The Hot Pressing of Dry-formed Wood-based Composites. Part III. Predicted Vapour Pressure and Temperature Variation with Time, Compared with Experimental Data for Laboratory Boards. *Holzforschung* 43.
- Bolton, A. J., P. E. Humphrey, and P. K. Kavvouras (1989): The hot pressing of dry-formed wood-based composites. Part VI: The importance of stresses in the pressed mattress and their relevance to the minimisation of pressing time, and the variability of board properties. *Holzforschung* 43(6): 406-410.
- Deppe, H-J, Ernst, K. (2000): Taschenbuch der Spanplattentechnik, 4. Auflage, DRW- Verlag, Leinfelden- Echterdingen
- Dinwoodie, J.M. (1981). Timber Its Nature and Behaviour. Van Nostrand Reinhold Company, London.
- Dunky, M. Pizzi, A. and Van Lemmput, M. (2002). Wood adhesion and glued products. Working group 1: wood adhesives. State-of-the-art report Volume 1, COST Action E31.

- Elias, R. and Irle, M.A. (1996). The Acidity of Stored Sitka Spruce Chips. *Holz als Roh-und Werkstoff* 54(1):65-68.
- Fischer, K. (1972). Modern Flaking and Particle Reductionizing. In Proceedings of the 6th International Particleboard Symposium, W.S.U.
- Fruehwald, A., Thoemen, H. (2008): The rise of wood based panels. Presentation during the 3rd International Wood Academy, University of Hamburg, 25.02-07.03.08
- Galbraith, C.J., Cohen, S.C., Ball, G.W. (1983). Self-Releasing Emulsifiable MDI Isocyanate: An Easy Approach for All-Isocyanate Bonded Boards. In Proceedings of the 17th International Particleboard Symposium, W.S.U.
- Geimer, R.L. (1982). Steam Injection Pressing. In Proceedings of the 16th International Particleboard Symposium, W.S.U.
- Gretten, K. (2008): Sensor technology for wood based panels. Presentation during the 2nd International Wood Academy, University of Hamburg, 18 -29.09.06
- Hasener, J.; Barbu, M.C. (2009): Overview on NDT technologies for on-line control in the wood-based panel industry and an outlook for future trends. Proceeding of COST E49 Workshop on “Processes and Performance of Wood-Based Panels”, 28-29 April, Istanbul, pag. 2-14
- Humphrey, P.E. & Bolton, A.J. (1989). The Hot Pressing of Dry-formed Wood-based Composites. Part II. A Simulation Model for Heat and Moisture Transfer, and Typical Results. *Holzforschung* 43(3):199-206
- Johansson, J. Pizzi, A. and Van Leemput, M. (Editors) (2002). Wood adhesion and glued products. Working group 2: glued wood products. State-of-the-art report Volume 2, COST Action E31 (ISBN 92-894-4892-X).
- Jain, N.C., Gupta, R.C. & Jain, D.K. (1967). Particleboard from Groundnut Shells. Proceedings 11th Silviculture Conference, May, 1967, India.
- Maloney, T.M. (1993). Modern Particleboard & Dry-Process Fibreboard Manufacturing. Miller Freeman Publications, San Francisco. (TS 875.M3)
- Meyer, B. (1981). Urea Formaldehyde Resins. Addison-Wesley Publishing Co., Inc. Massachusetts.
- Meinert, K. (2008): OSB production. Presentation during the 3rd International Wood Academy, University of Hamburg, 25.02-07.03.08

- Mitlin, L. (1968). Particleboard Manufacture and Application. Novello & Co. Ltd., Kent.
- Mosesson, J.G. (1980). The Processing and Use of Waste Straw as a Constructional Material. Conservation and Recycling, Vol. 3, pp. 389-412.
- Moslemi, A.A. (1974). Particleboard. Vol. 1 - Materials. Particleboard. Vol. 2 – Technology. Southern Illinois University Press. (TS 875.M6)
- Natus, G. (2008): Comparison of pressing systems. Presentation during the 3rd International Wood Academy, University of Hamburg, 25.02-07.03.08
- Pizzi, A. (1983). Wood Adhesives Chemistry and Technology. Marcel Dekker, Inc., New York.
- Ressel, J. (2008): Raw materials. Presentation during the 3rd International Wood Academy, University of Hamburg, 25.02-07.03.08
- Ressel, J. (2008): Particle generation and screening. Presentation during the 3rd International Wood Academy, University of Hamburg, 25.02-07.03.08
- Ressel, J. (2008): Particle drying. Presentation during the 3rd International Wood Academy, University of Hamburg, 25.02-07.03.08
- Ressel, J. (2008): Adhesive application. Presentation during the 3rd International Wood Academy, University of Hamburg, 25.02-07.03.08
- Ressel, J. (2008): Mat formation. Presentation during the 3rd International Wood Academy, University of Hamburg, 25.02-07.03.08
- Rexen, F. (1975). Straw as a Raw Material for Particleboard and Paper Production. Report on the First World Straw Conference. ed T. R. Miles, Eugene, Oregon.
- Roll, H., Barbu, M., Beck, P., Hoepner, D., Kaiser, U. & Lerach, K. (2001). Continuous Hot Press with Cooling Section for MDF. In Proceedings of the 5th European Panel Products Symposium, October, 2001.
- Rowell, R.M. & Norimoto, M. (1988). Dimensional Stability of Bamboo Particleboards made from Acetylated Particles. Mokuzaï Gakkaishi 34(7):627-629.

- Schniewind, A.P., Cahn, R.W., Bever, M.B. (1989). Wood and wood-based materials - Concise Encyclopedia. Pergamon Press Plc, Headington Hill Hall, Oxford OX3 0BW, England.
- Shumate, R.D., Schenkman, A.H. & Sloop, J.E. (1976). Experiences with Air Suspension Classifiers in Particleboard Manufacture. Proceedings of the 10th International Particleboard Symposium, W.S.U.
- Steffen, A. (2008): Particleboard mat forming. Presentation during the 3rd International Wood Academy, University of Hamburg, 25.02-07.03.08
- Steinwender, M.; Barbu, M.C. (2009): Environment Impact of the Wood based Panels Industry. Proceeding of ICWSE, 4-5 June, Brasov, pag. 767-775
- Stipek, J.W. (Translated by R.J. Vance) (1982). The Present and Future Technology in Wood Particle Drying. Proceedings of the 16th International Particleboard Symposium, W.S.U.
- Subramanian, R.V., Somasekharan, K.N., Johns, W.E. (1982). Acidity of Wood. Holzforschung 37(3):117-120
- Suchsland, O. & Woodson, G.E. (1986). Fibreboard Manufacturing Practices in the United States. USDA, Forest Service, Agriculture Handbook No. 640.
- Suchsland, O. & Woodson, G.E. (1986). Fiberboard Manufacturing Practices in the United States. USDA, Forest Service Agriculture Handbook No. 640.
- Thoemen, H. (2008): Pressing of panels. Presentation during the 3rd International Wood Academy, University of Hamburg, 25.02-07.03.08
- Thoemen, H. & Humphrey, P.E. (1999). The Continuous Pressing Process for Wood-Based Panels: An Analytical Simulation Model. In Proceedings of the Third European Panel Products Symposium, The BioComposites Centre, University of Wales, Bangor.
- Thoemen, H., Meyer, N., Barbu, M. (2006): Pressing from a fundamental point of view: actions to increase press performance. Proceeding of 4th "Press Users Club" Seminar, Shanghai, China, 23-26 October.
- Vasisth, R.C. & Chandramouli, P. (1975). New Panel Boards from Rice Husks. FAO Background Paper, FO/WCWBP/75.
- Wadsworth, J. (2001). Focus on Particleboard. Part 1: Europe and North America Revealed. Wood Based Panels International 21(5):9-25.

Walker, J.C.F. (1993). Primary wood processing: Principles and Practice. Chapman & Hall. London.

Walker, J.C.F. (2006). Primary wood processing: Principles and Practice 2nd Edition. Springer, Amsterdam.

Williams, W. (1995). The panel pioneers: an historical perspective. Wood Based Panels International 17(September):6.

Youngquist, J.A. (1999). Wood-based Composites and Panel Products. In Wood handbook - Wood as an engineering material. Gen. Tech. Rep. FPL-GTR-113. Madison, WI: U.S. Department of Agriculture, Forest Service, Forest Products Laboratory. 463 p.

Chapter 2

Water Absorption of Wood and Wood-Based Panels – Significant Influencing Factors

Peter Niemz

CHAPTER SUMMARY

Wood and wood-based materials absorb water from the air by sorption and from a fluid by capillary forces. The sorption behaviour of solid wood depends, amongst other factors, on the amount of extractives. The velocity of water absorption strongly depends on the cutting direction and on the anatomical structure of wood. It is clearly higher in the fibre direction than perpendicular to it. The formation of tyloses by hardwood species and the closed pits of softwoods considerably reduce the capillary water absorption. Wood based materials tend to absorb more water through their edges than through their faces.

The equilibrium moisture content (EMC) for wood based materials such as fibre boards, MDF or OSB is lower than for solid wood. This seems to be caused by the processing method. For wood based materials glued with phenol resin, however, the strong hygroscopic behaviour of alkali leads to higher EMCs than when other adhesives are used. The EMC has a strong influence on all physical and mechanical properties of wooden materials (MOE, MOR, IB, hardness, thermal conductivity etc.).

The swelling of particleboard and OSB in the direction of the plane is higher than that of solid wood in the fibre direction. The thickness swelling of particle board, OSB and MDF is much higher than that of solid wood perpendicular to the grain. This correlates with the densification of the particles.

2.1 INTRODUCTION

Wood is a macromolecular material. It has, on average, the following composition: 50 % carbon, 43 % oxygen, 6 % hydrogen, 1 % nitrogen. The **main components of wood** are:

- Cellulose (particularly in fibrils): 40-60 %
- Hemicelluloses: 6-27 %

- Lignin (matrix substance): 18-41 % (41 % for compression wood; 25-32 % for softwoods; 18-25 % for hardwoods)
- Secondary wood constituents (for example extractives): 0.3-20 %

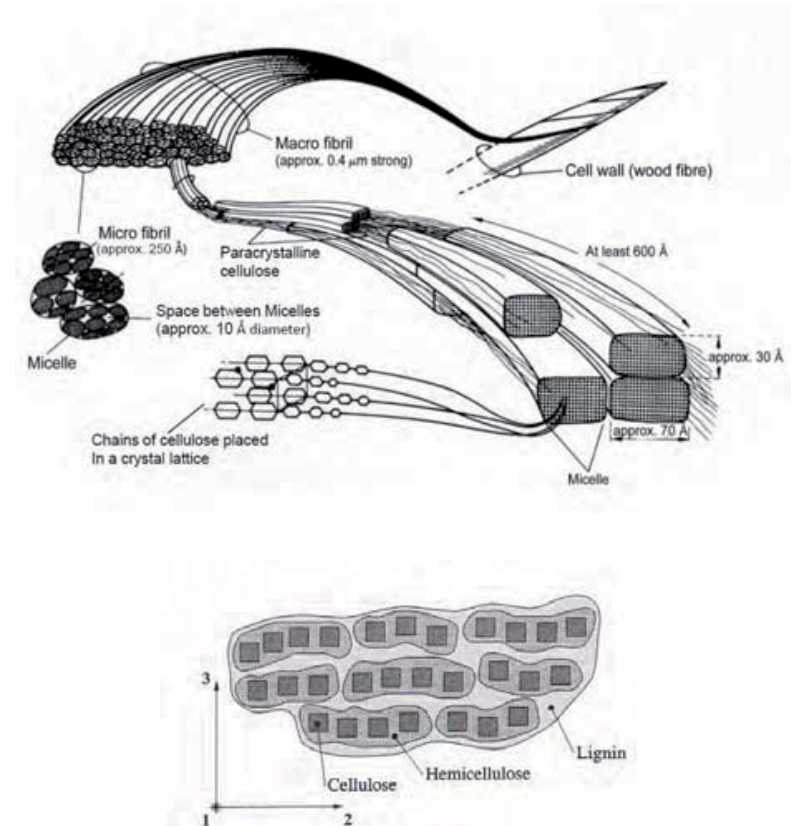


Figure 2.1: Wood structure (Schmitt, University of Hamburg).

The **cellulose** in wood acts as a reinforcement and lignin behaves as a matrix, similar to fibre-reinforced synthetics. Molecules of cellulose form micelles and these in turn form fibrils that are crystalline and amorphous (Figure 2.1). The middle lamellae of the cell wall consist mainly of **lignin**, the S_2 of cellulose. The alignment of the fibrils in the S_2 determines the mechanical properties and the swelling and shrinkage of wood in the fibre direction.

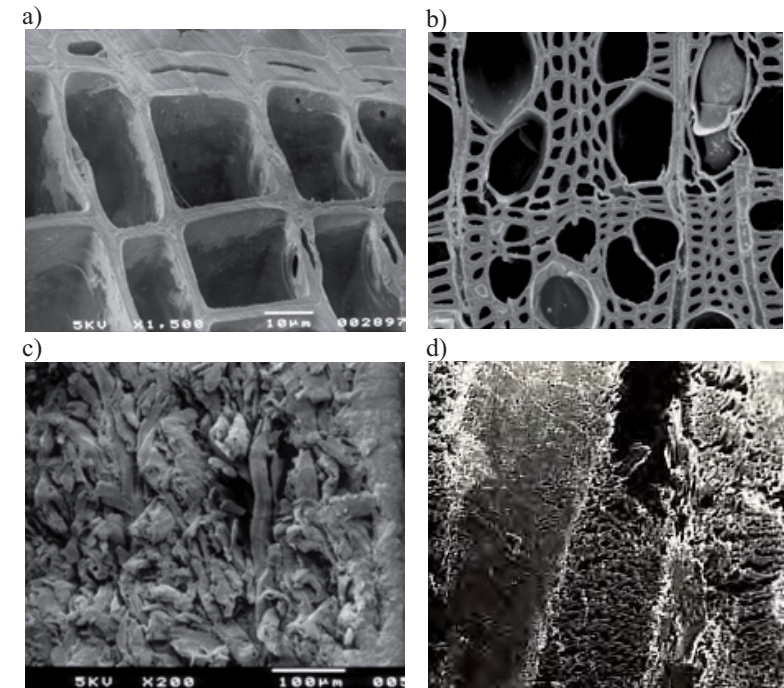


Figure 2.2: SEM images: a) Softwood (*Picea abies*), image: ETH Zurich, Wood Physics, b) Hardwood (*Nothofagus alpina*), image: ETH Zurich, Wood Physics, c) MDF, image: TU Dresden; Bäucker d) Particle board, image: ETH Zurich, Wood Physics.

Water can adhere in macroscopic as well as in microscopic (see Figure 2.2 a) and b) and sub-microscopic cavities of the cell wall. In a wooden material, water can also be in the cavities between the particles (see Figure 2.2c and d). **Extractives** are deposited in the cell wall and in the lumens (as in the case of oak where the heart wood is clearly darker than the sapwood). As a protective mechanism, hardwoods form tyloses whereas softwoods close their pits. Thereby, living trees are protected against fungi, preventing the transfer of water. The closing of pits, the formation of tyloses and the extractives content vary greatly between various kinds of trees, especially amongst many tropical trees, but also amongst temperate trees such as acacia (*Acacia ssp.*) or oak (*Quercus Robur L.*). These are distinct tylosis formers and produce a high amount of extractives. Spruce species, which are softwoods, are characterised by a high amount of closed pits.

Wood-based panels (plywood, particle boards, fibre boards, etc.) are composed of chopped or cut elements of wood (planks, veneer, chips, fibres) that are glued together. Synthetic bonding agents are frequently used (urea resin, phenolic resin, isocyanates). The **amount of adhesive** present varies with the panel type but does not often exceed 10 %, for floors up to 16 %. Wood based materials in static use often have a clearly higher density than solid wood (40-80 % higher). The kind of adhesive and the structure of the material influence the properties of the wood based material as well as the technology of the production (defibration, drying, gluing).

2.2 SORPTION BEHAVIOUR AND CAPILLARY WATER ABSORPTION

2.2.1 Ultimate State of Wood-Water

Wood is a capillary porous system. Water can be adsorbed in both, macro and micro pores (pores in the cell wall). Pores that are conditional on the anatomical structure have a diameter of 10-1 to 10-5 cm, whereas those conditional on the molecular structure are 10-5 to 10-7 cm in diameter.

The **wood-water system** can be divided into **three different states**:

- Absolutely dry = **oven-dry** (water is inexistent, wood moisture = 0 %).
- **Fibre saturation** (the complete micro pore system, i.e. intermicellar and interfibrillar cavities of the cell wall, is filled with water; the wood moisture content is approximately 28 % which can vary between wood species).
- **Water saturation** (both the micro and macro system are filled with water; wood moisture depends on the wood density and lies between 770 % (for Balsa, *Ochroma lagopus* SW) and 31 % (for *Lignum vitae*, *Guaiacum officinale* L. Data according to Trendelenburg and Mayer-Wegelin 1955).

Water adsorbed from absolute dry to the fibre saturation point (FSP) is called bound water because it is **hydrogen-bonded** to the wood cell wall polymers; water absorbed above the FSP is called **free water**.

The equilibrium moisture content (EMC) is calculated as follows:

$$EMC (\%) = \frac{\text{original weight} - \text{oven dry weight}}{\text{oven dry weight}} \quad (1)$$

For oven drying we used a temperature of 103±2°C.

2.2.2 Sorption Behaviour

2.2.2.1 Solid wood

Solid wood (the basic raw material for particleboards, OSB and MDF) has a large specific inner surface. For spruce it is about 220 m²/g (calculated according to the theory of Hailwood-Horrobin). Wood behaves hygroscopically; it takes up water from the air and gives it off by desorption. In Figure 2.3 (for solid wood) and 2.4 (for wooden materials) the different sorption stages can be seen. This works up to a relative air humidity of circa 100 % where the fibre saturation point is reached. The EMC of wood is correlated to a certain temperature and relative air humidity and depends on the wood species and the type of wooden material. In general, adsorption (increasing humidity) and desorption (decreasing humidity) can be distinguished. A **hysteresis** effect occurs between both; for this reason, the wood moisture content will be 1-2 % higher for desorption than for adsorption. There are three stages of water absorption:

- **Chemisorption** (build up of a monomolecular layer of water)
- **Physisorption** (build up of a polymolecular layer of water)
- **Capillary condensation** (condensation of water on the capillary caused by a saturation pressure that is smaller for capillaries than for plain surfaces (for example for a capillary radius of $r = 1,06 \cdot 10^{-4}$ cm, the relative vapour pressure is 99,9 %; for $r = 0,86 \cdot 10^{-7}$ cm, the relative vapour pressure is 30 %)

Below the FSP, the equalisation of moisture takes long periods of time as the moisture transport happens by diffusion (see moisture distribution in a board as a function of time; Figure 2.8).

Using a thermal or hygrothermal pre-treatment (such as high temperature drying) can reduce the EMC (Figure 2.3). **Treatment with heat** and pressure leads to a reduced amount of hemicelluloses and therefore to lower wood moisture percentage and a higher dimension stability.

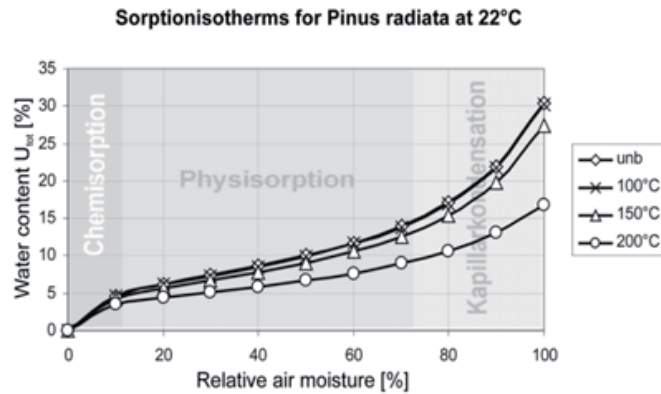


Figure 2.3: Sorption of *Pinus radiata* (influence of thermal treatment (unb = untreated)).

The EMC and swelling of wood are reduced to 50 % by using a thermal treatment at temperatures between 180 and 240 °C (in the case of solid wood). Densified wood has a slightly lower EMC in the range of capillary condensation and FSP than un-densified wood, while in the ranges of chemisorption and physisorption the EMC is slightly higher (Popper et al. 2002).

Simultaneous thermal or hygrothermal treatment and **densification** leads to a significant reduction of EMC compared to normal wood. Densification nevertheless is reversible by exposure to water (memory effect).

The relative humidity of air in buildings can be considerably influenced by the hygroscopic behaviour of wooden objects within them. Living spaces with a high amount of wood have smaller variations in relative air humidity than those with non-hygroscopic materials present. Wood adds a measurable contribution towards greater comfort in living spaces.

2.2.2.2 Wood-based panels

Wood-based panels (WBPs) are strongly influenced by adhesives, density and the production technology (drying, defibration, pressing at high temperatures). The EMCs of WBPs are lower than those of solid wood of the same species under the same conditions. There is a strong influence of particle drying (thermal modification), defibration (producing fibres) and hotpressing (thermal or hydrothermal treatment, densification). Partially, the moisture-related behaviour of WBPs can also

be explained with the presence of **adhesives**, which have different sorption behaviours compared to wood. For example, alkali-containing phenolic resin is highly hygroscopic (Figure 2.4). The wooden materials themselves also differ between each other. Furthermore, there is a strong **influence of the density** (Figure 2.5b).

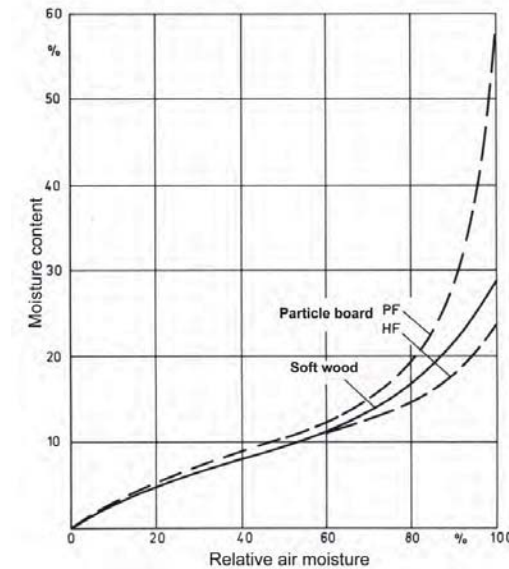


Figure 2.4: Comparison of the sorption behaviour of softwood, particle boards with phenolic resin (PF) and particle boards with urea resin (HF) (Seifert, cited in Kehr 1974).

The EMC of MDF is slightly lower than that of particleboards (Figure 2.5a). This is caused by the **hygrothermal processes** used to produce the fibres. The EMC of MDF is correlated to the vapour pressure used during the defibration process, the temperature and the defibration duration (Krug and Kehr 2001). With high pressures and long defibration durations, the thickness swelling of MDF decreases.

The sorption behaviour of WBP can be described for instance by the **Hailwood-Horrobin (HH)** or the **Brunauer-Emmet-Teller (BET)** method (see DIN ISO 9277:2003-05).

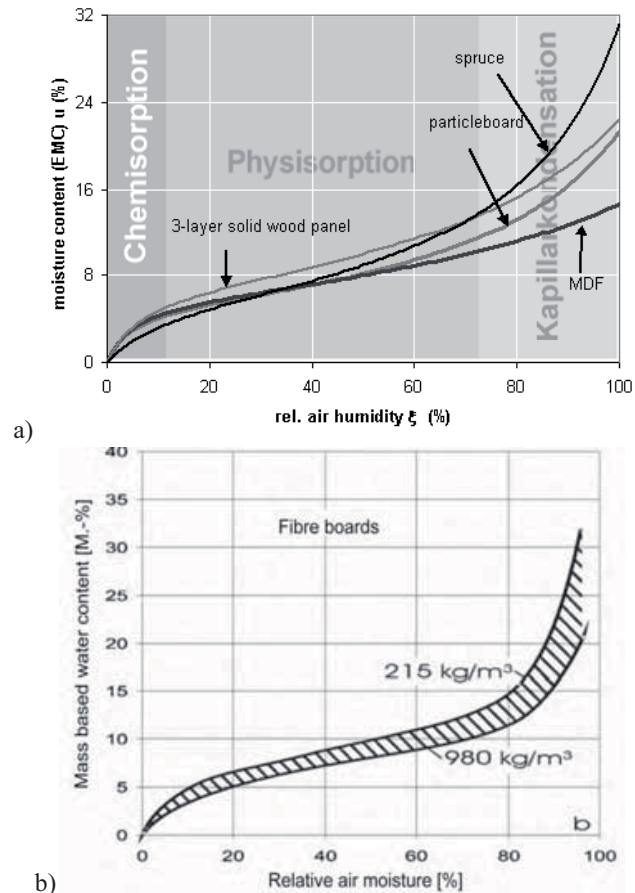


Figure 2.5: Sorption of different wood based panels: a) Sorption of different wood based panels (ETH Zurich), b) Influence of the density on the moisture content of fibreboards (Kiesl and Möller 1989).

2.2.3 Water Absorption by Capillary Forces

Mainly beyond the FSP, wood absorbs water (liquid water) by capillary forces. Moisture transport happens according to the laws of capillary physics (from wide to small capillaries). Closed pits (softwoods) or tyloses (hardwoods) strongly reduce the water uptake which also leads to

a lower uptake of immersion liquids. The velocity of water absorption is significantly influenced by:

- the density of the material (the higher the density, the lower the absorption velocity)
- the anatomical direction of wood (clearly higher velocity in the fibre direction than perpendicular to it)
- the wood species
- the content of paraffin
- the surface coating
- the sample size (dimensions)

Table 2.1 shows the coefficients of water absorption (**absorption of liquid water** by immersion (DIN EN ISO 15148) in $\text{kg}/(\text{m}^2\sqrt{\text{s}})$ for spruce and beech.

Table 2.1: Coefficients of absorption of liquid water by immersion (DIN EN ISO 15148).

	Spruce $\text{kg}/(\text{m}^2\sqrt{\text{s}})$	Beech $\text{kg}/(\text{m}^2\sqrt{\text{s}})$
Longitudinal	0.017	0.044
Radial	0.003	0.005
Tangential	0.004	0.004

For particle boards (density $670 \text{ kg}/\text{m}^3$) the coefficient in direction of the plain is 0.025 and perpendicular to the plain 0.0014.

The water absorption per unit of time is clearly higher in the direction of the fibre than in the radial or tangential directions, in direction of the plane higher than perpendicular to it. This relationship is also valid for water absorption from air humidity. This is the reason why large cross-sections (as used for building materials, e.g. Glulam) require long storage periods to reach the EMC over the complete cross section.

2.2.4 Swelling and Shrinkage

2.2.4.1 Solid wood

Changes of dimension occur with changes of moisture within the hygroscopic area (up to the FSP, Figure 2.6, left side). **Swelling** occurs

when water is taken up; **shrinkage** occurs when water is released. Swelling and shrinkage are different for the three principle directions of wood. It is small in longitudinal direction, whereas wood swells 10–20 times more in the radial direction (direction of the rays) and even 15–30 times more in the tangential direction (see Table 2.2).

The maximum swelling increases with wood density, although the time to achieve this increases too.

Table 2.2: Swelling and shrinkage of wood according to DIN 52184.

Species	Max. swelling (%)			Rel. swelling (%/%)	
	Longitudinal	Radial	Tangential	Radial	Tangential
Spruce	0.2 – 0.4	3.7	8.5	0.19	0.36
Pine	0.2 – 0.4	4.2	8.3	0.19	0.36
Beech	0.2 – 0.6	6.2	13.4	0.20	0.41
Oak	0.3 – 0.6	4.6	10.9	0.18	0.34

2.2.4.2 Wood based materials

In wood based materials, **swelling** in the direction of the **plain** is slightly higher than parallel to the grain in solid wood. It is also clearly higher perpendicular to the plain than for solid wood perpendicular to the grain (see Table 2.3). This is due to the reversal of densification of the particles that were compressed during the production of the board (Figure 2.6b). Swelling is largely reversible for solid wood but this is not the case for particleboards, fibreboards and compressed wood where some of the swelling is irreversible. Swelling increases with the density. The rel. swelling is calculated in % swelling/% change of the EMC. The swelling rate of particleboard and MDF is not linearly correlated with the RH (from oven dry to fibre saturation; Sonderegger und Niemz (2006), see also annex Table 2.12).

Figure 2.6c shows the **thickness swelling** as a function of moisture content. If the boards expand only by the volume of water absorbed, as solid wood does, thickness swelling would theoretically follow the dashed line. The particleboard swells considerably more which means that voids are created within board. The MDF does not. It behaves essentially like a solid wood (Suchland 2004).

For large cross-sections, the EMC can only be reached in the outer regions. As a result, a moisture profile will build up, causing internal stresses and possibly cracks.

Table 2.3: Swelling of wooden materials (%/%) EMC)

Material	Swelling/Shrinkage (%/%)	
	In the direction of the plane	Perpendicular to the plane (thickness)
Plywood	0.02	0.30
Particle-board	Phenol resin	0.025
	Other	0.015
Glulam	0.01	0.24
MDF	0.15..0.20	0.80

When zones of different moisture contents have developed in a board, a **warping** can be observed (Figure 2.7). This effect also applies to particleboards, MDF and OSB. In the case of particleboards and fibreboards, the density profiles (homogeneity, different densities at the upper and lower side of the board) and board thicknesses play an important role. The higher the thickness, the lower the warping. Figure 2.7 shows the warping of a solid wood panel with different middle layers made of wooden materials. There is a strong influence of the middle layer's MOE: the lower the MOE of the middle layer, the higher is the warping of the whole board. In elements with big dimensions, an equilibrium moisture content for the whole element will never be reached. Instead, a moisture profile is formed (Figure 2.8).

Apart from stresses inherent to the material, a considerable swelling pressure builds up when the component is firmly mounted. In fact, the pressure exerted by swollen wood was applied in ancient times to bust rocks. The measured swelling pressure in the case of hindered swelling is significantly smaller than the theoretically calculated one. This is because a substantial amount of the stresses is reduced due to (plastic) deformations and relaxation. The swelling pressure is higher in humid air than it is for immersions in water. The density of wood and the swelling pressure have proven to be correlated, with the one increasing with the other. A higher swelling pressure was observed parallel to the grain than perpendicular to it. A swelling pressure of 0.2-0.4 N/mm² was measured for MDF (density: 600 kg/m³). The swelling pressure in water is lower than in water vapour; it increases with the density.

Internal stresses also occur in glued elements with different properties (different element thicknesses, different fibre and grain angles, differences in the EMC). These stresses can cause **delamination**, cracks in the elements or destroy the structure of wood based panels after a natural weathering (see Figure 2.10).

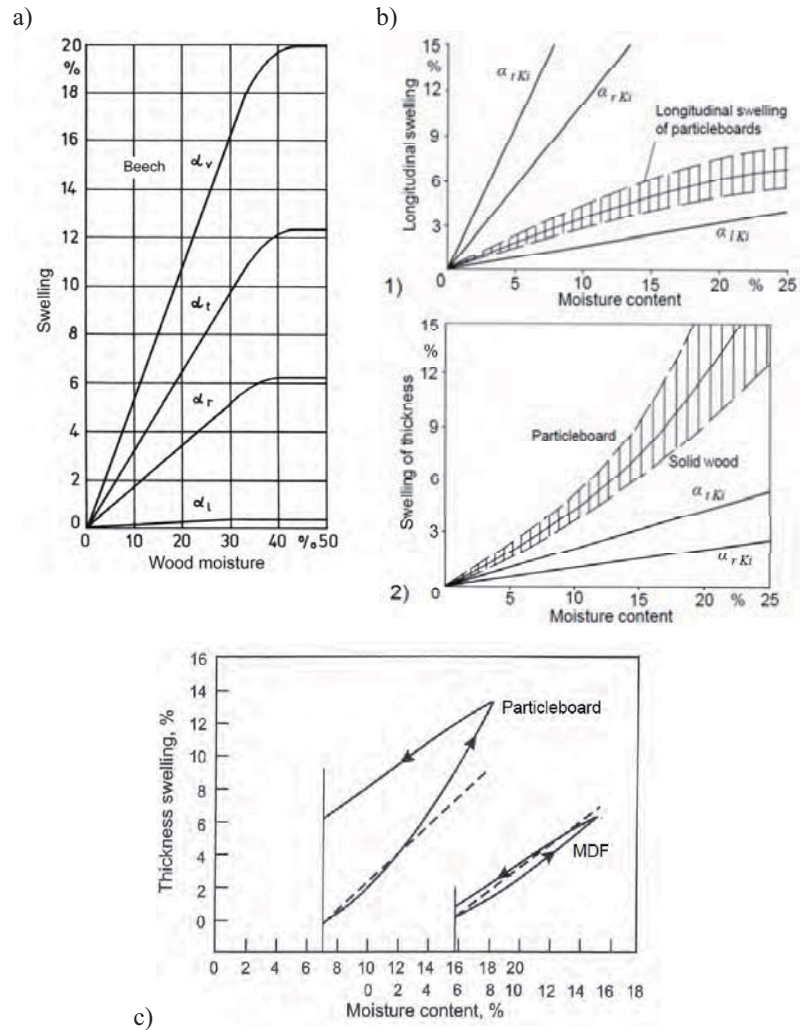


Figure 2.6: Swelling of wood and wooden materials: a) solid wood (Mörath 1932) ; l - longitudinal, r - radial, t - tangential, b) wood based materials (Teichgräber, cited in Kehr 1974); comparison of longitudinal swelling in relation to solid wood (1) and swelling of thickness (2) of particleboards with solid wood (pine), c) thickness swelling from particleboard and MDF during cyclic exposure (Suchsland 2004).

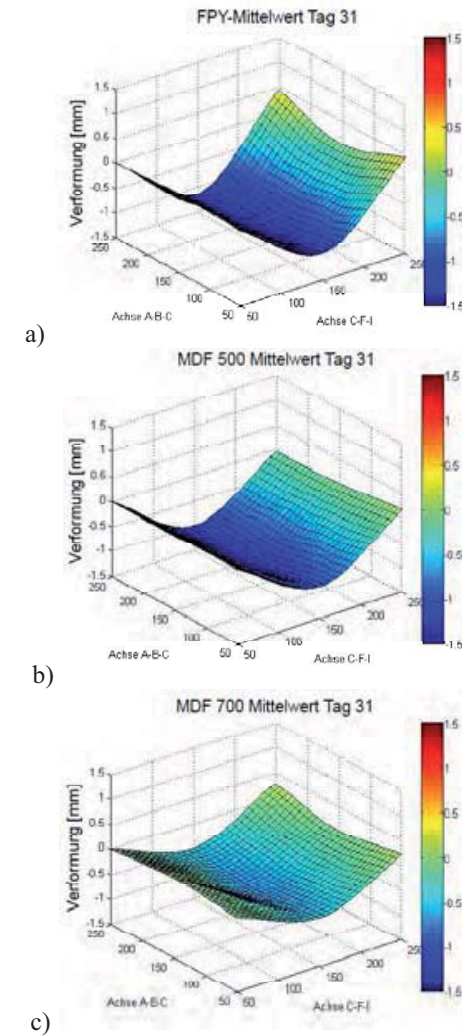


Figure 2.7: Warping of a three layer solid wood panel under different climatic conditions (upper side 1: 20°C/65%RH, lower side 2: 20°C/100%RH) and middle layer from different wooden materials: (a) solid wood, (b) MDF density 500kg/m³ and (c) MDF density 700kg/m³ (ETH Zurich, IfB, Wood Physics 2009).

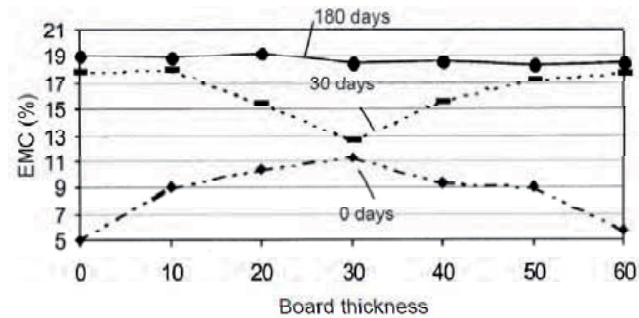


Figure 2.8: Moisture profiles in a wood panel after changing the climatic conditions from 20°C/65% RH to 2°C/90%RH, (Dunky and Niemz 2002).

2.2.5 Influence of Wood Moisture on the Surface Roughness of Wood-Based Materials

During manufacturing of wooden particle boards, the particles are strongly compressed. When the panels get moist (e.g. while aqueous adhesives are applied), thickness swelling of the densified particles occurs (spring-back effect), accompanied by an increase in surface roughness. The thicker the particles, the higher is the surface roughness. The **surface roughness** for particleboards is 60-80µm (veneer) and 40-60 µm (finish lamination). For high-quality surfaces (e.g. those to be coated with overlay papers), very small particles have to be used in the top layers. Thick particles become apparent after coating. Moreover, density variations of the panels (in the direction parallel to the panel surface) can cause a corrugated surface. Examples are shown in Figures 2.9 and 2.10. Weathering is strongly influenced by adhesive type and particle dimensions as well. We have a strong swelling from the particles in the surface, the roughness increased after weathering, for OSB the roughness is higher than for MDF (Figure 2.9).



Figure 2.9: OSB and MDF after a natural weathering, (ETH Zurich, IfB, Wood Physics).

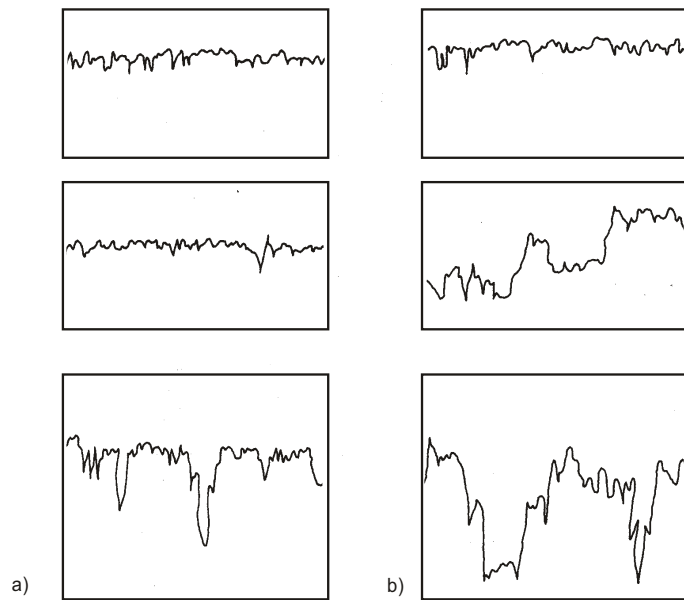


Figure 2.10: Surface roughness of particle board in dry (a) and wet (b) condition (Dunky and Niemz 2002).

2.3 THE RELATIONSHIP BETWEEN MOISTURE CONTENT AND PROPERTIES

The moisture content has a strong influence on most properties of wood (up to the FSP) and WBP. Strength (Figure 2.11), MOE and hardness (Table 2.4) decrease with increasing EMC; the thermal conductivity increases (Table 2.5) as well as the diffusion coefficient (Figure 2.12 and 2.13). Both are also strongly influenced by density.

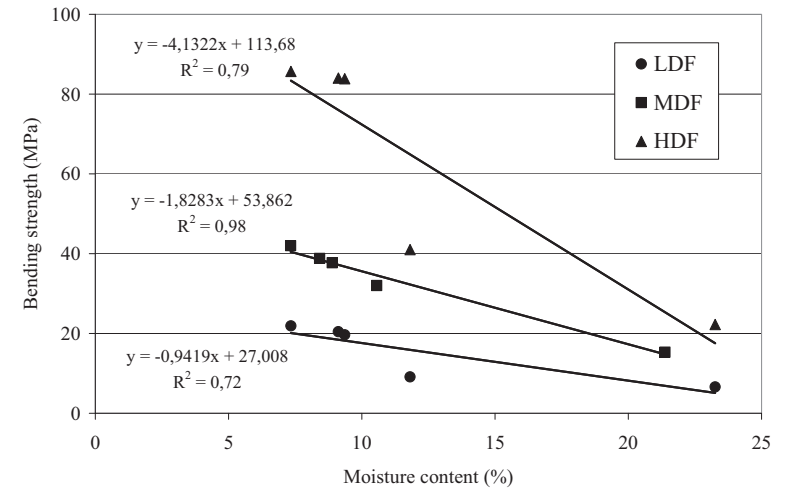


Figure 2.11: Relationship between EMC and bending strength for MDF with different densities (ETH Wood Physics, Bektha and Niemz 2009).

Table 2.4: Influence of the EMC on the Brinell hardness of wooden materials for different EMCs (ETH Wood Physics, Niemz 2009) (Load: 500N, v – coefficient of variation).

Particleboard 19 mm (HF – resin)		Particleboard 16 mm (PF – resin)		Solid wood panel (spruce) 25 mm	
EMC (%)	Brinell Hardness (N/mm ²)	EMC (%)	Brinell Hardness (N/mm ²)	EMC (%)	Brinell Hardness (N/mm ²)
0	45.6 v=18.0 %	0	85.1 v=17.4 %	0	19.4 v=31.6 %
7.7	33.5 v=14.6 %			8.8	14.6 v=23.1 %
8.2	44.0 v=18.9 %	9.4	38.5 v=24.4 %	10.5	15.6 v=24.4 %
12.7	24.6 v=12.2 %	16.3	26.7 v=14.2 %	16.9	12.5 v=16.8 %
17.45	18.0 v=17.2 %	27.5	19.7 v=15.8 %	24.12	10.4 v=14.4 %

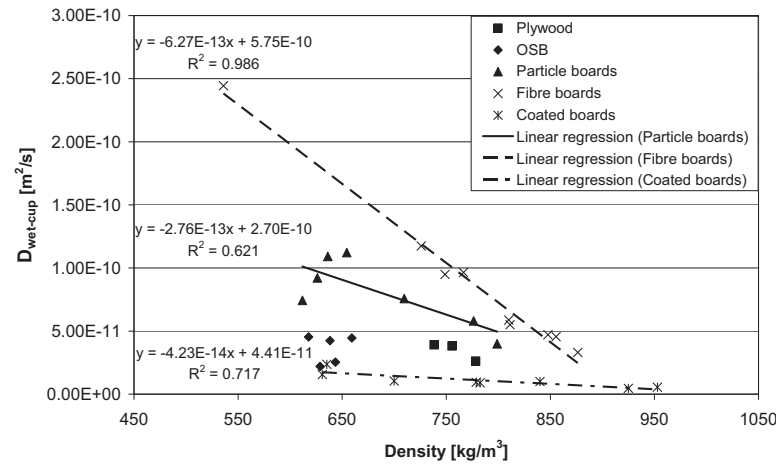


Figure 2.12: Diffusion coefficients (D) determined with wet cup tests depending on the density (mean values) (Sonderegger and Niemz 2009).

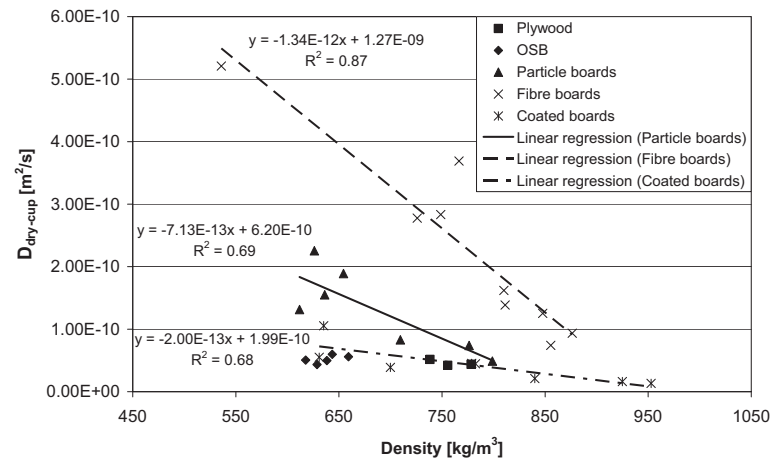


Figure 2.13: Diffusion coefficients (D) determined with dry cup tests depending on the density (mean values) (Sonderegger and Niemz 2009).

Table 2.5: Thermal conductivity (λ) depending on the moisture content. Mean values of 5 specimens per type (at dry condition only 3 specimens per type); $\lambda_{10.dry.reg(\omega)} = \lambda$ at dry condition and 10°C; $\Delta\lambda_\omega =$ change of λ per percent moisture content in W/(m·K) and in percent (Sonderegger and Niemz 2009).

Material	Thickness (mm)	Density (kg/m ³)	$\lambda_{10.dry.reg(\omega)}$ (W/(m·K))	$\Delta\lambda_\omega$ (W/(m·K·%))	$\Delta\lambda_\omega$ (%/%)
Plywood (beech), 25 mm	25.7	679	0.1304	0.00255	1.96
OSB 3, 18mm	18.4	562	0.0959	0.00074	0.77
Particle board (V20), 16 mm	16.4	597	0.0965	0.00128	1.32
MDF (V20), 3 mm	2.9	802	0.1104	0.00115	1.04
MDF (V20), 16 mm	16.2	696	0.0974	0.00121	1.24
Substrate of laminate flooring (HDF), 7 mm	6.6	785	0.1138	0.00151	1.32

In summary, wood moisture influences all properties of wood and wood based materials. The EMC of WBPs is slightly smaller than that of solid wood. The swelling in the direction of the panels is slightly higher than in the longitudinal direction of solid wood, whereas the thickness swelling is clearly higher than that of wood perpendicular to the grain due to the spring-back effect of the densified particles.

In the annex, various important properties of wood and wooden materials related to the moisture are listed.

2.4 REFERENCES

- Diverse authors: Holzlexikon (4th edition). DRW, Leinfelden-Echterdingen: 2003
- Bektha, P.; Niemz, P.: Effect of relative humidity on some physical and mechanical properties of different types of fibreboard. Euro. J. Wood Prod. (2009 on line)
- Bodig, J; Jayne, B.A.: Mechanics of Wood and Wood Composites. Krieger Publishing Company, Malibar, Florida: 1993
- Burmester, A.: Formbeständigkeit von Holz gegenüber Feuchtigkeit. Grundlagen und Vergütungsverfahren. Berlin, BAM report No. 4: 1970
- Dunky, M.; Niemz, P: Holzwerkstoffe und Leime. Berlin, Springer Verlag 2002
- Hailwood ,A.J. HorrobinS.: Absorption of water by polymers. Analysis in term of single model. Trans. Faraday Soc. 42B (1946)p.84-102
- Kehr, E. (Chapter 2) in „Werkstoffe aus Holz“; Fachbuchverlag, Leipzig 1974
- Kiessl, K.; Möller, U.: Zur Berechnung des Feuchteverhaltens von Bauteilen aus Holz und Holzwerkstoffen. Selektion feuchtetechnischer Parameter. Holz als Roh- und Werkstoff, Berlin 47 (1989) p. 317-322
- Krug, D.; Kehr, E.: Einfluss des Aufschlussdruckes bei der Faserstoffherstellung auf die Quellungsvergütung. Holz als Roh und Werkstoff, Berlin 59(2001) 342-343
- Künzel, H.: Risse in bewittertem Holz. Einfluss auf die Feuchteverhältnisse, Abhilfe. Bauen mit Holz, Karlsruhe (1993); 12, p. 1018-1022
- Kollmann, F.: Technologie des Holzes und der Holzwerkstoffe (volume 1, 2nd edition). Springer, Berlin: 1951
- Kollmann, F.; Coté, W.: Principles of Wood Science and Technology (volume 1). Springer, Berlin, Heidelberg: 1968
- Maloney, T.: Modern Particleboard and Dry Process Fibreboard Manufacturing. Miller Freeman, San Francisco: 1993
- Mörath, E.: Studien über die hygroskopischen Eigenschaften und die Härte der Hölzer. Darmstadt, 1932

- Niemz, P.: Physik des Holzes und der Holzwerkstoffe. DRW, Leinfelden-Echterdingen: 1993
- Niemz, P.; Sonderegger, W.: Untersuchungen zum Sorptionsverhalten von Holzwerkstoffen. Bauphysik, Berlin 31(2009): 244-249
- Popper, R.; Niemz, P.; Torres, M.: Einfluss des Extraktstoffanteils ausgewählter fremdländischer Holzarten auf deren Gleichgewichtsfeuchte. Holz als Roh- und Werkstoff 64 (2006), 491-496
- Popper, R.; Niemz, P.; Eberle, G.: Sorptions- und Quellungseigenschaften von verdichtetem Holz. Holzforschung und Holzverwertung, Wien (2002) 6, S.114-116
- Sonderegger, W.; Niemz, P.: Untersuchungen zur Quellung und Wärmedehnung
- von Faser-, Span- und Sperrholzplatten Holz als Roh- und Werkstoff 64(2006) 64: 11-20
- Sonderegger, W.; Niemz, P.: Thermal conductivity and water vapour transmission properties of wood based materials.
- Euro. J. Wood Prod. 67(2009):313-321 Suchsland, O. The swelling and shrinking of Wood. Forest Prod. Society, Madison: 2004
- Trendelenburg, R.; Mayer-Wegelin, H.: Das Holz als Rohstoff (2nd edition). Carl Hanser, München: 1955
- Walker, J.C.F.: Primary Wood Processing. Principles and Practice. 2nd edition, Springer 2006
- Willeitner, H.; Schwab, E.: Holz - Aussenverwendung im Hochbau. Verlagsanstalt Alexander Koch, Stuttgart: 1981

2.5 ANNEX: TABLES LISTING SELECTED PROPERTIES OF WOOD AND WOODEN MATERIALS

Table 2.6: Sorption of different wood species (ETH, Wood Physics 2010). (EMC = equilibrium moisture content, RH = relative humidity, x = mean, s = standard deviation).

Species		EMC (%)				
		35 % RH	50 % RH	65 % RH	80 % RH	90 % RH
Fir	x	7.16	8.84	10.18	13.42	17.63
	s	0.83	0.90	1.00	0.86	0.92
Spruce	x	7.69	9.65	11.31	15.18	19.07
	s	0.23	0.15	0.26	0.42	0.44
Pine	x	7.57	8.92	10.03	13.26	17.29
	s	0.62	0.64	0.64	0.36	0.29
Beech	x	7.17	8.92	10.33	14.61	18.78
	s	0.08	0.07	0.07	0.08	0.22
Chestnut	x	8.03	9.66	11.12	14.50	17.45
	s	0.29	0.31	0.30	0.33	0.45

Table 2.7: EMC of wood-based materials (after production) (Niemz 1993).

Material	Moisture content %
Plywood	5-15
Particleboard	9±4
Fibre hardboard	5±3
MDF	9±4
Spruce (20°C/65% RH)	12
Glulam	10±2

Table 2.8: EMC of fibre board (wet process) at different RH (Niemz and Sonderegger 2009).

Material	density	EMC (%) at RH				
	kg/m ³	35%	50%	65%	80%	90%
Fibreboard (wet process)	980	5.66	6.83	9.10	12.72	15.69
Fibreboard (wet process) for insulation (without adhesive)	150-200	6.55	8.34	11.1	15.37	19.72
Fibreboard minerally bounded	320	1.11	1.30	1.59	2.28	3.17

Table 2.9: EMC of wood-based materials (adsorption) at different (Niemz and Sonderegger 2009).

Material and thickness	density	EMC (%) at RH %				
	kg/m ³	35%	50%	65%	80%	93%
Plywood, beech, 25 mm	742	6.70	7.74	9.75	13.58	20.62
Plywood, beech, 35 mm	777	7.30	9.09	11.00	13.56	21.21
Plywood, beech, 50 mm	752	7.10	9.01	11.31	14.27	20.17
OSB, 12 mm	663	6.46	7.99	9.47	13.15	19.36
OSB, 15 mm	634	6.56	8.09	9.53	13.62	19.81
OSB, 18 mm	619	6.66	8.34	10.10	12.91	19.16
OSB, 22 mm	627	6.55	8.05	9.49	12.86	19.28
OSB, 25 mm	622	6.53	8.03	9.63	12.90	19.04
Particleboard, 10 mm	724	6.90	8.14	9.86	12.68	19.90
Particleboard, 16 mm	657	7.00	8.43	10.40	13.28	20.47
Particleboard, 16 mm, coated	683	6.53	7.72	9.27	12.23	20.45
Particleboard, 19 mm	630	7.27	8.53	10.40	13.55	21.16
Particleboard, 25 mm	615	7.59	8.11	9.75	12.93	20.72
particleboard, 25 mm, coated	636	6.53	7.85	9.49	12.26	20.37
Particleboard, 40 mm	633	6.79	8.14	9.79	13.22	21.44
Particleboard, 40 mm, coated	635	8.00	8.14	9.64	12.98	20.74
Particleboard, 6 mm	769	7.38	8.64	10.42	13.76	22.34
Particleboard, 7 mm	790	7.32	8.56	10.34	12.99	20.34
Particleboard, 7 mm, coated	826	6.97	8.27	9.91	12.36	18.59
MDF, 3 mm	825	6.37	7.74	9.31	11.40	19.18
MDF, 6 mm	843	5.98	7.08	8.07	10.77	18.93
MDF, 10 mm	803	5.98	7.15	8.22	10.89	18.84
MDF, 15 mm	532	6.11	7.67	9.40	12.50	18.18
MDF, 16 mm	728	5.50	6.83	8.47	11.92	19.13
MDF, 16 mm, coated	774	6.25	7.22	8.41	10.19	18.14
MDF, 19 mm	809	6.26	7.37	8.23	10.10	17.98
MDF, 25 mm	742	6.16	7.34	8.28	10.51	18.59
MDF, 25 mm, coated	777	6.28	7.32	8.66	11.04	18.44
MDF, 40 mm	763	5.70	6.73	7.60	9.97	16.98
HDF, 7 mm	871	5.29	6.38	8.09	11.28	17.56
HDF, 7 mm, coated	920	6.34	7.27	8.35	10.25	17.04
HDF, 8 mm, coated	934	6.23	7.25	8.35	10.43	17.23

Table 2.10: Coefficient of capillary water uptake (AW-coefficient of capillary water uptake DIN EN ISO 15148) (ETH Zurich, Wood Physics 2009).

Material	Thickness mm	Parallel to the board surface		Perpendicular to the board surface	
		Density (g/cm ³)	AW in (kg/m ² s ^{0.5})	Density in (g/cm ³)	(AW) kg/m ² s ^{0.5}
Solid wood panel	27	0.44	0.0115	0.42	0.0022
Plywood	15	0.51	0.0381	0.50	0.0026
Particle- board(V20)	19	0.67	0.0254	0.69	0.0014
MDF	22	0.69	0.0556	0.69	0.0125
OSB		0.65	0.0234	0.68	0.0018

Table 2.11: Diffusion properties of wooden materials (Niemz 1993).

Material	Density (kg/m ³)	Water vapour resistance factor μ
Spruce	Radial	470
	Tangential	-
MDF	470	20
Particleboard	900	50
	470	20
Strandboard	900	360
	470	65
Solid wood panel	900	1400
	450	40/400
Fibre insulation board	175	5
Hardboard (fibreboard)	1000	120

Table 2.12: Differential swelling for wood-based materials (Sonderegger and Niemz 2006) (p. - perpendicular, l. – longitudinal).

Material/ Thickness	Density (kg/m ³)	Swelling in (%/%)				
		in the direction of the plane			Perpend. to the plane	
		35 – 95% RH	35 – 80% RH	80 – 95% RH	65 – 95% RH	
MDF	756	0.016	0.040	0.010	1.07	
18 mm	v = 0.4	v = 3.6	v = 2.8	v = 7.4	v = 2.1	
OSB 3, 18 mm	l.	630	0.016	0.028	0.011	0.98
		v = 4.4	v = 17.3	v = 9.0	v = 29.5	v = 10.7
Particleboard V20, 8 mm	p.	649	0.018	0.034	0.011	0.91
		v = 2.5	v = 9.3	v = 8.4	v = 18.8	v = 10.7
Particleboard V20, 18 mm	p.	733	0.040	0.049	0.036	1.22
		v = 1.1	v = 2.5	v = 3.6	v = 3.1	v = 3.9
Particleboard V20, 30 mm	p.	649	0.027	0.036	0.023	0.93
		v = 1.9	v = 11.3	v = 8.0	v = 18.8	v = 4.6
Particleboard V313, 19mm	p.	596	0.032	0.040	0.029	0.87
		v = 0.7	v = 4.0	v = 5.6	v = 5.7	v = 3.1
Plywood larch 12,5mm	l.	649	0.035	0.041	0.031	0.92
		v = 1.6	v = 5.4	v = 5.2	v = 8.1	v = 4.8
3Plywood: beech 20mm	l.	665	0.010	0.017	0.006	0.22
		v = 1.6	v = 23.1	v = 17.2	v = 42.9	v = 10.2
p.	685	0.021	0.038	0.013	0.22	
	v = 3.6	v = 32.5	v = 31.7	v = 33.8	v = 9.3	
p.	780	0.012	0.024	0.006	0.42	
	v = 1.4	v = 29.4	v = 7.1	v = 36.9	v = 7.9	
p.	783	0.023	0.037	0.016	0.40	
	v = 1.0	v = 19.3	v = 12.7	v = 28.0	v = 5.4	
p.	766	0.022	0.034	0.015	0.41	
	v = 1.2	v = 13.5	v = 7.7	v = 22.9	v = 3.4	

Table 2.13: Water vapour resistance factors (μ) and diffusion coefficients (D) derived from dry and wet cup tests (Sonderregger and Niemz 2009) (MC - moisture content, μ_{mf} - Water vapour resistance factor of the melamine face)

Material	Thickness		Density [kg/m ³]	Dry cup				Wet cup					
	Required [mm]	Measured [mm]		MC [%]	μ_{dry} [-]	COV [%]	$\mu_{mf,dry}$ [-]	D _{dry} [m ² /s]	MC [%]	μ_{wet} [-]	COV [%]	$\mu_{mf,wet}$ [-]	D _{wet} [m ² /s]
Plywood (beech)	25	26.0	738	7.06	97.8	18.4		5.16 x 10 ⁻¹¹	15.95	44.1	23.2		3.92 x 10 ⁻¹¹
	35	35.4	778	8.15	100.8	18.8		4.38 x 10 ⁻¹¹	14.95	66.0	19.9		2.62 x 10 ⁻¹¹
	50	50.1	756	9.50	97.2	4.4		4.22 x 10 ⁻¹¹	15.01	48.8	15.2		3.82 x 10 ⁻¹¹
OSB 3	12	11.9	659	7.11	100.5	4.2		5.59 x 10 ⁻¹¹	18.02	42.8	14.8		4.46 x 10 ⁻¹¹
	15	15.0	638	6.98	116.8	0.1		4.97 x 10 ⁻¹¹	18.28	47.3	20.3		4.24 x 10 ⁻¹¹
	18	18.3	618	7.53	112.6	16.6		5.06 x 10 ⁻¹¹	18.15	47.6	5.7		4.54 x 10 ⁻¹¹
	22	22.0	644	7.18	98.8	17.7		5.97 x 10 ⁻¹¹	16.70	75.3	7.2		2.54 x 10 ⁻¹¹
	25	25.6	629	7.25	139.1	16.4		4.34 x 10 ⁻¹¹	15.91	93.3	26.3		2.20 x 10 ⁻¹¹
Particleboard (V20)	6	5.9	776	7.59	65.1	7.8		7.39 x 10 ⁻¹¹	16.50	27.1	4.2		5.81 x 10 ⁻¹¹
	10	10.3	710	8.15	56.9	8.6		8.29 x 10 ⁻¹¹	15.09	25.1	15.5		7.58 x 10 ⁻¹¹
	16	16.4	654	7.45	29.7	3.2		1.89 x 10 ⁻¹⁰	16.21	16.8	9.9		1.12 x 10 ⁻¹⁰
	19	18.9	636	7.75	35.1	3.3		1.55 x 10 ⁻¹⁰	17.52	18.5	5.5		1.09 x 10 ⁻¹⁰
	25	25.1	612	7.05	48.2	15.7		1.31 x 10 ⁻¹⁰	15.52	26.4	13.6		7.44 x 10 ⁻¹¹
	40	38.3	626	7.03	27.8	2.1		2.25 x 10 ⁻¹⁰	14.21	20.2	10.7		9.21 x 10 ⁻¹¹
Melamine faced board	16	15.5	700	7.80	146.3	20.4	8932	3.88 x 10 ⁻¹¹	10.52	162.8	22.2	11270	1.05 x 10 ⁻¹¹
	25	25.3	631	7.33	111.8	18.3	8117	5.50 x 10 ⁻¹¹	10.77	120.2	9.6	11925	1.55 x 10 ⁻¹¹
Substrate of laminated flooring (particle board)	40	38.6	635	7.46	57.9	14.5	5864	1.05 x 10 ⁻¹⁰	10.41	78.0	14.7	11162	2.37 x 10 ⁻¹¹
Laminated flooring (particle board)	7	6.6	799	7.58	94.8	3.1		4.90 x 10 ⁻¹¹	15.95	38.4	3.3		3.99 x 10 ⁻¹¹
Laminated flooring (particle board)	7	6.8	840	8.34	200.5	5.4	3689	2.11 x 10 ⁻¹¹	13.24	149.8	18.7	3862	1.01 x 10 ⁻¹¹

Table 2.13: continued

Material	Thickness		Density [kg/m ³]	Dry cup				Wet cup					
	Required [mm]	Measured [mm]		MC [%]	μ_{dry} [-]	COV [%]	$\mu_{mf,dry}$ [-]	D _{dry} [m ² /s]	MC [%]	μ_{wet} [-]	COV [%]	$\mu_{mf,wet}$ [-]	D _{wet} [m ² /s]
MDF (V20)	3	2.9	856	8.01	58.9	3.6		7.41 x 10 ⁻¹¹	11.88	31.1	8.5		4.55 x 10 ⁻¹¹
	6	6.0	848	6.73	42.4	4.1		1.25 x 10 ⁻¹⁰	12.15	27.1	7.5		4.71 x 10 ⁻¹¹
	10	9.9	811	6.61	39.0	4.0		1.39 x 10 ⁻¹⁰	14.70	24.8	1.0		5.51 x 10 ⁻¹¹
	16	16.7	726	6.98	20.4	6.5		2.78 x 10 ⁻¹⁰	14.11	13.4	5.8		1.17 x 10 ⁻¹⁰
	19	18.9	810	6.69	33.4	4.3		1.62 x 10 ⁻¹⁰	12.82	22.9	1.6		5.87 x 10 ⁻¹¹
Melamine faced board (MDF)	25	25.0	749	6.57	20.4	1.3		2.83 x 10 ⁻¹⁰	12.91	15.4	1.8		9.49 x 10 ⁻¹¹
	40	40.2	766	6.04	16.6	7.1		3.69 x 10 ⁻¹⁰	11.29	13.9	6.2		9.64 x 10 ⁻¹¹
	16	16.0	779	6.36	132.8	30.5	8900	4.52 x 10 ⁻¹¹	9.03	145.9	5.0	10556	9.39 x 10 ⁻¹²
Substrate of laminated flooring (HDF)	25	24.4	783	6.81	120.4	5.3	12085	4.47 x 10 ⁻¹¹	8.73	155.4	16.0	17059	9.03 x 10 ⁻¹²
Substrate of laminated flooring (HDF)	7	6.4	876	6.49	54.5	13.6		9.36 x 10 ⁻¹¹	12.81	36.7	3.6		3.31 x 10 ⁻¹¹
Laminated flooring (HDF)	7	6.5	925	6.73	289.0	5.1	5060	1.62 x 10 ⁻¹¹	9.50	251.3	4.4	4656	4.59 x 10 ⁻¹²
Laminated flooring (HDF)	8	7.6	953	6.47	349.8	11.9	7525	1.33 x 10 ⁻¹¹	10.95	207.6	18.1	4397	5.52 x 10 ⁻¹²
MDF wall panel	15	14.9	536	7.76	13.5	1.3		5.21 x 10 ⁻¹⁰	12.51	8.9	2.0		2.44 x 10 ⁻¹⁰

Chapter 3

Transport Phenomena

Luisa Carvalho, Jorge Martins, Carlos Costa

CHAPTER SUMMARY

Transport phenomena, as heat and mass transfer, are involved in several processes in the manufacture of wood-based products, such as drying of particles/fibres, hot-pressing and conditioning. The drying of fibres/particles and the hot-pressing operations involve simultaneous, heat and mass transfer. This chapter starts to focus on the basic mechanisms of transport phenomena that occur in porous media, as heat conduction, convection and radiation and also mass diffusion and convection. Then, the main operations involving these mechanisms in the production of wood-based panels are described: the drying of particles/fibres and the hot-pressing process. The drying regimes in convective drying, heat transfer and moisture movement are important issues treated in this chapter. The monitoring of the internal conditions in the mattress during the hot-pressing and the prediction of transport properties are also treated. Heat and mass transfer in conditioning (hot-stacking and normal stacking) is also covered. This chapter finishes with the diffusion of chemicals, resins, wax and other additives.

3.1 HEAT AND MASS TRANSFER MECHANISMS IN POROUS MEDIA

3.1.1 Introduction

Wood is a natural material and can be characterised as a capillary porous, cellular, hygroscopic, anisotropic and viscoelastic material. The particle/fibre mat is a complex structure at multiple levels, including the cellular structure of wood and the pseudo cellular structure of the mat (Kamke, 2004). So, fibre and particle mats are at the micro-level, heterogeneous and hygroscopic porous media. The description of transport mechanisms in a rigid porous media poses many problems, but the situation is even more difficult if the medium is compressible (Aguilar, 2006).

3.1.2 The Heat Transfer Mechanisms

There are three basic heat transfer mechanisms: **conduction**, **convection** and **radiation** (see Figure 3.1). Heat can also be generated inside the material if a source of energy is present.

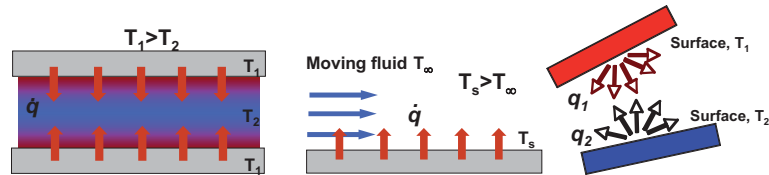


Figure 3.1: Conduction, convection and radiation heat transfer modes.

Heat conduction is defined as energy transferred by temperature difference or gradient and can occur in solids, liquids or gases. Heat flows from higher-temperature regions to those of lower temperature (Aguilar, 2006). In conduction, energy is transferred by atomic or molecular excitation from a higher to a lower-energy zone (Smith, 1994). Most metals are good conductors because their atoms are more readily set in a vibration mode by thermal excitation. Most inorganic compounds and organic molecules, such as polymers and wood are more difficult to set in a vibration mode and are poor conductors. The constitutive equation for conductive heat flux is known as **Fourier's first law** and can be written as:

$$\dot{q} = -k\nabla T \quad (1)$$

Where \dot{q} is **heat flux** in W/m, k is the **thermal conductivity** of the material in W/(mK), T is the temperature in K and ∇ the gradient operator (m^{-1}).

A second heat transfer mechanism is **convection**. For engineering purposes it is a subclass of conduction in a fluid where bulk flow or flow of the thermally excited molecules is the mechanism for transferring heated fluid to a colder region (Smith, 1994). The hot fluid must still transfer energy to a solid surface by molecular collision and then transfer it into solid by conduction. **Convection** may be augmented by forced flow to increase the rate of molecular collisions. For instance, in a gas phase, the convective heat flux (Wm^{-2}) can be expressed as:

$$\dot{q} = \rho_g C_{pg} v_g T \quad (2)$$

where ρ_g is the **gas density** (in kg/m^3), C_p the **gas specific heat** (in $\text{J}/(\text{kgK})$) and v_g is the **velocity of the gas phase** (in m/s). In certain conditions, as in combustion (gas generation) and in drying (phase change of water) the convection can be enhanced.

The convective heat flux at the boundary, from a surface to the ambient can be given by:

$$\dot{q}|_{\text{boundary}} = h(T_s - T_\infty) \quad (3)$$

where h is the **external heat transfer coefficient** in $\text{W}/(\text{mK})$ that is function of the system geometry, fluid properties, flow velocity and temperature difference between the surface (T_s) and the ambient (T_∞).

A third mechanism is **thermal radiation**, which is the transfer of heat by electromagnetic radiation. Externally generated radiation from a hot body travels at the speed of light to the object and is absorbed by both liquid and solid material. The wavelength of the radiant energy must match the product absorptivity for the best energy coupling and drying rates. Some materials act as a window to radiant energy at specific electromagnetic wavelengths and in many cases, hotter radiant heaters do not produce better energy transfer rates (Aguilar, 2006). Heat transfer by radiation (q in W) can be modelled by the **Stefan-Boltzmann law** for a grey body, at an absolute temperature T_1 and the surrounding enclosure at T_2 :

$$q = A\varepsilon\sigma(T_1^4 - T_2^4) \quad (4)$$

where A is the **grey body area** (body with an emissivity >1 which is independent of the wavelength), ε is the **emissivity** of this body, σ the Stefan-Boltzmann constant ($5.67 \times 10^{-8} \text{ W}/(\text{m}^2\text{K}^4)$), with the emissivity of wood being equal to 0.9 (Incropera and DeWitt, 1990). This value, however is subject to several conditions like surface properties and wavelength and ranges from 0.85 to 0.95.

Thermal energy can also be generated internally by an **exothermic chemical reaction**, but also by radio-frequency or microwave energy produced outside the material and converted to thermal energy inside. These electromagnetic wavelengths only heat dielectric products. The thermal excitation is selective to dipolar molecules such as water, and therefore, if the initial conditions are uniform, heating will be uniform, and consequently the temperature and moisture profiles after pressing. The heat generated in the medium depends primarily on three variables: the intensity of the electromagnetic field applied, its frequency and the material dielectric properties (Torgovnikov, 1993). Wood fibres are good electric insulators but interact with electromagnetic radiation due to their

composition of asymmetric molecules and water. This heating method is very capital intensive and nowadays is less viable because, energy costs are very high. **Electromagnetic radiation heating** has been used in the forest products industry for over 60 years and modern-day equipment makes this technique especially useful for wood drying and polymer curing in the manufacturing of wood composite products, such as particleboard, MDF and OSB, and solid-wood panels (Pereira *et al.*, 2004).

3.1.3 The Mass Transfer Mechanisms

In a fluid, **molecular diffusion** and convection (bulk flow) are the two basic mechanisms of mass transfer. In a porous web structure, additional mechanisms of capillary action, surface tension forces, wicking (movement along the fibre) and vaporization are also important (Aguilar, 2006). In addition, if a phase change takes place, a large quantity of thermal energy is involved (latent heat of vaporisation). For a material that is drying, this energy comes from the surface layers and therefore the surface temperature decreases. The effect, called evaporative cooling, occurs in all drying operations and can be compensated by heat transfer.

The rate of drying in many practical situations is controlled by internal mass transfer. In porous solids like wood or wood particle/fibre mattresses, internal mass transfer may occur within the solid phase or within the void space. Several mechanisms of internal mass transfer have been proposed in the literature including liquid and vapour diffusion, hydrodynamic or bulk flow and capillary flow. Table 3.1 lists the most important mechanisms of moisture transport in porous media.

For instance, in a mixture of air and steam, the **gaseous phase** is transferred by **convection** and each component is transferred by diffusion and convection in the whole phase. The **diffusive flux** can be obtained by Fick's first law (1833). **Fick's first law** established that the rate of diffusion is proportional to a concentration gradient, e.g. water vapour concentration in air:

$$\dot{n}_v = -D_v \nabla C \quad (5)$$

where \dot{n}_v is the **diffusive flux** in $\text{kg}/(\text{sm}^2)$, D_v is the **water vapour diffusivity** in air in m^2/s , C the **concentration of steam** in kg/m^3 .

Table 3.1: Moisture transport mechanisms through a fibrous porous media (Nilsson et al., 1993).

Transport Mechanisms	Phase	Local	Transport properties	
			Temperature dependency	Relative humidity (RH) dependency
Gas diffusion	Gaseous phase	Pores	Proportional to $T^{1.75}$	Independent (not considering swelling/ shrinking effects)
Knudsen diffusion	Gaseous phase in very small pores	Pores with diameter less than 10 nm	Proportional to $T^{0.5}$	Independent (not considering swelling/ shrinking effects)
Surface diffusion	Adsorbed phase	Fibres surface	Increase with T	Increase with RH
Solid internal diffusion	Adsorbed phase	Interior of cell wall material	Increase with T	Increase with RH
Capillary transport	Condensed phase	Pores		Only when the pores contain water

Convective mass flux (bulk flow) of water vapour in the gas phase can be expressed as:

$$\dot{n}_v = \rho_v v_g \quad (6)$$

where ρ_v is the **water vapour density** (in kg/m^3) and v_g is the **velocity of the gas phase** (in m/s).

When a fluid, for instance water vapour, is flowing outside a solid surface in **convection motion**, the rate of convective mass transfer is driven by a concentration difference of vapour between the solid surface (C_s) and the ambient air stream (C_∞):

$$\dot{n}|_{\text{boundary}} = k_c (C_s - C_\infty) \quad (7)$$

where k_c is the **convective mass transfer coefficient** (m/s).

Simultaneous heat and mass transfer occurs in all drying systems. In a simultaneous mass and heat transfer, the temperature gradient can cause mass transfer (Soret effect) and a mass concentration gradient can generate a heat flux (Dufour effect). Luikov (1966) was the first to use this approach, having applied the irreversible thermodynamics principles to describe the mechanisms of moisture transport in porous solids by thermal diffusion.

In a **porous media**, three types of flow can be considered: **viscous or laminar, turbulent and molecular slip flow or Knudsen flow**. **Laminar flow** occurs for Reynolds numbers below 2000. **Turbulent flow** is present for Reynolds numbers greater than 2300 (Siau, 1984). The **Knudsen flow** consists of molecular diffusion through a capillary due to the pressure gradient arising from the applied pressure differential. When the capillary radius is smaller or in the same order of the mean free path of the molecules Knudsen diffusion or split flow occurs. Flow in the interstices of a **porous media** is usually of low Reynolds number, *i.e.*, $Re \ll 1$, and in this case the pressure gradients drive the flow to balance the viscous stress gradients. The steady-state laminar bulk flow of fluids through porous media can be described macroscopically by Darcy's law (1856) (with no gravitational effect):

$$v = -\frac{K}{\mu} \nabla P \quad (8)$$

where v is the velocity of the fluid in m/s, μ is the viscosity of the fluid in Pa s, K is the permeability of the medium in m^2 , which is a measure of the resistance of a porous medium to flow through it, and ∇P is the pressure gradient (Pa). **Capillary flow** occurs as a result of pressure gradient induced by capillary forces. The Young-Laplace equation permits the calculation of the **capillary pressure** across the interface liquid-gas at equilibrium:

$$P_c = P_g - P_l = \frac{2\gamma \cos \theta}{r} \quad (9)$$

where P_g is the pressure in gaseous phase and P_l the pressure in the liquid phase below the meniscus, both in Pa, r the capillary radius (m), θ the contact angle between the liquid and the capillary wall ($^\circ$) and γ the liquid surface tension (N/m). In order to re-establish the equilibrium, there will be migration of water from the larger pores to the small ones, *i.e.* from the zones of low capillary potential to the zones of high capillary potential. Generally, this kind of transport only is considered for local moisture values above the **fibre saturation point (FSP)**, when the liquid phase is continuous. However, at the hygroscopic domain, **capillary condensation** can occur in tiny pores, which results from the proximity of the solid surface (adsorption effect), but also from the curvature of the meniscus (Kelvin effect) (Gregg and Sing, 1991). The first effect is restricted to a distance close to the diameter of fluid molecules. The relative vapour pressure through a liquid-vapour interface can be calculated, assuming cylindrical pores, using the **Kelvin equation**:

$$\ln \frac{P_v}{P_{sat}} = -\frac{2\gamma \cos \theta MM}{RT\rho r} \quad (10)$$

where P_v is the vapour pressure above the meniscus, P_{sat} the saturated vapour pressure, both in Pa, γ the liquid surface tension (N/m), MM is the molecular mass of water (kg/kgmol), ρ its density (kg/m^3), θ the contact angle ($^\circ$), r the capillary radius (m) of the gas-liquid interface, R the gas constant (8.314 J/(kgmolK)) and T the temperature in K. From this equation, it is possible to infer that if the meniscus is concave, which means that the liquid wets the solid ($\theta < 90^\circ$ *i.e.* $0 < \cos \theta < 1$), the capillary condensation in a pore of radius r will occur at a pressure below the saturation vapour pressure.

3.2 HEAT AND MOISTURE TRANSFER IN THE DRYING OF PARTICLES/FIBRES

3.2.1 Introduction

Drying is an important operation in the production of wood-based panels (WBP), which consumes a large amount of energy, affects product quality and without appropriate control, causes environmental concerns (Pang, 2001). The **drying of furnish** (particles/fibres) is very different from the **drying of solid wood**. In solid wood drying the operation can take days, while in drying of WBP furnish takes minutes or seconds at relatively high temperatures (Maloney, 1989). Although the fundamental mechanisms are the same, the drying operation is a little different in the manufacture process of particleboard, fibreboard and OSB. The operating conditions (temperature, applied pressure) and the moisture content of wood at dryer entry and exit are also different. In the case of particleboard, furnish arrives to the dryer with moisture content ranging from 10 to 200 %. Typical moisture contents are around 30-40 % during summer, and 60-70 % during winter. If the particles or fibres are to be used with a liquid resin, then they must be dried to about 2-7 %. In MDF, drying temperatures reach 160 $^\circ C$ for drying times between 2 and 5 seconds that leads to final resinated fibre moisture contents between 5 and 8 % (Ntalos and Grigoriou, 2001). In OSB strands have moisture contents of around 2 % after drying. The drying temperature depends on furnish moisture content and can vary from 260 to 870 $^\circ C$ (Maloney, 1989).

The most common **dryers** for particles/flakes are rotary single-pass or three-pass dryers. Modern **single-pass dryers** are long-retention dryers

incorporating pneumatic-mechanical conveying of the particles/flakes and operating at low inlet temperatures (400-500 °C). The **three-pass dryer** provides a pre-drying (interior pass) and a final drying (second and third passes) and the particles are dried directly with hot gases. The **rotary dryer** consists of a large horizontally oriented, rotating drum (typically 3 to 6 m in diameter and 20 to 30 m in length) (see Figure 3.2).



Figure 3.2: Dryer in a particleboard plant (Sonae Indústria, Oliveira do Hospital plant).

The wet wood particles are mixed directly with hot combustion gases, in a co-current flow pattern, at the inlet to the rotating drum. The gas flow provides the thermal energy for drying, as well as the medium for pneumatic transport of the particles through the length of the drum. Interior lifting flanges serve to agitate and produce a cascade of particles through the hot gases (Shu *et al.*, 2006). So, heat is transferred from the gas to the wet solids as a result of a temperature driving force, and the particles increase in temperature and lose moisture (Kamke and Wilson, 1986). The water vapour is then transferred to the gas stream under a vapour pressure gradient.

In the case of MDF, the mixture of wet fibres and steam flows through a blowline, where the adhesive and other additives are added to the fibres and then into a tube dryer. A **tube dryer** typically has a horizontal part followed by a vertical part and the total length is normally around 100 m. The mixture of air, steam and resinated fibres enters a cyclone for

separation (Pang, 2001). A number of operating conditions are associated with this operation, such as initial moisture content of furnish and its variation, particle geometry of furnish, variable ambient conditions, the feeding system to the dryer, contamination and discoloration and fire and explosion problems (Maloney, 1989).

The drying phenomena have been extensively studied for solid wood and several models have been proposed (Whitaker, 1977; Plumb *et al.*, 1985; Stanish *et al.*, 1986; Ben Nasrallah and Perré, 1988; Liu *et al.*, 1994; Kocaefe *et al.*, 2006). However, articles about the drying of particles, strands or fibres in WBP manufacture are scarce. Although the drying of solids in a rotary dryer has been extensively covered in the literature, drying of wood furnish has been studied by only a few researchers. Kamke and Wilson (1986a, 1986b) analysed the factors affecting the retention time of particles within a rotary dryer, as well as the heat and mass transfer with aim of developing a computer model to describe the drying behaviour. There are also few studies that deal with wood chips drying in superheated steam in pneumatic conveying (Fyhr and Rasmuson, 1996, 1997; Johansson *et al.*, 1997a).

3.2.2 Drying Regimes in Convective Drying

The **rate of drying** for lumber depends on the relative humidity of air, the air temperature, and the air velocity across the surfaces. The **drying process** is usually divided into two different regimes: the period of “**constant drying rate**”, where the process is determined by external conditions and the period of “**falling drying rate**”, where the internal moisture migration limits the drying rate (Johansson *et al.*, 1997a). In hygroscopic materials like wood, the drying by **forced convection** can be described as follows:

- First phase: After establishing the equilibrium and while the moisture content is above the FSP, the temperature of the wood does not change. So, all the heat transferred to wood is used to evaporate the water. The vapour pressure at the wood surface is equal to the saturation vapour pressure; drying is controlled by the external resistances to heat and mass transfer. This is the phase of “**constant drying rate**” and it cannot be observed if the external conditions are severe (high temperature and low relative humidity of air).
- Second phase: This phase occurs when the capillary water migration is lower than the evaporation flux. So, the moisture content at surface will fall below the FSP and the vapour pressure

is then lower than the saturated vapour pressure, according to the sorption isotherms. As drying progresses the moisture concentration gradient in wood becomes lower and so the rate of moisture migration, leading to a decrease of drying rate: it is called the “**falling drying rate**”. The resistance to the transfer of moisture inside the material becomes the most important mechanism.

- Third phase: When all the material is in the hygroscopic domain, drying continues slowly until the equilibrium between the material and the external air stream is reached. The drying rate is controlled by heat transfer, because the moisture adsorption decreases as temperature increases.

Due to wood anisotropy, the three phases can coexist, depending on the size of material and properties as water diffusivity in the transversal and longitudinal directions.

3.2.3 Heat Transfer

In drying of particles, it is important to consider the transport of heat inside the particles (internal flux) and also at the surface of the particles (external flux). So, heat is transported internally by convection and conduction whereas external heat transfer from the surface occurs via convection and radiation.

In the conventional drying of solid wood, the heat transfer by **convection** is less important than the transport by **conduction** (Liu *et al.*, 1994). The **convection** mechanism is only considered in drying by **forced convection** (Ben Nasrallah and Perré, 1988), by vacuum at moderate temperature (Fohr *et al.*, 1995) and **convective drying** at high temperature (Pang and Keey, 1995). In drying of wood particle/fibres, heat is transferred to the material primarily by convection air currents and so this mechanism is the most important. Therefore, the drying medium properties (air and water vapour) will affect the process. The period of **constant drying rate** which does not exist (or is very short) using air drying, becomes more significant with decreasing amounts of air in the drying medium, in particular when using pure superheated steam (Johansson *et al.*, 1997a,b). In case of MDF, because the fibre temperature at the **blowline** outlet is normally higher than the wet-bulb temperature at the dryer inlet, flash drying occurs immediately after the wet fibres and steam enter the dryer. Flash drying occurs in a very short distance, and so heat and also mass transfer can be evaluated using only the length of a single fibre (see Figure 3.3). Because heat and mass transfer coefficients between the fibre and the air stream are high, the

drying rate is dominated by internal **moisture movement** within the fibre walls (Pang, 2001).

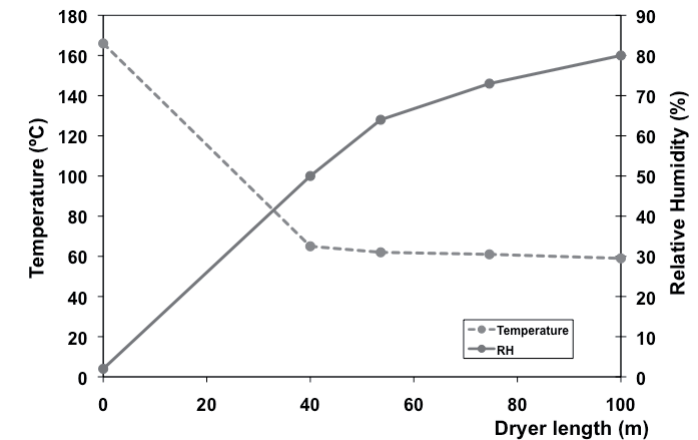


Figure 3.3: Example of a typical evolution of temperature and relative humidity (RH) along the fibre dryer in the production of MDF (Mangualde plant (Portugal) from Sonae Indústria, data collected by Pedro Reis).

3.2.4 Moisture Movement

Moisture in wood can exist in three forms: water vapour in the pores, capillary or free (liquid) water in the pores and hygroscopic or bound water in the cell walls (Simpson, 1983-84a, b). Considering the mechanisms of moisture movement in wood, two situations must be considered:

- Below FSP: Moisture movement as vapour through the cellular cavities and pit openings; adsorbed or bound water movement through the cell walls. Molecules are fixed at sorption sites by van der Waals forces and hydrogen bonds. Water molecules can only move if they have sufficient energy to escape from their adsorption sites and become activated molecules. (see Figure 3.4c)
- Above FSP: Free water movement due to a capillary pressure gradient or due to the increase of gas volume inside the cell lumens with the increase of temperature. (see Figures 3.4a and 3.4b)

So the mechanisms of mass transfer through wood during drying can be divided into two main classes according to Siau (1984):

- **Diffusion;** intergas diffusion, which includes the transfer of water vapour through the air in the lumens of the cells and bound water, within the cells walls;
- **Bulk flow** of fluids through the interconnected voids under the influence of a static or capillary pressure gradient.

In the first phase of wood drying, water in the liquid state migrates easily longitudinally and finds a transversal path (see Figure 3.4a). During the third phase, the water migration proceeds essentially along the thickness direction (see Figure 3.4c). During the second phase, there is a transition from a mechanism mainly longitudinal to a transversal mechanism for moisture transfer (see Figure 3.4b). The migration purely in the thickness direction settles when all the material is in the hygroscopic domain (see Figure 3.4c).

For drying processes at low temperature (conventional drying of solid wood), the migration of water to the surface is due to a difference of chemical potential, whereas at high temperature (drying of particles/fibres), the migration of water is mostly due to a pressure gradient in wood, due to a high temperature gradient. These statements are valid for both solid wood and for particles/fibres drying.

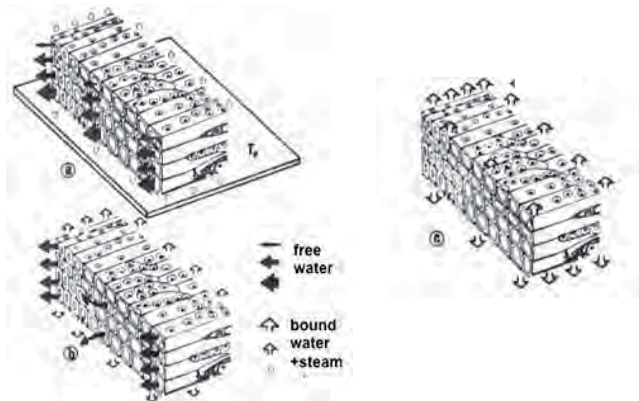


Figure 3.4: Mechanism of moisture movement during wood drying a-first phase (moisture above PSF), b-second phase c-third phase (all the material is in the hygroscopic domain) (from Moyne, 1983).

The **drying process** of fibres in MDF production was described by Pang (2001) as follows. In a micro-structural scale, the fibre wall contains both holes (pit openings) and fine pores due to the mechanical action of the refining. At the dryer entrance, fibres are very wet and covered with liquid water (from the refining operation and from the adhesive spraying) and therefore the fibre surface is vapour saturated. During drying, the liquid flows outwards through pit openings (with a diameter of about 4 μm) and then through the large pores. The process persists until the fibre moisture content is decreased to below 50%. At this point, some liquid still remains in very fine pores and this liquid will evaporate within the material. At the same time the vapour diffuses through the fibre material towards the outer surface. Once the remaining liquid water has been removed drying slows down and become controlled by bound water diffusion and water vapour movement within the cell walls (Pang, 2001)

3.2.4.1 Moisture diffusion

Water vapour diffusion in air can be described by Fick's law, driven by a partial pressure gradient and is much more rapid than **bound water diffusion**. Bound water diffusion in wood is sometimes described by Fick's law, but this has generated some controversy, regarding the driving force used (moisture content, partial pressure of water vapour and chemical potential). The traditional approach assumes the moisture gradient as the driving force for diffusion (Stamm, 1959; Siau, 1984; Simpson, 1993). Another line of thought considers bound water diffusion as a response to a vapour pressure gradient (Bramhall, 1976). The vapour pressure gradient presents more consistency with the experimental results and has a more universal application, as in the non-isothermal drying. At low moisture content, diffusion is probably best described by chemical potential driving forces (Siau, 1984). Below FSP (hygroscopic domain), water movement can follow a continuous path through cell wall or through a combination of cell walls and cell cavities. Stamm (1964) analysed this situation with an electrical analogy using parallel and series networks of diffusion paths.

3.2.4.2 Bulk flow of gaseous phase

In case of drying, only **bulk flow** of the gaseous phase has interest. Bulk flow of liquids has practical applications in wood preservation (pressure or vacuum treatment) and the impregnation of wood with chemicals, e.g. pulping, wood polymer composites. **Darcy's law** is considered a good approximation to describe the one-phase flow through wood (Plumb *et al.*, 1985; Siau, 1984), although some special situations in which Darcy's

law would not be obeyed are reported by Siau (1984). This is the case of turbulent flow that perhaps could occur in the largest earlywood vessels of red oak and the presence of nonlinear flow due to kinetic energy losses where fluids enter pit openings from vessel or tracheid lumens. It can occur at Re numbers between 0.04 and 16, assuming radii from 0.005 to 2 mm and a pit membrane thickness approximately 0.1 μm .

3.2.4.3 Capillary flow of liquid

The flow of free water above FSP requires both a continuous passageway for flow and a driving force. The continuous passageway is provided mainly by cell cavities and interconnecting pits (pit openings range from 0.1 to 1 μm in diameter (Simpson, 1983-84a). The driving force is the **capillary pressure** (difference between the pressure in the gas phase and in liquid phase). Bulk flow of liquid water can be described using Darcy's law and is determined by liquid permeability.

The capillary pressure is calculated using the **Young-Laplace equation**. For a 10 μm radius ($\gamma = 73 \text{ mJ/m}^2$ and complete wettability $\theta = 0^\circ$), which could be the typical value of a softwood tracheid, the capillary pressure will be 14.6 kPa, while for a 1 μm radius, typical of a large pit opening, the capillary pressure will be 146 kPa. If the gas pressure is 1 bar (100 kPa), then the pressure below the meniscus is -46 kPa. This negative pressure is called capillary tension (Siau, 1984). These elevated capillary tensions that are generated in wood during drying are responsible for phenomena as the collapse of wood and pit aspiration that reduces permeability. As it was mentioned above, even below FSP, capillary condensation can occur in pores. In case of wood, and considering for instance a relative humidity of 90 %, i.e. a relative pressure of 0.9, the maximum radius for which capillary condensation will occur at ambient temperature, is 0.01 μm ($\gamma = 73 \text{ mJ/m}^2$ and complete wettability $\theta = 0^\circ$), a little lower than the range of pit membranes openings (around 0.05 μm).

3.2.5 Effects of Wood Chip Properties

3.2.5.1 Permeability

For wood, **permeability** is dependent on wood structure. The permeability of wood cannot be solely related to its porosity but also to the availability of interconnecting pits and perforation plates between its cells (Siau, 1995). Several authors proposed models to estimate the **permeability** of wood considering its anatomical aspects (Comstock, 1970; Spolek and Plumb, 1980; Siau, 1984). Experimental measurements

of liquid and gas permeabilities were also performed for some species (Siau, 1984). Longitudinal permeabilities range from 10^{-10} for red oak to 10^{-15} m^2 for Douglas-fir heartwood. Transverse permeabilities range from 10^{-16} to 10^{-18} respectively (Siau, 1984). For softwood, the ratio transverse-to-longitudinal is around 1/20000 (Comstock, 1970). For hardwoods they are even lower due to the high connectivity of vessels. Wood permeability affects drying behaviour: the period of constant drying is longer for high permeability species, because the capillary forces tend to keep the surface above FSP; the falling rate period is faster for higher permeability species in the longitudinal direction.

3.2.5.2 Geometry

The size and the shape of the individual particles in a furnish are significant factors that influence wood drying. With existing technology it is impossible to achieve uniform particles (Maloney, 1989). The total drying time increases with the chip thickness: if the thickness is halved, the total drying time is approximately halved too. In thinner chips, the maximum overpressure in the centre of material is higher, because the distance for the transport of heat from the surface is halved and the main pressure release occurs in the longitudinal direction. When the longitudinal dimension is doubled the maximum overpressure increases by a factor of more than two because of the larger length of longitudinal flow necessary for pressure equalisation. The total drying time is not as sensitive to the wood chip length. So for equal volumes, a thin chip is better for drying purposes than a short one, due to the highest resistance to flow in the thickness direction (Fhyr and Rasmuson, 1997).

Suggested R&D Topics include:

- Influence of the drying conditions on the subsequent wettability and absorption of the resin
- Influence of the drying conditions (moisture internal profile) on the industrial press operation
- Influence of the drying conditions on the final product VOC emissions

3.3 HEAT AND MASS TRANSFER MECHANISMS IN HOT PRESSING

3.3.1 Introduction

Matpress consolidation of a WBP is achieved through hot-pressing. The thermal energy is used to promote the cure of the thermosetting adhesive and soften the wood elements. The mechanical compression is needed to increase the area of contact between the wood elements to allow the possibility of adhesive bond formation. This operation has a major effect on the balance of properties of the resulting panel; a rigorous control of all processing variables is necessary to achieve appropriate product quality and to minimise pressing time. Several coupled physico-chemical-mechanical phenomena are involved during hot-pressing, making this operation very complex (see Figure 3.6). Besides heat and mass transfer, other mechanisms are also involved as the polymerization of the adhesive and the rheological behaviour of the wood elements. Several researchers have described these mechanisms with the aim of modelling the hot-pressing process. These include Bolton and Humphrey (1988), Humphrey and Bolton (1989a), Thoemen (2000), Zombori (2001), Fenton *et al.* (2003), Carvalho *et al.* (2003), Dai and Yu (2004), Pereira *et al.* (2006), and Thoemen and Humphrey (2001, 2006).

Several types of presses can be used: batch or continuous, steam injection, plate and/or radio-frequency or micro-wave heated. The most common type is the **batch press** with heated plates (multi-opening), but in the last decade, continuous presses (see Figure 3.5) with moving heated belts are substituting batch presses, particularly for **particleboard** and **MDF** manufacture. Regardless of the press design, the mechanisms of heat and mass transfer in the mat are the same, but vary by degree of importance and direction of flow (Kamke, 1994). In this operation a number of factors are involved, related not only with the material itself but also the operating conditions, including resin type, catalyst, press temperature, wood species and fibre/particle geometry, mat moisture level content and distribution, pressing time (batch process), pressing speed (continuous process), mat volume and its relation to the board density profile, steam pressure within the board during pressing and pre-cure and post-cure of the resin (Maloney, 1989).



Figure 3.5: Continuous press in a particleboard plant (Sonae Indústria, Oliveira do Hospital plant).

The mat of wood particles/fibres is a capillary porous material in which the voids between and within particles/fibres contain a gas mixture of air and steam. Globally, the most important mechanisms of **heat and mass transfer** are (Pereira *et al.*, 2006):

- Heat is transferred by conduction due to temperature gradients and by convection due to the bulk flow of gas: conduction follows Fourier's law;
- The gaseous phase (air and water vapour) is transferred by convection; each component is transferred by diffusion and convection in the whole phase. Diffusion follows Fick's law and the gas convective flow follows Darcy's law: the driving force for gas flow is the total pressure gradient and for diffusive flow is the partial pressure gradient;
- The migration of water in the adsorbed phase occurs by molecular diffusion due to the chemical potential gradient of water molecules within the adsorbed phase;
- Phase change of water from the adsorbed to the vapour state and vice-versa.

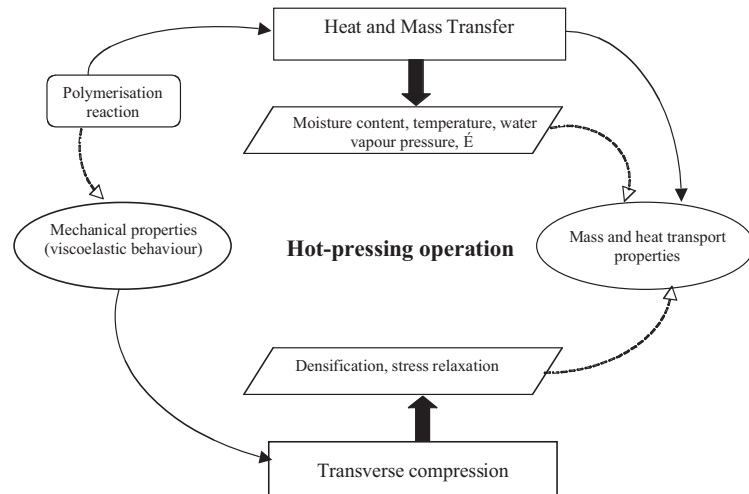


Figure 3.6: Mechanisms involved during the hot-pressing of wood-based panels and their interaction.

3.3.2 Heat Transfer

3.3.2.1 Heat transfer by conduction

The **conduction** is one of the more important mechanisms of heat transfer in the hot-pressing of WBP, mostly in case of batch pressing, in which almost all the heat supplied to the mat comes from the heated platens. Heat is transferred through the interface plate/mat to the interior by conduction and will be used to resin polymerisation and to remove water presented in the mat as bound water. To remove this water it is necessary to supply energy equal to the sum of the water latent heat of vaporization and the heat of wetting (or sorption) sufficient to break hydrogen bonds between water and wood constituents.

3.3.2.2 Heat transfer by convection

Convection occurs because the heat transferred from the hot platens causes the vaporization of moisture, increasing the water vapour pressure. A gradient of vapour partial pressure is formed across the board thickness, causing a convective flux of vapour towards the mat centre. On the other hand, the increase of gas pressure will cause a horizontal

pressure gradient that will create a flux of heat by convection to the edges. When the temperature of the medium exceeds the ebullition point of water, imposed by the external pressure, the horizontal pressure gradient becomes the more important driving force (Constant *et al.*, 1996). However, it is not necessary to attain the ebullition point of free water to have a vapour flow. Any change in temperature will affect the EMC of wood and so the vapour partial pressure in the voids (Humphrey and Bolton, 1989a). Also, if the vapour is cooled, it will condense, liberating the latent heat and a rapid rise of temperature will occur. So, there is also a phase change associated with the bulk flow, which imparts the temperature change (Kamke, 2004). This condensation will happen continuously from the surface to the core and not as a discrete event, which complicates the modelling of this system.

3.3.2.3 Heat transfer by radiation

Heat transfer by radiation is usually neglected, since for the relatively lower range of temperatures (< 200 °C), it would be insignificant compared with conduction and convection. However, during press closing and before the platen makes contact with the mat, as well as during the first instants of pressing while mat density is relatively low, heat transfer by radiation can be a significant part of the total heat transferred (Humphrey and Bolton, 1989a). On the other hand, on the exposed edges the heat is continuously transported to the surroundings by radiation (Zombori, 2001).

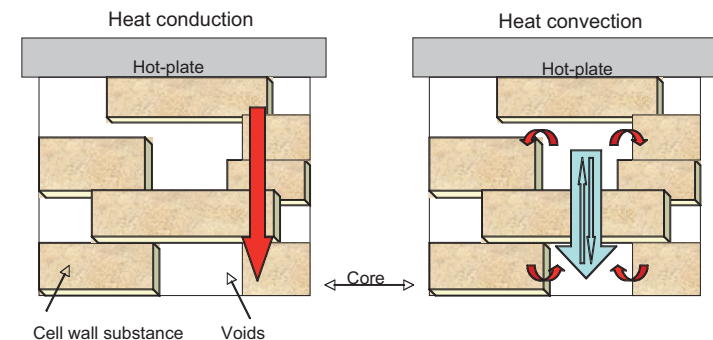


Figure 3.7: Heat transfer mechanisms in a WBP mat (adapted from Thoemen and Humphrey, 2001).

3.3.2.4 Other sources

The other possible sources are the exothermic reaction of the resin cure and the **heat of compression**. The contribution of the heat of compression is generally neglected. Bowen (1970) estimated that its contribution for heat transfer was around 2%. The contribution of the exothermic polymerisation of the resin depends on the reaction rate and condensation enthalpy. Bowen (1970) showed that as much as 22% of the total heat came from this reaction, although 10 to 15% may be a more reasonable level (Maloney, 1989).

Suggested R&D Topics include:

- Amount of heat that originates from conduction and from the condensation of vapour
- Percentage of heat transfer by convection and by conduction
- How can heat transfer be maximized?

3.3.3 Mass Transfer

3.3.3.1 Mass transfer by convection

In WBP hot-pressing, it is generally assumed that moisture content is below the FSP and so the water is present as vapour in cell lumens and voids between particles/fibres and bound water in cell wall (Kavvouras, 1977; Humphrey, 1982; Carvalho *et al.*, 1998; Carvalho *et al.*, 2003; Zombori, 2001; Thoemen and Humphrey, 2006; Pereira *et al.*, 2006).

Two main mass phases are then considered, the gaseous phase (air + water vapour) and the bound water and local thermodynamic equilibrium is also assumed. The gaseous phase is transferred by **convection** due to a gas pressure gradient (bulk flow) and the vapour is transferred by **diffusion**.

The **bulk flow** occurs in response to a gas pressure gradient caused by the vaporisation of moisture present in mat. In conventional hot-pressing, this bulk flow is generally assumed to be laminar and the contributions of other mechanisms (turbulent and Knudsen) of gas flow are neglected (Sokunbi, 1978; Humphrey, 1982; Denisov *et al.*, 1975; von Haas *et al.*, 1998). So, the **gas convective flow** follows Darcy's law (Carvalho *et al.*, 2003; Zombori, 2001; Fenton *et al.*, 2003; Thoemen and Humphrey, 2006). In the case of steam injection pressing, this assumption is not valid, since turbulent flow is likely to be of some importance (Hata *et al.*, 1990).

Diffusion inside the mat during hot-pressing includes **vapour diffusion** and **bound water diffusion**. The driving force for the diffusive flow of vapour is the partial pressure gradient. The convective and diffusive fluxes occur simultaneously, but it is widely accepted that convective gas flow is the predominant mass transfer mechanisms during hot-pressing (Denisov *et al.*, 1975; Thoemen and Humphrey, 2006).

3.3.3.2 Mass transfer by diffusion

The migration of water in the adsorbed phase occurs by molecular diffusion and follows Fick's first law with the chemical potential gradient of water molecules within the adsorbed phase as the driving force to diffusive flux. This is a slow process and thus it is often considered negligible by some authors (Carvalho *et al.*, 2003) in comparison with steam diffusion. Zombori and others (2003) studied the relative significance of these mechanisms and they found that the diffusion is negligible during the short time associated to the hot-pressing.

Local equilibrium is in general assumed to describe the mass transfer. The local moisture content is equal to the EMC. The adsorbed water and steam are related by a sorption equilibrium isotherm. Any change in temperature will affect the EMC and thus the partial pressure of the vapour in the surrounding air (Humphrey and Bolton, 1989).

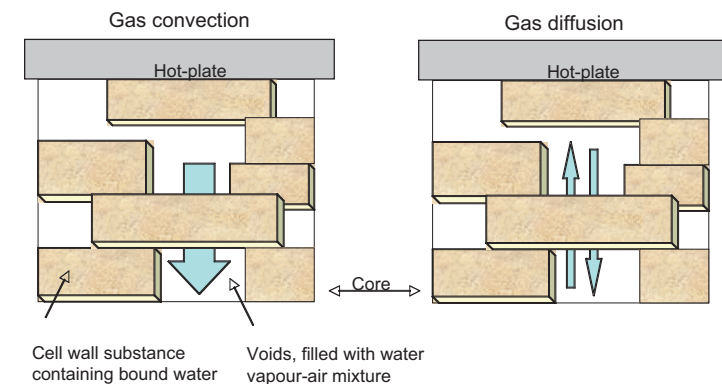


Figure 3.8: Mass transfer mechanisms in a WBP mat (adapted from Thoemen and Humphrey, 2001).

3.3.3.3 Capillary transport

At press entry the moisture content of the furnish is relatively low (generally below 14 %) and although a possible presence of liquid water brought by the adhesive and capillary condensation in some tiny pores, it is generally assumed that the whole mat is below the FSP (Kavvouras, 1977; Humphrey, 1982; Zombori, 2001; Thoemen and Humphrey, 2006). In case of particleboard, the moisture content at the press entry might be 11 %, while the particle moisture content before resin blending could be around 2-4 %. During blending, considerable quantities of water are added with the resin (water content around 50 %), and so unless the equilibrium is achieved by the furnish before entering the press (in that case, the water will be adsorbed in the cell walls of wood) some capillary translation might occur (Humphrey and Bolton, 1989). In case of MDF, the **fibre drying** after the resin spraying in the blow-line results in the decrease of moisture and it is reasonable to consider that the equilibrium will be attained before the hot-pressing, and thus the water will be adsorbed in the fibres (Carvalho, 1999).

There is also a possibility of **capillary condensation** in tiny pores. In case of WBPs, the relative humidity does not exceed 90 % (Humphrey, 1984, Kamke and Casey, 1988) and considering a temperature of 115°C, inside the mat, the maximum pore diameter filled with water will be 0.007 μm . This will correspond to capillary pressures of 14.6 to 20 kPa, which are an order of magnitude less than the predicted maximum vapour pressure differential between the centre and the edges of board (at atmospheric pressure). So, even if some fine capillaries do fill by capillary condensation, it is unlikely that capillary translation of liquid will occur (Carvalho, 1999).

3.3.4 Internal Mat Conditions

During the hot-pressing cycle, the internal conditions of the mat change in space and time. The transient and simultaneous phenomena of momentum, heat and mass transfer inside the mat do not allow a straightforward prediction of the internal mat environment. Although experimental measurements of these conditions are useful, its prediction demands mathematical modelling, which also provides knowledge for a better understanding of the phenomena involved.

Temperature and gas pressure affect the **hot-pressing process** and so the properties of WBPs. High temperatures are needed to achieve rapid cure of the adhesive and assist mat compaction by wood plasticization. Due to the compaction and the vaporisation of water, gas pressure builds up. The

level of gas affects heat convection. A high level of gas pressure can cause local or even a complete delamination of the mat, when the pressure is released during press opening and the resin bond strength is not sufficient to resist this pressure drop.

3.3.4.1 Monitoring the internal conditions

With the aim of studying the effects of several hot-pressing variables on the final board properties, several researchers have attempted to monitor this operation by measuring the temperature and gas pressure inside the mat during lab trials, but also in industrial presses (Maku *et al.*, 1959; Strickler, 1959, Kamke and Casey, 1988a,b; Humphrey, 1991; Bolton *et al.*, 1989b; García, 2002; García *et al.*, 2001, 2003).

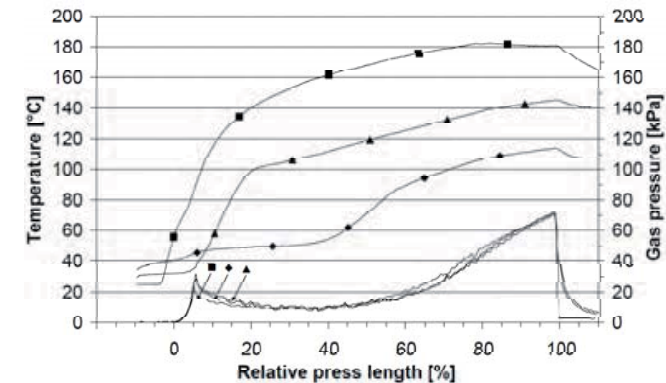


Figure 3.9: Temperature and gas pressure within a mat for a 16 mm particleboard during continuous hot pressing ■=surface layer, ▲=intermediate layer, ◆=core layer. Top three lines=temperature curves (from Meyer and Thoemen, 2007).

Temperature was measured by using thermocouples and the total gas pressure was measured by using a pressure probe consisting of a small diameter stainless steel tube connected to a pressure transducer. The tube and the transducer may be filled with a low vapour pressure fluid, as silicon oil, to reduce the dead volume in the hydraulic line (avoiding condensation of water vapour inside the tube) and also transfer the pressure change at the open end of the microbore tubing to the pressure sensitive diaphragm in the transducer well (Kamke and Casey, 1988a). This technique was developed and demonstrated by Kavvouras (1977) and Kamke and Casey (1988). They measured the gas pressure inside a flakeboard with 510 x 160 x 19 mm and target density of 720 kg/m³, a platen temperature of 190 °C and press closure time of 1 minute and they

obtained maximum values from 40 kPa to 200 kPa for initial moisture contents between 6 and 15 %. Bolton *et al.* (1989a) observed that for a particleboard with 283 x 283 x 15 mm, platen temperature of 160 °C and final density from 450 to 850 kg/m³ vapour pressure attained values of the same magnitude, from 20 to 200 kPa. They found significant differences in vapour pressure inside an industrial board and inside a laboratory board made with the same furnish and press conditions (Humphrey and Bolton, 1989a). In a 15 mm thick board (1.8 x 3.65 m) of 650 kg/m³ density, initial moisture content 16 % for surface layers particles and 12 % for core layer particles, the maximum core vapour pressure was at least 200 kPa at the end of press cycle, while in the laboratory board, they obtained a maximum of 60 kPa, 150 s after press closure. Steffen *et al.* (1999) monitored temperature and gas pressure inside a mat in movement during continuous pressing. The entire measurement equipment including the cable travelled through the hot press. A miniature pressure transducer covering a range from 0 to 700 kPa was imbedded in a plastic case. The sensor was prepared for sealed connection with air-filled stainless tubes (diameter 2 mm). A portable system PressMAN® was developed by the Alberta Research Council and measures mat thickness, hydraulic pressure, core temperature and gas pressure (Alexopoulos, 1999).

Meyer and Thoemen (2007) monitored the continuous hot-pressing of particleboard using this system. Deng *et al.* (2006) also used the PressMAN® to monitor the internal conditions during the hot-pressing of laboratory MDF mats that were pre-heated with microwaves. During the preheating with microwaves or HF, temperature is measured with fibre optic sensors (Deng *et al.*, 2006; Celeste *et al.*, 2004) (see Figure 3.10).

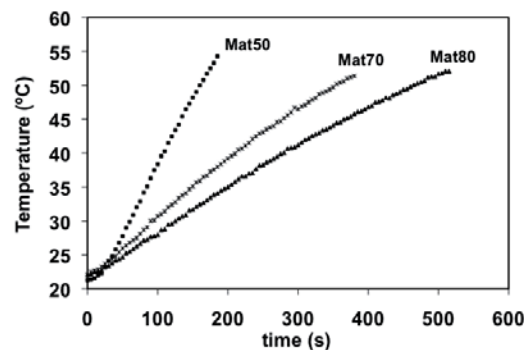


Figure 3.10: Temperature time evolution at board centre during the pre-heating of MDF for mats with thicknesses of 50, 70 and 80 mm (adapted from Pereira *et al.*, 2004).

Suggested R&D topics include:

- Development of new on-line sensors for monitoring the mat internal conditions, especially in continuous pressing
- Development of systems for the correct positioning the probes during continuous pressing
- How to treat the collected data and deal with its uncertainty?
- How to overcome the problems encountered in the measurement of gas pressure originated by the rheological transformations in the mat during pressing?
- How to overcome the difficulties to measure moisture content at several positions inside the mat?

3.3.4.2 Evolution of the internal conditions during hot-pressing

A typical trend of the evolution of temperature and vapour pressure during the hot-pressing can be described as follows. Heat is transported by **conduction** from the hot platen to the surface. This leads to a rapid rise in temperature, vaporising the adsorbed water in the surface and thus increasing the total gas pressure. The gradient between the surface and the core results in the flow of heat and vapour towards the core of the mattress, therefore increasing the gas pressure. As a consequence, a positive pressure differential is established from the interior towards the lateral edges, and then a mixture of steam and air will flow through the edges. The rate of temperature rise is larger at the superficial layers, because the core temperature is less affected by platen temperature (Kamke and Casey, 1988a,b) (see Figure 3.11). The temperature rise at the core is the balance of two mechanisms: the gradient of gas pressure that causes the flow of vapour to the centre and the effect of water loss from the board. This temperature rise at the core is thus linear. The ratio between the amount of heat lost by moisture escaping from the board edges and the input of heat from press platens is smaller in an industrial press than in a laboratory one. So, due to a higher steam production at board centre in an industrial press, a higher build up of gas pressure is observed (Humphrey and Bolton, 1989b). If the water vapour gives up enough heat to the surrounding mat during its journey to the centre it will condense (Kamke, 2004). If the water vapour reaches the equilibrium with the moisture content at the prevailing temperature, it will be adsorbed and become bound water, if not it will remain as liquid water.

A progressive decrease in the rate of temperature rise occurs after this period, which may be attributed to a decrease in heat transfer to the system as the temperature gradients near the surface of the board decrease and also to the increase of vapour loss from the edges of the board. Humphrey (1982) also attributes this fact to the increase of heat of wetting as the moisture content falls, thus resulting in a reduction of water evaporated per unit of energy input from the heated platens. The change of temperature at the surface attains almost a plateau, when the rate of vapour gain from the surface becomes smaller than the rate of lateral vapour loss from surface layers, which implies a decrease of the gas pressure. When venting begins (prior to press opening), water vapour pressure decreases and equalizes through the mat, while temperature stays high. The venting gas may move to the edges and toward the surfaces of the mat.

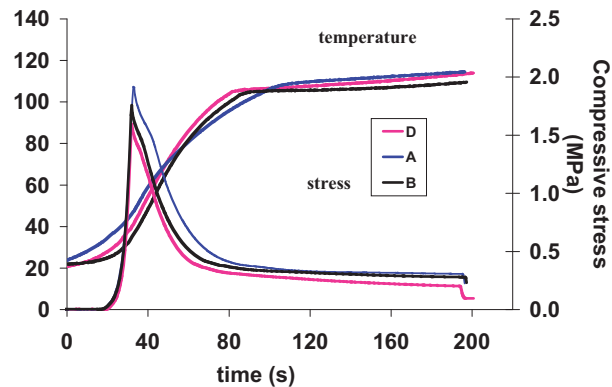


Figure 3.11: Compressive stress and temperature time evolution at board centre during the hot-pressing of MDF mats for three platen temperature: A-140 °C; B-150 °C and D-160 °C (from Pereira, 2002).

Suggested R&D topics include:

- How to control the steam flux through the edges to have a uniform density profile?
- How to measure gradients of steam pressure and temperature from board centre to edges?
- How the change in water vapour pressure affects the resin polymerisation reaction?

3.3.4.3 Influence of pressing parameters on the internal conditions

The levels of temperature and gas pressure are affected by pressing parameters, namely press closing time, initial moisture content and platen temperature. A faster press closing time results in a larger rate of mat densification. This leads to a rapid build-up of steam pressure in the surface region and thus a faster rate of convective heat transfer to the core (Kamke and Casey, 1988b). Low moisture content and low platen temperature result in a low gas pressure. High initial moisture content increases the rate of temperature rise in the core region but the maximum temperature may not be higher than the temperature found in a lower moisture content mat. Kamke and Casey (1988a) showed that high platen temperature and high moisture content mats results in a large deviation of gas pressure between the surface and core layers after press closing.

Temperature and gas pressure will also influence the **viscoelastic behaviour** of the mat and so the formation of a **vertical density profile**. Wolcott *et al.* (1990) investigated the interaction of temperature, moisture content, and compaction on the formation of a vertical density gradient in the board. On the other hand, particle geometry, wood density and the compression of wood particles will affect the porosity and permeability. A larger **permeability** allows for a larger rate of gas flow through the edges, which will retard the pressure build-up and thus lead to a lower plateau temperature. Winistorfer *et al.* (2000) developed a radiation-based system for the in-situ measurement of **density** during board consolidation. This system coupled with former ones for temperature and gas pressure measurements should lead to better insight of the consolidation and formation of vertical profile. García *et al.* (2003) measured the internal temperature and vapour pressure responses to flake alignment during OSB hot-pressing. The results indicated that lower density mats will heat faster and have lower internal gas pressure. Less aligned mats will initially heat faster and have higher internal gas pressure, but towards the end of pressing they will take slightly longer to heat.

The measurement of the evolution of moisture content throughout the mat during the **hot-pressing** is also important as it affects the rheology of the wood and the cure of the adhesive. There is evidence that the cure of resins that polymerize by condensation reactions is affected by the relative humidity of the surrounding air (Carvalho, 1999). This kind of data would give also information for a qualitative understanding of the dimensional stability of the panels. Other transport properties, such as **conductivity**, are also influenced by moisture content. Unfortunately, there are still difficulties of measuring moisture content on line and thus

the prediction of this variable by **mathematical modelling** is of great importance.

Suggested R&D topics include:

- A quantitative understanding of responses of pressing variables is needed
- More lab-scale trials at limit conditions (high moisture content) and different wood furnishes
- Need for correlations between lab and industrial presses data

3.3.5 Transport Properties

Transport properties are dependent on changing physical properties that vary with respect to space and time during hot-pressing. They are a function of temperature, moisture content and vapour pressure. Additionally, the physical properties are dependent on mat structure and so, the transport properties are direction-dependent. Although all WBP are comprised mainly of wood their very different in structures and compressibilities causes the transport properties of plywood, particleboard, MDF, and OSB to be very different from one another. On the other hand, they are not well known in some cases, considering the environment of high temperature and gas pressure. So, they are generally estimated using empirical correlations that sometimes were not obtained for the kind of WBP in study, but for another kind (mostly particleboard) or even for solid wood.

Suggested R&D topics include:

- More data on physical and mechanical properties of mats during hot-pressing are needed
- How to deal with changing wood raw material mix (wood species mix and geometry of wood particles) and their influence on material and transport properties?

3.3.5.1 Thermal conductivity

Like solid wood, WBPs are relatively good insulators, especially in the direction perpendicular to the plane of the board, where there is high resistance to flow due to the interruption of the path by the poorly conducting air-filled pores. In particular, softboard or ultra-light MDF that are low-density fibreboards, are especially designed to be insulators in construction applications. In any flat-pressed WBP, as **particleboard**

or **fibreboard**, where the particles tend to lay randomly in a plane parallel to the plane of the board (Kamke, 2004), there will be a difference between the out-of-plane (thickness) and the in-plane (width and length) thermal conductivity. The transversal conductivity was considered by Siau (1984, 1995) as a combination of the **thermal conductivity** of cell walls, the conductivity of air and the conductivity of moisture. He considered a geometrical model for a single wood cell with cubic geometry. To derive the transverse conductivity, he considered the conductance of the cross walls (cell-wall substance) in series with the conductance of the lumen (air) and the side walls (cell-wall substance). Based on this approach, Zombori (2001, 2002) considered for a strand board the following expression for the **thermal conductivity** in the thickness direction:

$$k_a = \frac{k_a k_T}{k_a(1 - \zeta_{sm}) + k_T \zeta_{sm}} \quad (11a)$$

$$k_T = SG(k_{cw} + k_w M) + k_a v \quad (11b)$$

where k_a is the conductivity of air (0.024 W/(mK)), k_T the conductivity of wood in transverse direction (W/(mK)), k_{cw} the conductivity of cell wall substance (0.217 W/(mK)), k_w the conductivity of water (0.4 W/(mK)), ζ_{sm} the space fraction of the mat, v the porosity of wood, M the moisture content of wood (fraction) and SG the specific gravity of wood. The **thermal conductivity** of the mat in the lateral direction was estimated in a similar manner, considering the orientation of the strands quantified through a degree of alignment. The longitudinal thermal conductivity of solid wood was considered as 2.5 times higher than the transverse conductivity (Siau, 1995). For the thermal conductivity of a particleboard in the thickness direction, Humphrey (1982) derived an experimental relationship and included a correction term for temperature (Kuhlmann, 1962; Humphrey, 1982) and another for moisture content (Kollmann and Malmquist, 1956; Humphrey, 1982):

$$k_z = (0.01172 + 0.0001319)FmFt \quad (12a)$$

$$Fm = 0.000103M + 1.00000 \quad (12a)$$

$$Ft = 0.001077T + 0.97$$

For the **conductivity** parallel to the board plane (k_x), Humphrey (1982) assumed a value given by equation (12a) multiplied by 1.5, based on experimental work of Ward and Skaar (1963) with an UF (urea-formaldehyde) bonded particleboard. The same expression was used by Carvalho *et al.* (1998, 2003), Pereira *et al.* (2006) and Nigro and Storti (2001). Fenton *et al.* (2003) and Lee *et al.* (2006) used for an OSB mat, the equation 11a combined with the correction for temperature in 11b. Thoemen (2000) and Thoemen and Humphrey (2006) used the following expression for MDF, where the thermal conductivity perpendicular to the plane in W/(m·K) is calculated by the sum of $k_T^{0.30}$, which denotes the thermal conductivity measured at 0 % moisture content and 30 °C in function of density ρ in kg/m³ (von Haas, 1998) and a correction factor derived by Haselein (1998) to account the moisture content M (%) and temperature T (°C) effects:

$$k_T = k_T^{0.30} + \Delta k_T \quad (13a)$$

$$k_T^{0.30} = 4.86 \cdot 10^{-8} \rho^2 + 4.63 \cdot 10^{-5} \rho + 4.38 \cdot 10^{-2} \quad (13b)$$

$$\Delta k_T = 4.9 \cdot 10^{-3} M + (1.1 \cdot 10^{-4} + 4.3 \cdot 10^{-5} M)(T - T_{exp}) \quad (13c)$$

with T_{exp} being the average experimental temperature used in the measurements of thermal conductivity (here, 30 °C).

Suggested R&D topics include:

- What is the contribution of thermal conductivity to the increase of temperature inside the mat?
- What is the thermal conductivity of modern-day fibre and particle mattresses?

3.3.5.2 Specific heat

The specific heat of the mat is the amount of heat necessary to increase the temperature of one unit of mass by one degree in (C or K). It is generally estimated by adding the specific heat of dry wood and that of water according to the material porosity and assuming full saturation. The **specific heat** C_p (J/(kg·K)) increases with temperature T(K) and moisture content M(%) as derived by Siau (1984):

$$C_p = 4180 \frac{0.268 + 0.0011(T - 273.15) + M}{1 + M} \quad (14)$$

This expression was used by Carvalho *et al.* (1998, 2003), Pereira *et al.* (2006) and Nigro and Storti (2001). Zombori (2001) used a similar expression given by Skaar (1972):

$$C_p = \frac{\rho_d}{1000} \frac{0.268 + 0.0011(T - 273.15) + \frac{\rho_b + \rho_v}{\rho_d}}{0.293} \quad (15)$$

where ρ_d , ρ_v and ρ_b are respectively, the density of dry-wood, air and bound water in kg/m³. Thoemen (2000) and Thoemen and Humphrey (2006) used an expression from Haselein (1998) derived using a mixture rule to account for moisture:

$$C_p = \frac{1131 + 4.19T + 4190M}{1 + M} \quad (16)$$

Fenton *et al.* (2003) and Lee *et al.* (2006) calculated the specific heat (J/kg·°C) using an expression from Simpson (1999) only in function of temperature (°C):

$$C_p = 103.1 + 3.86(T + 237.15) \quad (17)$$

Suggested R&D topics include:

- New correlations are needed for mat specific heat for different types of furnish

3.3.5.3 Permeability

The rate of **convective heat transfer** to the panel core is controlled by its **permeability** in thickness direction. Permeability in the plane of the board also controls the flow of vapour to the panel edges (Hood, 2004). In the transverse direction, the permeability of WBPs is highly dependent on panel densification. So, this property will change during the hot-pressing operation; during the press closure the permeability is high, after press closure the permeability will be considerably lower and when the venting begins, the press opens slowly, generating additional gaps between particle/fibres and thus increasing the permeability.

This property is dependent on panel structure which in turn is a function of the size and form of particles/fibres, density of wood and the degree of the compression of the mat. Due to the pore structure, the transverse permeability is usually very much higher than the longitudinal

permeability and very much higher than the transverse permeability of the wood from which the board is made, which seems to indicate that permeability is mainly determined by the pores between the wood particles in the mat, than by the particles themselves (Denisov *et al.*, 1975; Bolton and Humphrey, 1994). In a strand mat there are relatively wide particles, and the gas must move around the particles and not through them. It will follow the path of least resistance and so in the transverse direction the OSB strands tend to hinder gas flow because they lie flat in the plane of the panel, whereas gas flow parallel to the plane can follow the edges of strands rather than having to go around them. Hood (2004) measured the **permeability** through the mat thickness and in the plane of OSB mats (with no vertical density profile) as a function of compaction ratio and flake thickness. He found that the permeability through the thickness of the mat was highly dependent on **compaction ratio** (mat density to wood density) and to a lesser extent on flake thickness (Hood *et al.*, 2005). A high **compaction ratio** implies a larger compression strain of the particles and thus smaller and fewer gaps between particles (Kamke, 2004). **Permeability** in the plane of the mat decreases also with increasing compaction ratio, but in a less severe manner than through the mat thickness. Transverse and in-plane permeabilities were higher for mats comprised of thicker flakes, which is thought to be caused by a reduction in flow-path tortuosity.

The density of wood species can also influence **permeability**; for the same target panel density, high density wood species lead to high mat permeabilities than low-density wood species. Several authors presented data for the specific permeability of particleboard in the thickness direction as a function of board density (Bowen, 1970; Sokunbi, 1978; Humphrey, 1982). Carvalho and Costa (1998) fitted an exponential curve to the data presented by Humphrey and Bolton (1989) for **transverse permeability** of particleboard (in m^2) as a function of mat density (in kg/m^3):

$$K_{gz} = 1.74 \cdot 10^{-12} \exp(-0.806 \cdot 10^{-3} \rho_{mat}) \quad (18)$$

This expression was also considered by Zombori (2001) and also by Nigro and Storti (2001). Fenton *et al.* (2003) used the following expression derived by Marceau (2001) to calculate the cross-sectional permeability of an OSB mat:

$$K_{gz} = 10^{-15} \exp(14.444 - 0.0192 \rho_{OSB}) \quad (19)$$

To estimate the **longitudinal permeability**, Humphrey and Bolton (1989) established a ratio of 59:1 between the permeabilities parallel and normal

to the board plane. In the absence of a more reliable relationship (the parallel data was based on permeability measurements on extruded particleboard), other researchers have used this ratio (Carvalho and Costa, 1998; Carvalho *et al.*, 2003; Nigro and Storti, 2001; Zombori, 2001; Zombori *et al.*, 2003; Fenton *et al.*, 2003; Lee *et al.*, 2006).

Thoemen (2000) and Thoemen and Humphrey (2006) used two alternative sets of permeability data obtained by Haselein (1998) and von Haas *et al.* (1998) for MDF mats. Both sets of data give permeability (in m^2) as a function of density (in kg/m^3) and expressed also by an exponential equation of the form:

$$K_{gz} = \exp(a + b\rho + c / \ln \rho) \quad (20)$$

The coefficients a, b and c are presented in Table 3.2.

Table 3.2. Coefficients a, b and c of equation 20.

Flow direction		a	b	c
Haselein (1998)	in-plane	-0.006	2.95×10^{-6}	-0.199
	cross-sectional	-0.026	4.98×10^{-6}	-0.074
von Haas <i>et al.</i> (1998)	in-plane	-0.041	9.51×10^{-6}	-0.015
	cross-sectional	-0.037	1.10×10^{-5}	-0.037

Pereira (2002) and Pereira *et al.* (2006) used the same expression with the coefficients of von Haas *et al.* (1998) to calculate the in-plane and the cross-sectional permeabilities of a MDF mat.

Suggested R&D topics include:

- How do the geometry, alignment and size of particles (fines, strands) affect mat permeabilities?
- When wood crosses the glass transition temperature, what changes in mat permeability will take place?

3.3.5.4 Diffusivity of water vapour

Water vapour diffusion occurs due to a partial pressure in the voids of the mat. The interdiffusion coefficient of an air-vapour mixture (binary diffusion coefficient) is calculated by the following semi-empirical equation (Stanish, 1986), in m^2/s :

$$D_{va} = 2.20 \cdot 10^{-5} \left(\frac{101325}{P} \right) \left(\frac{T}{273.15} \right)^{1.75} \quad (21)$$

with the gas pressure P in Pa and temperature T in K. This equation was used by several researchers, who studied the heat and mass transfer in wood-composite mats (Carvalho and Costa, 1998; Carvalho *et al.*, 2003; Nigro and Storti, 2001; Zombori, 2001; Zombori *et al.*, 2003; Fenton *et al.*, 2003; Lee *et al.*, 2006). Thoemen and Humphrey (2006) used a similar expression based on data presented by Cussler (1984).

To estimate the **effective diffusivity of steam** in air within the voids of a wood composite mat, it is necessary to account for the porous structure and the tortuous path. The following expression was then considered, in which the diffusivity is reduced by the square of porosity (ε) and is multiplied by a tortuosity factor (ζ):

$$D_{eff} = \frac{\varepsilon^2}{\zeta} D_{va} \quad (22)$$

Pereira *et al.* (2006) considered an empirical **tortuosity factor** equal to 2 in both the vertical and horizontal directions. Hata *et al.* (1990) used the following expression for the effective diffusivity of steam in the thickness direction for a particleboard:

$$D_{eff} = 0.1D_{va} \quad (23)$$

In the horizontal directions, Hata *et al.* (1990) considered that the **diffusivity of steam** among the particles is equal to that in open air: $D_{vx} = D_{vy} = D_a$. Stanish *et al.* (1986) used an attenuation factor α to account for closed pores resulting from the cellular nature of the solid:

Zombori (2001) set this attenuation value to 0.5 in both the vertical and horizontal directions, assuming that the pathway is similar for steam diffusion horizontally and vertically in the mat structure. Fenton *et al.* (2003) and Lee *et al.* (2006) used the same value.

The **diffusivity of steam** decreases during the consolidation of the mat due to an increase in board density. Jensen and Emmeler (1996) obtained the diffusivity of steam in the transversal direction of MDF mats with different densities, at ambient temperature. Carvalho (1999) fitted this data and obtained the following equation:

$$D_{eff} = \alpha \varepsilon^2 D_{va} \quad (24)$$

Zombori (2001) set this attenuation factor (α at a value of 0.5 in both the vertical and horizontal directions, assuming that the pathway is similar for steam diffusion horizontally and vertically in the mat structure. Fenton *et al.* (2003) and Lee *et al.* (2006) used the same value.

The **diffusivity of steam** decreases during the consolidation of the mat due to an increase in board density. Jensen and Emmeler (1996) obtained the diffusivity of steam in the transversal direction of MDF mats with different densities, at ambient temperature. Carvalho (1999) fitted this data and obtained the following equation:

$$D_v = 1.72 \cdot 10^{-4} - 6.21 \cdot 10^{-8} \rho_s - 1.06 \cdot 10^{-10} \rho_s^2 \quad (25)$$

Thoemen and Humphrey (2006) considered that a porous medium offers a resistance to molecular gas diffusion that can be expressed by an obstruction factor k_d . They used experimental data obtained in steady-state experiments on MDF samples (with homogeneous density profiles) fitted by an exponential equation, relating the dimensionless obstruction factor in the cross-sectional direction with the material density (kg/m^3):

$$k_d = 0.334 \exp(5.08 \cdot 10^{-3} \rho) \quad (26)$$

3.3.5.5 Diffusivity of bound water

It is believed that bound water flux by diffusion through the particles and fibres is small compared to the movement of water by convection. So, many researchers have neglected this mechanism (Carvalho *et al.*, 2003; Nigro and Storti, 2001).

Bound water diffusivity was determined by Stanish *et al.* (1986). With the lack of more reliable data, several researchers (Zombori, 2001; Pereira, 2002; Pereira *et al.*, 2006) considered the bound water diffusivity to be constant and equal to the same value given by Stanish *et al.* (1986), for the temperature and moisture content range expected during hot-pressing:

$$D_b = 3 \cdot 10^{-13} \text{kg/sm}^3 \quad (27)$$

3.3.5.6 Thermodynamic relationships

The description of heat and mass transfer during drying and hot-pressing needs some thermodynamic relationships. The most important of these as

used by several researchers for modelling these operations, are given in the following pages.

The heat of vaporisation of water (in J/kg) as a function of temperature (in K) can be given by the Clausius-Clapeyron equation:

$$\lambda = 2.511 \cdot 10^6 - 2.48 \cdot 10^3(T - 273.15) \quad (28)$$

As an alternative, Stanish *et al.* (1986) fitted a polynomial to steam tables and obtained:

$$\lambda = 2.792 \cdot 10^6 - 160T - 3.43T^2 \quad (29)$$

The enthalpy of air, steam and bound water can be calculated using the following expressions (Stanish *et al.*, 1986; Zombori *et al.*, 2003). The enthalpy of air as a function of temperature is:

$$H_a = C_{p \text{ air}}(T - 271.15) \quad (30)$$

where $C_{p \text{ air}}$ is air heat capacity (1000 J/(kgK)).

The enthalpy of water vapour can be calculated as (Stanish *et al.*, 1986; Zombori *et al.*, 2003):

$$H_v = 1.65 \cdot 10^6 + 1950T - 2070T_{dp} - 3.43T_{dp}^2 \quad (31)$$

where the temperature of the dew point as a function of the vapour partial pressure (P_v in Pa) is described by:

$$T_{dp} = 230.9 + 2.10 \cdot 10^{-4}P_v - 0.639\sqrt{P_v} + 6.95\sqrt{P_v^3} \quad (32)$$

The differential enthalpy of bound water at any concentration is equal to the free water enthalpy minus the differential heat of sorption. For wood, Stanish *et al.* (1986) assumed that the differential heat of sorption varies quadratically with **bound water content** and at zero bound water content is equal to 40 % of the heat of vaporization:

$$H_p = C_{pw}(T - 273.15) - 0.4\lambda \left(1 - \frac{\rho_b}{\rho_b^{fsp}} \right) \quad (33)$$

where C_{pw} is the specific heat of water (4180 J/(kgK)) and ρ_b^{fsp} is the bound water density at FSP. At full saturation, the differential enthalpy of bound water reaches a maximum and decreases as the bound water is

depleted. Fenton *et al.* (2003), Lee *et al.* (2006) and Zombori *et al.* (2003) used this relationship.

The enthalpy of dry wood (in J/kg) can be estimated as (Stanish *et al.*, 1986):

$$H_{wood} = 1.360(T - 273.15) \quad (34)$$

Fenton *et al.* (2003) and Lee *et al.* (2006) used an expression by Simpson and Tenwolde (1999).

$$H_{wood} = 103.1T + 1.93335T^2 \quad (35)$$

The differential heat of desorption (in J/kg) for the wood-water system depends on the moisture content (M) according to the equation of Bramhall (1979) and this expression was used by Humphrey (1982), Carvalho and Costa (1998), Carvalho *et al.* (2003), Pereira *et al.* (2006):

$$Q_l = 1.176 \cdot 10^6 \exp(-0.15M) \quad (36)$$

Thoemen *et al.* (2006) used an equation, presented by Humphrey and Bolton (1989a) which includes both the heat of sorption (equation 36) and the latent heat of vaporisation (equation 28).

The **saturation vapour pressure** can be adequately described by the following expression fitted to the data of Keenan and Keyes (1936):

$$\log P_{sat} = 10.745 - \frac{2141.0}{T} \quad (37)$$

The **viscosity of water vapour** (in Pa s) as a function of temperature (in K) can be calculated using an expression derived by Humphrey and Bolton (1989a) who fitted an equation from Sutherland (1893) to experimental data from Keenan and Keyes (1966):

$$\mu_v = 1.12 \cdot 10^{-5} - \frac{T^{1.5}}{(T - 273.15) + 3211.0} \quad (38)$$

This expression was used by several researchers (Pereira *et al.*, 2006; Thoemen and Humphrey, 2006). Thoemen and Humphrey (2006) used the same approach and derived the viscosity of air:

$$\mu_a = 1.37 \cdot 10^{-6} - \frac{T^{1.5}}{(T - 273.15) + 358.9} \quad (39)$$

Fenton *et al.* (2003) and Lee *et al.* (2006) used expressions from the Perry's Chemical Engineers handbook. The **viscosity** of the air-vapour mixture was obtained from a linear combination of the component viscosities weighted by the mole fraction in the mixture (Thoemen and Humphrey, 2006; Fenton *et al.* 2003; Lee *et al.*, 2006).

3.4 HEAT AND MOISTURE TRANSFER IN CONDITIONING

3.4.1 Introduction

Upon leaving the press, most boards are cooled, generally in a star cooler. This is the case for WBP bonded with amide-based resins because cooling minimises hydrolysis of the adhesive, but also to facilitate the subsequent sanding operation. Cooling is also thought to help balance moisture content distribution and stresses. After a pre-calibration in sanders, boards are stored as packs for conditioning. Other boards, generally bonded with phenolic resins, but also with special formulations of UF resins are hot-stacked. This operation serves to equalize differences of temperature and moisture content, but also to complete the cure of the resin. WBPs like MDF, particleboard or OSB leave the hot-press with surface temperatures of about 210 °C and above. However, resin is not completely cured especially at the core layers and for PF resins, which need more time to cure compared with UF or MUF.

Existing know-how about the effects of this operation is based on 30 year-old investigations, but nowadays this knowledge is of limited use, because significant advances have occurred with respect to process technology and resin systems (Ohlmeyer and Kruse, 1999). Moreover, there is rather little fundamental literature research that could be useful to understand the mechanisms of heat and mass transfer during the conditioning (hot stacking and normal stacking).

3.4.2 Internal Conditions during Conditioning

The temperature, moisture content and vapour pressure changes dynamically during hot pressing, but it continues during the **hot-stacking or normal stacking** (after cooling). When leaving the hot press, board temperature decreases rapidly, especially at the surface layers so that very quickly the temperature of the surface layers is lower than the core layers (see Figure 3.12). In addition, the moisture content of the surface layers is considerably lower than that of the core layers.

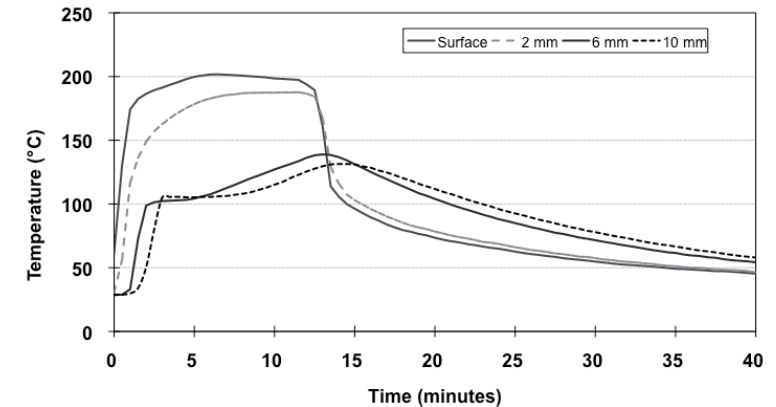


Figure 3.12: Temperature variation in a mattress pressed to 20 mm at 200°C (data collected by Mark Irle).

Measurement of the internal conditions of boards during conditioning could be useful not only for predicting the final board properties through modelling and simulation, but also to the development of new resin formulations. However, few studies have focused on this step. Ohlmeyer and Kruse (1999) measured the temperature and moisture content in different layers for **normal stacked** (initial temperature around 60 °C) and hot-stacked UF-panels (initial temperature around 90 °C) and for **hot-stacked** PF boards (initial temperature around 100 °C). They observed that when storing UF-panels in a stack, the temperature decreases slowly and it took up to 10 days to cool the panels in the centre of the stack to room temperature. The temperature in the outer parts of the stack decreased at a much faster rate. When the boards were separated for sanding and re-stacked in smaller stacks, the cooling rate increased. On the other hand, they observed that moisture content changed only marginally when boards are stored in a stack and that the differences in moisture content between the layers of hot-stacked panels was lower when compared with normal stacked panels. During the transport from the press outlet via the cross-cut saw to the cooling zone convection due to the movement causes a surface temperature decrease. When boards are lying in the cooling zone the surface temperature can increase again due to heat flux from the core.

3.4.3 Relevant Heat and Mass Transfer Mechanisms

During **hot stacking and normal stacking**, heat will be transferred by convection driven by a temperature gradient between and within panels in the stack and the environment. Inside the stacks, heat will be mainly transferred by **conduction**. The use of controlled temperature air could accelerate heat transfer by **convection** and thus panel cooling. Handling of the panels to smaller stacks could result in a faster heat transfer, due to an increase of the ratio surface area to volume of the stack. Initial stack temperature will also affect heat transfer. In hot stacking, heat transfer is faster at surface than at core layers, while in normal stacking, differences between the layers on temperature drop rate are not significant.

Mechanisms for **mass transfer** during hot stacking and normal stacking include **bulk flow of gas** (air and water vapour) from the board to the environment and **moisture diffusion** inside the stack. For hot-stacking, when the total pressure gradients are significant, convection is still an important mechanism for moisture movement, while for normal stacking when the total pressure gradients have decreased, diffusion will become more significant. The migration of water towards the surface will be mostly due to a chemical potential gradient. So, **hot-stacking** will result also in a faster moisture movement inside the panel, due to the decreasing resistance to diffusion with increasing temperatures and the increased rate of water desorption at higher temperatures (Haas and Fruehwald, 1999).

Suggested R&D topics include:

- Monitoring of mat conditions during hot-stacking and normal stacking
- More quantitative understanding of responses to these conditions
- Post-curing of adhesives during hot-stacking
- Influence of hot-stacking physical and mechanical properties on the final boards

3.5 DIFFUSION OF CHEMICALS

3.5.1 Introduction

The diffusion of chemicals, for example adhesives, wax and other additives during the hot-pressing of WBPs will certainly affect the properties of the final products. However, there is a lack of information, not only in the evaluation on transport properties of these substances but also about the interaction of these substances with wood during this process. The diffusion of these chemicals will depend on their physical state. In general, resin and wax are added as aqueous solutions, as well as wood preservatives and fire retardants, but in some cases they can be added in powder form. On the other hand, under the conditions they are subjected during drying, blending and hot-pressing, phase changes and reactions will produce other products, namely volatile substances such as formaldehyde and other **volatile organic compounds (VOC)**.

3.5.2 Diffusion of Resins

The amount of resin in wood composites is relatively low (usually less than 14 % by oven-dry weight of wood), but the development of bond strength due to resin cure and interaction with wood is crucial for physical and mechanical performance of the final boards. Ideally, resin cure should be sufficient by the end of the press cycle and it may continue during subsequent stages. However before gelation, the mobility of resin might have importance to its possible redistribution and penetration in wood cells during the pressing cycle.

There are some investigations about the distribution of resin in WBPs, but no fundamental studies exist about their transport processes. Brady and Kamke (1988) have studied the effect of the hot-pressing parameters on phenol-formaldehyde resin penetration by using **fluorescence microscopy** and a manual digitalisation technique. They concluded that the uniformity of resin penetration is more influenced by the natural variability of wood than by pressing conditions (temperature, moisture content, time, pressure). However, these conditions influence **resin penetration** by controlling the viscosity of resin: pressure is the driving force for **bulk flow**; moisture content and temperature have direct effect on resin viscosity. Gindl *et al.* (2002) studied the diffusion of MUF resin in cell walls of spruce wood using UV-microscope. Thumm and Grigsby (2002) achieved the simultaneous visualisation of wax and resin UF in MDF boards using a labelling technique for wax and resin and a **confocal laser scanning microscope**. They provide some clues about the movement of resin into the fibre wall. Xing *et al.* (2005) used the same

technique with a toluidine blue O staining system to study the penetration of UF resin into MDF fibres and they concluded that the penetration of resin is very easy under high moisture and temperature conditions and it is at a maximum during the second drying stage. The migration of phenol-formaldehyde resin was also studied by DMA (dynamic mechanical analysis) (Laborie *et al.*, 2002). Xu (2009) investigated resin penetration into wood particles under press conditions using FPA-FTIR spectroscopy at microscopic scale. She found that PMDI penetrates much deeper into the cell structure than UF.

The movement of the resin inside the board during the hot pressing operation is linked to resin properties such as **resin “flow”** and **viscosity**, but also with mat properties such as permeability, density and moisture content. **Resin “flow”** is the ability of a resin to remain fluid under heat and pressure, wetting new surfaces and accommodating particle movement before being immobilized by loss of solvent and/or polymer growth (Maloney, 1989). The **resin curing** should normally take place after the platens have achieved target thickness. However, in some boards resin pre-cure can occur at board surfaces leading to low density surfaces. An optimum value of resin flow permits maximum board consolidation and internal bond strength, with a minimum loss of surface hardness due to resin pre-cure. On the other hand, a high resin flow can cause loss of board strength due to the excessive resin penetration into furnish. **Resin viscosity** is crucial in the application process (spraying and blending), but will also influence the permeability. Some adhesives are sensitive to the relationship between the liquid carrier content and the cross-linking reaction: if the carrier is removed too rapidly the adhesive molecules will not have the mobility necessary for optimum cure. If the carrier is removed too slowly full cure may not be achieved. So permeability will affect the transport of resin carrier and thus the bond quality.

Suggested R&D topics include:

- How much resin penetrates in wood during the blending operation or during hot-pressing?
- How does resin mobility affect curing and bond strength development?

3.5.3 Diffusion of Wax and Other Additives

Wax only affects the absorption of liquid water and not of water vapour. The initial penetration of liquids in board is through the voids between the particles or fibres, which can be considered as irregularly shaped capillaries. So, the liquid water will enter the board mainly due to

capillary forces. Capillary pressure increases with decreasing capillary radius and decreases with increasing liquid contact angle. So, the sizing agents will decrease the surface wettability, thus decreasing the capillary forces.

During the hot-pressing and stacking, the flow of wax can occur if the temperature is above the melting point of the wax for a sufficiently long time. In general, longer press times and hot-stacking helps the wax efficiency. However, it is also necessary that the wax particles adhere to wood. For this, it is necessary that the water present in the emulsion is absorbed by wood, leaving the wax surrounded by the surfactant at the surface. Secondly, it is necessary that the surfactant releases wax particles to permit that the wax adheres to wood. This mechanism will depend upon the more or less complete destruction of the surfactant in the hot press cycle (Maloney, 1989). Thumm and Grigsby (2002) observed that if the wax is applied first and then the resin in MDF fibres, the wax will reduce the movement of resin into the fibre wall if it forms a layer over part of fibre surface.

An optimal wax emulsion should minimize water absorption and thickness swelling, but also hydrocarbon emissions without affecting other properties as **internal bond** (Eckert and Edwardson, 1998). So, the evaporation of hydrocarbons from wax will occur during the **hot-pressing** and could lead to fires above the press due to accumulation of hydrocarbons in the ventilation system. The diffusion of these chemicals should be similar to other volatile compounds from wood (terpenes, alcohols) or from resins (formaldehyde).

The mass transport of **volatile compounds** occurs either by **internal diffusion** within the gas phase (air and water vapour), driven by a concentration gradient, by **convection** (bulk flow of gas) inside the mat and by convection across the surface boundary layer, driven by a difference between the concentration of the component at the surface and its concentration on bulk air. These mechanisms involve transport properties, such as the **diffusivity** of a given component, e.g. formaldehyde, into other component (as air), permeability and convective mass transfer coefficients. Mass transport coefficients from the mat to the surroundings will depend on local air flow parameters (velocity, flow regime and temperature). In near steady state conditions, e.g. **board conditioning**, it would be expected that the controlling mechanisms are the internal diffusion and the transport of vapour through the board-air inter-phase. However, during hot-pressing, first the evaporation and then the bulk flow (the water vapour will transport the volatile compounds) will be the controlling mechanisms. These volatile compounds obviously

will contribute to an increase in gas pressure inside the mat. Mat conditions will affect their transport. Moisture is an agent that will extract and transport the volatile compounds and also contribute to a faster heat transfer to the core, increasing the mat temperature (Wang and Gardner, 1999). The mat temperature will promote the formation and the diffusion of these compounds. It was observed that the total VOCs and formaldehyde emissions increase with platen temperature (Makowski and Ohlmeyer, 2006).

Other additives that are used include **preservatives** and **fire retardants**. The diffusion of these chemicals will depend on their characteristics, mostly if they are aqueous solutions. In general, preservatives are not used widely, as if they are then only for exterior boards. The recent systems are aqueous solutions and are mixed with resin, which permits an even distribution of the **preservatives** over the particles.

Fire retardants are used in some boards. In general, they are added to the furnish, in the blender, in powdered or liquid form in small quantities. They can be mixed with the liquid resin. Some, such as the borates, have high diffusivities. The salts are diffused by concentration gradients into the interior of the particles. The blender conditions but also the pressing conditions can affect the diffusion of these chemicals, in particular in systems, which contain water-soluble monomers that polymerize to an insoluble state at elevated temperature. Geimer *et al.* (1994) investigated the injection of three different gases into wood composites: a fire retardant (methyl borate), a resin catalyst (methyl formate) and an accelerator for cement-bonded panels (carbon dioxide).

Suggested R&D topics include:

- Contribution of volatile compounds (e.g. formaldehyde) to the increase in total gas pressure inside the mat relatively to water vaporization
- Is the diffusion of wax really important in affecting water sorption and resin penetration?

3.6 REFERENCES

- Aguilar, H. (2006) Study of the rheology of deformable porous media: application to paper production. PhD Thesis in Chemical Engineering, Faculty of Engineering from University of Porto, Portugal.
- Alexopoulos, J. (1999) OSB Pressing optimisation and problem solving using monitoring of temperature and gas pressure. In: Proc. of the third European panel Products Symposium. Llandudno, Wales, pp.190-208.
- Ben Nasrallah, S., Perré, P. (1988) Detailed study of a model of heat and mass transfer during convective drying of porous media. *Int. J. of Heat and Mass Transfer*, **31**(5), 957-967.
- Bird, R.B., Stewart, W.E., Lightfoot, E.N. (1966) *Transport Phenomena*. John Wiley and Sons, New York.
- Bloch, J.F. (1992) *Transfers de Masse et de Chaleur dans les Milieux Poreux deformables Non Saturés: application au Pressage du Papier*. Thèse Doctorat, Institut National Polytechnique de Grenoble, Grenoble, France.
- Bolton, A.J. and Humphrey, P.E. (1988) The Hot Pressing of Dry-formed Wood-based Composites. Part I. A Review of the Literature, Identifying the Primary Physical Processes. *Holzforchung*, **42**(6), 403-406.
- Bolton, A.J., Humphrey P.E. and Kavvouras, P.K. (1989a) The Hot Pressing of Dry-formed Wood-based Composites. Part III. Predicted Vapour Pressure and Temperature Variation with Time, Compared with Experimental Data for Laboratory Boards. *Holzforchung*, **43**(4), 265-274.
- Bolton, A.J., Humphrey P.E. and Kavvouras, P.K. (1989b) The Hot Pressing of Dry-formed Wood-based Composites. Part IV. Predicted Variations of Mattress Moisture Content with Time. *Holzforchung*, **43**(5), 345-349.
- Bolton, A.J., Humphrey P.E. and Kavvouras, P.K. (1989c) The Hot Pressing of Dry-formed Wood-based Composites. Part VI. The Importance of Stresses in the Pressed Mattress and their Relevance to the Minimisation of Pressing Time, and the Variability of Board Properties. *Holzforchung*, **43**(6), 406-410.
- Bolton, A.J., and Humphrey, P.E. (1994) The permeability of WBPs. Part 1. A Review of the Literature and some unpublished work. *Holzforchung*, **48** (Suppl), 95-100.

- Bowen, M.E. (1970) Heat transfer in particleboard during hot-pressing. PhD dissertation, Colorado State University, Corvallis, USA.
- Brady, D.A., and Kamke F.A. (1988) Effects of hot-pressing parameters on resin penetration. *For. Prod. J.*, **38**(11/12), 63-68.
- Bramhall, G. (1976) Fick's law and bound-water diffusion. *Wood Sci. and Technol.*, **8**(3), 153-161.
- Bramhall, G. (1979) Mathematical model for lumber drying I-Principles involved. *Wood Sci. and Technol.*, **12**(1), 14-21
- Carvalho L. (1999) Estudo da Operação de prensagem do Aglomerado de Fibras de Média Densidade: Prensa descontínua de pratos quentes (Study of the hot-pressing of Medium Density Fiberboard (MDF): batch platen press). PhD Thesis in Chemical Engineering, Faculty of Engineering of University of Porto, Portugal.
- Carvalho, L.H., Costa, M.R.N. and Costa, C.A.V. (2003) A Global Model for the Hot-Pressing of Medium Density Fiberboard (MDF). *Wood Sci. and Technol.*, **37**, 241-258.
- Carvalho, L.M., Costa, C.A.V. (1998) Modeling and simulation of the hot-pressing process in the production of medium density fiberboard (MDF). *Chem. Eng. Comm.* **170**, 1-21.
- Comstock, G.L. (1970) Direction permeability of softwoods. *Wood Fibre*, **1**, 283-289 (1970)
- Constant, T., Moyne, C., Perré, P. (1996) Drying with internal heat generation: theoretical aspects and application to microwave heating. *AIChE J.*, **42**(2), 359-368.
- Cussler, E.L. (1984) Diffusion. Mass transfer in fluid systems. Cambridge Univ. Press, UK.
- Dai, C., Yu, C. (2004) Heat and mass transfer in wood composite panels during hot-pressing: Part I. A physical-mathematical model. *Wood and Fibre Sci.*, **36**(4), 585-597.
- Darcy, H.P.G. (1856) *Les Fontaines Publiques de la Ville de Dijon*, Victor Dalmont, Paris.
- Deng, J., Xie, Y., Feng M. (2006) An experimental study of microwave pre-heating of an MDF fibre mat: Moisture and temperature distribution and the impact on hot-pressing. *For. Prod. J.*, **56**(6), 76-81.

- Denisov, O.B., Anisov, P., Zuban P.E. (1975) Untersuchung der Permeabilität von Spanvliesen. *Holztechnologie*, **16**(1), 10-14.
- Dorri, B., Emery A.F., Malte P.C. (1985) Drying rate of wood particles with longitudinal mass transfer. *J. of Heat Transfer*, **107**, 12.
- Droin-Josserand, A., Taverdet, J.L., Vergnaud, J.M. (1989) Modeling the process of moisture absorption in three dimensions by wood samples of various shapes: cubic, parallelepipedic. *Wood Sci. and Technol.*, **23**(3), 259-271.
- Fenton, T., Budman, H., Pritzker, M., Bernard, E., Broderick, G. (2003) Modeling of Oriented Strand Board Pressing. *Ind. Eng. Chem. Res.*, **42**, 5229-5238.
- Fhyr, C., Rasmuson (1997) Some aspects of the modelling of wood chips drying in superheated steam. *Int. J. Heat Mass Transfer*, **40**(12), 2825-2842.
- Fhyr, C., Rasmuson (1996) Mathematical model of steam drying of wood chips and other hygroscopic porous media. *AIChE J.*, **42**(9), 2497-2502.
- Fick, A (1833) On diffusion. *Annalen der Physic*, **Ser 2**, 94, 59-85.
- Fohr, J.P., (1995) Vacuum drying of oak wood. *Drying Technology*, **13**(8&9), 1675-1693.
- García, P.J. (2002) Three-dimensional heat and mass transfer during oriented strand board hot-pressing, PhD Thesis, Faculty of Forestry, The Univ. of British Columbia, Vancouver, British Columbia, Canada.
- García, P.J., Avramidis, S., Lam, F. (2001) Internal temperature and pressure response to flake alignment during hot-pressing. *Holz Roh-Werkst*, **59**, 272-275.
- García, P.J., Avramidis, S., Lam, F. (2003) Horizontal gas pressure and temperature distribution responses to OSB flake alignment during hot-pressing. *Holz Roh- Werkst*, **61**, 425-431.
- Geimer, G.L., Leão, A., Arnebruster, D., Pablo, A. (1994) Property Enhancement of wood composites using gas injection. In: *Proceedings of the 28th International Particleboard/Composite Materials Symposium*, Washington State Univ., Pullman, WA, USA, pp.243-259
- Gindl, W., Dessipri, E., Wimmer, R. (2002) Using UV-Microscopy to Study the diffusion of Melamine-Urea-Formaldehyde Resin in Cell Walls of Spruce Wood. *Holzforshung*, **56**(1), 103-107

- Gregg, S.J., Sing, J.S. (1991) Adsorption, Surface Area and Porosity, Academic Press, London.
- Haselein, CR, (1998) Numerical Simulation of pressing wood-fibre composites. Ph.D. Thesis, Oregon State Univ., U.S.A.
- von Haas, G., Steffen A. and Fruehwald, A. (1998) Untersuchungen zur Permeabilität von Faser-, Span- und OSB-Matten für Gase. Holz Roh-Werkst. **56**(6), 386-392.
- von Haas, G., and Fruehwald, A. (1998) Einfluß der Temperatur auf die Geschwindigkeit der sorptiven Wasseraufnahme von Furnieren. Holz Roh- Werkst, **57**, 77-78.
- Hata T., Kawai, S., Sasaki, H. (1990) Computer simulation of temperature behavior in particle mat during hotpressing and steam injection pressing. Wood Sci. and Technol., **24**, 65
- Hood, J., (2004) Changes in Oriented Strandboard Permeability during hot-pressing. MSc Thesis, Faculty of Virginia Polytechnic Institute and State University, Blacksburg, Virginia, U.S.A.
- Hood, J.P., Kamke, F.A., Fuller, J. (2005) Permeability of oriented strandboard mats. For. Prod. J., **55**(12), 194-199.
- Humphrey PE, (1991) Pressing issues in panel manufacture: Internal behavior during pressing and its impact on time minimization, properties and profit. In; Proceedings of the International Particleboard Symposium, Pullman, WA, USA, pp.99-108.
- Humphrey, P.E. (1982) Physical aspects of wood particleboard manufacture. Ph.D. Thesis, Univ. of Wales, U.K.
- Humphrey, P.E. and A.J. Bolton (1989a) The Hot Pressing of Dry-formed Wood-based Composites. Part II: A Simulation Model for Heat and Moisture Transfer, and Typical Results. Holzforschung, **43**(3), 199-206.
- Humphrey, P.E. and A.J. Bolton (1989b) The Hot Pressing of Dry-formed Wood-based Composites. Part 5 :The Effect of Board Size: Comparability of Laboratory and Industrial Pressing. Holzforschung, **43**(6), 401-405.
- Hunter, A. J. (1993) On movement of water through wood-The diffusion coefficient", Wood Sci. and Technol., **27**, 401-408.
- Incropera F.P., Witt, D.P. (1990) Fundamentals of heat and mass transfer, John Wiley & Sons, New York.

- Jensen, U., Emmeler, R. (1996) Diffusion resistance of MDF and particleboard. In: Proceedings of the 1996 International Conference on Wood Mechanics, FMFA, Stuttgart, Germany, pp. 345.
- Johansson, A., Fhyr, C., Rasmuson, A. (1997a) High temperature convective drying of wood chips with air and superheated steam. Int. J. Heat Mass Transfer, **40**(12), 2843-2858.
- Johansson, A., Fhyr, C., Rasmuson, A. (1997b) Influence of the drying medium on high temperature convective drying of single wood chips. Int. J. Heat Mass Transfer, **15**(6-8), 1801-1813.
- Kamke F.A., Wolcott, M.P. (1991) Fundamentals of flakeboard manufacture: wood-moisture relationships. Wood Sci. and Technol., **25**, 57.
- Kamke, F.A., Wilson, J.B. (1986a) Computer simulation of a rotary dryer. Part I: Retention time. AIChE J., **32**(2), 263-268.
- Kamke, F.A., Wilson, J.B. (1986b) Computer simulation of a rotary dryer. Part II: Heat and Mass transfer. AIChE J., **32**(2), 269-275.
- Kamke, F.A., Casey, L.J. (1988a) Fundamentals of flakeboard manufacture: internal-mat conditions. For. Prod. J., **38**(6), 38- 44.
- Kamke, F.A. and Casey, L.J. (1988b) Gas pressure and temperature in the mat during flakeboard manufacture. For. Prod. J., **38**(3) 41-43.
- Kamke, F.A., (2004) Physics of Hot-pressing. In: Fundamentals of Composite Processing: Proceedings of a Workshop, pp. 3-18, USDA Forest Service, General Technical Report FPL-GRT-149, Madison WI, U.S.A.
- Kamke, F.A., Watson, L.T., Lee, J-N, Shu, J. (2006) A Web-based problem solving environment for the wood-based composites industry. For. Prod. J., **56**(9), 26-32.
- Kavvouras, P.K. (1977) Fundamental process variable in particleboard manufacture, Ph.D. Thesis, Univ. of Wales, U.K.
- Keenan, J.H., Keyes, F.G. (1936) Thermodynamic properties of steam. John Wiley and Sons, London.
- Keey, R., Langrish, T., Walker, J.C. (1999) Kiln-Drying of Lumber. Springer Series in Wood Science, Springer Verlag, Berlin.

- Kocaefe, Younsi, R., Chandry, B., Kocaefe, Y. (2006) Modeling of heat and Mass transfer during high temperature treatment of aspen. *Wood Sci. and Technol.*, **40**, 371-391.
- Kollmann, F., Malmquis, L., (1956) Über die Wärmeleitzahl von Holz und Holzwerkstoff. *Holz Roh-Werkst.* **14**(16), 201-204.
- Krischer, O., Kroll, K., (1956) Die wissenschaftlichen Grundlagen der Trocknungstechnik. Springer Verlag, Berlin.
- Kuhlmann, G. (1962) Untersuchung der technischen Eigenschaften von Holz und Spanplatten in Abhängigkeit von Feuchtigkeit und Temperatur im hygroskopischen Bereich. *Holz Roh-Werkst.* **20**(7), 259-270.
- Laborie, M.P., Salmén, L., Frazier, C.E. (2002) The cooperativity analysis of segmental motion in wood adhesive interphase: A probe of nanoscale morphology. In: Proceedings, 6th Pacific-rim Bio-based composites Symposium & Workshop on the chemical modification of celluloses, Portland, Oregon, pp. 18-25.
- Lee, C., Budman, H., Pritzker, M. (2006) Simulation and Optimisation of the Continuous Oriented Strand Board Pressing Process. *Ind. Eng. Chem. Res.*, **45**(6), 1974-1988.
- Lee, J., Kamke, F., Watson, L. (2006) Simulation of the hot-pressing of a multi-layered wood strand composite. *J. of Comp. Mat.* published on line.
- Liu, J., Avramidis, S., Ellis, S. (1994) Simulation of Heat and Moisture Transfer in Wood During Drying under Constant Ambient Conditions. *Holzforshung*, **48**(3), 236-240.
- Luikov, A.V. (1966) Heat and mass transfer in capillary-porous bodies. Pergamon Press, London.
- Maku, T., Sasaki, R., Hamada, H. (1959) Studies on the particle board. Repor IV. Temperature and moisture distributions in particle board during hot-pressing. *Wood Res.* **21**, 34-46.
- Makowski, M., Ohlmeyer, M. (2006) Influences of hot pressing temperature and surface structure on VOC emissions from OSB made of Scots pine. *Holzforshung*, **60**, 533-538
- Maloney, T. (1989) Modern Particleboard and Dry-Process Fiberboard Manufacturing. 3rd Edition, Miller Freeman Publications, San Francisco.
- Marceau, P. (2001) Rapport préliminaire: perméabilité au gaz des panneaux, unpublished report.

- Meyer, N., Thoemen, H. (2007) Gas pressure measurements during continuous hot pressing of particleboard, *Holz Roh Wekst.*, **65**(1), 49-55.
- Moyne, C. (1983) Séchage. In: Le matériau bois: Propriétés, Technologie, Mise en oeuvre, A.R.B.O.L.O.R., Nancy.
- Nigro N., Storti, M. (2001) Hot-pressing process modelling for medium density fibreboard (MDF). *Int. J. Math and Math Sci.*, **26**(12), 713-7129.
- Nilsson, L., Wilhelmsson, B., Stenström, S. (1993) The diffusion of water vapour through pulp and paper. *Drying Technology*, **11**(6), 1205-1225.
- Ntalos, G., Grigoriou, (2001) Particleboards. In: State of the Art of Report of COST E13 (Wood Adhesion and Glued Products), Johansson, Pizzi, Van Leemput eds.
- Ohlmeyer, M., Kruse K. (1999) Hot Stacking and its effect on panel properties, In: Proceedings of the 3rd European Panel Symposium, pp., Llandudno, Wales.
- Pang, S. (2001) Improving MDF fibre drying operation by application of a mathematical model. *Drying Technology*, **13**(5-7), 1395-1409.
- Pang, S. and R.B. Key (1995) Drying Kinetics of Pinus Radiata Boards at Elevated Temperatures, *Drying Technology*, **19**(8), 1789-1085.
- Pereira, C. (2002) Estudos da Operação de Prensagem e Cura do Aglomerado de Fibras de Media Densidade (Studies of the Hot-pressing and Curing of Medium Density Fiberboard. PhD Thesis, Faculdade de Engenharia da Universidade do Porto, Porto, Portugal.
- Pereira, C., Carvalho, L.H., Costa, C.A.V. (2004) High Frequency Heating of Medium Density Fiberboard (MDF): Theory and Experiment. *Chem. Eng. Sci.*, **59**(4), 735-745.
- Pereira, C., Carvalho, L.H., Costa, C.A.V. (2006) Modeling the continuous hot-pressing of MDF. *Wood Sci. and Technol.*, **40**, 308-326.
- Perré, P., Degiovani, A. (1990) Simulation par volumes finis des transferts couplés en milieu poreux anisotropes. *J. of Heat and Mass Transfer*, **33**(11), 2463-2478.
- Perry's Chemical Engineers' Handbook, 7th ed.; Perry, R.H., Green, D.W., Maloney, J.O. eds.; Mc Graw Hill, New York, 1984, pp.2-320-2-322.

- Plumb, O.A., Spolek, G.A., Olmstead, B.A. (1985) Heat and mass transfer in wood during drying. *Int. J. of Heat and Mass Transfer*, **28**(9), 1669.
- Reis, P. (2009) Estudos da Operação de Prensagem e Cura do Aglomerado de Fibras de Media Densidade (Studies of the Hot-pressing and Curing of Medium Density Fiberboard). PhD Thesis, Faculdade de Engenharia da Universidade do Porto, Porto, Portugal.
- Shu, J., Watson, L.T., Zombori, B.G. (2006) WBCSim: an environment for modelling WBPs manufacture. *Engineering with Computers*, **21**, 259-271.
- Shusheng, P., Keey, R.B. (1995) Modelling the temperature profiles within boards during the high-temperature drying of *Pinus radiata* timber: the influence of airflow reversals. *Int. J. Heat and Mass Transfer*, **38**(2), 189-205.
- Siau, J.F. (1984) *Transport process in wood*, Springer-Verlag, Berlin.
- Siau, J.F. (1995) *Wood. Influence of moisture on physical properties*. Virginia Polytechnic Institute and State University, NY.
- Simpson, W. T. (1993) Determination and use of moisture diffusion coefficient to characterize drying of northern Red oak (*Quercus rubra*). *Wood Sci. and Technol.*, **27**, 409-420.
- Simpson, W., TenWolde, A. (1999) *Physical Properties and Moisture Relations of Wood*. In: *Wood Handbook-Wood as an Engineering material*, USDA Forest Service, Forest Products Laboratory, Madison, WI, USA.
- Simpson, W.T. (1983-84a) Drying wood: a review. I. *Drying Technology*, **2**(2), 235-264.
- Simpson, W.T. (1983-84b) Drying wood: a review. II. *Drying Technology*, **2**(3), 353-368.
- Skaar, C. (1972) *Water in wood*. Syracuse University Press, Syracuse, New York.
- Smith, T.M. (1994) Heat transfer dynamics. *Tappi J.*, **77**(8), 239-245.
- Sokunbi, O.K. (1978) Aspects of particleboard permeability. M.Sc. Thesis, Univ. of Wales, U.K.
- Spolek, G.A., Plumb, O.A. (1964) A numerical model of heat and mass transfer in wood during drying, *Drying'80*, vol 2, In: *Proceedings of the*

- Second International Symposium on Drying*, Mac Graw Hill University, pp. 84-92.
- Stamm, A.J. (1959) Bound-water diffusion into wood in the fiber direction. *For. Prod. J.*, **9**(27), 27-32.
- Stamm, A.J. (1964) *Wood and Cellulose Science*. Ronald Press, New York.
- Stanish, M. A., Schajer G. S., Kayihan, F. (1986) A mathematical model of drying for hygroscopic porous media, *AIChE J.*, **32**(8), 1301.
- Steffen A, Haas, G., Rapp, A., Humphrey, P., Thoemen, H. (1999) Temperature and Gas Pressure in MDF-mats during Industrial Continuous Hot-Pressing. *Holz Roh- Werkst.*, **57**, 154-155.
- Strickler, M.D. (1959) The effect of press cycles and moisture content on properties of Douglas fir flakeboard, *For. Prod. J.*, **9**(7), 203-207.
- Sushland, O. (1967) Behaviour of particleboard mat during the press cycle. *For. Prod. J.*, **17**(2), 51-57.
- Sutherland, W. (1893) The viscosity of gases and molecular force. *The London, Edinburgh, and Dublin Philosophical Mag. Journ. Sci.*, **36** (fifth series)(223), 507-531.
- Thoemen H., Humphrey P.E. (2003) Modeling the continuous pressing process for wood-based composites. *Wood and Fibre Sci.*, **35**, 456-468.
- Thoemen, H., Humphrey, P.E. (2006) Modeling the physical processes relevant during hot pressing of wood-based composites. Part I. Heat and Mass transfer. *Holz Roh- Werkst.*, **35**, 456-468.
- Thoemen, H. (2000) *Modeling the Physical Processes in Natural Fibre Composites During Batch and Continuous Pressing*. Ph.D. Thesis, Oregon State Univ., USA.
- Thoemen, H., Humphrey, P. (2001) Hot pressing of wood-based composites: selected aspects of the physics investigated by means of a simulation. In *Proceedings of The Fifth European Panel Products Symposium*, Llandudno, Wales, UK, pp. 18-30.
- Thoemen, H., Humphrey, P.E. (1999) The Continuous pressing process for WBPs: an analytical model. In: *Proceedings of The Third European Panel Products Symposium*, Llandudno, Wales, UK, pp. 18-30.
- Thumm, A., W. Grigsby (2002) Interaction of wax and UF resin in MDF: quantitative analysis of the relationships between wax and resin on MDF

fibres. In: Proc. of the Sixth European Panel Products Symposium, Llandudno, Wales, UK, pp. 51-59.

Torgovnikov, G.I. (1993) Dielectric Properties of Wood and Wood-Based Materials. Springer-Verlag, Germany.

Wang, W. and Gardner, D. (1999) Investigation of volatile organic compound press emissions during particleboard production. For. Prod. J., **49**(3), 65-72.

Ward, R.J., Skaar, C. (1963) Specific heat and conductivity of particleboard as a function of temperature. For. Prod. J., **13**(1), 32.

Whitaker, S. (1977) Simultaneous heat, mass and momentum transfer in porous media: a theory of drying. Advances in Heat Transfer, **13**, 119-203.

Winistorfer, P.M. (2000) Fundamentals of vertical density profile formation in wood composites. Part I. In-situ density measurement of the consolidation process. Wood and Fibre Sci., **32**(2), 209-219.

Wolcott, M.P., F.A. Kamke, D.A. Dillard (1990) Fundamentals of flakeboard manufacture: viscoelastic behavior of the wood component. Wood and Fibre Sci., **22**(4), 345-361.

Xing, C., Riedl, B., Cloutier, A., Shaler, S. (2005) Characterization of urea-formaldehyde resin penetration into medium density fiberboard fibres. Wood Sci. and Technol., **39**, 374-384.

Xu, Yan (2009) Investigations on adhesive bonding of wood and particle boards using UF resins and PMDI (in German). PhD Thesis, Technical University, Faculty of Life Sciences, Braunschweig, Germany

Yrjölä, J., Saatanainen, J.J. (2002) Modelling and practical operation results of a dryer for wood chips. Drying technology, **20**(6), 1077-1099.

Zombori B. (2001) Modeling the transient effects during the Hot-Pressing of Wood-based Composites. PhD Thesis, Faculty of the Virginia Polytechnic Institute and State University, Blacksburg, Virginia, USA.

Zombori B, Kamke, F.A., Watson, L.T. (2002) Simulation of the internal conditions during the hot-pressing process. Wood and Fibre Sci., **35** (1), 2-23.

Zombori B, Kamke, F.A., Watson, L.T. (2002) Sensitivity analysis of internal mat environment during hot-pressing. Wood and Fibre Sci., **35** (1), 2-23.

Chapter 4

Advanced Imaging Techniques in Wood-Based Panels Research

Lech Muszyński and Maximilien E. Launey

CHAPTER SUMMARY

Although **numerical modelling** seems to be a promising tool in virtual prototyping of new composite materials, the prevailing empirical practice does not adequately address the complexity of **bio-based materials** such as wood **composites**, and the outputs are generally incompatible with the requirements of contemporary modelling tools. The innovative material characterization techniques based on **advanced imaging** technologies and **inverse problem methodology** seem particularly suitable for complex heterogeneous **composites**.

Advanced **image analysis** techniques provide new means for quantitative characterization of **wood-based** composite materials. Particularly non-destructive methods based on **computed tomography** yield an unprecedented insight in the morphology and micromechanics of **particulate composites**, which enables a new comprehensive approach to experimental determination of material characteristics. Combination of **full-field measurements** with **inverse problem methodology** brings the material testing on new level of efficiency by removing many limitations of the traditional test methods. Such integrated approach to material characterization supports development of morphology-based **numerical modelling** for rapid prototyping of new enhanced materials and manufacturing processes.

4.1 INTRODUCTION

Wood-based composites, and prominently panel products are examples of complex, anisotropic, and heterogeneous materials, which allow various levels of flexibility in engineering their properties to the requirements of the final use. A key to securing the leading position in the market is not only developing stronger and more durable materials, characterized by mechanical performance carefully tailored to the requirements of the end use, but ability to bring breakthrough innovations e.g. in the technology, which would allow widening sustainable raw material base. In developing enhanced manufacturing processes, new

adhesive formulations and **bonding** techniques the focus is on the **internal bond**, providing composite integrity and mechanical performance. However, despite long history of research in this area relatively little is known on the actual **micro-mechanical** interaction between the adhesive and wood within the **bond interphase**. While contemporary adhesive formulators are capable of engineering the interaction between the adhesive and constitutive wood polymers on the molecular level, the **micro-mechanics** of the **bond** on the scale of wood anatomical features is rarely considered as a diagnostic tool or even investigated. Across the industry, **bond** performance is assessed through a number of standardized tests on relatively bulk product specimens. The principle qualifying criterion may in most cases be reduced to the general requirement that the **bond** be stronger than the wood substrate. Only few of these tests return true qualitative data and none addresses the actual micromechanics of the **interphase**. Significant progress in this area requires a more holistic approach, and is hard to imagine this progress occurring without better understanding of the composite performance and **internal bond durability** on the **micro-mechanical** level, as well as reliable modelling based on that understanding (Wolcott and Muszyński 2008). In this respect, **wood-based composites** may become a model for a larger family of other **bio-particulate composites**. However, despite substantial research effort in material characterization of **wood-based composites**, reliable modelling poses a significant challenge. The principle obstacles are the inherent complexity of the raw material (various grades of wood: veneer sheets, strands, particles, fibres) and of the composite interaction in the **internal bond** on the **micro-mechanical** level, as well as that the body of quantitative knowledge generated in the field is hardly compatible with the required inputs of available modelling tools.

The complexity of the internal structure and the compatibility of the experimental output with the requirements of the contemporary modelling techniques can be effectively addressed by application of **advanced imaging techniques** coupled with **numerical modelling** of the composite structure.

“**Imaging techniques**” is a collective name used to refer to all kind of experimental techniques recording data in form of two- or three-dimensional images. In most general sense, this category includes micrographs from light, electron or atomic force microscopes, radiographs, images acquired from thermographic cameras, ultrasonographs, as well as three-dimensional data acquired via **medical** and industrial **computed tomography (CT)** based on x-ray or gamma radiation, nuclear magnetic resonance and other techniques. Their

common denominator is the format of the output: features visible and hidden for human eye are represented as visual maps of light intensity and/or colour for the researchers to behold and analyze.

For many years, increasingly **advanced imaging techniques** have been used as a primary or supporting reference tool providing invaluable insight in the internal structure of biological systems and complex materials. With time, cameras fitted on light or fluorescent microscopes became a commonplace. Electron scanning microscopes and **CT** scanning devices are becoming more accessible, less expensive and more common, too. In most cases, however the actual use of images generated by those techniques had not extended beyond visual inspection and qualitative assessment of features within the **field of view** by an expert eye. This approach is quite effective in fields of research where conclusions can be drawn based on comparison of certain visible aspects or characteristics in the analyzed images to a standard image of the same object, or where existence (or not) of such characteristics can inform the decision making process. This is for instance the case when finished surfaces are visually compared to a standard, or when a presence of visible checks, knots and repairs is a base of disqualification of plywood sheets from decorative grades. Visual inspection is however much less effective when quantification of the findings (counting multiple objects, measurements etc.) is of interest, like for instance when the level of discoloration or the size of knots and checks is to be measured, and their number within the **field of view** counted.

The value of the output generated by **imaging techniques** goes far beyond what is available for visual inspection. Information coded in digital images can and is being harnessed more effectively by application of advanced, quantitative **imaging techniques** coupled with tools for automatic image processing and analysis. These techniques seem to be particularly suitable to address the complexity of the internal structure of **wood-based** products. They also have a potential for bridging the gap between experimentation and modelling in the area of **wood-based** panel products.

In this chapter, opportunities and principal challenges to bridging experimentation and modelling with **advanced imaging techniques** in the area of **wood-based composites** research are discussed. Several of promising material characterization techniques based on **advanced imaging** technologies and **inverse problem methodology**, which seem particularly suitable for providing necessary input data for numerical models are also presented.

4.2 VIRTUAL PROTOTYPING: OPPORTUNITIES AND CHALLENGES

Numerical models are important tools for discovery. Scientific models are being created to **predict** behaviour of physical objects and phenomena of various level of complexity. Numerical models are used for prototyping and virtual testing of hypotheses and are particularly desirable whenever physical tests are too complex, impractical, or too expensive. Accurate models capable of correlating our understanding of how various processing regimes and treatments affect morphology and **micro-mechanics** of the **composites** with their bulk properties and service performance would be critical for prototyping and developing new, advanced **bio-based materials** and products. Such models would be also important tools for improving properties of those already present on the market.

It is not surprising then, that modelling many aspects of physical and mechanical nature of **wood-based** materials has been in focus of quite vigorous research activity. In his bibliography of **finite element** (FEA) modelling in wood research Mackerle (2005) lists more than 260 papers published just in one decade between 1995 and 2004.

However, actual implementation of virtual prototyping based on material modelling to development of new and improved **wood-based** panels still seems to be a concept from the future. Two principal obstacles seem to be the inherent complexity of the internal structure of **wood-based composites** and the incompatibility between the outputs of contemporary testing approaches commonly used in wood **composites** research and the input requirements of most numerical models.

4.2.1 Levels of Complexity in the Internal Microstructure of the Composites

Modelling of complex heterogeneous particulate **bio-based composites** is not a trivial task. In the case of **wood-based composites**, with one exception for plywood, the naturally variable wood structure is reduced to small irregular units (wafers, strands, particles, fibres), henceforth addressed collectively as particles, characterized by wide distribution of geometries and sizes. The original cellular structure of wood is disrupted and modified to various degrees during the comminution process, and further during the consolidation, which particularly for panel products includes hot-pressing under dynamic temperature and changing moisture content conditions.

Another level of complexity comes from the new arrangement of these particles in the composite, which although not entirely random, is nevertheless far from deterministic (Zhou et al. 2008). The rearranged microstructure will also include additional voids in inter-particle spaces, cured adhesive or, in case of **wood plastic composites**, a continuous polymer matrix. In the most general case the resulting size, shape, orientation and distribution of the component elements (strands, particles, fibres, adhesive and voids) are of interest for **predicting** the bulk properties of the **composites**. All of the morphological characteristics listed above are best described in statistical terms, and the description must be based on large number of measurements. Because of the metamorphosis the particles undergo in the consolidation process, **in situ characterization** would be preferred as input for reliable numerical models.

These models must also address the **internal bonding**, which provides integrity to the reconstituted **composites** and facilitates load transfer between the components. In most **wood-based composites**, the **bonding** is provided by polymer adhesives, which do not form a distinct continuous matrix assumed by most composite theories. In addition, models developed for synthetic and mineral **composites** assume that the **bond** is formed on a well defined **interface** between the impermeable components. This is certainly not the case with **wood-based composites**. Instead, microscopic evidence shows a substantial **inter-phase** where the adhesive penetrates the porous cell structure on the particle perimeter (Marra 1992; Kamke and Lee 2007). Although there are many publications reporting tests on **bonds** between isolated strands (e.g. Smith 2005), fibres and properties of fibre-polymer **interfaces** (Mott et al. 1996; Shaler et al. 1997; Egan and Shaler 2000; Tze et al. 2003), the contribution of the **interphase** to the **micro-mechanical** performance of the **internal bond**, and the performance of the composite as a whole are not completely understood.

Such complexity may be best addressed through **multi-scale modelling**, which refers to correlation of phenomena and properties observed on various levels of material organization (load transfer through the **interphase**, contributions of individual particles, and properties of bulk composite).

4.2.2 Compatibility between Testing Approaches and Numerical Models

The **predictive** power of numerical models depends as much on sound constitutive theory as on reliability of the input data: morphology,

boundary conditions, and bulk characteristics of the modelled object acquired through measurement and empirical tests. In the same time, the prevailing approach in material characterization in the area of wood **composites** is that of simplified comparative tests responding to the industry's need for inexpensive tools to assess their quality against an accepted standard. In most cases however, this approach does not produce characteristics compatible with the inputs of modelling software based on the principles of theoretical mechanics. The traditional testing and measurement methods, where the bulk mechanical characteristics are determined from relatively simple analytical solutions derived for small deformations in idealized homogeneous and isotropic solids, are generally not adequate for the level of complexity found in particulate bio-**composites**. Collecting viable input data for modelling of such **particulate composites** requires better understanding and cooperation between modellers and experimentalists and may require revision of traditional testing practices and approach to material testing.

4.3 THE ADVANCED IMAGING TECHNIQUES

The complexity of the internal structure and the compatibility of the experimental output with the requirements of the contemporary modelling techniques can be effectively addressed by application of **advanced imaging techniques** and coupling them with three-dimensional **numerical modelling** of the composite structure. By contrast to the traditional methods, recent progress in modern high-resolution non-contact imaging and **full-field measurement** techniques makes it possible to explore enhanced approaches to experimental procedures. Although many of the **imaging techniques** discussed below are by no means new, the amount and value of the information carried by images is often underestimated.

There are generally two ways to approach the geometrical aspects of the composite microstructure in **morphology-based modelling**. One, often applied in **finite element method (FEM)**, is to generate the element mesh based on generalized knowledge of the **micro-structure** of the composite, where various morphological characteristics are either created explicitly using idealized average parameters, or generated using stochastic methods in order to reflect the variability of the real material in a more realistic manner. The other approach, often used in the **material point method** (to be discussed later in this chapter) is to use a digitized structure of an actual material sample as captured with one of the **imaging techniques**. Note, that also in the first approach a reliable knowledge of the variability of the morphological structure is assumed.

4.3.1 Digital Image Analysis

High resolution digital microscopy, scanning electron microscopy (SEM), **computed tomography (CT)** based on x-ray, gamma and neutron radiation (Wellington and Vinegar 1987; ASTM 2000; Macedo et al. 2002; Richards et al. 2004), nuclear magnetic resonance (NMR) relaxometry, and other advanced instruments (Park et al. 2003; Pétraud et al. 2003) return digital images carrying a wealth of spatial information coded in discrete color or greyscale values. Virtually all have been successfully used for visualization of the internal structure of solid wood (e.g. Mannes et al. 2010), and various morphological aspects in **wood-based composites**. These values representing method-specific quantities (e.g. real colours, densities, x-ray attenuation, temperatures) assigned to millions of pixels or voxels arranged in two- or three-dimensional arrays. The data may be manipulated and effectively analyzed by employment of robust algorithms for automated **image enhancement**, pattern recognition, and quantitative characterization of spatial distribution of various physical features: e.g. components, phases, inhomogeneities and void spaces resulting from various processing and loading regimes.

4.3.1.1 Image enhancement

Presence of noise in raw images obtained from various **imaging techniques** blurs the boundaries between regions and objects and may interfere with automatic processing. Therefore, prior to analysis digital images are often subjected to **image enhancing** procedures like noise removal, edge and contrast enhancement. Despite the conceptual similarity of **image enhancement** to one-dimensional signal filtering not all one-dimensional signal processing techniques do naturally extend to higher dimensions (Mallat 1989; Coifman and Donoho 1995; Candes and Donoho 1999). Among the alternative methods the most prominent is nonlinear **anisotropic diffusion** algorithm first proposed by Perona and Malik (Perona and Malik 1990; Catta et al. 1992; Weickert 1999), which allows effective noise removal in two- and three-dimensional image data while preserving edges between regions of consistently different intensities. A coherence-enhanced **anisotropic diffusion** particularly suitable for relatively low resolution **CT** reconstructions was proposed by Frangakis and Hegerl (Frangakis and Hegerl 2001; Sheppard et al. 2004). Comprehensive lists of **image enhancement** techniques are available in the literature (Gonzalez and Wintz 1987; Pratt 1991).

4.3.1.2 Image segmentation

Image segmentation usually refers to processing of images with the goal of automatic detection of objects or phases presented in the image. The difficulty of this task depends largely on the number and uniformity of objects or phases being analyzed as well as on the definition of their boundaries. While **phase segmentation**, or division of the image into regions of common characteristics can be achieved using relatively elementary operations like colour separation or thresholding the greyscale intensity (e.g. Sahoo et al. 1988; Chen et al. 2010), definition and characterization of individual particles within the image may pose a serious challenge. This is certainly true in case of particulate **wood-based composites** (OSB, particleboards, fibreboards), where irregular particles are tightly packed together with multiple contact points.

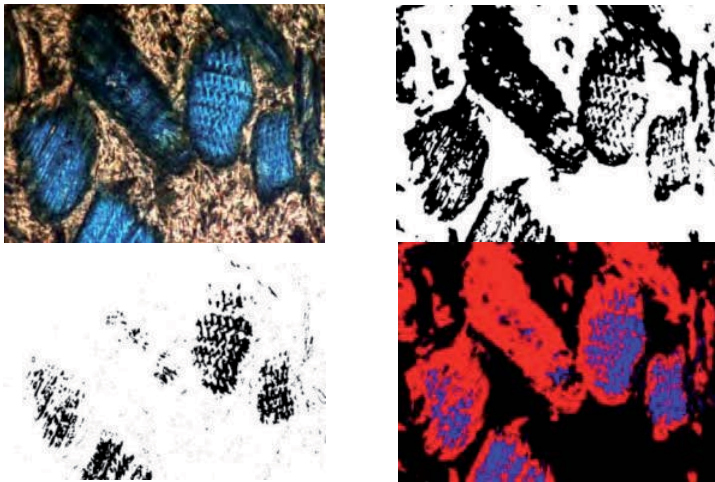


Figure 4.1: Colour segmentation of a microscopic image of wood particles embedded in PVC matrix reveals extensive inter-phase (red zone in the bottom right picture) where cell walls and lumens appear penetrated by the matrix material (Wang 2007).

For instance, in a recent study the density distribution in commercial panel products is evaluated in terms of greyscale intensity frequency distributions in combined radiographs of the panels (Chen et al. 2010). A series of images presented in Figure 4.1 illustrate how **phase segmentation** based on RGB colour aspects of a micrograph generated in a fluorescent microscope is used to separate and quantify extensive **inter-phase** between wood flour particles and polymer matrix in a **wood-polymer composite** sample. The **interphase**, where cell walls and

lumens appear penetrated by the matrix material, is clearly visible in the original colour micrograph, but only the two-stage colours **segmentation** technique allowed automatic recognition of the zone and calculation of relative areas of clear wood, matrix, and the **interphase** visible as the red zone in the bottom right picture (Wang 2007).

Similar approaches may be employed for **segmentation** of X-ray **computed tomography** (CT) data generated through computational reconstruction of internal feature of heterogeneous samples from a series of X-ray projections of the samples recorded at different angles. In the following example, a small sample of OSB shown in Figure 4.2a was scanned at resolution of $\sim 6 \mu\text{m}/\text{voxel}$. Images in Figures 4.2b and c show the central vertical and horizontal sections of the 3D data. The histogram represents the intensity distribution in the specimen.

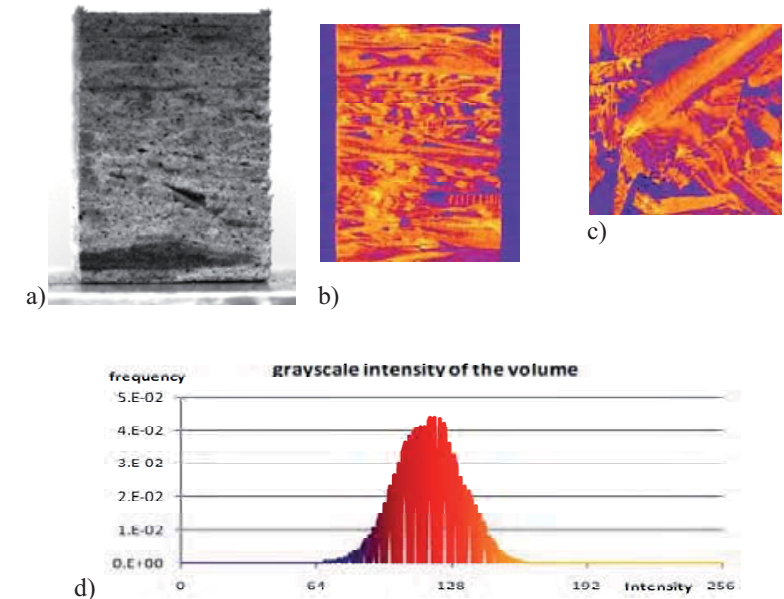


Figure 4.2: XCT scans of an OSB sample (a) at resolution of $\sim 6 \mu\text{m}/\text{voxel}$: central vertical section (b), and central horizontal section (c). The histogram (d) represents the intensity distribution in the specimen.

Three-dimensional renderings of a particle board specimen in Figure 4.3 demonstrate the comparison of the initial volume (a) with three

consecutive stages of **phase segmentation** based on thresholding of the volume intensity range (b-d).

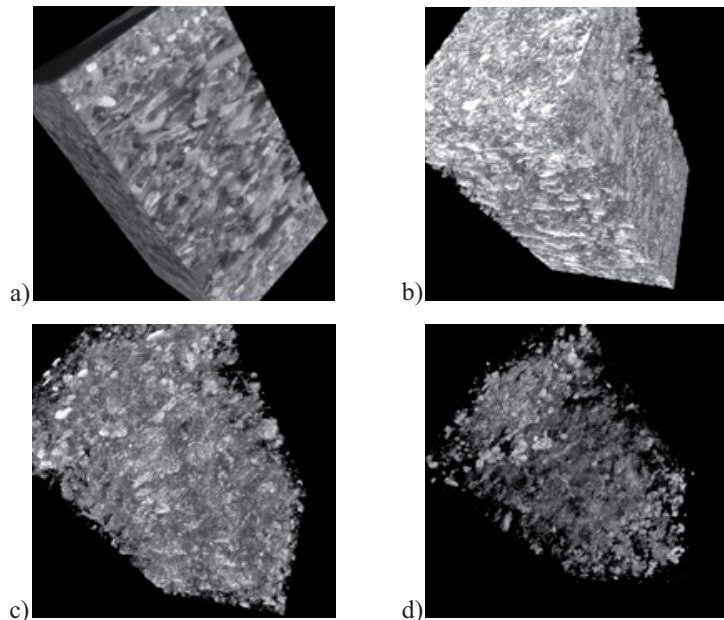


Figure 4.3: Three-dimensional renderings of a particle board specimen: the initial volume (a) is compared with three consecutive stages of phase segmentation based on thresholding of the volume intensity range (b-d).

While **phase segmentation** may be very helpful in assessing relative volumes of voids, woody particles and adhesive in the composite, it provides only visual clues as to the number, shape and position of the individual particles. These characteristics can be quantified using a group of procedures collectively referred to as **particle analysis**.

A great variety of **particle analysis** algorithms have been developed in the last few decades and this number continually increases each year. Several review papers for **segmentation** techniques have been presented in the literature (Fu and Mui 1981; Haralick and Shapiro 1985; Borisenko et al. 1987; Pal and Pal 1993; Freixenet et al. 2002). Some of these techniques use spatial details such as boundary (Davis 1975) and region (Zucker 1976) based methods, some use hybrid techniques such as watershed transform (Vincent and Soille 1991) and seeded region

growing (Adams and Bischof 1994) while other use fuzzy set theoretic approaches (Bezdeck 1981; Bezdeck 1992). Most of these techniques are not suitable for noisy data, which stresses the importance of effective **image enhancement** procedures. More computationally involved procedures are needed to work with noisy data (e.g. Hansen and Elliott 1982; Hertz et al. 1991; Kosko 1991).

However, there is no single method which can be considered good for all images, nor are all methods equally good for a particular type of image. Most of these sophisticated methods have been developed in the **medical** field because of the simplicity of patterns studied and the thorough knowledge of their characteristics (Ozkan *et al.* 1993; Chen *et al.* 1998; Pardo *et al.* 2001; Hibbard 2004; Zhang *et al.* 2006). In heterogeneous **particulate composite** materials, the geometry of the particulate component is more complex and irregular; therefore the **segmentation** is more complicated.

Currently many commonly accessible image-processing software bundles offer various machine vision tools for 2-dimensional images, including efficient **edge detection** and **particle analysis** algorithms capable of isolating and quantitatively describing multiple particles. Standard **particle analysis** returns distribution of sizes, areas and orientation of irregular particles.

Numerous generalized algorithms have also been proposed for the analysis of 3-dimensional data (Price 1995; Garboczi 2002; Thompson et al. 2006). An example in Figure 4.4 demonstrates two stages of **particle analysis** of a closely packed particulate composite performed on a binarized X-ray **CT** image of a sample reported by Thompson et al. (2006). The **segmentation** allows automated statistical analysis of the axial dimensions, volumes, and orientation of all the particles within the analyzed sample. Recently a similar approach was attempted to segment, visualize and analyze random cellulosic fibrous networks based on X-ray **CT** data (Faessel et al. 2005; Walther and Thoemen 2009).

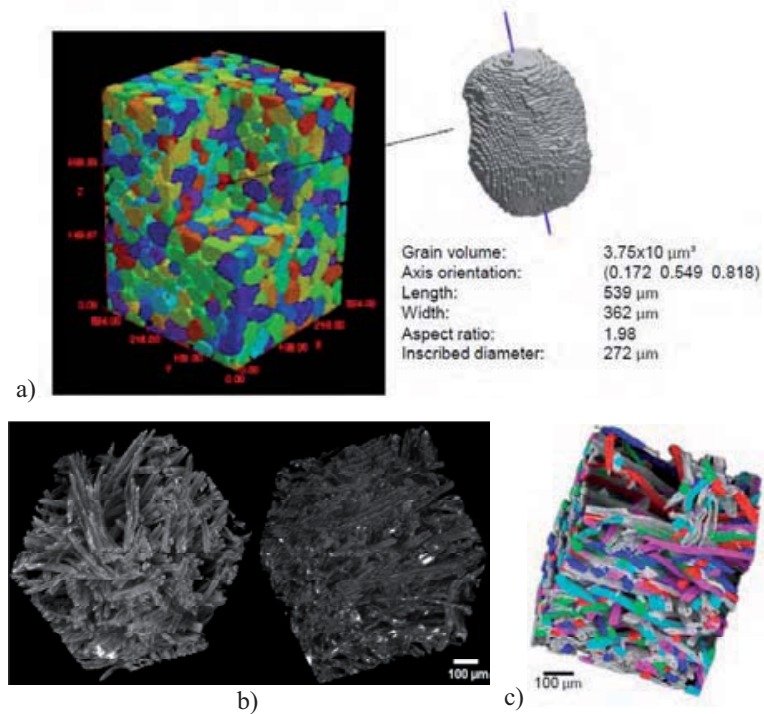


Figure 4.4: Segmented and binarized X-ray tomography images of (a) a particulate material and visualization of the segmented particle-scale reconstruction of the volume (Thompson et al. 2006); (b-c) a random cellulosic fibrous network (Walther and Thoemen 2009).

4.3.1.3 Importance of the representative volume

Usually, mechanical testing is done on macroscopic samples with volumes extremely large when compared to order of magnitude of known features of the composite **micro-structure**. Since modelling of such a huge volume cannot be practically accomplished on contemporary computers, it is generally assumed that the ensemble average of a given physical property obtained on smaller volumes is equal to its volume average in the infinite-volume limit. However, the assumption makes sense only if the medium is statistically homogeneous, i.e., the statistical properties of all regions of space are similar. This assumption should be

particularly carefully checked in case of the **wood-based composites**, where the scale of the component particles may differ by levels of magnitude (for instance compare strands, particles and fibre bundles used in panel products).

Effective properties are evaluated by methods of **edge detection** or averaging of microscopic variables like stresses and strains over a **representative volume element (RVE)** of the microstructure, which is an important parameter on the micromechanical analysis of composite materials. The concept of **RVE** was introduced by Hill (Hill 1963) as a micro-structural sub-region that is representative of the entire microstructure in an average sense. Hashin and Shtrikman (Hashin and Shtrikman 1962, 1963) extended the concept and introduced **representative volume** as a reference cube that is small compared to the entire body, for which the volume average of variables like strain, stress, or phase volume fraction are the same as those for the whole body. The consequences for **wood-based** panel products are that the smallest volume to be meaningfully analyzed for morphological characteristics or modelled has to include a good representation of the component elements, that is: strands, particles or fibres. Obviously, **RVEs** for OSB, particleboards and fibreboards will be very different. It will also depend on the specific morphological features being characterized. For instance, the size of **representative volumes** appropriate for characteristics describing local density variation, shape and size distributions of voids or cured adhesive spots in OSB, may be levels of magnitude smaller than these required to characterize the **in-situ** strand geometry.

4.3.2 Multi-Scale and Multi-Modal Correlation

One of the common problems in morphological analysis and characterization of **wood-based composites** is the trade off between the resolution and the **field of view**. The resolution of digital images is related to the fixed number of elementary sensors (pixels) in the detector array, which transforms the physical signal into the digital image. Consequently, increasing the spatial resolution of the images is achieved by decreasing the size of the **field of view**. Problems arise when morphological features of different scales are of interest at the same time, as in the case of strand geometry and adhesive spot distribution in OSB panels mentioned above. The geometry, distribution and orientation of the strands have to be considered at the centimetre scale, but then sub-millimetre or micron scale features of the adhesive spots cannot be resolved. In such cases image representations of the same sample at two different resolution levels have to be generated and the position of the high resolution detail should be registered with the related region in the low resolution image.

In fact, this registration process can span several steps over multiple levels of magnitude (centi- to nano- meters).

Similarly, different **imaging techniques** (or **modalities**) may be used in order to visualize different aspects of the same region of interest. This is a commonplace in fluorescent microscopy, where micrographs generated with different light spectra are correlated with each other, but is also performed between micrographs generated using imaging instruments based on entirely different physical principles and returning images of different scales. **Multi-modal correlation** may for instance allow precise registration of images generated using light-, fluorescence-, electron- and atomic force microscopy, as well as two-dimensional micrographs of physically exposed sections with three-dimensional **CT** data of the same sample acquired before the cut up. Figure 4.5 illustrates an attempt at a manual registration of a detail recorded in fluorescent microscope on a physical section of a WPC sample in a virtual section of three-dimensional data for the same sample before cutting (Rahmati and Muszyński 2009).

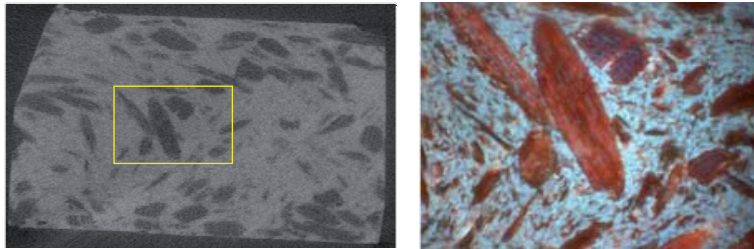


Figure 4.5: A CT section (3.0 mm x 2.1 mm) of wood plastic composite (a) compared with a fluorescence micrograph (b). Manual extraction of subsamples and registration of the images was a serious challenge and could not be accomplished with the desired precision (Rahmati and Muszyński 2009).

Novel techniques for numerical **multi-scale** and **Multi-modal correlation** of image data, collectively referred to as **correlative microscopy**, are developed mainly in the field of biomedical research (e.g. Vicidomini et al. 2010). **Correlative microscopy** is considered a new frontier of the advanced **image analysis** and each year brings another wave of interesting techniques with multiple potential applications in **wood-based** panel research.

4.3.3 Optical Measurement of Deformations and Strains

Digital images and volumetric data are also used for non-contact **full-field measurement** of deformations and strains in heterogeneous anisotropic solids under various loading regimes with sub-pixel accuracy by means of digital speckle **photogrammetry (DSP)** based on the **digital image correlation (DIC)** algorithms (Ranson et al. 1987; Sutton and Chao 1988; Bruck et al. 1989; Vendroux and Knauss 1998). **DSP** allows determination of displacements of a dense mesh of selected points on surfaces of deformed specimens by comparing successive images acquired during tests and cross correlating the gray intensity patterns of the direct neighbourhood of the points (or the **reference areas**). **DSP** has been already successfully applied to determine strains in specimens of solid wood subjected to external loads and climate changes (Muszyński et al. 2006), individual wood fibres and paper (Sutton and Chao 1988; Choi et al. 1991; Mott et al. 1996), fibre reinforced plastics (FRP) (Russell and Sutton 1989; Muszyński et al. 2000), concrete (Choi and Shah 1997), and adhesive films (Muszyński et al. 2002).

In late 1990s, a similar algorithm has been developed for volumetric data dubbed **digital volume correlation (DVC)** (Bay et al. 1999; Smith et al. 2002). **DVC** allows calculation of 3D internal strain fields in the analyzed volume by comparing data from x-ray tomographic scans of the same specimen acquired in unloaded and loaded states. This method was found to be very accurate in mapping the strain intensities in porous media such as bone tissue polymer and aluminium foams (Bay et al. 1999; Smith et al. 2002; Sutton 2004), and recently similar approach was demonstrated with wood sample by Forsberg et al. (Forsberg et al. 2008; Danvind et al. 2009).

4.3.4 Inverse Problem Approach

Two- and three- dimensional full-field methods provide displacement and strain data equivalent to hundreds of strain gages and are capable of capturing localized deformation gradients and strain concentrations that could not be possibly detected through discrete measurements from traditional instrumentation, such as extensometers, LVDTs, displacement gages or strain gages. In addition, the output format is readily compatible with many **numerical modelling** packages based on **FEM**, so that the displacement and strain fields measured by means of the full-field methods may be compared with the results of theoretical simulations of the same test configurations using existing models. In this approach, known as the **inverse problem methodology**, the measured and theoretical strain fields are used as input data in order to determine

localized material properties even for heterogeneous anisotropic materials and for specimens of complex geometries (Grediac and Pierron 1998; Pierron and Grediac 2000; Lecompte et al. 2005). The general idea of this method is shown on the schematic diagram in Figure 4.6.

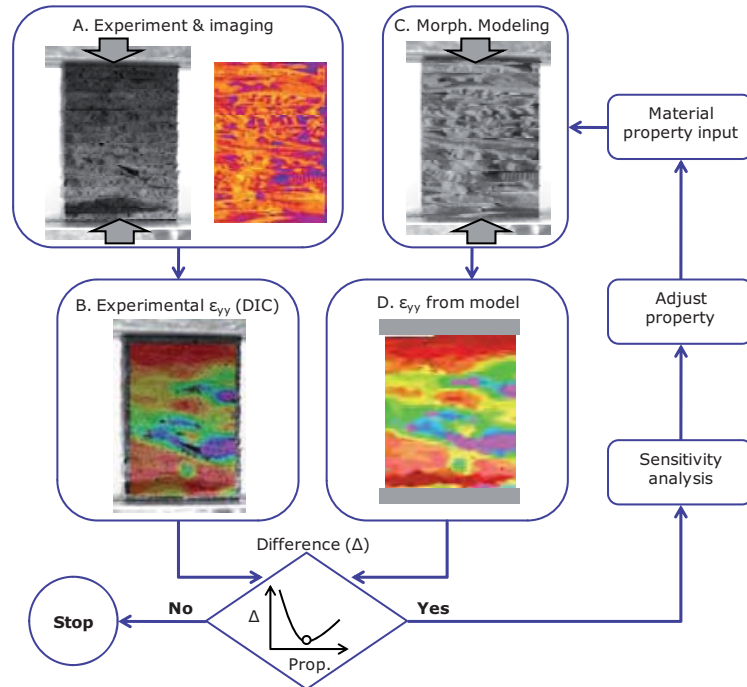


Figure 4.6: Flow chart of the material parameter identification problem by coupling full-field techniques in material testing, FEM modelling and inverse problem methodology (Muszyński and Nairn 2008).

In fact, the combination of **full-field measurements** with **inverse problem methodology** brings the material testing on a whole different level of efficiency by removing one of the limitations of the traditional test methods, which is the requirement that the mechanical material tests are reduced to simplest load cases. By combining the **full-field measurements** with **inverse problem methodology** and careful design of specimen geometries, loading, and boundary conditions, it is possible to determine all involved terms of anisotropic compliance matrices in a single test (Lecompte et al. 2005). The great number of virtual measurement points returned by full-field methods provides enough

statistical redundancy for even very complex constitutive models. It follows quite naturally, that the existing models are perfectly suited tools to assist in design and development of such complex test configurations, while on the other hand the results of the tests may provide validation to the models' assumptions.

4.3.5 New Developments in Modeling

New developments may be also expected in the area of modelling. Some time ago, a **material point method (MPM)** was proposed by Sulsky (1994) as an alternative to **FEM**, which is particularly suited for modelling heterogeneous solids based on their morphology. In this method, digital images of heterogeneous surfaces may be used directly as digitized input of the material geometry removing rather difficult task of generating complex **FEM** meshes. The **MPM** method is as suitable for application with the **inverse problem methodology** as **FEM**, and was successfully used for modelling wood at various levels of material organization (Nairn 2003; Nairn and Guo 2005; Nairn 2007). An **MPM** algorithm is available in public-domain as a 3D parallel code (Parker 2002).

4.4 REFERENCES

- Adams, R. and L. Bischof (1994). Seeded Region Growing. *Ieee Transactions on Pattern Analysis and Machine Intelligence*, 16(6): 641-647.
- ASTM (2000). ASTM E 1441-00: Standard Guide for Computed tomography (CT) Imaging. in: AMERICAN SOCIETY FOR TESTING AND MATERIALS. West Conshohocken, PA.
- Bay, B. K., T. S. Smith, D. P. Fyhrie and M. Saad (1999). Digital volume correlation: Three-dimensional Strain Mapping Using X-ray Tomography. *Experimental Mechanics*, 30(3): 217-226.
- Bezdeck, J. C. (1981). *Pattern Recognition with Fuzzy Objective Function Algorithms* Springer, New-York.
- Bezdeck, J. C. P., S.K. (1992). *Fuzzy Models for Pattern Recognition: Methods That Search for Structures in Data* IEEE Press, New-York.
- Borisenko, V. I., A. A. Zlatopolskii and I. B. Muchnik (1987). Image segmentation (State-of-the-Art SuRVEy). *Automation and Remote Control*, 48(7): 837-879.
- Bruck, H. A., S. R. McNeill, M. A. Sutton and W. H. I. Peters (1989). Digital image correlation Using Newton-Raphson Method of Partial Differential Correction. *Experimental Mechanics*, 28(3): 261-267.
- Candes, E. J. and D. L. Donoho (1999). Ridgelets: a key to higher-dimensional intermittency? *Philosophical Transactions of the Royal Society of London Series a-Mathematical Physical and Engineering Sciences*, 357(1760): 2495-2509.
- Catte, F., P. L. Lions, J. M. Morel and T. Coll (1992). Image Selective Smoothing and Edge-Detection by Nonlinear Diffusion. *Siam Journal on Numerical Analysis*, 29(1): 182-193.
- Chen, C. W., J. B. Luo and K. J. Parker (1998). Image segmentation via adaptive K-mean clustering and knowledge-based morphological operations with biomedical applications. *Ieee Transactions on Image Processing*, 7(12): 1673-1683.
- Chen, S., X. Liu, L. Fang and R. Wellwood (2010). Digital X-ray analysis of density distribution characteristics of wood-based panels. *Wood Science and Technology*, 44(1): 85-93.

- Choi, D., J. L. Thorpe and R. B. Hanna (1991). Image analysis to measure strain in wood and paper. *Wood Science and Technology*, 25(2): 251-262.
- Choi, S. and S. P. Shah (1997). Measurement of Deformations on Concrete Subjected to Compression Using Image Correlation. *Experimental Mechanics*, 37(3): 307-313.
- Coifman, R. R. and D. L. Donoho (1995). Lecture Notes in Statistics. in: G. O. Anestis Antoniadis, Ed. *Lecture Notes in Statistics*. New-York, Springer. 103: 225.
- Danvind, J., F. Forsberg, R. Mooser, M. Arnold, E. Hack and P. Wyss (2009). An example on acquiring wood ultra-structure, density and strain in 3D using non-destructive Synchrotron Radiation Micro Computed tomography and Digital volume correlation. in: *Proceedings of COST Action FP0802 Workshop: "Experimental and computational methods in wood micromechanics"*, Vienna, Austria, May 11-13, 2009. 123.
- Davis, L. S. (1975). A SuRVEy of Edge detection Techniques. *Computer graphics and image processing*, 4: 248-270.
- Egan, A. and S. M. Shaler (2000). *Fracture and Mechanics of Fracture for Resin Coated Single Wood Fibres*. Fourth Panel Products Symposium. Llandudno, Wales, UK: 95-103.
- Faessel, M., C. Delisée, F. Bos and P. Castéra (2005). 3D Modelling of random cellulosic fibrous networks based on X-ray tomography and image analysis. *Composites Science and Technology*, 65(13): 1931-1940.
- Forsberg, F., R. Mooser, M. Arnold, E. Hack and P. Wyss (2008). 3D micro-scale deformations of wood in bending: Synchrotron radiation [mu]CT data analyzed with digital volume correlation. *Journal of Structural Biology*, 164(3): 255-262.
- Frangakis, A. S. and R. Hegerl (2001). Noise reduction in electron tomographic reconstructions using nonlinear anisotropic diffusion. *Journal of Structural Biology*, 135(3): 239-250.
- Freixenet, J., X. Munoz, D. Raba, J. Marti and X. Cufi (2002). Yet another suRVEy on image segmentation: Region and boundary information integration. in: *Computer Vision - Eccv 2002 Pt Iii*. 2352: 408-422.
- Fu, K. S. and J. K. Mui (1981). A SuRVEy on Image segmentation. *Pattern Recognition*, 13(1): 3-16.

- Garboczi, E. J. (2002). Three-dimensional mathematical analysis of particle shape using X-ray tomography and spherical harmonics: Application to aggregates used in concrete. *Cement and Concrete Research*, 32(10): 1621-1638.
- Gonzalez, R. C. and P. Wintz (1987). *Digital Image Processing*. Addison-Wesley, Reading, MA.
- Grediac, M. and F. Pierron (1998). T-shaped specimen for the direct characterization of orthotropic materials. *International Journal for Numerical Methods in Engineering*, 41(2): 293-309.
- Hansen, F. R. and H. Elliott (1982). Image segmentation Using Simple Markov Field Models. *Computer Graphics and Image Processing*, 20(2): 101-132.
- Haralick, R. M. and L. G. Shapiro (1985). Image segmentation Techniques. *Proceedings of the Society of Photo-Optical Instrumentation Engineers*, 548: 2-9.
- Hashin, Z. and S. Shtrikman (1962). On Some Variational Principles in Anisotropic and Nonhomogeneous Elasticity. *Journal of the Mechanics and Physics of Solids*, 10(4): 335-342.
- Hashin, Z. and S. Shtrikman (1963). A Variational Approach to the Theory of the Elastic Behaviour of Multiphase Materials. *Journal of the Mechanics and Physics of Solids*, 11(2): 127-140.
- Hertz, J., A. Krogh and R. G. Palmer (1991). *Introduction to the Theory of Neural Computation* Addison-Wesley, New York.
- Hibbard, L. S. (2004). Region segmentation using information divergence measures. *Medical Image Analysis*, 8(3): 233-244.
- Hill, R. (1963). Elastic Properties of Reinforced Solids - Some Theoretical Principles. *Journal of the Mechanics and Physics of Solids*, 11(5): 357-372.
- Kamke, F. A. and J. N. Lee (2007). Adhesive penetration in wood - A review. *Wood and Fiber Science*, 39(2): 205-220.
- Kosko, B. (1991). *Neural Networks and Fuzzy Systems: A Dynamical Systems Approach to Machine Intelligence*. Prentice Hall, Englewood Cliffs, NJ.
- Lecompte, D., H. Sol, J. Vantomme and A. M. Habraken (2005). Identification of Elastic Orthotropic Material Parameters Based on ESPI

- Measurements. SEM Annual Conference & Exposition on Experimental and Applied Mechanics. Portland, OR: paper #: 119/045.
- Macedo, A., C. M. P. Vaz, J. C. D. Pereira, J. M. Naime, P. E. Cruvinel and S. Crestana (2002). Wood Density Determination by X- and Gamma-Ray Tomography. *Holzforschung*, 56: 535-540.
- Mackerle, J. (2005). Finite element analyses in wood research: a bibliography. *Wood Science and Technology*, 39: 579-600.
- Mallat, S. G. (1989). A Theory for Multiresolution Signal Decomposition - the Wavelet Representation. *Ieee Transactions on Pattern Analysis and Machine Intelligence*, 11(7): 674-693.
- Mannes, D., F. Marone, E. Lehmann, M. Stampanoni and P. Niemz (2010). Application areas of synchrotron radiation tomographic microscopy for wood research. *Wood Science and Technology*, 44(1): 67-84.
- Marra, A. A. (1992). *Technology of wood bonding : principles in practice*. Van Nostrand Reinhold, New York. 454 p.
- Mott, L., S. M. Shaler and L. H. Groom (1996). A novel technique to measure strain distributions in single wood fibers. *Wood and Fiber Science*, 28(4): 429-437.
- Muszyński, L., R. Lagana and S. M. Shaler (2006). Hygro-mechanical Behavior of Red Spruce in Tension Parallel to the Grain. *Wood and Fiber Science*, 38(1): 155-165.
- Muszyński, L., R. Lopez-Anido and S. M. Shaler (2000). Image Correlation Analysis Applied to Measurement of Shear Strains in Laminated Composites. in: *Proceedings of the SEM IX International Congress on Experimental Mechanics*, Orlando, FL, June, 5-7, 2000. 163-166.
- Muszyński, L. and J. Nairn (2008). Coupling Advanced imaging Analysis and Morphology Based Modeling for Integrated Characterization of Micro-mechanics of Wood And Wood-based Composites. *International Conference PHOTOMECHANICS 2008*. Loughborough, UK (poster).
- Muszyński, L., F. H. Wang and S. M. Shaler (2002). Short-term creep tests on phenol-resorcinol-formaldehyde (PRF) resin undergoing moisture content changes. *Wood and Fiber Science*, 34(4): 612-624.
- Nairn, J. A. (2003). Material point method calculations with explicit cracks. *Computer Modeling in Engineering & Sciences*, 4: 649-664.

Nairn, J. A. (2007). A Numerical Study of the Transverse Modulus of Wood as a Function of Grain Orientation and Properties. *Holzforschung*, 61: 406-413.

Nairn, J. A. and Y. Guo (2005). Material point method Calculations with Explicit Cracks, Fracture Parameters, and Crack Propagation. in: *Proceedings of 11th Int. Conf. Fracture*, Turin, Italy, Mar 20-25.

Ozkan, M., B. M. Dawant and R. J. Maciunas (1993). Neural-Network-Based Segmentation of Multimodal Medical Images - a Comparative and Prospective-Study. *Ieee Transactions on Medical Imaging*, 12(3): 534-544.

Pal, N. R. and S. K. Pal (1993). A Review on Image segmentation Techniques. *Pattern Recognition*, 26(9): 1277-1294.

Pardo, X. M., M. J. Carreira, A. Mosquera and D. Cabello (2001). A snake for CT image segmentation integrating region and edge information. *Image and Vision Computing*, 19(7): 461-475.

Park, B.-D., S. G. Wi, K. H. Lee, A. P. Singh, T.-H. Yoon and Y. S. Kim (2003). Characterization of Rice Husk Using Microscopic and Micro-Analytical Techniques for Rice Husk/Thermoplastic Composites. the 7th International Conference on Woodfiber-Plastic Composites. Madison, WI: 323-331.

Parker, S. G. (2002). A Component-based Architecture for Parallel Multi-Physics PDE Simulation. International Conference on Computational Science (ICCS2002) Workshop on PDE Software. P. M. A. Sloot, C. J. K. Tan, J. J. Dongarra and A. G. Hoekstra. Amsterdam, The Netherlands Springer-Verlag, Berlin. 2331: 719-734.

Perona, P. and J. Malik (1990). Scale-Space and Edge-Detection Using Anisotropic Diffusion. *Ieee Transactions on Pattern Analysis and Machine Intelligence*, 12(7): 629-639.

Pétraud, M., N. Labbé, J.-C. Lartigue, B. De Jéso and G. Sébe (2003). Nuclear Magnetic Resonance Relaxometry Applied to Wood Fibers. in: *Proceedings of 7th International Conference on Woodfiber-Plastic Composites*, Madison, WI. 358.

Pierron, F. and M. Grediac (2000). Identification of the through-thickness moduli of thick composites from whole-field measurements using the Iosipescu fixture: theory and simulations. *Composites - Part A: Applied Science and Manufacturing*, 31(4): 309-318.

Pratt, K. (1991). *Digital Image Processing*. Wiley, New-York.

Price, K. (1995). *Annotated Computer Vision Bibliography*. Institute for Robotic and Intelligent System School of Engineering (IRIS), University of Southern California. <http://iris.usc.edu/Vision-Notes/bibliography/contents.html>. Last update: April 2, 2009. Access date: April 4, 2009.

Rahmati, H. and L. Muszyński (2009). Correlating fluorescent micrographs with volumetric x-ray CT scans of wood plastic composite (WPC) samples. Unpublished data. Corvallis, OR, Oregon State University.

Ranson, W. F., M. A. Sutton and W. H. Peters (1987). Holographic and Speckle Interferometry. in: A. S. Kobayashi, Ed. *SEM Handbook of Experimental Mechanics*. Englewood Cliffs, New Jersey, Prentice-Hall, Inc.: 388-429.

Richards, W. J., M. R. Gibbons and K. C. Shields (2004). Neutron tomography developments and applications. *Applied Radiation and Isotopes*, 61: 551-559.

Russell, S. S. and M. A. Sutton (1989). Strain Field Analysis Acquired Through Correlation of X-Ray Radiographs of a Fiber Reinforced Composite Laminate. *Experimental Mechanics*, 29: 237-240.

Sahoo, P. K., S. Soltani, A. K. C. Wong and Y. C. Chen (1988). A Survey of Thresholding Techniques. *Computer Vision Graphics and Image Processing*, 41(2): 233-260.

Shaler, S. M., A. Egan, L. Mott and E. N. Landis (1997). Fracture and Micromechanics of Resinated Fibers. in: *Proceedings of 4th International Conference on Woodfiber-Plastic Composites*, Madison, WI. 32-39.

Sheppard, A. P., R. M. Sok and H. Averdunk (2004). Techniques for image enhancement and segmentation of tomographic images of porous materials. *Physica a-Statistical Mechanics and Its Applications*, 339(1-2): 145-151.

Smith, G. (2005). The lap-shear strength of bonds between Oriented Strand Board (OSB) like strands coated with pMDI resin. *European Journal of Wood and Wood Products*, 63(4): 311-312.

Smith, T. S., B. K. Bay and M. M. Rashid (2002). Digital volume correlation Including Rotational Degrees of Freedom during Minimization. *Experimental Mechanics*, 42(3): 272-278.

Sulsky, D., Z. Chen and H. L. Schreyer (1994). A particle method for history-dependent materials. *Comput. Methods Appl. Mech. Engrg.*, 118: 179–186.

Sutton, M. (2004). An attempt to track and quantify micro-damage within rigid cellular polyurethane foam under uni-axial compression. Department of Mechanical Engineering, Oregon State University. Corvallis, OR. 7pp.

Sutton, M. A. and Y. J. Chao (1988). Measurement of strains in a paper tensile specimen using computer vision and digital image correlation. *TAPPI Journal*, 71(3): 173-175.

Thompson, K. E., C. S. Willson and W. L. Zhang (2006). Quantitative computer reconstruction of particulate materials from microtomography images. *Powder Technology*, 163(3): 169-182.

Tze, W. T. Y., S. C. O'Neill, D. J. Gardner, C. P. Tripp and S. M. Shaler (2003). Coupling Polystyrene and Cellulose Fibers with Hydrophilic and Hydrophobic Silanes: Effects on Interfacial Properties. in: *Proceedings of the 7th International Conference on Woodfiber-Plastic Composites*, Madison, WI, May 19-20, 2003. 29-35.

Vendroux, G. and W. G. Knauss (1998). Submicron Deformation Field Measurements: Part 2. Improved Digital image correlation. *Experimental Mechanics*, 38(2): 86-92.

Vicidomini, G., M. C. Gagliani, K. Cortese, J. Krieger, P. Buescher, P. Bianchini, P. Boccacci, C. Tacchetti and A. Diaspro (2010). A novel approach for correlative light electron microscopy analysis. *Microscopy Research and Technique*, 73(3): 215-224.

Vincent, L. and P. Soille (1991). Watersheds in Digital Spaces - an Efficient Algorithm Based on Immersion Simulations. *Ieee Transactions on Pattern Analysis and Machine Intelligence*, 13(6): 583-598.

Walther, T. and H. Thoemen (2009). Synchrotron X-ray microtomography and 3D image analysis of medium density fiberboard (MDF). *Holzforschung*, 63(5): 581-587.

Wang, Y. (2007). Morphological Characterization of Wood plastic Composite (WPC) with Advanced imaging Tools: Developing Methodologies for Reliable Phase and Internal Damage Characterization. PhD Thesis. Oregon State University. Corvallis, OR. 123 pp.

Weickert, J. (1999). Coherence-enhancing diffusion filtering. *International Journal of Computer Vision*, 31(2-3): 111-127.

Wellington, S. L. and H. J. Vinegar (1987). X-ray Computerized Tomography. *Journal of Petroleum Technology*, August: 885-898.

Wolcott, M. and L. Muszyński (2008). Position paper: “Materials and Wood-based Composites” in: “Wood Engineering Challenges in the New Millennium - Critical Research Needs”. *Materials of Pre-Conference Workshop for ASCE Structures Congress*. Vancouver, BC, Canada 41-50.

Zhang, L., G. Wang and W. Wang (2006). A new fuzzy ART neural network based on dual competition and resonance technique. in: *Advances in Neural Networks - Isnn 2006*, Pt 1. 3971: 792-797.

Zhou, C., C. Dai and G. D. Smith (2008). A generalized mat consolidation model for wood composites. *Holzforschung*, 62(2): 201-208.

Zucker, S. W. (1976). *Region Growing: Childhood and Adolescence*. *Computer graphics and image processing*, 5: 382-399.

Chapter 5

Adhesive Bond Strength Development

Milan Sernek and Manfred Dunky

CHAPTER SUMMARY

The **bond strength** of **thermosetting adhesives** develops during the hardening or **curing process**, which is usually carried out in a hot-press at a defined pressure and temperature, and for a defined period of time. The **mechanical properties** of the adhesive during curing can be examined by any of the following methods: **Thermomechanical analysis (TMA)**, **Dynamic mechanical analysis (DMA)**, **Torsional braid analysis (TBA)**, Integrated pressing and testing system (**IPATES**), and Automated bonding evaluation system (**ABES**). Among these, ABES and IPATES are to be preferred from the practical point of view since these techniques provide data on the **shear strength** of the adhesive bond (ABES) or internal bond (IPATES), whereas TMA, DMA and TBA measure the changes of the different moduli. A short description and principles of the mentioned methods is given. Examples of typical results obtained with each technique are presented and briefly discussed. References for detailed information on results from these methods are provided.

5.1 INTRODUCTION

Adequate bond strength and long-term performance of the wood-based panels such as particleboard, fibreboard (MDF), oriented strand board (OSB) and plywood is achieved with sufficient adhesive curing during pressing. At the end of the **press time** – when the press opens or when the board leaves the continuous press – a certain degree of bond strength (i.e. certain mechanical hardening) is necessary in order to withstand the various internal forces in the board (**spring back**) due to (i) mechanical stresses caused by deformation of the wood substance (reduced by relaxation processes within the board) and (ii) by the **internal steam pressure** built up during the hot-press process. The full **chemical curing** however can be completed afterwards outside of the press (e.g. during hot stacking).

If the sufficient adhesive bond strength is not developed, the compressed panel will exhibit either a low performance (**internal bond**, shear strength, etc.) or it will delaminate (blister) when the press pressure is released and the press opens. A stronger adhesive bond can be achieved to a certain limit by a prolongation of the pressing time, but this increases the cost of heat energy supplied, and reduces production capacity. Manufacturers of wood-based panels are thus continually trying to find an optimal pressing time, which provides a good balance between the required performance of the panel and acceptable production costs. In order to enable shorter pressing times and therefore reduced production costs an early, quick and instantaneous formation of the bond strength is important.

5.2 FUNDAMENTALS

bond strength between the wood substrate and the adhesive develops during the **hardening** or **curing** of the adhesives, which involves conversion of a liquid adhesive through **gelation** and **vitrification** to fully cured adhesive. Gelation marks the transition from liquid to a rubbery state and it retards macroscopic flow. The gel corresponds to the formation of an **infinite network** in which polymer molecules are cross-linked and form a macroscopic molecule. The viscosity and modulus of a polymer increase dramatically when the gel point is achieved.

Vitrification occurs when the **glass transition temperature** (T_g) of the formed network rises to the temperature of cure. In adhesive curing it marks the transformation from a rubber to a gelled glass. T_g is the critical temperature that separates glassy behavior from rubbery behavior. The strength of adhesion between adherents increases linearly as the amount of interlinking between the two adherent layers increases. **Cross-linking** (as effect within the adhesive resin) affects many of the physical and mechanical characteristics of thermosetting adhesives. It improves their strength and durability, and also increases solvent and high temperature resistance. Hardening and gelling of thermosetting adhesives and resins can usually be monitored by:

- **The exo- or endothermic behaviour** (Figure 5.1) during gelling and hardening (chemical curing); suitable test methods are the Differential Thermal Analysis (DTA) or the Differential Scanning Calorimetry (DSC).

- **The further reactions** of the thermosetting resins (chain elongation, branching, and crosslinking) to a more or less three dimensional network with a theoretical endless high molar mass, generating an insoluble resin which is not longer thermoformable (thermoplastic). These reactions can also be followed by means of various **spectroscopic methods**, taking as measure the changes in the portion of various specific structural elements in the adhesive. Suitable methods are Infrared (**IR**), Nuclear Magnetic Resonance (**NMR**) ^{13}C or solid state NMR.
- **The solidification of the adhesive** (Figure 5.2) during curing by building up the three-dimensional network, also described by the achievable degree of cross-linking; usual test methods for this mechanical curing are the Dynamic Mechanical Analysis (DMA), the Thermal Mechanical Analysis (TMA), the Torsional Braid Analysis (TBA), the **Thermal Scanning Rheometry** (Stefke and Dunky 2006) as well as various **gel test methods** at different temperatures and using various hardeners (Stefke and Dunky 2006), using the moment (or period) of formation of the gelled state as measure.
- **The formation of the bond strength** between two adherents (materials being bonded); this can be followed by methods like the Automated Bonding Evaluation System (ABES) (Humphrey 1993), the Composite Testing System (**ComTeS**) (Heinemann 2004), the Integrated Pressing and Testing System (IPATES) (Heinemann 2004, Roos 2000) or also any other type of tests where bonds are created under certain conditions (especially in dependence of time) and then tested (Sernek et al. 2005). The easiest procedure, even time consuming, is to press a series of plywood samples with different press times applied and to test the already generated and still generating bond strength in a suitable procedure like the shear mode. Similar tests can be performed with lab particleboards or lab MDF/HDF, with following testing of the internal bond or other properties describing the formation of bond strength and material cohesion.

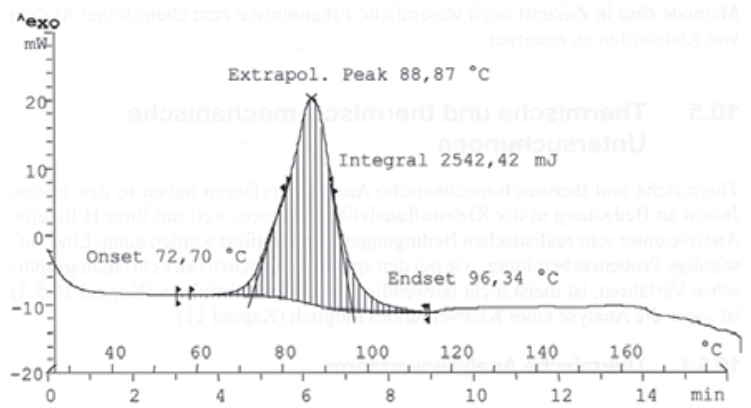


Figure 5.1: DSC-plot of an UF-resin (Dunky 1996).

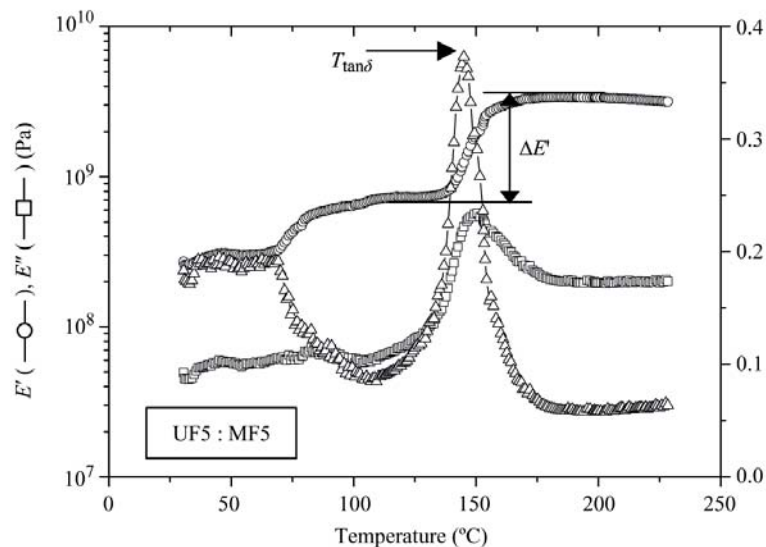


Figure 5.2: DMA-plot of an aminoplastic adhesive resin (Kim et al. 2006).

The bond strength generated and measured when testing lab particleboards or lab MDF/HDF, however, does not only reflect the **mechanical degree of curing**, but also is influenced by **residual stresses**

in the pressed board, which are caused by (i) the steam pressure in the board, and (ii) the residual mechanical stresses due to the densification of the particle or fibre mat and even the deformation of the particles and fibre themselves.

Humphrey und Ren (1989) pressed plywood under nearly isothermal conditions and constant moisture content. The bonding strength was determined immediately after the end of the various press times and increased with the press time up to a certain level when full curing occurred. By plotting the steepness of these curves for different temperatures versus the reciprocal absolute temperature a so-called **reactivity index**, similar to an **activation energy**, can be calculated.

The processes taking place during hardening depend on the basic chemical type of the adhesive. Adhesives can consist of reactive components with various molar masses, from low molecular weight species as reactive monomers up to already more or less polymeric structures still having reactive groups within their chains or at the end points of the oligomeric or polymeric molecules; in the latter case chemical crosslinking of rather thermoplastic structures can occur.

For thermosetting adhesives the usual reactions taking place are **polycondensation** or **polyaddition**, with the hardened and, most probably, three-dimensional network state as final structure. At the same time, the development of the mechanical bond strength between the two adherents as a consequence of the increase in cohesive bond strength by these further reactions takes place.

The curing process usually is performed at higher temperatures depending on the process used; but also hardening at room temperature or at slightly elevated temperatures is possible. The pH conditions of this step vary with the type of resin:

- With usually acidic condensation taking place for aminoplastic resins,
- Rather alkaline conditions with phenolic resins,
- Resins based on resorcinol prefer even neutral conditions.

The reactions are very much accelerated by heat based on the well-known temperature dependence of the rate of chemical reactions as described by the **equation of Arrhenius** (Figure 5.3). In this example the inverse gel time was taken as a measure for the rate of the hardening reaction. The slope of the lines indicates the energy of activity of these chemical processes.

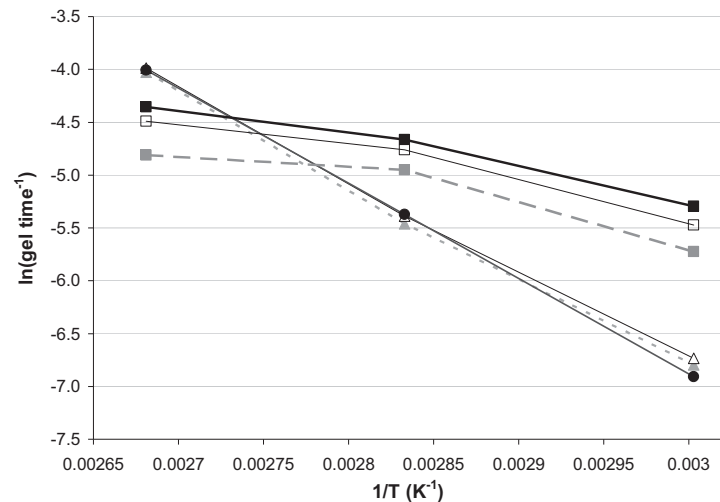


Figure 5.3: Arrhenius plots of the logarithmic inverse gel time with the gel times expressed in seconds plotted against the reciprocal absolute temperature ($1/K$) for a straight UF resin as measure for the hardening rate with various hardeners at three temperatures. ■ 3.2% Acetic acid, □ 2.3% Acetic acid, ■ 1.6% Acetic acid, △ 2.3% Ammonium sulphate, ▲ 1.2% Ammonium sulphate ● 2.3% Ammonium chloride.

5.3 MONITORING THE DEVELOPMENT OF ADHESIVE BOND STRENGTH

The development of the adhesive bond strength during curing can be observed by different methods such as:

- Thermomechanical analysis (TMA),
- Dynamic mechanical analysis (DMA),
- Torsional braid analysis (TBA),
- Automated bonding evaluation system (ABES),
- Integrated pressing and testing system (IPATES),

- Others: rheological techniques, Composite Testing System (Com-TeS), etc.

5.3.1 Thermomechanical Analysis (TMA)

Thermomechanical analysis (TMA) involves measurements of the dimensional changes of material under controlled conditions of force, atmosphere, time and temperature. Force can be applied in different modes such as compression, flexure or tension. TMA measures the intrinsic properties of the material (**Young's modulus**, **glass transition**, **thermal expansion coefficient**) and also processing or product performance parameters. The viscoelastic properties of the material (creep or stress relaxation) can be observed. The degree of **crosslinking** in an adhesive can be determined through detecting the **glass transition temperature** (T_g). The schematic principle of the TMA is shown in Figure 5.4. There are different experimental configurations for the TMA, with the three point flexion as the most useful one for monitoring the curing of a wood adhesive.

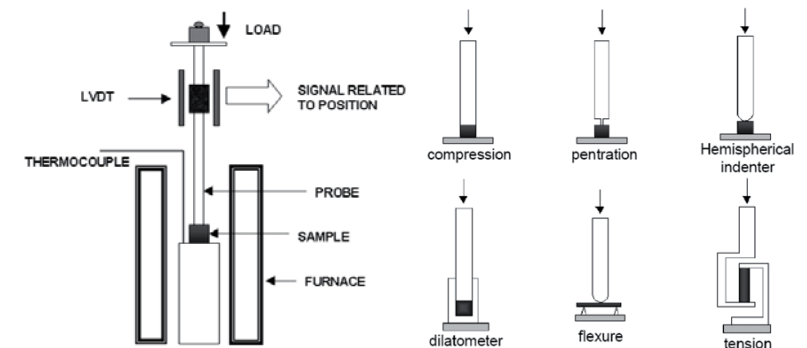


Figure 5.4: Schematic principle of TMA (left) and different type of mounting configuration (right) (<http://www.anasys.co.uk/library/tma1.htm>).

Both, non-isothermal and isothermal TMA are useful methods to forecast the internal bond (IB) of a particleboard (Laigle et al. 1998) and to investigate the influence of different mixture of adhesives on the crosslinking and hardening process of adhesives (Yin et al. 1995). This study is an instructive example for application of TMA investigating some thermosetting wood adhesives (UF, MUF and PMUF). The TMA results are presented in terms of the evaluation of relative elastic moduli as a

function of temperature. Three significant zones can be recognized related to the change of the relative modulus of the adhesive during curing:

1. First zone with low modulus: at the onset of curing and before gelling, the adhesive behaves as a liquid, which cannot yet transfer the stresses between the wood adherents.
2. Second zone with increasing modulus: gelling of the adhesive creates three-dimensional structures, by transforming the adhesive from a liquid to a rubbery state; the relative elastic modulus of the adhesive and thus of the bond increases, assuming a sufficient adhesion situation. The start of this second zone can be defined as a gel temperature (T_{gel}).
3. Third zone with a slight decrease of the modulus after reaching a maximum, which is due to thermal degradation processes in aminoplastic adhesives as well as to the differences in the relative expansion coefficient of wood and adhesive. Hardening temperature (T_v) can be defined as a temperature where the rate of increase of the elastic modulus attains its maximum.

TMA was also used in several other studies in order to evaluate the adhesive bond strength development: Laigle et al. (1998), Pichelin et al. (2000), Garnier et al. (2002), Zanetti and Pizzi (2002), Lecourt et al. (2003), George et al. (2003).

5.3.2 Dynamic Mechanical Analysis (DMA)

Dynamic mechanical analysis (**DMA**) (sometimes referred to as Dynamic mechanical thermal analysis (**DMTA**)), is a widely used technique in order to study the mechanical properties of materials. DMA analyses a response of a material subjected to a sinusoidal stress, which generates a corresponding sinusoidal strain. Characteristic values like the modulus, the viscosity, and the damping factor can be determined from measurements of the amplitude of the deformation at the peak of the sine wave and the lag between the stress and strain sine waves (Menard 1999). Particularly, the **storage modulus** (E') (Figure 5.5) and the **loss modulus** (E'') can be determined from the measurements. The **mechanical damping term** $\tan\delta$ is defined as E''/E' . Hardening phenomena such as gelation and vitrification of an adhesive can be clearly identified from these parameters.

DMA is very useful technique for observing the viscoelastic nature of polymers and also for examining the curing of adhesives. The cure results

(i.e. mechanical cure) are based on the monitoring of the adhesive stiffness and the $\tan\delta$ as a function of temperature.

Many of the DMA studies on wood adhesives were conducted with a glass filter as substrate, which was impregnated with adhesive (Christiansen et al. 1993, Umemura et al. 1996), whereas some of the DMA experiments were done using wood samples as substrates for the adhesives (Wang et al. 1996, Bučar and Tišler 1997, He and Yan 2005).

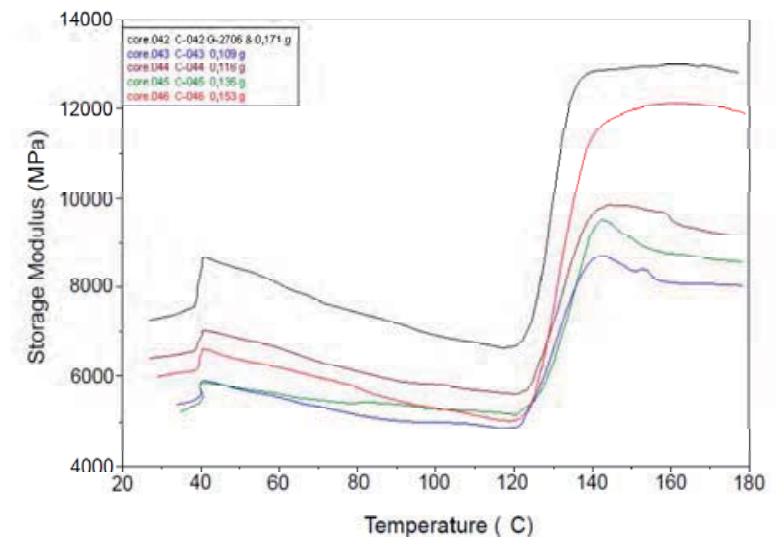


Figure 5.5: DMA study of amino resins (Courtesy: Jose Gomez-Bueso).

5.3.3 Torsional Braid Analysis (TBA)

Torsional braid analysis (TBA), the processor of DMA, is an excellent technique to characterize the cure properties of polymeric materials such as adhesives. The techniques are useful in measuring the glass transition temperature (T_g), the elastic modulus (E') and the loss modulus (E''). These parameters are useful to characterize the transformation of a liquid to the solid state (hardening). A schematic model of a torsion pendulum is shown in Figure 5.6. The adhesive sample is clamped at the two extremes. The upper clamp is bound to an inertial rotating counterbalanced system. Torsional oscillations are induced by applying a torque.

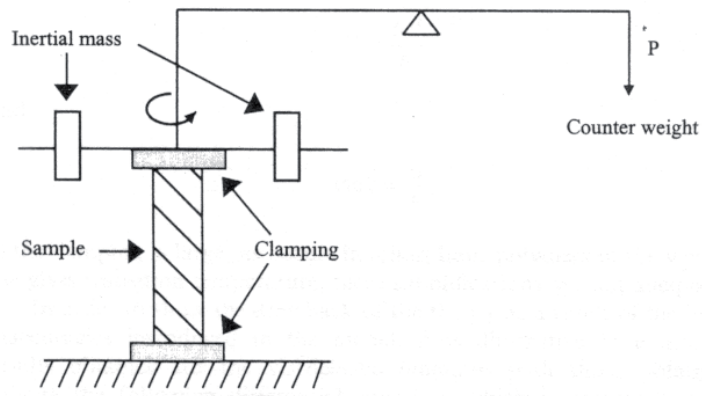


Figure 5.6: Scheme of an inverted torsion pendulum (Riande 2000).

The temporary dependence of the angular displacement is measured. The analyzed material is cured at different temperatures and the data are collected over time. Values of T_g are obtained in order to construct the **time-temperature-transition (TTT) diagram** (Figure 5.7).

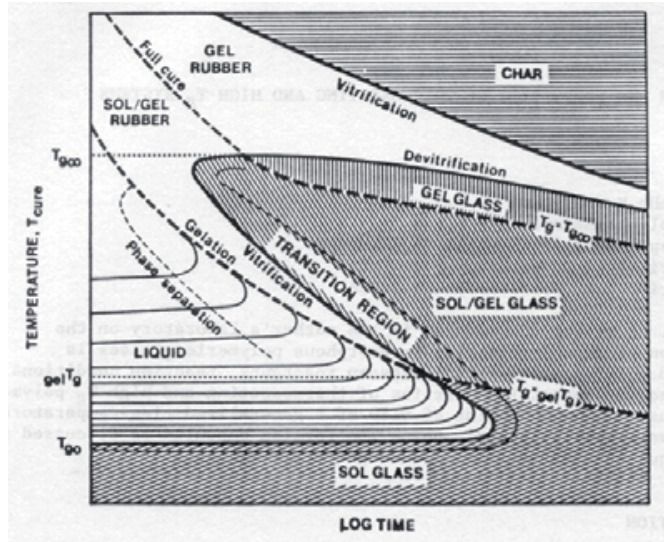


Figure 5.7: Schematic TTT diagram for a thermosetting system (Gillham 1997).

A TTT cure diagram is a plot of the times, required to reach **gelation** and **vitrification** functions during isothermal cure of adhesive as a function of curing temperature. Several events occur through curing time. These events include the onset of phase separation, gelation, vitrification, full cure, and **devitrification**.

Much of the behaviour of a thermosetting material can be understood in terms of the TTT diagram through the influence of gelation, vitrification, and devitrification on the properties of the material investigated. Gelation marks the transition from liquid to a rubbery state. It retards macroscopic flow, and retards growth of a dispersed phase. Vitrification occurs when the glass transition temperature rises to the temperature of cure. It marks the transformation from a rubber to a gelled glass or from a liquid to an ungelled glass. Vitrification retards the possible further chemical reactions. Devitrification occurs when T_g decreases again due to excessive heat impact. Devitrification, due to thermal degradation, marks the lifetime for the material. An excellent introduction to study the cure of thermosetting systems by TBA is given by Gillham (1997); TBA was also used in several studies on different wood adhesive types: Steiner and Warren (1981), Steiner and Warren (1987), Ohyama *et al.* (1995), Tomita *et al.* (1994).

5.3.4 Automated Bonding Evaluation System (ABES)

The so-called automated bonding evaluation system (ABES) has been developed and patented by Humphrey (1993). The ABES enables the determination of strength development characteristics of different adhesives in combination with an adherend. The system includes bonding and testing of a lap-shear specimen under controlled conditions (Figure 5.8).

The system uses a pair of relatively thin adherend strips (e.g. veneer, wood or metals) and the adhesive, which is applied to the end of one strip. The strips are put together to form a lap-shear specimen. The specimen is put in the testing device and pressed by side like in a small hot-press. After a certain press time, this small press opens and the specimen is immediately (or after a defined cooling interval of few seconds) tested in tension shear mode (Figure 5.9).

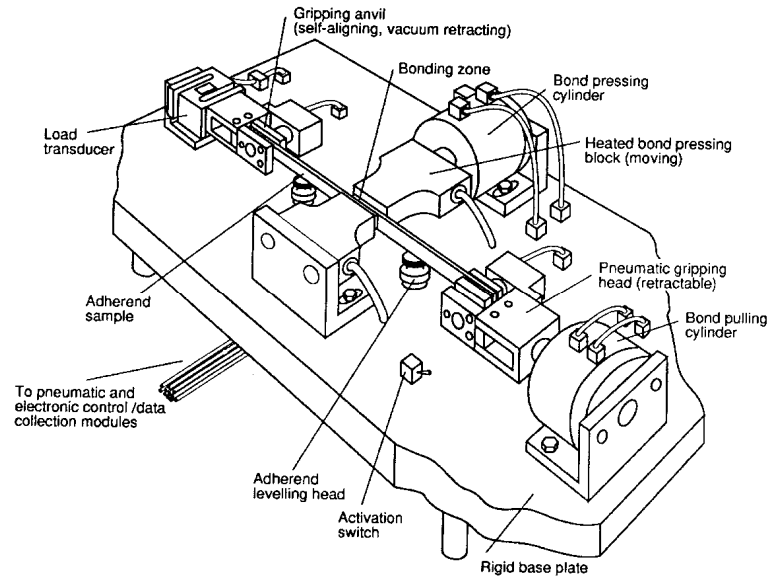


Figure 5.8: Automated Bonding Evaluation System (Humphrey; US-patent 5176028).

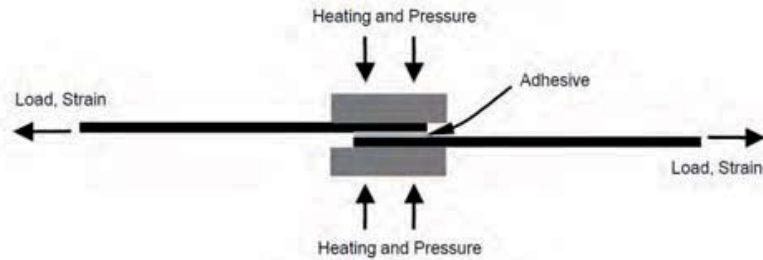


Figure 5.9: Schematic picture of the ABES principle.

The technique provides valuable data on the shear strength of the adhesive bond as a function of the pressing parameters (e.g. time and temperature) and conditions (e.g. the cooling effect) (Humphrey 2006) (Figure 5.10). The measured time dependent shear strengths describe the formation of the pure cohesive bonding strength, without wood failure. As soon as wood failure occurs, the test series has to be stopped.

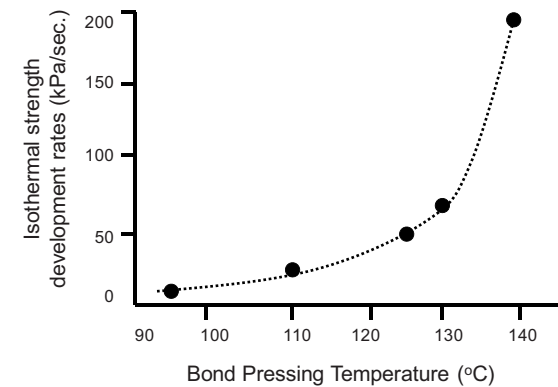
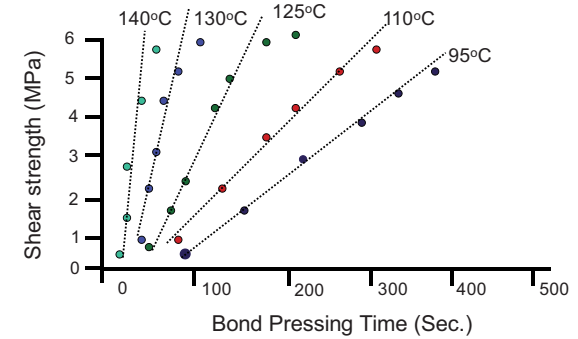


Figure 5.10: A typical set of isothermal strength development plots for UF adhesive-to-maple bonds (top), with a derived plot of regressed bonding rate against temperature (bottom) (Humphrey 2006).

ABES and similar adapted methods have been found to be useful for determining the development of bond strength for various adhesive types under different pressing conditions (Kreber *et al.* 1993; Prasad *et al.* 1994; Chowdhury and Humphrey 1999; Kim and Humphrey 2000; Heinemann *et al.* 2002a; Heinemann *et al.* 2002b; Lecourt *et al.* 2003). ABES is an excellent technique for strength development determination because it reveals the mechanical properties (e.g. shear strength) of the adhesive bond. For practice, mechanical testing of the adhesive bond line

is the method which is used to determine the quality of the adhesive cure and the effectiveness of the wood-adhesive interaction (Steiner and Warren 1981). A shortcoming of ABES compared to DMA is that only one data point of shear strength per test is provided, since ABES is a destructive test.

5.3.5 Integrated Pressing and Testing System (IPATES)

The so-called Integrated Pressing and Testing System (IPATES) was developed for the determination of the adhesive cure in wood fibre and particle mats. The principle is similar to the principle of ABES. A mat is formed on a disc as steel press platen with 100 mm in diameter (Figure 5.11). The mat is heated by two electrically heated blocks and compressed by the universal testing machine. A special adhesive is used to ensure the proper linkage between the press platens and the sample being tested. After pressing, the specimen is destructively tested in tension mode for determination of the internal bond (Heinemann *et al.* 2002a). A similar method (ComTeS) has been used for testing wood composites (Heinemann *et al.* 2002b).

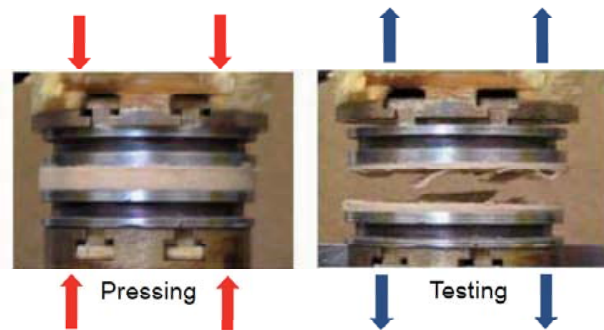


Figure 5.11: Integrated pressing and testing system (IPATES).

Heinemann *et al.* (2002a) investigated the influence of temperature (80-160 °C), mat density (500-800 kg/m³) and resin consumption (gluing factor) (7-13 %) on the internal bond (IB) of MDF. The strength development of the used UF adhesive resin as a function of pressing time and temperature is shown in Figure 5.12. It is evident that the development of IB is much slower at lower pressing temperatures (especially 80 °C), and it does not reach the same level as for the samples pressed at higher temperatures.

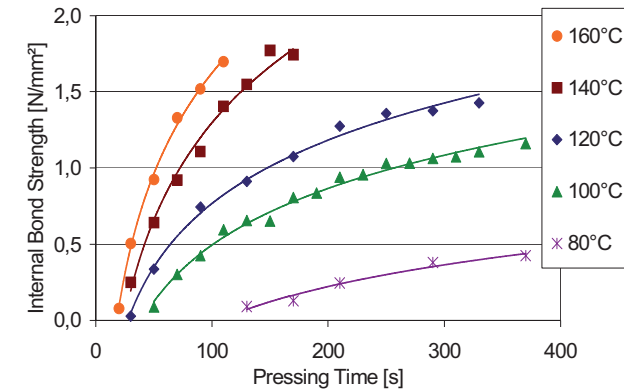


Figure 5.12: Development of internal bond strength obtained by IPATES (Courtesy: C. Heinemann).

5.3.6 Other Techniques

There are some other techniques for investigating the development of adhesive bond strength such as **acoustic test procedures** (Biernacki and Beall 1996, Chen and Beall 2000) and mechanical tests. A classical shear test with an adapted ABES principle (heating) and with a possibility for **dielectric analysis (DEA)** of the adhesive cure is shown in Figure 5.13 (Sernek *et al.* 2006).

This simple technique allows the evaluation of the development of adhesive bond strength (measured as shear strength and wood failure) as a function of the pressing time. An example of the development of adhesive bond strength during phenol-formaldehyde resin curing is shown in Figure 5.14. The strength development curve shows that the shear strength was zero at the beginning of the pressing (first stage), since the adhesive was still in a liquid state. With longer pressing time and increased temperature of the adhesive, gelation occurred and the adhesive mechanical strength started to build up. In the second stage, the shear strength increased almost linearly with the pressing time. Intensive polycondensation and cross-linking yielded more and more linkages in the three dimensional network, which allowed the adhesive to withstand higher stresses. Further curing led to the last stage where the shear strength curve leveled off and reached a maximum value. A model was used to describe the development of adhesive bond strength as a function of time (solid line).

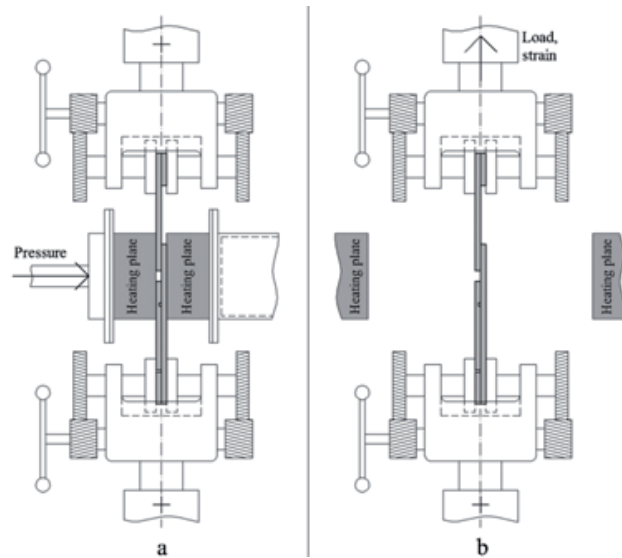


Figure 5.13: Device for investigation of the physical-chemical and mechanical properties of a specimen during resin curing: (a) pressing of the specimen and monitoring the curing by DEA; (b) determination of the shear strength of the adhesive bond.

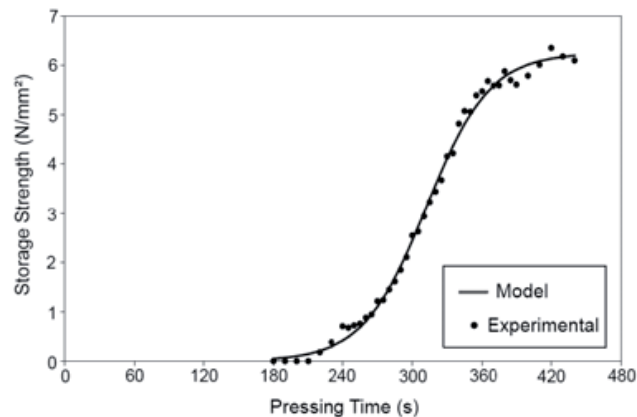


Figure 5.14: Development of the shear strength of a phenol-formaldehyde adhesive bond.

5.4 OPEN QUESTIONS

Main task of a comprehensive evaluation of the ongoing processes include reliable correlations between these parameters. Still a partly unclear question is the description and prediction (i) of the suitability of adhesives for bonding two surfaces and (ii) of the achievable properties of the bond line and the bonded products. Hence valuable, but still controversial information concerning the curing behaviour of various resins is gained by comparing the progress of both, the chemical and the mechanical curing; up to now only few examples in literature describe especially this connection of these two hardening processes as they can be monitored using different methods; one reason for this fact might be the difficult experimental realization. The following types of presentations are possible:

- Plotting the achieved partial **degrees of curing** after a certain time span in an x-y-plot can reveal the comprehensive hardening pattern of a resin (Figure 5.15) (Geimer *et al.* 1990). Such a correlation plot of the degree of chemical cure (*e.g.* measured by DSC) and the increase of mechanical strength (*e.g.* measured by DMA or ABES) can be regarded as a fingerprint of the curing behaviour of a resin.

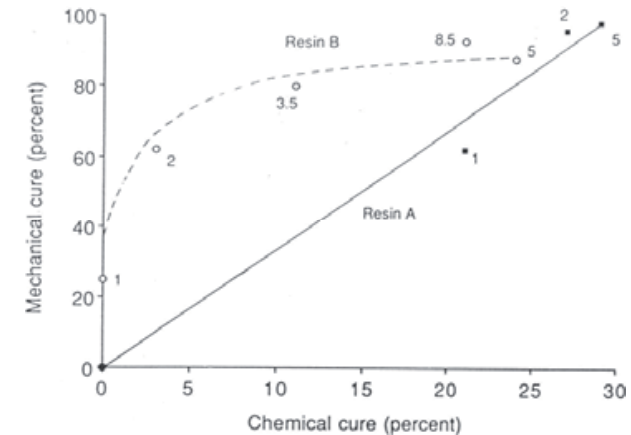


Figure 5.15: Chemical-mechanical hardening plot for two different PF resins; prehardening temperature 140 °C, times in minutes (Geimer *et al.* 1990).

- Monitoring the course of both reactions over time (Geimer and Christiansen 1991, 1996).

- Monitoring the course of the chemical hardening during the press time up to the moment where the press opens and therefore some certain bond strength must be reached (Heinemann *et al.* 2004).

It has been recognized, that the various test methods to describe the hardening behaviour and the formation of the bond strength not necessarily show the same course of the changes in the resins; this is quite obvious, because all methods are based on different changes in the adhesive during curing.

Especially the forming of the bond strength is influenced by much more parameters than just reflecting the chemical curing as seen (i) as the thermal reaction in DTA or DSC or (ii) by monitoring the increase in molar mass or (iii) looking at the changes in the portion of various structural elements in the resin. All these parameters rather describe the covalent behaviour of the adhesive in the bond line; bond strength however includes parameters like wetting and penetration (including over-penetration), since forming of adhesively acting bonds is mainly based on secondary attraction forces.

Target of the development of reactive adhesives is to achieve a reactivity as high as possible, however under consideration of *e.g.* the storage stability of the adhesive, the pot life of the adhesive mix and the existing process parameters. The reactivity of an adhesive (mix) hence is determined by various parameters:

- Type of the adhesive,
- Composition and cooking procedure,
- Type and amount of hardeners,
- Additives which might accelerate or retard the hardening process,
- Hardening temperature: press temperature, temperature in the bond line, temperature in the core layer,
- Properties of the wood surfaces.

Since no universal method exists describing all aspects of gelling and hardening as well as of formation of bond strength, still various methods must be used side by side. Combining experiences of chemical reaction pathways and results of the various test procedures as described above give a good chance when further developing and tailor making adhesive resins and adjusting their behaviour to special bonding processes.

5.5 REFERENCES

- Biernacki J.M., Beall F.C. 1996. Acoustic monitoring of cold-setting adhesive curing in wood laminates. *International Journal of Adhesion and Adhesives*, 16, 3: 165-172
- Bučar D.G., Tišler V. 1997. Curing dynamics of tannin-based adhesives. *Holzforschung und Holzverwertung*, 48, 6: 101-104
- Chen L., Beall F.C. 2000. Monitoring bond strength development in particleboard during pressing, using acousto-ultrasonics. *Wood and Fiber Science*, 32, 4: 466-477
- Chowdhury M.J.A., Humphrey P.E. 1999. The effect of acetylation on the shear strength development kinetics of phenolic resin-to-wood bonds. *Wood and Fiber Science*, 31, 3: 293-299
- Christiansen A.W., Follensbee R.A., Geimer R.L., Koutsky J.A., Myers G.E. 1993. Phenol-formaldehyde resin curing and bonding in steam-injection pressing. Part II. Differences between rates of chemical and mechanical responses to resin cure. *Holzforschung*, 47, 1: 76-82
- Dunky, M. unpublished results (1996, 2004)
- Garnier S., Pizzi A., Huang Z. 2002. Dry I.B. forecasting of commercial tannin adhesives-bonded particleboard by TMA bending. *Holz als Roh- und Werkstoff*, 60, 5: 372
- Geimer, R.L., Christiansen A.W. 1996. Critical values in the rapid cure and bonding of PF-resins. *For.Prod.J.* 46, 11/12: 67 - 72
- Geimer, R.L., A.W.Christiansen. 1991. Adhesive curing and bonding: response to real time conditions. *Proceedings Adhesives and Bonded Wood Products*, Seattle, WA, 12 - 29
- Geimer R.L., Follensbee R.A., Christiansen A.W., Koutsky J.A., Myers G.E. Resin characterization. *Proceedings 24th Wash. State University Int. Particleboard/ Composite Materials Symposium*, Pullman, WA, 1990, 65 - 83
- George B., Simon C., Properzi M., Pizzi A., Elbez G. 2003. Comparative creep characteristics of structural glulam wood adhesives. *Holz als Roh- und Werkstoff*, 61, 1: 79-80
- Gillham J.K. 1997. The TBA torsion pendulum: a technique for characterizing the cure and properties of thermosetting systems. *Polymer International*, 44(3): 262-276

He G.B., Yan N. 2005. Effect of wood species and molecular weight of phenolic resins on curing behavior and bonding development. *Holzforschung*, 59(6): 635-640

Heinemann C., Fruehwald A., Humphrey P.E. 2002a. Evaluation of adhesive cure during hot-pressing of wood-based composites. COST E13, Workshop Proceedings, 3rd Workshop – Vienna, 19-20 September 2002: 1-8. http://www.bfafh.de/bfh-pers/pdf/publ_heinemann_02_3.pdf

Heinemann C., Lehnen R., Humphrey P.E. 2002b. Kinetic response of thermosetting adhesive systems to heat: physico-chemical versus mechanical responses. Proceedings of the 6th Pacific Rim Bio-Based composites symposium. Portland/USA, 10.-13.11.2002, Corvallis: Oregon state university: 34-44

Heinemann, C., R. Mitter, M. Dunky, Thermokinetic simulation of a hot press cycle in the production of particleboards. Eighth European Panel Products Symposium, Llandudno (North Wales) 2004

<http://www.anasys.co.uk/library/tma1.htm>

Humphrey 2006. Temperature and reactant injection effects on the bonding kinetics of thermosetting adhesives. Proceedings Wood Adhesives 2005, San Diego, CA

Humphrey, P.E., S. Ren. 1989. Bonding kinetics of thermosetting adhesive systems used in wood-based composites: the combined effect of temperature and moisture content. *J.Adhesion Sci.Technol.* 3: 397 - 413

Humphrey, P.E. 1990. Device for testing adhesive bonds. USP 5176028

Kim J.W., Humphrey P.E. 2000. The effect of testing temperature on the strength of partially cured phenol-formaldehyde adhesive bonds. Proceedings Wood Adhesives 2000, South Lake Tahoe, CA

Kim S., Kim, H.-J., Kim, H.-S., LeeY.-K., YangH.-S. Thermal analysis study of viscoelastic properties and activation energy of melamine-modified urea-formaldehyde resins. *J.Adhesion Sci. Technol.* 20 (2006) 8, 803 - 816

Kreber B., Humphrey P.E., Morrell J.J. 1993. Effect of polyborate pre-treatment on the shear strength development of phenolic resin to Sitka spruce bonds. *Holzforschung*, 47, 5: 398-402

Laigle Y., Kamoun C., Pizzi A. 1998. Particleboard IB forecast by TMA bending in UF adhesives curing. *Holz als Roh- und Werkstoff*, 56, 3: 154

Lecourt M., Pizzi A., Humphrey P. 2003. Comparison of TMA and ABES as forecasting systems of wood bonding effectiveness. *Holz als Roh- und Werkstoff*, 61, 1: 75-76

Menard, K.P. 1999. Dynamic mechanical analysis : a practical introduction. CRC press. Boca Raton, 208 p.

Ohyama M., Tomita B., Hse C.Y. 1995. Curing property and plywood adhesive performance of resol-type phenol-urea-formaldehyde cocondensed resins. *Holzforschung*, 49, 1: 87-91

Pichelin F., Pizzi A., Fruehwald A. 2000. OSB adhesives rate of strength development on single strands couples. *Holz als Roh- und Werkstoff*, 58, 3: 182-183

Prasad T.R.N., Humphrey P.E., Morrell J.J. 1994. The effects of chromated copper arsenate and ammoniacal copper zinc arsenate on shear strength development of phenolic resin to Sitka spruce bonds. *Wood and Fiber Science*, 26, 2: 223-228

Riande, E., *Polymer Viscoelasticity*, 86, 2000.

Roos, T., Diploma Thesis, University of Hamburg, 2000

Sernek M., Kokalj A., Jošt M. 2006. The development of adhesive bond strength during phenol-formaldehyde resin curing. Wood resources and panel properties : conference proceedings : Cost Action E44-E49, Valencia, Spain, 12-13 June 2006. Valencia: AIDIMA, Furniture, wood and packaging technology institute: 89-96

Stefke, B., M. Dunky, Catalytic influence of wood on gelling of formaldehyde based glue resins. *J.Adhesion Sci. Technology* 20 (2006) 8, 761 – 785

Steiner P.R., Warren S.R. 1981. Rheology of wood-adhesive cure by torsional braid analysis. *Holzforschung*, 35, 6: 273-278

Steiner P.R., Warren S.R. 1987. Behavior of urea-formaldehyde wood adhesives during early stages of cure. *Forest Products Journal*, 37, 1: 20-22

Tomita B., Ohyama M., Itoh A., Doi K., Hse Ch.-H. 1994. Analysis of curing process and thermal properties of PUF cocondensation resins. *Mokuzai Gakkaishi (J.Japan Wood Res.Inst.)* 40, 2: 170-175

Umemura K., Kawai S., Mizuno Y., Sasaki H. 1996. Dynamic mechanical properties of thermosetting resin adhesives II. Urea resin. *Mokuzai Gakkaishi*, 42, 5: 489-496

Wang X.M., Riedl B., Geimer R.L., Christiansen A.W. 1996. Phenol-formaldehyde resin curing and bonding under dynamic conditions. *Wood Science and Technology*, 30, 6: 423-442

Yin S., Deglise X., Masson D. 1995. Thermomechanical analysis of wood/aminoplastic adhesives joints cross-linking - UF, MUF, PMUF. *Holzforschung*, 49, 6: 575-580

Zanetti M., Pizzi A. 2002. Time delay effect in TMA methods for MUF resins testing. *Holz als Roh- und Werkstoff*, 60, 5: 3

Chapter 6

Innovative Methods for Quality Control in the Wood-Based Panel Industry

Jochen Aderhold and Burkhard Plinke

CHAPTER SUMMARY

The objective of this chapter is to review some innovative techniques for quality control in the wood-based panels industry which are not yet commercially available. The authors selected those techniques which they think are most likely to find industrial application in the near future: infrared thermography, near infrared reflectometry, and nuclear magnetic resonance.

6.1 INTRODUCTION

Wood based panel companies face their customer's increasing demand for high and consistent quality of their products and for flexible production. At the same time, the cost pressures intensify. Quality assurance systems following standards such as ISO/EN/DIN 9000 become more and more important. Just in time delivery concepts require the production of up to 20 different panel types on the same production line within 24 hours (Nielsen 1994). In order to meet these requirements, a careful **monitoring of the production** process and preventive measures to avoid production failures are necessary (Deubel 1992a, Deubel 1992b). This includes appropriate testing procedures for the final products, the panels. Panel testing methods roughly fall into two categories: on-line methods and off-line methods. On-line methods should be integrated into the production process and work non-destructively. In many cases, every single panel can be tested. Some points of interest are measurement of the raw density and the mechanical strength as well as the detection of structural failures such as delaminations. Off-line techniques on the other hand will always be limited to spot samples which can be tested for properties not accessible with on-line testing.

Regarding on-line techniques, a variety of **testing methods** have developed over the years, many of which are already available on the market, including ultrasonic, microwave, and x-ray techniques as well as

image processing. These commercially available techniques are not within the scope of this chapter since they are described in detail elsewhere (e.g. Welling 1998).

Recently, some new techniques have evolved, including infrared thermography, near infrared reflectometry, and nuclear magnetic resonance. These three new methods will be described in detail in the following sections since the authors believe that these techniques are most likely to find applications in the industry in the near future.

6.2 INFRARED THERMOGRAPHY

6.2.1 Principles of Infrared Thermography

The basis of infrared thermography is the fact that every object having a temperature above absolute zero emits electromagnetic radiation which is called thermal or Planck radiation. At a given wavelength the radiated power density (for a so-called black body) depends on the temperature only so that the temperature can be calculated by measuring the radiated power density. The dependence of the power density on temperature and wavelength is given by the famous **Planck equation** (Planck 1900):

$$M_{\lambda}^0 = \frac{C_2 \lambda^{-5}}{\exp(C_2 / \lambda T) - 1} \quad (1)$$

In this equation M_{λ}^0 is the power density per wavelength interval emitted by an ideal ("black") radiator (unit: W/m^3), whereas λ stands for the wavelength and T for the absolute temperature. The constants C_1 and C_2 contain only natural constants such as h (Planck's constant), c (speed of light) and k_B (Boltzmann's constant):

$$C_1 = 2\pi h c^2 = 3.742 \cdot 10^{-16} W m^2 \quad (2)$$

$$C_2 = hc / k_B = 0.014388 mK \quad (3)$$

Figure 6.1 shows the thermal radiation of a black radiator for the temperature range between 300 K and 700 K. It is apparent that the overall power density (the areas under the curves) increases strongly with increasing temperature. This fact is mathematically described by the **Stefan-Boltzmann law** which can be obtained by integrating Planck's equation:

$$M^0 = \int_0^{\infty} M_{\lambda}^0 d\lambda = \sigma T^4 \quad (4)$$

with:

$$\sigma = \frac{2\pi^5 k_B^4}{15h^3 c^2} = 5.670 \cdot 10^{-8} W m^{-2} K^{-4} \quad (5)$$

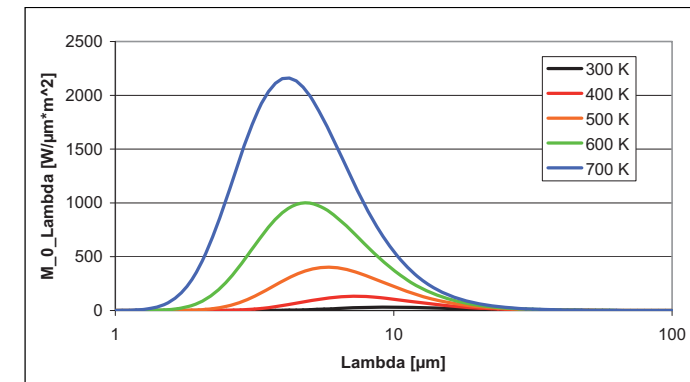


Figure 6.1: Thermal radiation of a black radiator between 300 K and 700 K.

Furthermore, the peak position of the power density λ_{max} shifts to smaller wavelengths for increasing temperatures. This is described by Wien's displacement law:

$$\lambda_{max} T = 2898 \mu m K \quad (6)$$

Historically, both the Stefan-Boltzmann law and **Wien's displacement law** were discovered before Planck's law (Stefan 1879, Boltzmann 1884, Wien 1893).

Since M_{λ}^0 depends on temperature only, one can estimate the temperature of an object by measuring the power density if Planck's equation is valid, i. e. when the atoms or molecules of the object are in thermal equilibrium. In most practical cases this will be true. Gas discharges and similar phenomena are an exception from Planck's law. Consequently, the temperature of gas discharges cannot be measured in the described way.

At temperatures between room temperature and 450°C, most of the radiated intensity is in the so-called thermal infrared (IR) region of the electromagnetic spectrum having wavelengths of 2.5 μm and longer. Of practical importance are the regions labelled as mid-wave IR (MWIR, 3 μm ... 5 μm) and long-wave IR (LWIR, 8 μm ... 12 μm) where suitable detectors are available, and where the atmosphere is sufficiently transparent.

The "black" body describes the ideal, theoretical case. Real objects will under given conditions emit less power density than black bodies. This fact is usually described by a factor which is called emissivity. It is represented by the Greek letter ϵ and can, by definition, have values between 0 and 1.

The **emissivity** of an object depends on the nature of its surface. Empirical values for many materials can be taken from the literature (Gaussorgues 1994). Many organic materials, water and glass have emissivities of 0.9 or higher. Strongly reflecting surfaces on the other hand have normally very low emissivities. In the infrared region of the electromagnetic spectrum this is especially true for metallic surfaces. In these cases reflected thermal radiation from the environment can exceed the object's thermal radiation, which can lead to misinterpretations. In particular, the infrared image can show a reflection of the camera itself, so that the cooled detector appears as a very cold spot. This is the so-called narcissus effect. Examinations of metallic surfaces using thermography thus require extreme care. In many cases, problems with low emissivity surfaces can be solved by covering them with special high emissivity paints.

6.2.2 Infrared Cameras

A huge number of different infrared cameras having different detection principles are available. Today, almost all cameras have focal plane arrays, i.e. matrices from single detector pixels as in normal digital cameras. From a practical point of view, the most important difference is between cameras having cooled photovoltaic detectors or microbolometer detectors, respectively. **Cooled photovoltaic detectors** are made from compound semiconductor materials. Infrared photons having an energy larger than the band gap can be absorbed, generating an electron-hole pair, and consequently electric current. The number of semiconductors having a suitably small band gap is limited, including InSb (Indium Antimonide) and HgCdTe (Mercury Cadmium Telluride, MCT or CMT) as the most important materials. These semiconductors are difficult to grow in high quality, and production yield of focal plane arrays is low,

causing high cost. Furthermore, to improve signal-to-noise ratio, they have to be cooled down to 90 K or lower. In the past this was mainly done by cooling with liquid nitrogen. Today, mechanical coolers, so-called Stirling coolers, can do the cooling. However, these are again expensive. Consequently, prices for cameras with cooled detectors are in the range of 70 k€. Their temperature resolution is around 15 mK. Frame rates can be as high as 1 kHz.

The pixels of **microbolometer detectors** are essentially very thin silicon plates with an absorbing layer. When an infrared photon is absorbed by these plates their temperature and consequently their electric resistance rises, which can be used for detecting the photons. Since the production of these structures is similar to the well-developed silicon CMOS technology, these detectors are much cheaper than InSb or MCT detectors. Although the temperature of microbolometer detectors should be well-controlled as well, and although Peltier coolers are often applied, these devices do not require expensive Stirling coolers. Consequently, prices for microbolometer cameras start from 10 k€. A temperature resolution of 100 mK and frame rates up to 50 Hz can be achieved. Since this is sufficient for many applications, it is expected that microbolometer cameras will become more and more important and will allow new applications of thermography in many areas for which cooled photovoltaic cameras would be too expensive.

It should be noted that glass and quartz are not transparent in the thermal IR so that expensive special lenses from Si, Ge, ZnSe or suchlike are required for any camera type.

6.2.3 Thermography for Non-Destructive Testing

As explained before, an object's infrared radiation depends on its emissivity as well as on its temperature. Both dependencies can be used for infrared machine vision in the wood-based panel industry.

In classical machine vision in the visible spectral range, differences in intensity of the light reflected from the object under study are utilized in order to draw conclusions about possible defects or foreign bodies. In a similar manner, **emissivity differences** can be used. Objects having different emissivities radiate thermal radiation of different intensity even if they are at the same temperature. Thus, they have different grey values in the infrared image. Alternatively, the objects can be illuminated by infrared radiators so that the light reflected by them can be detected. The contrast in the infrared can be very different from that in the visible part of the spectrum. For instance, metal and glass surfaces are highly

reflective in the visible range, whereas in the infrared this is only true for metal surfaces. Glass has a high emissivity and consequently a low reflectivity in the infrared range.

Apart from emissivity differences, and more importantly, **temperature differences** can be used for panel testing and process control. In systems where heat and mass transfer is possible (which is true in most practical cases) temperature differences are always connected with heat flow. Temperature differences will cause heat flow, and a heat flow caused by some reason will lead to temperature differences, the amount of which will depend on the object's thermal properties. If no inner heat sources (such as exothermic chemical reactions) and no bulk flows are present, as will be the case for wood-based panels a certain time after pressing, heat flow and consequently temperature differences will occur only when the object is not in thermal equilibrium with its environment. This means that the object must cool down or heat up in some way. In such a cooling or heating process, regions of different thermal conductivity and/or capacity can have different surface temperatures and can thus be differentiated in the infrared image. This can be used for panel testing since many defects differ in thermal conductivity (air inclusions, delaminations) or thermal capacity (moisture) from the good regions. The defects need not be at the surface in order to be detected but may be deeper in the material. The exact penetration depth of the technique depends on many factors.

How can the necessary **cooling or heating processes** be generated? The easiest case are objects which cool down (or heat up) anyway as a consequence of the production process. Wood-based panels produced by hot pressing are a good example. In this case, it is sufficient to simply observe the object with an infrared camera (passive heat flow thermography, see Figure 6.2). Surface regions under which defects with a low thermal conductivity can be found will cool down more rapidly since less heat can be supplied from the hot interior. Air inclusions and delaminations are examples for such defects. In such a way, they can be detected in the infrared image.

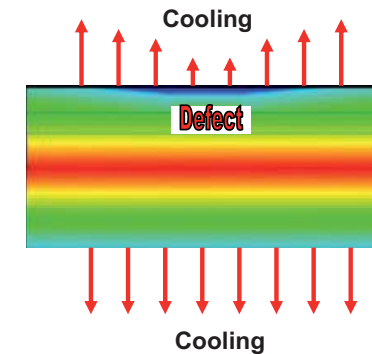


Figure 6.2: Principle of passive heat flow thermography.

If it is not possible to utilize cooling or heating processes caused by the production process, the object can be exposed to an exterior heat pulse (active heat flow thermography, see Figure 6.3). In the easiest case, this can be done if the object passes an infrared heater on a conveyor belt. This will cause a heat wave which penetrates into the object while the surface cools down. If the conduction of heat is retarded by defects of low thermal conductivity, the surface above the defect will stay warm for a longer time, which can again be detected in the infrared image. As a rule of thumb one can expect to see a defect if its distance from the surface does not exceed its diameter.

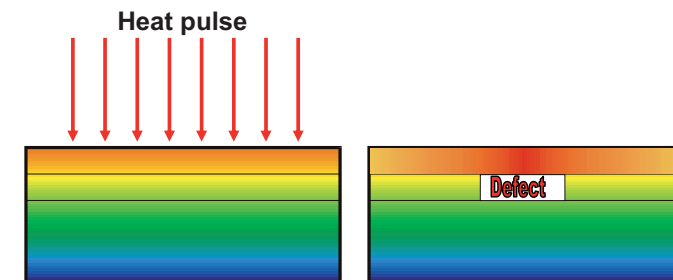


Figure 6.3: Principle of active heat flow thermography.

6.2.4 Application and Examples

Since wood-based panels are mostly manufactured by hot-pressing, quality control is in many cases possible by passive heat flow

thermography. Here the cooling of the objects to be tested is observed by an infrared camera. The camera is installed typically directly behind the press (Figure 6.4).



Figure 6.4: Set-up for passive thermography behind the press.

Many defects differ in thermal capacity and/or conductivity from the good areas and become thus apparent by different surface temperatures. If, for example there is a **delamination**, the surface above this spot cools down faster, because due to the lower heat conductivity of the defect less heat follows from the inside than in good areas.

Typical defects detectable this way include:

- Blisters in particleboards
- Delaminations between wood-based panels and decorative papers
- Defective gluing in plywood
- Fallen out knots in the internal veneers of plywood
- Variable glueline thicknesses

Thermography has successfully been used for the testing of boards with thicknesses between 3 mm and 38 mm and at production speeds of up to 30 m/min. The surface temperatures of the wood-based panels can vary

between 40 °C (coating with decorative papers) and more than 100 °C (OSB). Figure 6.5 shows infrared images of blisters in particleboards of 22 mm thickness as an example. The images were taken after the application of decorative papers.

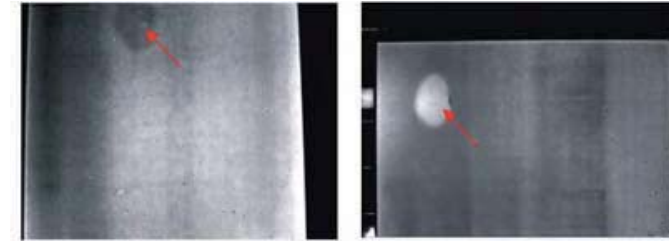


Figure 6.5: Infrared images of blisters in 22 mm thick particleboards. The dark (cool) spot in the left imager shows a blister in the lower layer while the light (warm) spot in the right image shows a blister in the upper layer.

Infrared images of **particleboards** can be easily evaluated automatically because of their homogeneous structure. A bit more complicated is the situation for plywood, where the natural wood structure is still recognizable when applying decorative papers. Nevertheless, defects like fallen out knots or defective gluing can be detected (Figure 6.6).

A further field of application of the passive thermography in the wood-based panel industry is the detection of fluctuations in density and moisture content in the production of **oriented strand boards (OSB)**. Such inhomogeneities involve corresponding differences in the thermal capacity leading to a different cooling behaviour. Figure 6.7 shows a freshly pressed OSB laboratory board with intentional defects such as over-moistening (top right) and excess raw density (left below). The infrared image (right) was taken at a time where the thermal contrast between defect and good material was maximized.

After an appropriate calibration the density measurement can be done quantitatively. To this end a number of test boards was first characterized by thermography and then cut into small pieces, the density of which was determined by weighing. The density distribution obtained this way corresponds both qualitatively (Figure 6.8) and quantitatively (Figure 6.9) very good with the gray values of the infrared image.

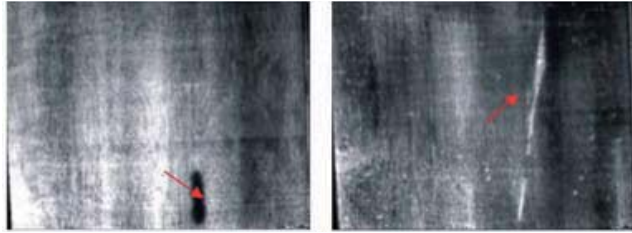


Figure 6.6: Infrared image of plywood boards of 5 mm thickness. The left image shows a fallen out knot in the middle layer, while the right image shows a defective gluing of the veneers.

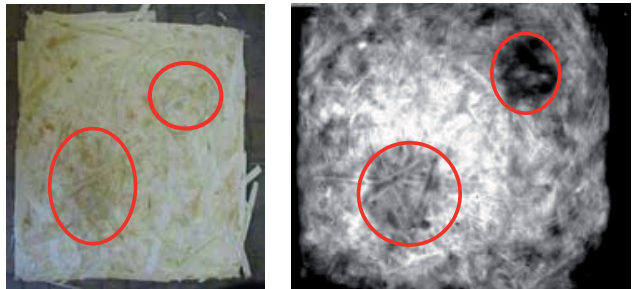


Figure 6.7: Freshly pressed OSB laboratory board with intentional defects.

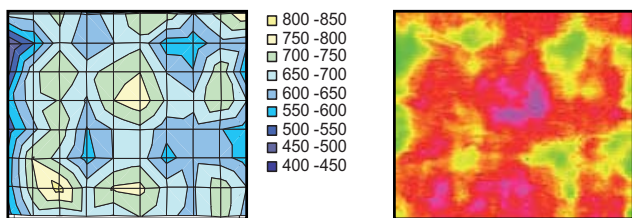


Figure 6.8: Comparison of gravimetrically determined density distribution (left) and infrared image (right) of an OSB laboratory board. Density scale in kg/m^3 .

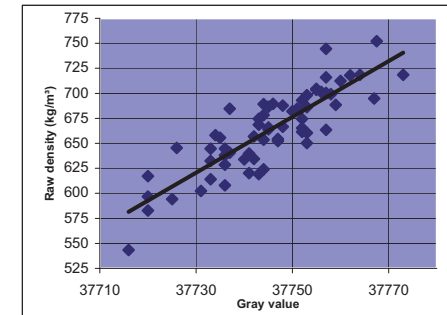


Figure 6.9: Quantitative comparison between density and grey value.

In case that no cooling processes inherent to the process can be used, the active variant of the heat flow thermography (Figure 6.10) can be used where the boards are transported on a conveyor belt passing first an infrared heater and then the infrared camera. Important applications here also are the testing of **plywood** regarding gluing defects and fallen out knots as well as of high-quality solid wood (wood for musical instruments or pencils) regarding density inhomogeneities.

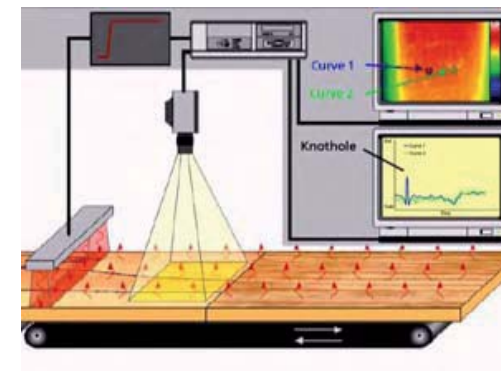


Figure 6.10: Principle of the online active heat thermography.

Black knots in solid wood can also be detected by means of ultrasonic excitation. Black knots cause problems because they can fall out easily. The ultrasonic excitation causes **frictional heat** in the black knots which can easily be detected by thermography. Good knots give no signal (Figure 6.11).

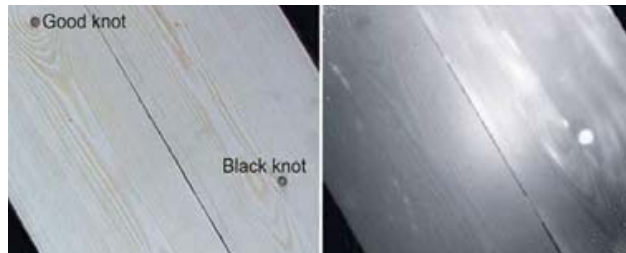


Figure 6.11: Solid wood piece with good knot (left top) and black knot (right above). The black knot appears as light area in the infrared image.

Suggested R&D topics include:

- Automated defect detection in wood-based panels having an inhomogeneous structure such as massive wood or plywood
- Techniques for compensating parasitic effects such as changing background conditions, heat sources in the surrounding, sunlight etc.
- Building a solid fundament for density measurements by means of thermography

6.3 NAR INFRARED REFLECTOMETRY

6.3.1 Origin of NIR Spectra

The infrared spectral region contains the wavelength interval between 0.7 μm and 1000 μm and is subdivided in the near, mid-wave and far infrared (Table 6.1). Please note that this definition is a little different from that given in the thermography chapter.

Many molecules have strong spectral lines in this region. The reasons for this are **molecular rotations and vibrations**. Molecular rotations cause spectral lines in the far infrared and are not important here. Molecular vibrations, i.e. stretching and bending oscillations of the chemical bond, lead to complicated spectra in the near and mid-wave infrared. If the chemical bond is approximated by a harmonic oscillator and treated quantum mechanically, a spectrum of equidistant energy levels is obtained. Transitions between these levels are connected with emission or absorption of infrared radiation. Following the rules of quantum

mechanics, only transitions between neighbouring levels would be allowed which all would have the same frequency in the mid-wave infrared since the levels are equidistant. Near infrared spectral lines would not exist.

Table 6.1: The infrared spectral region (Osborne 1993).

Spectral range	Characteristic transitions	Wavelength range [μm]
Near Infrared (NIR)	Molecular vibrations: overtones and mixing frequencies	0,7 ... 2,5
Mid-wave Infrared	Molecular vibrations: fundamental frequency	2,5 ... 50
Far Infrared	Molecular rotation	50 ... 1000

The existence of NIR spectral lines is due to deviations of the chemical bond from the harmonic oscillator model. If nonlinearities are included, transitions between levels other than immediate neighbours are allowed as well, leading to so-called overtones. They are not necessarily integer multiples of the fundamental frequency since nonlinearity also leads to non-equidistant levels. Furthermore, frequency mixing is possible. Consequently, NIR spectra are more complicated, but also contain more information than spectra at longer wavelengths.

The position of **NIR spectra** lines for a given bond has been extensively studied and can be found in the literature. Table 6.2 shows the position of some spectral lines for some bonds which are important for adhesives used in the wood-based panel industry. The exact positions depend on the structure of the complete molecule.

Table 6.2: Some NIR spectral lines relevant for adhesives used in the wood-based panel industry (Osborne 1993).

Type of bond	Contained in ...	λ_1 [nm]	λ_2 [nm]	λ_3 [nm]
H ₂ O	Water	~1458	~980	~744
-CH ₂	Formaldehyde	1738-1795	1170-1209	890-913
-NH ₂	Urea	1501-1535	1014-1031	
-CH (aromatic)	Phenol	~1684	~1134	~859
ROH	Phenol	1398-1421	~979	

6.3.2 NIR Reflectometry

The appearance of spectral lines which are specific for a given molecule in the infrared spectral region can be used to identify many (mostly

organic) substances or even to measure their quantity in compounds. The NIR range has some advantages over other spectral ranges:

Since NIR spectra are due to anharmonicities, they are more differentiated than spectra in other infrared ranges. The object's thermal radiation normally does not play a role and does not disturb the measurements. Cheap conventional optical materials such as glass and quartz can be used whereas expensive special optics made from Ge, ZnSe and suchlike are needed in the mid-wave and far infrared. Due to the shorter wavelength the ratio of scattered and absorbed radiation is larger than in the other infrared regions. This fact is utilised in NIR reflectometry. A ray of light striking a surface can be reflected in a mirror like way (Figure 6.12a) or penetrate into the sample. The light penetrating into the sample can be absorbed (Figure 6.12c) or reflected diffusively (Figure 6.12b). It is the diffusively reflected part of the light which contains spectral information of the sample. It can easily be collected by a lens and subsequently analyzed.

Unlike other spectroscopic techniques, NIR reflectometry does not require sample surfaces of high optical quality. Elaborate sample preparation is not necessary. Furthermore, the samples need not to be transparent. For this reasons NIR reflectometry is a suitable tool for **online process monitoring** in the wood-based panel industry. However, calibration procedures and multivariate statistical methods (chemometry) are necessary for evaluating NIR data.

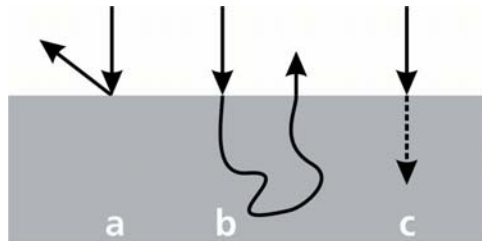


Figure 6.12: Mirror like reflection (a), diffuse reflection (b) and absorption (c) of a ray of light (Givens 1997).

6.3.3 Panel Properties and NIR Spectra

In the wood-based industry NIR reflectometry is already being used for the measurement of **moisture content**. Many other applications have been discussed in literature but they have not found industrial applications in a broader frame. For example, Niemz et al. have shown that the amount

of **adhesive** as well as the mixing ratio of softwood and hardwood can be measured in the mat of a particleboard line (Niemz 1994).

Recovered wood can be recycled into particleboards. However, it is important to sort out wood treated with paint or preservatives. For this purpose, NIR reflectometry has been proposed as well (Feldhoff 1998).

Gindl et al. have shown a clear correlation between the mechanical **strength** of European larch and the NIR reflection spectrum – with possible applications in strength grading (Gindl 2001).

Since NIR spectra are temperature dependent (Thygesen 2000), the spectra can in principle also be used for temperature measurement.

6.3.4 Multivariate Techniques for Data Analysis

The evaluation of NIR data can be done by modern multivariate techniques such as **principal components analysis (PCA)** and related techniques. Mathematically, PCA is a coordinate transformation. It assumes that any measured spectrum having N data points can be described by a point in a coordinate system having N dimensions. The measured spectra for a given set of samples which differ in some relevant property consequently form a point cloud in this coordinate system. PCA now transforms this coordinate system into a new one which is orthogonal, and where the variance of the data is largest for the first axis. The variance is a measure for the information content of a data set. The second axis has the second largest variance and so on. This coordinate transformation is described by a transformation matrix whose column vectors are the sought-after principal components. The idea is to consider only the first few principal components whose variances describe a sufficient part of the overall variance. This is equivalent to choosing a few wavelengths at which the samples show the largest differences. By evaluating only these selected wavelengths, the amount of data to be processed can be dramatically reduced.

6.3.5 Technical Aspects

As in other spectroscopic techniques, NIR has three functional blocks: excitation source, dispersive element, and detector. The easiest excitation sources are thermal radiators such as halogen lamps.

The most popular dispersive elements are holographic gratings. More advanced devices are acousto-optical tuneable filters (AOTFs) and line spectrographs. A line spectrograph transforms a line from the object under study onto the matrix detector of a normal camera in such a way

that one dimension of the array contains the spatial information along the line, whereas the other dimension contains the optical spectrum of a given point on the line. By moving the object under test along a conveyor band it can be scanned line by line, resulting in a complete set of spectra for every single point on the surface, limited only by the pixel number of the camera (**spectral imaging**). Line spectrographs are available for spectral ranges from the ultraviolet to the thermal infrared. In the NIR range, of course a NIR camera has to be used as a detector.

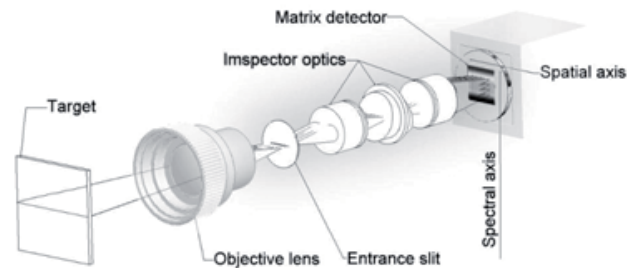


Figure 6.13: Principle of a line spectrograph.

On the detection side, semiconductor detectors are used most frequently which utilize photoconductivity (e.g. PbS detectors) or photovoltaic effects (e.g. InGaAs detectors). PbS detectors have a broader spectral range (800 nm to 3.0 μm) than InGaAs detectors (900 nm to 2.0 μm), but they are less sensitive than InGaAs by about one order of magnitude. Both detectors can be used to build NIR cameras. InGaAs focal plane array cameras were introduced to the market for acceptable prices some years ago.

6.3.6 Applications and Examples

Images which comprise complete reflexion spectra for each pixel (rather than three intensity values for red, green and blue like in conventional imaging) are called **hyperspectral images**. To achieve such an image a line spectrograph and a NIR camera are used to scan a moving surface. Figure 6.14 (top left) shows a mat formed with OSB strands. It was scanned using a demonstration set-up for NIR spectral imaging (Plinke, Ben-Yacov 2009) at a resolution of approximately 3 mm/Pixel in moving direction and of 1 mm/Pixel across. A hyperspectral image with a spectral resolution of 316 intensity values for the wavelength range 1050 to 1650 nm is stored and evaluated in a specific image processing program.

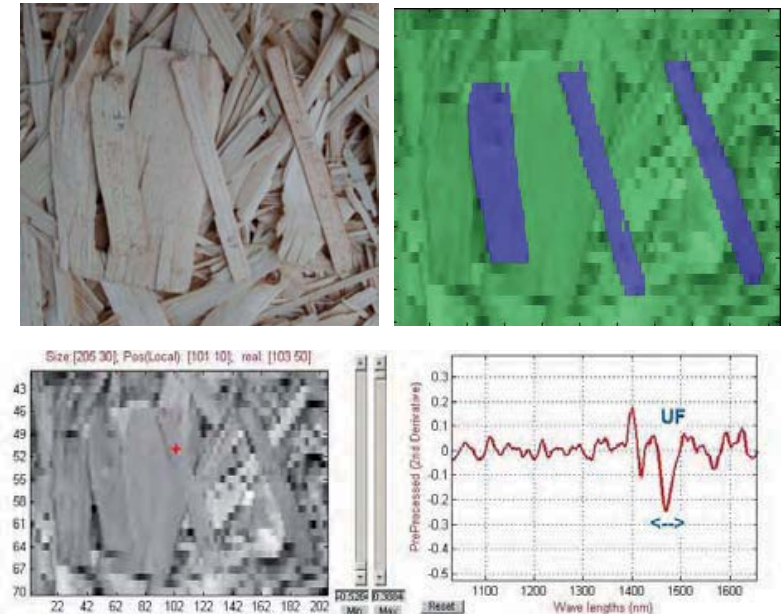


Figure 6.14: Application of Spectral Imaging for resin detection on wood particles, (Top left: Original scene showing strands with and without UF application, Bottom left: Mean NIR intensity per Pixel shown as gray value, Bottom right: local spectrum with characteristic UF peak, Top right: Image segmented by peak area, strands with UF application are marked blue).

The grey value image in Figure 6.14 (bottom left) was computed from the mean intensity of each pixel in such a way that image structures and strand shapes are roughly visible. Further steps are necessary to extract information from the hyperspectral image: The spectra of each pixel (typically 25000 per image) are smoothed, normalized to absorption spectra and transformed to their 2nd derivation. Then compounds such as resins or water can be detected by their **absorptions at typical wavelengths**. In Figure 6.14 (bottom left) the absorption spectrum of the pixel marked to the left of the diagram is shown. Beside the peaks due to surface moisture (around 1400 nm) the peak typical for UF-based resins appears. In Figure 6.14 (top right) all pixels showing this peak in their spectra are marked as blue. Thus, strands with an UF application can be distinguished from those without resin.

Classical **chemometry** offers more sophisticated evaluation methods for spectra (Kessler 2007). With PCA, a set of spectra can be decomposed

into their principal components, i.e. a new set of matrices of scores, loadings and residues. During the decomposition process, the variation of the spectra is transformed into a small set of principal components for each spectrum (scores) and loadings which show the dependency from the wavelengths. The elements in the score matrix can be used to form a score space as a good expression of the similarity of spectra. If their scores are in close vicinity in the score space then they probably comprise NIR signals of the same compounds. However, this method can only be applied successfully if other effects to the spectra than chemical composition (e.g. scattering, measurement geometry, drift of illumination, surface properties etc.) can be excluded or controlled by selection of specific principal components. Then it is possible to build a mathematical model from a set of training data and use it to predict the composition of compounds from their spectra.

An application of PCA used to segment a hyperspectral image is demonstrated in Figure 6.15: The top image is a scene with strands without resin in the background (red) and with three types of resin (UF, blue; PMDI, brown; MUPF, green). The colour classification of the pixels is derived from the scores of their 1st and 2nd principal components. Their score space is shown in Figure 6.15 (bottom) as one dot for each pixel. The scores of PC-1 and PC-2 show distinct clusters, and therefore the pixels in the left image are coloured according to the membership of their PC set to one of the clusters. Again, it must be emphasized that several conditions must be fulfilled to use PCA for an evaluation of hyperspectral images. The images in Figure 6.14 and 6.15 were generated with the **software tool** “SpectraWalker” which has been developed for this purpose.

Other than moisture measurement, there are few industrial applications of NIR reflectometry and especially NIR spectral imaging reported for the wood-based panel industry. Hutter et al. (2003) published a study that aimed at improving fibreboard production by a **design of experiments** procedure. In this study wet-process fibreboard production was systematically investigated in order to better understand the process and to address ways for future improvements. Experimental Design was applied to examine the effects of different wood mixtures and processing variables on visual and physical properties of the final fibreboard. All designed experiments were done without adding any synthetic adhesive or hydrophobic agent. Response Surface Methodology was used to visualise fibreboard properties and to carry out multiple response optimisation.

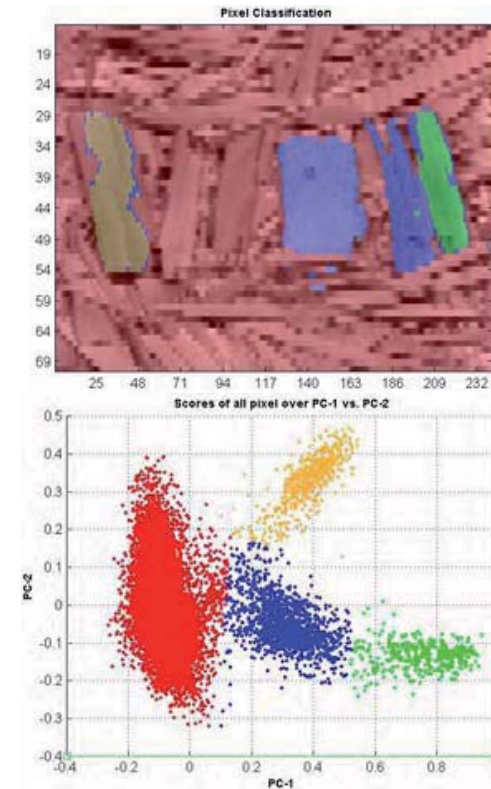


Figure 6.15: Application of PCA in spectral imaging to detect different resin types (Top: Strands, coloured according to resin type (red: no resin; blue: UF; brown: PMDI; green: MUPF), Bottom: Score plot of two principal components of the pixels in the left image).

NIR reflectometry methods are considered to be an important tool for gathering process data. Problems such as fluctuations of the light source, “flutter” effects (i.e. a rising or falling surface, measuring out of focus) as well as optical density fluctuations, e.g. on the fast moving conveyor belt, were addressed. A control system ensured the functionality, performed calibrations automatically and aligned the system with internal reference standards. The prototype was developed in close co-operation with the industry. The on-line control system was complemented by a high level multivariate data analysis including appropriate calibration models (Kessler 2000).

Metso Panelboard has used NIR technology as the basis for their PanelPro™ system for monitoring important parameters in MDF production. Engström (2008) of Casco Adhesives, Sweden, described real time determination of **formaldehyde emission** from particleboards using NIR spectroscopy. There is also some similar work on OSB (Taylor and Via 2009).

Suggested R&D topics include:

- Adapting NIR reflectometry to harsh industrial environments
- Exploring potential applications of NIR Reflectometry in industry

6.4 NUCLEAR MAGNETIC RESONANCE

6.4.1 Nuclear Spin

Nuclear Magnetic Resonances (NMR) is a technique which is based on the fact that many atomic nuclei have intrinsic magnetic moments which are characterized by the so-called **magnetic quantum number** m . It is related to a nuclear property called spin which is characteristic for a given nucleus and which can take values that are integer multiples of one-half (0, $\frac{1}{2}$, 1, $\frac{3}{2}$, ...). For a given spin, there are $(2I+1)$ possible values of m ranging from $-I$ to $+I$ in integer steps.

Because of their relative simplicity, nuclei having a spin of $I=\frac{1}{2}$ such as ^1H , ^{13}C , ^{15}N , ^{19}F , ^{29}Si und ^{31}P are of particular importance for NMR since they can have only two magnetic states, namely $\frac{1}{2}$ and $+\frac{1}{2}$. In the absence of a **magnetic field**, these two states have the same energy. If, however, a magnetic field is applied, the energy of the states differs by an amount which is proportional to the magnetic field strength. Transitions between these states are possible by absorption or emission of electromagnetic radiation with a characteristic frequency.

The effective magnetic field at the nucleus can be different from the external field due to shielding by other nuclei and also by electrons. Therefore, the transition frequency is different for different nuclei and also for nuclei having a different chemical environment. Therefore, the nature of the nucleus and of the chemical bond of which it is a part can be analyzed by measuring the transition frequency. This is generally done by exciting the transition by a transient electromagnetic pulse and a subsequent observation of **resonance absorption**.

6.4.2 Panel Properties and Nuclear Spin

The most commonly known application of NMR is in medicine where it is used to represent and differentiate different kinds of tissue. Over the last years, it has become a more and more important tool for process control and materials analysis. It works best for liquids, but can also be applied for solids.

Since wood is an organic compound, it contains many of the abovementioned nuclei with a spin of $I=\frac{1}{2}$, especially ^1H (protons). Consequently, wood gives a strong NMR signal. An important feature is the fact that protons in different molecules such as water, wood constituents, adhesives etc. give different NMR signals. In such a way it is possible to measure the **moisture content** and the **raw density** of wood or wood-based panels independently. Therefore, NMR has frequently been used to monitor the drying of various wood products or to study the internal structure of wood. However, applications to the field of wood-based panels mostly refer to studies of adhesive curing. There are only few papers on non-destructive testing of wood based panels using NMR. This is mainly due to the high cost of NMR equipment and to the limited penetration depth of the technique. However, it can provide information not accessible by other techniques.

6.4.3 Applications of NMR in the Wood Based Panel Industry

In the wood sector NMR has been used mainly for fundamental research (drying of wood, reactions of adhesives in wood-based panels, cellular structure of wood etc.). There are only few publications concerning the use of NMR for process monitoring and quality control in the wood-based panel industry. Possible applications are the measurement of raw density and moisture content in particleboards, the estimation of the degree of curing of adhesives and the detection of adhesion defects.

Among other quantities such as strength, stiffness, and dimensional accuracy, the **moisture content** is an extremely important property of logs, sawn timber, and wood-based products. For optimum processing conditions in the paper industry, the moisture variation of logs should be as low as possible. Sorting the logs according to moisture content would be very helpful for a stable and economic production of paper products. The moisture content of sawn timber and wood-based panels has to meet a certain target value in order to avoid problems with cracks, distortion, and decay. It also influences the measurement of other important properties including distortion. The lack of reliable, precise, and fast techniques for moisture determination often causes wood products to fall

short of the customer's expectations. Finally, drying timber to the target moisture is very energy intensive. A better control of this process will diminish energy consumption. The precise estimation of moisture content and of the raw density profile is very important in the wood-based panel industry as well since they will have a strong effect on the practical value of the product.

The moisture content can only be precisely determined if the local density is also known. Unlike other techniques, NMR can measure these quantities at the same time, giving more accurate and also more stable results.

It is also possible to obtain **moisture and density profiles** perpendicular to the surface and to achieve a certain lateral resolution.

This was demonstrated in a publication by Bloem et al. (1997). These authors designed a special hand-held NMR device which works with one-sided access to the plate only (Figure 6.16). They were able to measure the moisture content and simultaneously the raw density of a 26 mm thick particleboard (Figure 6.17). The system acquires NMR signals of a disc-shaped measuring volume at a certain depth inside the board's cross section. The raw density measured by NMR was in excellent accordance with data obtained from x-ray measurements (Figure 6.18).

Suggested R&D topics include:

- Adapting NMR to harsh industrial environments
- Increasing penetration depth by two-sided access



Figure 6.16: Hand-held NMR device for one-sided access.

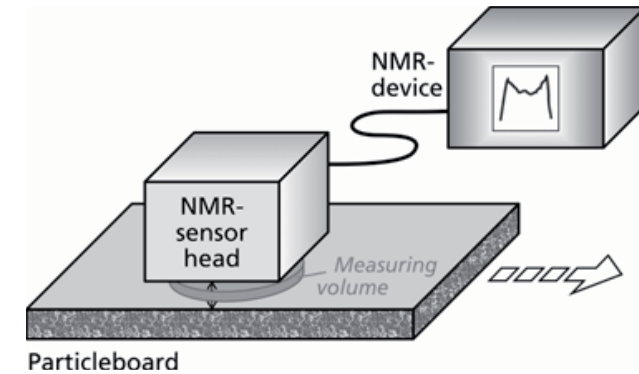


Figure 6.17: Principle of simultaneous on-line moisture and density measurement (Wolter et al. 1997).

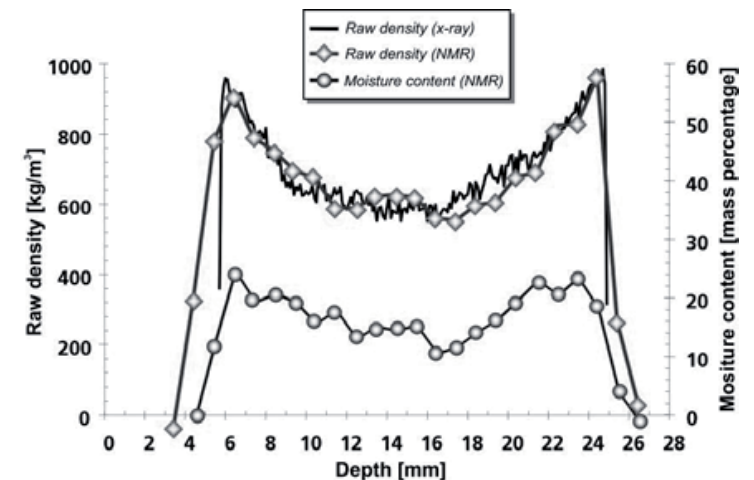


Figure 6.18: Typical raw density and moisture profile of a particleboard, measured by NMR.

6.5 REFERENCES

- P. Bloem, D. Greubel, G. Dobmann, O. K. Lorentz, B. Wolter, NMR for Non-Destructive Testing of Materials, Materials, functionality & design, Proceedings of the 5th European Conference on Advanced Materials and Processes and Applications. Vol. 4: Characterization and production/design : EUROMAT 97, Maastricht, NL, 21 - 23 April 1997
- L. Boltzmann, Ableitung des Stefan'schen Gesetzes, betreffend die Abhängigkeit der Wärmestrahlung von der Temperatur aus der elektromagnetischen Lichttheorie, Annalen der Physik 22 , 291 (1884)
- P. Deubel, Einführung moderner Qualitätssicherungssysteme in der Möbelindustrie (1), Holz- und Kunststoffverarbeitung 27(9), 942 (1992)
- P. Deubel, Einführung moderner Qualitätssicherungssysteme in der Möbelindustrie (2), Holz- und Kunststoffverarbeitung 27(10), 1104 (1992)
- B. Engström, Real Time Determination of Formaldehyde Emission from Particleboards Using NIR-Spectroscopy, International Panel Products Symposium 2008, 39
- R. Feldhoff, T. Huth-Fehre, K. Cammann, Detection of inorganic wood preservatives on timber by near infrared spectroscopy, J. Near Infrared Spectrosc. 6, A171 (1998)
- G. Gaussorgues, Infrared Thermography, Chapman & Hall 1994
- W. Gindl, A. Teischinger, M. Schwanninger, B. Hinterstoisser, The relationship between near infrared spectra of radial wood surfaces and wood mechanical properties, J. Near Infrared Spectrosc. 9, 255 (2001)
- D. I. Givens, J. L. De Boever, E. R. Deaville, The principles, practices and some future applications of near infrared spectroscopy for predicting the nutritive value of foods for animals and humans, Nutrition Research Reviews 10, 83 (1997)
- T. Hutter, R.W. Kessler, J. Zander, A. Ganz, Characterisation of modern wet-process fibreboard production using experimental design, 7th Europ. Panel Products Symp., (2003) pp. 14-25
- R.W. Kessler, T. Reinhardt, W. Kessler, H. Zimmer: Adaptive processing of wood for fibreboards by high level spectroscopic on-line control. 4th Europ. Panel Products Symp. (2000), pp. 227-235

- Kessler, W.: Multivariate Datenanalyse für die Pharma-, Bio- und Prozessanalytik. Weinheim : Wiley-VCH, 2007
- S. H. Nielsen, L. Jensen, Vollautomatisierte Produktion für Just-in-Time-Lieferung, Schenck-Automatisierungssymposium für die Plattenindustrie, Darmstadt, 13.-14. Oktober 1994, 1-6
- P. Niemz, F. Dutschmann, B. Stölken, Möglichkeiten zum Nachweis des Klebstoffanteils in beleimten Spänen, Holz als Roh- und Werkstoff 52, 6 (1994)
- B. G. Osborne, T. Fearn, P. H. Hindle, Practical NIR Spectroscopy with Applications in Food and Beverage Analysis, Longman Scientific and Technical 1993
- M. Planck, Über eine Verbesserung der Wien'schen Spektralgleichung, Verhandl. Dtsch. phys. Ges. 2, 202 (1900)
- B. Plinke, D. Ben-Yacov: Überwachung der Klebstoffverteilung im OSB-Vlies mit ortsauflösender Spektroskopie. 8. Holzwerkstoffkolloquium, Dresden, 10.-11.12.2009
- J. Stefan, Über die Beziehung zwischen der Wärmestrahlung und Temperatur, Sitzungsberichte der Akademie der Wissenschaften II 79, 391 (1879)
- A. Taylor, B. K. Via, Potential of visible and near infrared spectroscopy to quantify phenol formaldehyde resin content in oriented strand board, Eur. J. Wood Prod. 67, 3 (2009)
- L. G. Thygesen, S.-O. Lundqvist, NIR measurement of moisture content in wood under unstable temperature conditions. Part 1. Thermal effects in near infrared spectra of wood, J. Near Infrared Spectrosc. 8, 183 (2000)
- J. Welling (Ed.), Directory of non-destructive testing methods for the wood-based panel industry, Luxembourg : Off. for Off. Publ. of the Europ. Communities, 1998
- W. Wien, Eine neue Beziehung der Strahlung schwarzer Körper zum zweiten Hauptsatz der Wärmetheorie, Berliner Berichte, 55-62 (1893)
- B. Wolter, U. Netzelmann, G. Dobmann, O. K. Lorenz, D. Greubel, Kontrastierende 1H-NMR-Messungen in Aufsatztechnik zur Bestimmung von Feuchteverteilungen in

Chapter 7

Carbon Materials and SiC-Ceramics made from Wood-Based Panels

Olaf Treusch

CHAPTER SUMMARY

This chapter describes the manufacture process of monolithic porous carbon materials from specific wood-based panels. These carbon materials can serve among other things as precursors for SiC-Ceramics which is also illustrated here.

7.1 INTRODUCTION

A new approach to technology is to develop dense or porous monolithic **carbon materials** using cellulose containing preforms (e.g. wood, bamboo or flax). These **carbon materials** can be used directly in various applications (e.g. electrodes or structural materials) or be further converted to **silicon carbide** (SiC) ceramics. Combustion chambers or heat exchangers dominate in the ordinary field of applications for **SiC-ceramics**. These materials (C and SiC) can be produced from a renewable resource.

The process is capable of converting not only solid wood but also all its derivatives such as wood-based panels or paper and cardboard. Compared to conventional **precursors** (synthetic resins) for **carbon materials** or **SiC-ceramics**, wood-based composites are low-cost materials, since they are basically manufactured from low-cost raw materials such as wood chips and particles. Moreover, in contrast to natural solid wood, the isotropy of the wood-based materials is higher and their characteristics are easily reproducible.

Wood-based materials have been on the market for decades and there is wide range of products (e.g. oriented strand board, particleboard and medium density fibreboard) with certain characteristics for particular applications. These materials are generally suitable as **precursors** for **carbon materials** or **SiC-ceramics** but they have to be modified in order to attain specific properties. This is an additional advantage of wood-

based materials, as it is possible to adjust their properties by selecting specific components and by varying the processing parameters.

The manufacturing process of **carbon materials** and **SiC-ceramics** can be described in three stages: the production of specific wood-based composites, thermal degradation to **carbon materials (carbonization)** and **silicon infiltration** to generate the ceramics (Figure 7.1).

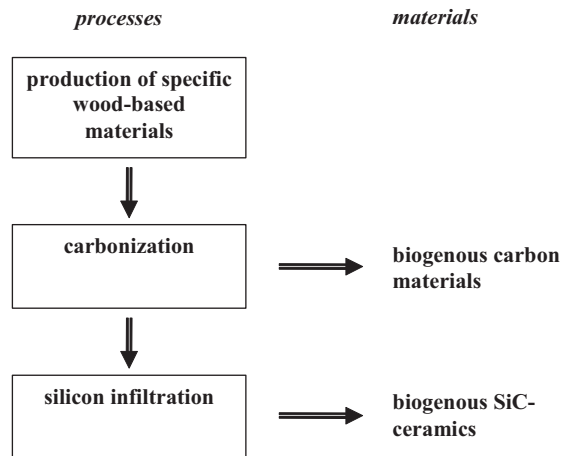


Figure 7.1: Manufacturing process of biogenous carbon materials and SiC-ceramics.

7.2 SPECIFIC WOOD BASED MATERIALS

Apart from solid wood, wood-based materials can serve as **precursors** for biogenous **carbon materials** and **silicon carbide** ceramics. Various studies have used conventional wood-based panels for the production of these materials. It could be shown that these are more appropriate starting materials for these processes than solid wood (Kercher and Nagle 2002; Schmidt et al 2001; Krenkel et al. 1999) due to their reproducible properties as well as their greater homogeneity and isotropy. As the conventional wood-based panels are designed for completely different purposes the properties of the resulting carbon or ceramic material respectively were not satisfactory for industrial utilization. However, one of the advantages of wood-based materials is that desired structures or

properties can be influenced specifically by selecting particle shapes and sizes as well as densities and adhesive types to suit the purpose.

In recent years various projects have been aimed at the systematic investigation of the potential of specifically designed wood-based composites as preform for biogenous **carbon materials** and **SiC-ceramics**. The studies have shown that one of the most important parameters for the manufacture of wood-based materials is the particle size of the wood component (Hofenauer et al. 2004; Treusch et al 2004; Herzog et al. 2006)

7.2.1 Raw Materials and the Manufacturing Process

For the fabrication of wood-based materials wood fibres, particles and powders (30-120 µm) have to be mixed with liquid or powdery resin in a stirring device or a charge mixer. So far different phenolic resins and pitch have been proven to be suitable for the subsequent thermal treatment of the boards. In the previous experiments the adhesive content was between 5 and 50 % related to the dry mass of the wood component. Depending on the bulk density desired, a specific amount of the wood resin mixture has to be evenly distributed into a mould for predensification. Finally the mixture has to be pressed to achieve the thickness required and then heated to at least 120 °C to cure the resin. To avoid a density profile in the resulting board the densification has to take place at room temperature.

7.2.2 Characterisation

The specific wood-based materials can be characterized by means of thermo-gravimetric analysis, light microscopy and mechanical testing. For the observation of the material by light microscopy they have to be embedded in acrylic resin and cut into 1 µm slides. As the density has an important impact on the properties of the resulting materials, especially on the possibility of infiltration, the density and the density profiles have to be measured.

Suggested R&D Topics include:

- Preceramic polymers as adhesives (e.g. silans, siloxans)
- Biogenous resins

- Moulding techniques to produce near net shape wood-based composites (e.g. extrusion and injection moulding with duroplastic resins)
- Optimization of particle geometry (size distribution)
- Applying additives (e.g. carbon fibres, chemicals)
- Homogeneous density distribution

7.3 CARBON MATERIALS

Most industrial **carbon materials** are produced from organic compounds of petrochemical origin, which were heat-treated in an inert atmosphere. Conventional starting materials for the production of porous carbons are phenol formaldehyde polymers, pitch, epoxy resins and furfuryl resins (Fitzer et al. 1969; Constant et al. 1995; Liu et al. 1996; Czosnek et al. 2002; Puziy et al. 2002).

Monolithic porous **carbon materials** can also be obtained by carbonising wood in a controlled thermal decomposition process. In this process the cellular anatomic features of wood are retained in the new carbon material (Byrne and Nagle 1997; Moor et al. 1974; McGinnes et al. 1971). Okabe et al. (1996a) describe a method for the production of **carbon materials** based on the **carbonization** of wood impregnated with phenolic resin. The phenolic resin reinforces the material and prevents the development of cracks. As the authors define ceramics as inorganic materials with ionic or covalent bonds they call these materials “wood ceramics”.

Conventional wood-based panels can also serve as **precursors** for crack-free, monolithic porous **carbon materials**. Kercher and Nagle (2002) used commercially available medium-density fibreboards (MDF) for the production of porous **carbon materials**. This investigation has shown that the electrical, mechanical and structural properties of carbonised MDF materials make them excellent candidates for lithium-ion and fuel cell components.

One of the advantages of wood-based materials used as **precursors** for porous **carbon materials** is, as already mentioned, the possibility to make adjustments for a wide range of macro- and micro-structures by selecting different densities, types and amounts of adhesive as well as particle sizes. Thus the tailoring of the properties of the materials derived thereof in terms of structure (e.g. porosity, pore size) and mechanical properties is

enabled. A broad variety of specifically developed wood-based materials were carbonized to produce crack free, monolithic porous **carbon materials**. The results indicated how the wood-based material parameters affect the properties of the resulting **carbon materials** (Treusch et al. 2004).

7.3.1 Carbonization

The **carbonization** of the wood-based materials is carried out in an inert atmosphere (e.g. N₂). To make sure the **carbon materials** remain crack free and without any deformations, a slow heating rate (approx. 1 K/min) has to be applied up to 500 °C. Subsequently a higher heating rate (approx. 5-10 K/min) can be applied up to the peak temperature (900-1500 °C). During this process, the exact replica of the former macroscopic structure of the wood-based composite remains (Figure 7.2) (Treusch et al. 2004; Herzog et al. 2006).

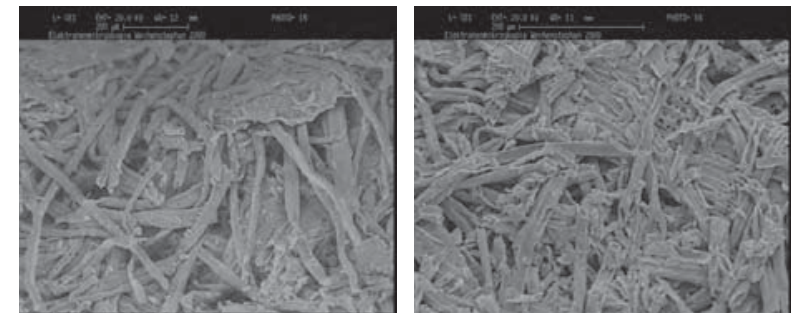


Figure 7.2: Fibreboard before (a) and after (b) carbonization.

Wood-based materials shrink and lose weight during **carbonization**. Similar to mass loss, dimensional changes are greatest at temperatures between 300 and 350 °C, which is consistent with the decomposition of cellulose in this temperature range (Shafizadeh, 1983). At 350 °C the material lost almost 60 % of its weight as well as 25 % of its transverse and 10 % of its plane dimensions. Shrinkage in the plane ranges between 30 and 40 % (Figure 7.3). Mass loss for the different types of specific wood-based materials lies between 55 and 80 %. Because of the fibre arrangement in the direction of the plane during hot-pressing, shrinkage in the plane is less than in transverse direction.



Figure 7.3: Dimensional changes during carbonization.

7.3.2 Characterisation

The structure of **carbon materials** can be analyzed by scanning electron microscopy (SEM) or by incident-light microscopy after embedding and polishing. To investigate dimensional changes and mass loss, dimensions and masses have to be measured before and after **carbonization** in their dry state. Mechanical testing of the **carbon materials** is carried out by determining flexural strength by the three point method (DIN 51902) or by determining compressive strength (DIN 51910-A). The specific surface area can be measured with a gas sorption analyser, and the BET surface area can subsequently be calculated from the isotherms by the Brunauer-Emmett-Teller (BET) equation. The electrical conductivity can be measured according to the 4-probe method, applying low currents so as to avoid Joule heating. The conducting properties allow these materials to be used as porous electrodes and light electromagnetic shields. Due to their rather high heat-treatment temperature (900-1400 °C), the **carbon materials** consist of almost pure carbon. Elemental analysis leads to the following elemental massic composition: C 98 %, H 0.5 %, O 1.5 % (1000 °C).

Apart from the internal structure, physical and mechanical properties are mainly influenced by wood-based material parameters such as particle size, adhesive type, adhesive content and density.

7.3.3 Potential Applications

Carbon is the basis for a multitude of materials with a broad variety of industrial applications. Potential fields of application for monolithic porous carbons can be found where properties like porosity, permeability,

mechanical strength, thermal and electrical conductivity as well as their microscopic structure have to be matched with each other (Pierson 1993). Porous **carbon materials** can be used for example as filters, adsorbents, electrodes and catalyst supports (Rodríguez-Reinoso and Linares-Solano 1982; Barton et al. 1999; Burchell 1999). More recently biogenous **carbon materials** have been found as **precursors** for composite materials and for reaction-formed structural ceramics (silicon or titan carbide) (Byrne and Nagle 1997; Zhang et al. 2003).

Suggested R&D Topics include:

- Reducing mass loss and dimensional changes during **carbonization**
- Improving shaping procedures for **carbon materials**
- Increasing the mechanical properties at high porosities
- Upscaling
- Finally, dispersing small catalytic particles onto such conducting high-area rigid supports is recommended

7.4 SiC-CERAMICS

Silicon carbide (SiC) is a well-known industrial ceramic material characterized by outstanding properties like high mechanical strength at temperatures up to 1300 °C, and excellent thermal shock, wear and corrosion resistance. Furthermore SiC shows high hardness at a low density (3,14 g/cm³) as well as low thermal extension. These properties make the material suitable for high temperature technologies and chemical instruments (Gadow 1986).

Apart from the sintering technique, conventional **SiC-ceramics** can be manufactured by the infiltration of a porous preform consisting of primary **silicon carbide** (SiC) powder and elemental carbon (C) with molten silicon (Si). During the infiltration process the secondary SiC, formed by the reaction ($\text{Si} + \text{C} \rightarrow \text{SiC}$), bonds the primary SiC grains, and the residual pores are filled with elemental silicon. In **silicon carbide** ceramics of common quality, the SiC content is in the range of 85 to 90 vol.-% leading to bending strengths between 300 and 500 N/mm² (Cohrt 1985). There have also been several attempts to manufacture **SiC-ceramics** without using primary SiC. Polymer-derived porous carbons, fibre-reinforced **carbon materials** and carbon fibres have been used for

the infiltration with liquid silicon (Singh and Behrendt 1994; Krenkel 2000).

In recent years carbonized wood from various species including bamboo subjected to **pyrolysis** were successfully infiltrated with liquid or gaseous silicon or silica sol resulting in silicon ceramics. In these biomorphic ceramics the structure of the biological **precursors** is preserved. A combination is thus achieved of the wood structure with the chemical and physical characteristics of the ceramic material (Byrne and Nagle 1997; Martinez-Fernandez et al 2000; Singh and Salem 2002; Qiao et al. 2002; Sieber et al. 2000; Arellano-Lopez 2004; Greil 2001; Kaindl 2000). Due to its inhomogeneity, anisotropy and the difficulties involved in adjusting its characteristics, the use of solid wood as a **precursor** for technical ceramics is limited. Commercial wood-based panels (e.g. veneer panels, particleboards) have been used as **precursors** for **SiC-ceramics** as these materials show higher isotropy and easily reproducible characteristics (Krenkel et al. 1999; Schmidt et al. 2001).

By optimizing the wood based panels with regard to their density, internal structure and adhesive content, **SiC-ceramics** were formed with a structure and mechanical properties (400 N/mm²) that are promising and show a high potential for industrial use. The mechanical strength of the resulting ceramic depends on its structure and phase composition, which is correlated with the structure of wood-based composite and the carbon template respectively. The strength rises with increasing **silicon carbide** content and decreases with residual silicon and carbon content as well as with higher porosity (Hofenauer et al. 2003; Gahr et al. 2004; Hofenauer et al. 2006; Herzog et al. 2006)

7.4.1 Siliconisation

Silicon infiltration of the carbon templates takes place in vacuum conditions at temperatures of approx. 1650°C and can be carried out in liquid or gaseous form (Figure 7.4). In the case of liquid **silicon infiltration**, silicon reception takes place under vacuum by capillarity of the existing cavity of the carbon body – one part of silicon reacts and another remains in the cavities. During gaseous **silicon infiltration** Si gas streams into the hollow spaces, while carbon and silicon combine to pure SiC. Hereby the porosity of the original material is retained. Siliconization in liquid or gaseous form leads to no further dimensional changes, so that a shaped C-template can be converted near net shape to SiC (Gahr et al., 2003; Hofenauer et al., 2003)

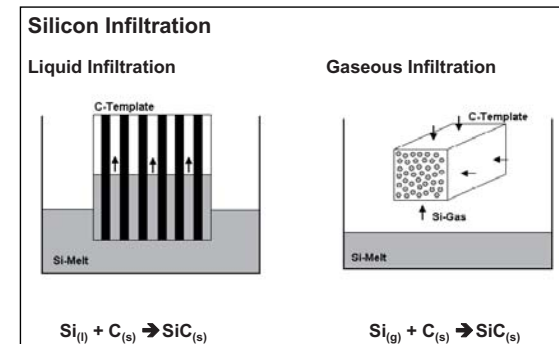


Figure 7.4: Silicon infiltration into porous carbon materials (Sieber and Kaindl 1998).

In a further approach to convert the **carbon materials** into **SiC-ceramics**, the carbon-templates formed were infiltrated with various kinds of silica sol (SiO₂). The resulting SiO₂/C composite is subsequently transformed into a SiC-ceramic via carbothermal reduction (Klingner et al. 2003; Herzog et al. 2006).

7.4.2 Characterisation

To determine the free carbon content of the ceramized materials, they can be heated for 1 h at 1000°C in air in an oxidation furnace with a record of the weight change (Herzog et al. 2006) or by image analysis of the cross section. Taking into account the bulk density of the carbon template as well as the carbon content and the bulk density of the resulting ceramic, the phase composition of the ceramic can be calculated. The phase composition declares the relative amount of SiC and residual carbon and silicon. To analyse the microstructure of the ceramics scanning, electron microscopy can be applied. Three or four point bending tests can be conducted to determine the strength of the ceramic material.

7.4.3 Potential Applications

Examples of the ordinary field of application for monolithic **SiC-ceramics** are combustion chambers, gas turbines, heat exchangers, seal rings, valve discs and ceramic engine parts (Hofenauer et al. 2003). Due to the melting point of the certain amount of residual silicon, the range of use is limited up to approx. 1380°C. Porous **SiC-ceramics** provide interesting applications in the field of filtration of hot and corrosive media and as perform material for infiltration with light metals to fabricate metal matrix composites (Herzog et al. 2006).

Suggested R&D Topics include:

- Optimization of the high temperature process
- Composition of the wood-based material (additives, adhesives)
- Increasing the SiC content
- Increasing fracture toughness
- Upscaling

7.5 REFERENCES

- Arellano-Lopez, A.R.; Gonzales, P.; Dominguez, C.; Fernandez-Quero, V.; Singh, M. (2004): Biomorphic SiC: A new Engineering Ceramic Material. *Int. J. Appl. Ceram. Technol.*, **1**(1), 56-67
- Barton, J.T.; Bull, L.M.; Klemperer, G.; Loy, D.A.; McEnany, B.; Misono, M.; Monson, P.A.; Pez, G.; Scherer, G.W.; Vartuli, J.C.; Yaghi, O.M. (1999): Tailored Porous Materials. *Chem. Mater.*, **11**, 2633-2656
- Burchell, T.D. (Hrsg.)(1999): Carbon Materials for Advanced Technologies. Pergamon, Amsterdam
- Byrne, C.E.; Nagle, D.C. (1997): Cellulose derived Composites - A method for materials processing. *Mater. Res. Innov.*, **1**, 137-144
- Cohrt, Z. (1985): Herstellung, Eigenschaften und Anwendung von reaktionsgebundenem, siliciuminfiltrierten Siliciumcarbid. *Z. Werkstofftech.*, **16**, 277
- Constant, K.P.; Lee, J.-R.; Chiang, Y.-M. (1996): Microstructure development in furfuryl resin-derived microporous glassy carbons. *J. Mater. Res.*, **11**, 2338-2345
- Czosnek, C.; Ratusek, W.; Janik, J.F.; Olejniczak, Z. (2002): XRD and ²⁹Si MAS NMR spectroscopic studies of carbon materials obtained from pyrolyses of a coal tar pitch modified with various silicon-bearing additives. *Fuel Process. Technol.*, **79**, 199-206
- Fitzer, E.; Schaefer, W.; Yamada, S. (1969): The formation of glasslike carbon by pyrolysis of polyfurfuryl alcohol and phenolic resin. *Carbon*, **7**, 643-648
- Qiao, R. Ma, N. Cai, C. Zhang, Z. Jin, "Mechanical Properties and Microstructure of Si/SiC materials derived from native Wood," *Mat. Sci. Eng.*, **A323**, 301-305
- Gadow, R. (1986): Die Silizierung von Kohlenstoff. Dissertation an der Universität Karlsruhe
- Gahr M., Schmidt J., Krenkel W., Hofenauer A., Treusch O. (2003): SiC-Keramik auf der Basis von Holzwerkstoffen. In: Hans-Peter Degischer (Editor) *Verbundwerkstoffe: 14. Symposium Verbundwerkstoffe und Werkstoffverbunde*, Wiley Europe

- Gahr M., Schmidt J., Krenkel W., Hofenauer A., Treusch O. (2004): Dense SiSiC ceramics derived from different wood-based composites: Processing, Microstructure and Properties. Proc. of HT-CMC 5, Seattle
- Greil, P. (2001): Biomorphic Ceramics from Lignocellulosics. J. Eur. Ceram. Soc. **21**, 105-118
- Herzog, A.; Vogt, U.; Kaczmarek, O.; Klingner, R.; Richter, K.; Thoemen, H. (2006): Porous SiC Ceramics Derived from Tailored Wood-Based Fiberboards. J. Am. Ceram. Soc. **89**(5), 1499-1503
- Hofenauer A., Treusch O., Tröger F., Wegener G., Fromm J., Gahr M., Schmidt J., Krenkel W. (2003): Dense Reaction Infiltrated Silicon/Silicon Carbide Ceramics Derived from Wood Based Composites. Advanced Engineering Materials, **5**, 794-799
- Hofenauer A., Treusch O., Tröger F., Wegener, G., Fromm J. (2004): High Strength SiSiC Ceramics derived from fine Wood Powders. Proc. of 28 th International Cocoa Beach Conference and Exposition on Advanced Ceramics & Composites, Cocoa Beach 26.-30. January
- Hofenauer A., Treusch O., Tröger F., Wegener, G., Fromm J. (2006): Silicon infiltrated silicon carbide ceramics (SiSiC-ceramics) derived from specific wood-based composites. Holz als Roh- und Werkstoff, **64**, 165 – 166
- Kaindl, A. (2000): Zellulare SiC-Keramik aus Holz. Dissertation, Universität Erlangen-Nürnberg
- Kercher, A.K.; Nagle, D.C. (2002): Evaluation of carbonized medium-density fibreboard for electrical applications. Carbon **40**, 1321-1330
- Klingner, R.; Sell, J.; Zimmermann, T.; Herzog, A.; Vogt, U.; Graule, Th.; Thurner, Ph.; Beckmann, F.; Müller, B. (2003): Wood-Derived Porous Ceramics via Infiltration of SiO₂-Sol and Carbothermal Reduction. Holzforschung, **57**, 440-446
- Krenkel, W.; Hall, S.; Seitz, S. (1999): Biomorphe SiC-Keramiken aus technischen Hölzern. DGM-Tagung „Verbundwerkstoffe und Werkstoffverbunde“, Hamburg 5.-7. Oktober
- Krenkel, W. (2000): Entwicklung eines kostengünstigen Verfahrens zur Herstellung von Bauteilen aus keramischen Verbundwerkstoffen. Forschungsbericht 2000-04, Deutsches Zentrum für Luft- und Raumfahrt e.V.

- Liu, Y.; Xue, J.S.; Zheng, T.; Dahn, J.R. (1996): Mechanism of Lithium insertion in hard carbons prepared by pyrolysis of epoxy resins. Carbon, **34**, 193-200
- M. Singh, J. A. Salem (2002): Mechanical Properties and Microstructure of biomorphic Silicon Carbide Ceramics fabricated from Wood Precursors. Journal of the European Ceramic Society, **22**, 2709-2717
- Martínez-Fernández, J.; Valera-Feria, F.M.; Singh, M. (2000): High Temperature Compressive Mechanical Behavior of Biomorphic Silicon Carbide Ceramics. Scripta Mater., **43**, 813-818
- McGinnes, E.A.; Kandeel, S.A.; Szopa, P.S. (1971): Some structural changes observed in the transformation of wood into charcoal. Wood Fiber, **3**, 77-83
- Moor, G.R.; Blankenhorn, R.; Beall, F.C.; Kline, D.E. (1974): Some physical properties of birch carbonized in a nitrogen atmosphere. Wood Fiber, **6**, 193-199
- Pierson, H.O. (1993): Handbook of carbon, graphite, diamond and fullerenes. Noyes/William Andrew Publishing, Park Ridge
- Puziy, A.M.; Poddubnaya, O.I.; Gawdzik, B.; Sobiesiak, M.; Dziadko, D. (2002): Heterogeneity of synthetic carbons obtained from polyimides. Appl. Surf. Sci., **196**, 89-97
- Rodríguez-Reinoso, F.; Linares-Solano, A. (1982): Microstructure of Activated Carbons as Revealed by Adsorption Methods. In: Thrower, P.A. (Hrsg.) Chemistry and Physics of Carbon. Marcel Dekker Inc. New York, 1-146
- Schmidt, J.; Hall, S.; Seitz, S.; Krenkel, W. (2001): Microstructure and properties of biomorphic SiSiC ceramics derived from pyrolysed wooden templates. Proceedings of the 4th Int. Conference on High Temperature Ceramic Matrix Composites (HTCMC4), München 1.-3. Oktober
- Shafizadeh, F. (1983): The chemistry of Pyrolysis and Combustion. In: R. Rowell (Hrsg.), The Chemistry of Solid Wood, American Chemical Society, Seattle
- Sieber, H.; A. Kaindl (1998): Biomimetik: Der Weg vom Holz zur Keramik. Leaflet of FAU Erlangen
- Sieber, H.; Hoffmann, C.; Kaindl, A.; Greil, P. (2000): Biomorphic Cellular Ceramics. Adv. Eng. Mater., **2**(3), 105-109

Singh, M.; Berendt, D.R. (1994): Microstructure and mechanical properties of reaction-formed silicon carbide (RFSC) ceramics. *Mater. Sci. Eng.*, **A187**, 183-187

Treusch O., Hofenauer A., Tröger F., Fromm J., Wegener G. (2004): Basic Properties of Specific Wood-Based Materials Carbonised in a Nitrogen Atmosphere. *Wood Science and Technology* **38**, 323-333

Zhang, D.; Xie, X.Q.; Fan, T.X.; Sun, B.H.; Sakata, T.; Mori, H.; Okabe, T. (2003): Microstructure and properties of ecoceramics/metal composites with interpenetrating networks. *Mater. Sci. Eng.*, **A351**, 109-116

formed wood fiber/polymer fiber composites. *Forest Products Journal*, **42(6)**, 42-48

Chapter 8

Thermally and Chemically Modified Wood-Based Panels

Wulf Paul and Martin Ohlmeyer

CHAPTER SUMMARY

The modification of wood aims to alter the absorptive behaviour of wood and thus gives an advantage in terms of dimensional stability. The two main methods of wood modification are chemical and thermal treatments; both result in an irreversible change of the wood cell components. The polyoses as main carrier of hydroxyl groups contribute most to moisture uptake and thus to the risk of dimensional changes.

The principle of a chemical modification is to replace the hydroxyl groups by a reagent; most study has undergone the substitution by acetyl groups referred to as acetylation of wood. Any chemical modification process results in a weight increase and keeps the wood in its swollen state. In contrast, thermal modification is always accompanied by a weight loss. The principle is to remove hydroxyl groups by thermal degradation thus leaving wood in its shrunken state. Wood modification has been subject to numerous studies and thermally modified solid wood became commercially viable whereas chemical modification processes often lack economical advantages due to high process and chemicals costs.

Increasingly, over recent years the focus is on applying those methods described on wood based panels as well. But despite promising results no commercial viability could be achieved yet.

This article gives an overview about different modification processes, their advantages but also negative impacts on board properties and highlights the limits in practical and economical terms.

8.1 INTRODUCTION

Wood modification implies all those treatments which result in a change of wood properties. Mostly, modification processes aim to change the hydrophilic nature of wood. Since the **hygroscopicity** of wood is accompanied by anisotropic changes in dimension, swelling and shrinking

may result in a loss of **dimensional stability**. Furthermore, crack formation might occur as a consequence of the dimensional changes and thus provoke constructional failures (Lukowsky and Böttcher 2001, Niemz 2002). Hence, especially for timber construction (e.g. window frames) high dimensional stability is needed.

For wood-based panels (WBP) anisotropic changes in dimension are minor, at least across the width and the length of a board. The limitation of common WBP if exposed to high relative humidity or frequent moisture changes (e.g. by weathering) is due to their tendency of **thickness swell**, i.e. a change of dimension across the thickness of a board. In contrast to solid wood, a change in dimension of WBP consists of two elements, a **reversible** and an **irreversible** one. While the reversible component is only due to the hygroscopic behaviour of the raw material itself, the irreversible component can be traced back to the production process (Adcock and Irlle 1997).

During hot-pressing the particles are compressed and thus stresses are induced into the mat. Subsequently, if a panel is exposed to high humidity or gets in contact with water, these stresses are released and thus lead to an irreversible increase of thickness which exceeds the reversible component by magnitude.

Thickness swell not only has a negative impact on the appearance of the panel, but also results in a decrease of its mechanical properties. If stress build-up exceeds the strength of the adhesive bonds between the particles, internal bond strength decreases. The stresses that develop inside the wood due to wetting are very high (Tarkow and Turner 1958) which no adhesive can permanently withstand. Therefore the adhesive bonds in a WBP in its swollen state are damaged if not broken, but stressed at the very least.

Thus, an improvement of WBP in terms of reduced thickness swell may be facilitated by both, a change of the hygroscopic nature of wood but also by an improved compressibility of the raw material by altering its visco-elastic properties.

For WBP principally two ways of modification exist: Either a modification of the raw material prior to blending and hot-pressing or a modification of the panel. In the following an overview of different modification methods is given.

As mentioned above, improving dimensional stability of WBP requires both, a reduced moisture uptake as well as a change of visco-elastic properties. Hence, only those modification methods will be considered

here, which lead to a chemical change of the cell wall components. Since the main target of wood modification is to limit the moisture uptake, any modification method aims to alter the hydroxyl groups as they contribute most to the absorption of water; Figure 8.1 gives a schematic overview of different mechanisms.

In the following, two methods will be described: The mechanism behind thermal modification is the degradation of hydroxyl groups, while the hydroxyl groups in the wood's polysaccharides form covalent bonds with the chemical reagent during chemical modification.

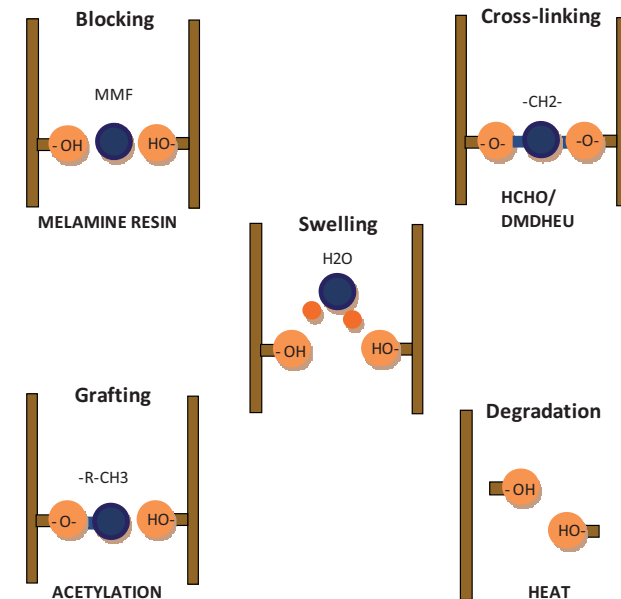


Figure 8.1: Mechanism of different modification methods to reduce swelling of the wood cell wall, (adapted from Rapp et al. 2000).

8.2 CHEMICAL MODIFICATION

Chemical modification of wood has early been recognized as an effective way to reduce its hygroscopicity and to improve its dimensional stability (Stamm 1964).

Rowell et al. (1988) defined chemical modification as any reaction between the abundant **hydroxyl groups** in the wood's polysaccharides with single chemical reagents, forming covalent bonds. Thus, the chemical configuration of the cell wall components is changed, resulting in altered wood properties. On the one hand, chemical modification leads to improved dimensional stability and to increased resistance against fungal attack and weathering. On the other hand there is a reduction in tensile strength and elasticity.

The aim of any modification process is to maintain the mechanical properties of wood while improving dimensional stability. Hence, wood modification always is a compromise between improved properties and reduced strength.

In accordance with Rowell (1975) suitable reagents for chemical modification should contain functional groups to form covalent bonds with hydroxyl groups. Furthermore it is necessary for the reagent to swell the wood in order to allow access to all reactive sites. The process should be carried out under mild conditions at temperatures up to 120 °C in order to allow simple and fast reactions. The catalysts used should be mildly alkaline with a low boiling point to avoid corrosion.

The mechanism of chemical modification is to replace hydroxyl groups in lignocellulosic materials. The reaction is accompanied with an increase of weight; the degree of modification is expressed as **weight percent gain** (WPG). To enhance the degree of hydroxyl group substitution, the reaction ideally follows a single site reaction, i.e. a reaction between the reagent and the hydroxyl group in a molar ratio of 1:1. Different reagents are used for chemical modification, e.g. anhydrides, epoxides, isocyanates, acid chlorides, carboxylic acids, lactones, alkyl chlorides, and nitriles. Among all types of chemical modifications, the substitution of hydroxyl groups by acetyl groups referred to as acetylation has been studied the most. A schematic overview about the reaction of acetic anhydride with hydroxyl groups of the wood is shown in Figure 8.2.



Figure 8.2: Acetylation of wood.

The chemical modification of fibres or particles prior to hot pressing rather than modification of entire panels can be regarded a relatively effective method because the raw material provides a large surface area, allowing the reagent to easily penetrate the wood.

Several studies reported in the literature deal with WBP made of chemically modified particles (fibres, particles, strands). The modification results in decreased TS and reduced moisture uptake. Sudo (1979) investigated fibreboards made from acetylated fibres and found a reduction of TS after 24 hours of water immersion. Arora et al. (1981) used a catalyzed liquid-phase process to acetylate particles. The PF-bonded panels made of acetylated particles showed considerably lower thickness swell at high relative humidity than boards made of non-acetylated particles.

Acetylated flakeboards bonded with PF-resin show lower moisture content, improved dimensional stability and improved decay resistance (Hadi 1992).

This coincides with work about **acetylation** of strands made of fir to improve the dimensional stability of OSB (Papadopoulos and Traboulay 2002). Ring-cut strands were acetylated at 120 °C using acetic anhydride. Test panels bonded with PF-resin showed significantly lower TS and water absorption. A chemical modification of wood chips using propionic anhydride was performed by Papadopoulos and Gkaraveli (2003); modification resulted in improved dimensional stability of particleboards manufactured with these chips. The TS values of the UF bonded boards were more than 50 % lower than controls.

Beside reduced TS and water absorption, chemical modification is often accompanied with lower strength properties. Youngquist et al. (1986) and Rowell et al. (1987) found for particleboards made of acetylated aspen particles and bonded with PF-resin a reduction in MOR of about 34 %. MOE was reduced by about 11 % and IB was decreased about 36 %, compared with panels made of non-treated flakes. Hardboards made from acetylated hemlock fibres and bonded with 7 % phenol-formaldehyde adhesive were tested by Youngquist et al. (1990). In static bending, MOR was reduced by 23% and MOE by 16 % as compared to control boards of non-acetylated fibres. Tensile strength parallel to the surface was reduced by 5 % but there was no change in the tensile strength perpendicular to the surface in acetylated boards compared to controls.

Rowell et al. (1991) tested fibreboards made from acetylated aspen fibres, using 8 % phenol-formaldehyde resin, in static bending. They found that MOR increased by 15 % and MOE increased by 40 % in acetylated fibreboards compared to controls. According to the authors, the acetylated boards had a more uniform density and a more consolidated surface as compared to controls.

Concerning the bonding behaviour as determined by internal bond strength (IB), chemical modification leads to a decrease, at least if bonded with formaldehyde resin systems (Chow et al. 1996, Youngquist et al. 1986, Fuwape and Oyagade 2000, Papadopoulos and Traboulay 2002, Papadopoulos and Gkaraveli 2003). From these studies it is apparent that IB decreases with increasing WPG. By means of electron micrographs Rowell et al. (1987) showed that fragmentation of the wood matrix increased with an increasing level of acetylation, i.e. with higher WPG. The authors did not attribute these defects to glue line failures since these defects were found only in the outermost layer of surface. Besides, their studies showed that failures during test occurred more often in the glue line for panels made of acetylated flakes compared to panels of non-acetylated flakes.

In considering the work of Youngquist et al. (1986), Rowell et al. (1987) considered that the press pressures required for flakeboards led to glue line failures. The reduced moisture content of the acetylated flakes made them less compressible and hence higher press pressures were needed.

Another explanation might be the low wettability of modified wood particles, and therefore poor penetration of water soluble formaldehyde resins into the particles (Papadopoulos and Traboulay 2002, Papadopoulos and Gkaraveli 2003).

Youngquist and Rowell (1990) as well as Papadopoulos et al. (2005) showed that using an isocyanate resin to bond the particles results in a much lower difference in IB between modified and non-modified particles. According to Papadopoulos et al. (2005) this might be due to the pH independent character of isocyanate resin as well as that it completely cures during hot pressing. Another possible explanation is the high mobility of isocyanate resins into the wood surface which causes penetration to considerable depth into compressed particles and can result in their total impregnation (Roll 1997).

Therefore it is suggested that the isocyanate resin system is more suitable for use in boards made from modified raw material than the formaldehyde resin system.

Despite such research efforts, no commercial applications have yet been fully realised for the acetylation of wood. First attempts, one in the United States in 1961 and one in the former USSR in 1974, came close to commercialisation but were discontinued, presumably because they were not cost-effective as described by Rowell et al. (1986a).

All of the procedures to acetylate wood developed over the years are complicated reaction schemes, using either a catalyst or an organic cosolvent and have required long reaction times.

Therefore, Rowell et al. (1986a, 1989) developed a non-catalyzed liquid phase acetylation process in order to achieve a modification of large batches to facilitate industrial processing. This method was investigated in several studies; panels made from acetylated fibres showed reduced moisture uptake and water absorption as well as decreased TS. However, significant improvements required more than 10 % WPG, based on dry wood mass (Chow et al. 1996, Rowell et al. 1986b–d, 1991, Tillman et al. 1987, Vick et al. 1991, Youngquist et al. 1986).

In terms of an industrial application, this means a great amount of chemical loading and thus a cost-intensive process as well.

Sheen (1992) reported about the production of acetylated fibres with a relatively simple, no solvent or catalyst process at a commercial pilot plant. Although the acetylation results were promising, full scale production was not realised because of high production costs as mentioned above. Consequently, the production costs had to be compensated by high prices of the final panel product.

8.3 THERMAL MODIFICATION

Another approach to alter wood properties is **thermal modification**. The target of this procedure is the same as for chemical modification, i.e. to change the hygroscopic nature of wood. Contrary to chemical modification the mechanism of action is to degrade hydroxyl groups instead of substitute them by a chemical reagent. The chemical loading keeps the wood in its swollen state and is accompanied with an increase in weight. A thermal modification results in a weight loss and the wood is kept in its shrunken stage.

Thermal modification in the typically applied temperature range of 180–250 °C leads to a degradation of hydroxyl groups following the mechanism of an acidic hydrolysis; Figure 8.3 gives an overview about the basic chemical changes that the main cell wall components undergo during thermal degradation. There are numerous studies dealing with the mechanism behind the decomposition of wood components due to heat treatment, e.g. Kollmann and Fengel (1965), Bourgois and Guyonnet (1988), Garrote et al. (1999).

The modification firstly affects the thermal instable polyoses. In comparison with cellulose, which is less affected by thermal degradation, their structure is rather amorphous with a high portion of hydroxyl groups. Thus, they contribute most to the sorption of water but also are sensitive to hydrolysis. For cellulose, a thermal modification only affects the amorphous regions within the otherwise crystalline structure, resulting in an increased degree of crystallinity. Thermal degradation proceeds in three steps, starting by deacetylation. The released acetic acid acts as a catalysing agent which then accelerates the depolymerisation of the polysaccharides. Alongside the depolymerisation, the heat leads to dehydration of the monosaccharides. Depending on their ring structure (furanosidic or pyranosidic), either furfural (out of xylose) or 5-hydroxymethylfurfural (out of glucose) are formed (Bobleter and Binder 1980). Especially the former substance is very reactive and leads to cross linking reactions with the lignin complex. At a temperature of about 200 °C the lignin itself undergoes a demethoxylation, leaving reactive sites which reticulate by auto condensation forming a hydrophobic network.

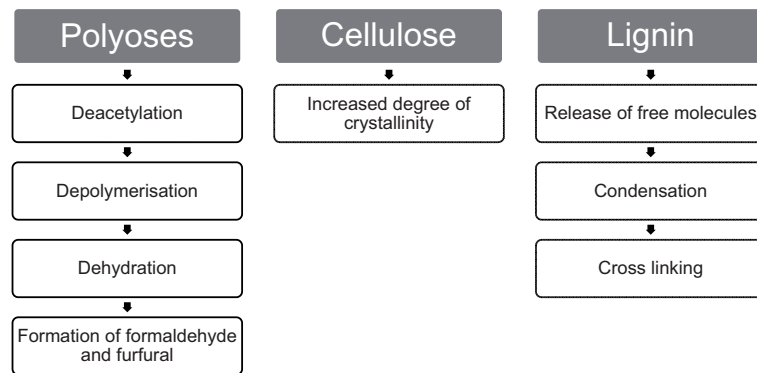


Figure 8.3: Decomposition of the main cell wall components due to thermal degradation (adapted from Esteves and Pereira 2009).

Heat treatment of solid wood is well known for decades and published in several works (e.g. Stamm et al. 1946, Seborg et al. 1953, Kollmann and Schneider 1963, Stamm 1964, Kollmann and Fengel 1965, Noack 1969, Burmester 1973, Burmester 1975, Giebeler 1983, Hillis 1984, Bourgois and Guyonnet 1988).

But also thermal modification of WBP to improve dimensional stability has been investigated for more than 40 years and still is of interest (e.g. Matsu and Sasaki 1956, Lehmann 1964, Heebink and Hefty 1969, Shen 1973, Burmester 1974, Tomimura and Matsuda 1986, Hsu et al. 1988, Subyanto et al. 1991, Sekino et al. 1997, Goroyias and Hale 2002a, Ohlmeyer and Lukowsky 2004, Paul and Ohlmeyer 2005, Paul et al. 2006).

Since the rate of hydrolysis is accelerated by temperature and pressure, mostly thermal modification is carried out under pressure and moist conditions. Most investigations deal with steam pre-treatment processes where pressures between 5 to 10 bar are applied, and temperature ranges from 160 °C to over 200 °C. Generally, increasing treatment temperature and time is very effective for improving dimensional stability, i.e. reducing TS. However, Sekino et al. (1998) found a significant reduction of the bond strength if temperatures above 200 °C are applied. This might be explained by the partial conversion of the polyoses into furfural polymers. This results in an increased embrittlement and a significant reduction of shear strength (Stamm 1964).

Boonstra et al. (2006) applied a two-stage heat pre-treatment according to the commercially established Plato-process for modifying solid wood (Boonstra et al. 1998, Tjeerdsma et al. 1998). The temperature was below 200 °C and the process was performed in two separate stages with an intermediate drying stage. In the first stage of the heat-treatment (hydro-thermolysis) the chips were treated in an aqueous environment at superatmospheric pressure with saturated steam (8–10 bar). In the second stage, after drying, the chips were heat treated in a kiln under dry and atmospheric conditions at 180 °C (curing-treatment). During this stage superheated steam or nitrogen was used as a shielding gas to exclude oxygen in order to reduce fire risks and preventing undesired oxidation reactions. The MUF-bonded particleboards made from modified chips show reduced thickness swell; best results were obtained if chips were only hydro-thermolysed (first stage) without the curing step. The bonding behaviour as determined by IB decreased.

All the treatment methods mentioned above have in common that heated steam is used and pressure has to be applied. That means in terms of an industrial upscale extensive reconstruction of the panel production process.

Tomek (1966) at first discussed the possibility to using the drying process to modify wood particles. The process was performed with a dryer heated by smoke gas; the oxygen content was less than 15 %. The moisture content of the particles prior to drying was set to 40 % and treatment was

carried out at a maximum temperature of 300 °C for four minutes. Although this process had potential to modify wood particles by an industrial drying process it is limited to laboratory scale. Since the dryer Tomek (1966) used was static it was necessary to spread out the wood particles in an equal layer thickness. That was important in order to achieve a homogenous temperature distribution within the wood particles. In terms of an industrial upscale this requirement is hardly to fulfil.

Investigations using a rotary dryer (at laboratory scale) allow thermal modification of larger batches and thus more potential to industrial upscale (Paul and Ohlmeyer 2005, Paul et al. 2006). The authors applied a one-step treatment of wood particles (strands, chips) with an initial moisture content of app. 5 %; Figure 8.4 displays particles of spruce (*Picea abies*) before and after the process; the modified chips show the typical discoloration following a thermal degradation. This effect is linked to coloured degradation products of the polyoses due to the hydrolytical decomposition which is similar to a Maillard reaction (Sehlstedt-Persson 2003). But also extractives are believed to contribute to the colour change of heat-treated wood (McDonald et al. 1997, Sundqvist and Morén 2002).

The process was carried out under atmospheric pressure in a dry and oxygen reduced atmosphere to avoid ignition. The reduction of oxygen was achieved by temporary inducing spray of water into the treatment chamber; besides, gaseous reaction products discharged remaining oxygen (oxygen content in the dryer was less than 15 %). Hence, the treatment could be performed at temperatures above 200 °C to allow short-time modification.



Figure 8.4: Chips of spruce (*Picea abies*) before (left) and after thermal modification.

The panels (bonded with formaldehyde-based resins and isocyanate, respectively) showed improved dimensional stability (thickness swell reduced by 50 %). Depending on the panel type (particleboard, OSB) the decrease of internal bond strength was minor for panels bonded with isocyanate. But the investigations have shown that pre-treatment of wood furnish prior to blending and pressing is not restricted to specific types of

adhesives. An example of particleboard made of thermally modified chips of spruce by the method described is shown in Figure 8.5.



Figure 8.5: Particle board made of untreated and thermally modified chips of spruce (*Picea abies*).

8.4 MODIFICATION OF PANELS

Steam treatments can also be effective at improving the dimensional stability of densified WBP. Besides pre-treatment by steaming of the wood furnish before forming a mattress (see above) a number of papers have been published on treatments during (simultaneous) and after hot pressing. Two different approaches may be distinguished: steam injection pressing in which steam not only treats the wood but affects adhesive cure as well (e. g. Shen 1973; Subyanto et al. 1991), and post-treatment steaming of a panel after hot-pressing (e. g. Heebink and Hefty 1969).

Another approach to apply a simultaneous treatment was presented by Goroyias and Hale (2002b) using a hot press without steam injection. The authors investigated the effect of elongated pressing times on the dimensional stability of PF-bonded OSB. The results show that thickness swell decreased with rising press temperature and pressing time. At the same time internal bond strength increased. The bending strength on the other hand decreased due to the treatment.

A post steam treatment of PF-bonded panels is an effective method for improving dimensional stability without significant detriment to the mechanical properties (Heebink and Hefty 1969). The principle is based on the plastification of wood, resulting in a fixation after cooling and thus preventing thickness swell. Another approach is presented by Del Menezzi and Tomaselli (2006). In their work they describe the effect of a simple heating of PF-bonded panels in a hot press without applying pressure. They found a reduction of thickness swell with increasing heating time.

A post treatment in terms of an industrial production is provided by storing the panels in stacks after hot pressing. The stacking is used for

conditioning the panels, mainly to achieve a unified temperature and moisture distribution in the horizontal and vertical planes of the panel. Another important effect is that stacking influences the properties of the final product. By varying the temperature of the stack and the duration of storage panel properties are changed. With increasing temperature and duration of storage a reduction of thickness swell can be achieved (Ohlmeyer 2002).

Although simultaneous and post treatments improve dimensional stability, these modification methods are restricted to adhesive systems which are resistant to hydrolysis, such as isocyanates and PF resins. In terms of an industrial upscale, simultaneous treatment is considered to be less expedient since hot pressing is known to be the bottle neck of the panel production process. That means increasing pressing time is not reasonable from an economical point of view. A post treatment by storing panels in a stack at elevated temperatures for several hours is difficult to realise. Due to the dimension of industrially produced panels it is time consuming and thus cost-intensive to achieve a homogenous temperature distribution within the panel. Furthermore, post treatments might result in shrinkage of the wood particles, affecting the wood-adhesive bond network (e.g. breakages of glue lines).

Post treatment using chemical modification was performed by Klinga and Tarkow (1966). The authors acetylated non-heat-treated wet-process hardboard by an uncatalyzed vapour phase process. The acetylation process resulted in board swelling and surface roughening, but it reduced reversible and irreversible thickness swell in subsequent water soak tests.

Murphy and Turner (1989) investigated the vapour phase preservative treatment of manufactured wood-based board materials including particleboards, MDF, aspen wafer boards and OSB using esterified borate in the vapour phase to obtain complete impregnation. Chemical modification applications to fibre boards can reduce water absorption and swelling of wood fibre and polymer fibre composites (Youngquist et al. 1992).

8.5 CONCLUSION

Modification of wood, regardless of which method is applied, is an effective way of improving dimensional stability and durability. There is a wide field of applications for which modified solid wood is already in use, e.g. deckings, claddings, parquet, garden furniture, to name just a few. But unlike for solid wood there is currently no marketable application for modified wood-based panels.

Due to the improved dimensional stability it appears to be possible from a general point of view to consider using modified wood-based panels for any of those applications where moisture resistance is required, e.g. flooring or cladding.

However apart from moisture resistance and dimensional stability, boards for these fields of application also need to fulfil certain standards regarding the strength, no matter whether those standards are of normative or industrial character.

The main objection to using modified wood based panels as a substitute for common ones is the loss of mechanical strength; while the effect on MOE is minor, the internal bond and particularly bending strength are affected more. Especially the degradation of the polyoses has major impact on the strength loss. Apart from being the main source for sorption of water, the polyoses also contribute to the visco-elasticity of wood which provides dynamic strength.

To a certain degree, the strength loss could be compensated by higher resin levels; but some treatment methods may even require a different resin system to allow for a sufficient glue joint or simply to withstand the modification itself, e.g. when applying a post treatment.

Another disadvantage is the currently high cost impact on the process in terms of thermal energy or chemicals. WBP are relatively low-value products and so cannot support high price increases. Therefore, modified wood-based panels would have to be used for special applications and niche products for which the extra cost of manufacturing will pay off.

A lot of research has been done and still is ongoing in the field of wood modification with the focus on applying successful methods to wood based panels. The outcome is promising and further research should investigate how modification methods could be altered in order to benefit from an improved dimensional stability but maintain the mechanical properties which are crucial for the final application. Also, the question of economical viability needs to be addressed and ways have to be found to integrate the modification using existing production techniques.

8.6 REFERENCES

- Adcock, T. and Irle, M.A. (1997): The effect of compaction ratio on the dimensional recovery of wood particles pressed perpendicular to the grain. In: Proceedings of The First European Panel Products Symposium, Llandudno, 9-10 October, 1997
- Arora, M.; Rajawat, M.; Gupta, R. (1981): Effect of acetylation on properties of particle boards prepared from acetylated and normal particles of wood. *Holzforschung und Holzverwertung*, **33**(1), 8–10.
- Bobleter, O.; Binder, H. (1980): Dynamischer hydrothormaler Abbau von Holz. *Holzforschung* 34: 48-51
- Boonstra, M.J.; Tjeerdsma, B.F.; Groeneveld, H.A.C. (1998): Thermal modification of non-durable wood species. In: Part 1. The Plato technology: thermal modification of wood. International Research Group on Wood Preservation, Document no. IRG/WP 98-40123
- Boonstra, M.J.; Pizzi, A.; Zomers, F.; Ohlmeyer, M; Paul, W. (2006): The effects of a two stage heat treatment process on the properties of particleboard. *Holz als Roh- und Werkstoff*, **64**(2), 157-164
- Bourgois J, Guyonnet R (1988) Characterization and analysis of torrefied wood. *Wood Sci Tech*, **22**, 143–155
- Burmester, A. (1973) Einfluss einer Wärme-Druck-Behandlung halbtrockenen Holzes auf seine Formbeständigkeit. *Holz Roh- Werkst*, **31**, 237–243
- Burmester, A. (1974): Erfolgreiche Quellungsvergütung mit einfachen Mitteln, part 1 and 2. *Holz- und Kunststoffverarbeitung*, **8 and 9**, 534-538 and 610-617
- Burmester A (1975): Zur Dimensionsstabilisierung von Holz. *Holz Roh-Werkst*, **33**:333–335
- Bourgois, J.; Guyonnet, R. (1988): Characterization and analysis of torrefied wood. *Wood Science and Technology* 22: 143-155
- Chow, P.; Bao, Z.; Youngquist, J.A.; Rowell, R.M.; Muehl, J.H.; Krzysik, A. (1996): Properties of hardboards made from acetylated aspen and southern pine. *Wood Fiber Sci.*, **28**(2), 252–258
- Del Menezzi, C.H.S.; Tomaselli, I. (2006): Contact thermal post-treatment of oriented strandboard to improve dimensional stability: A preliminary study. *Holz als Roh- und Werkstoff*, **64**(3), 212-217

- Esteves, B.M.; Pereira, H.M. (2009): Heat treatment of wood. *Bio Resources*, **4**(1), 370–404
- Fuwape, J.A.; Oyagade, A.O. (2000): Strength and dimensional stability of acetylated Gmelina and Sitka spruce particleboard. *J. Tropical Forest Prod.*, **6**(2), 184–189
- Garrote, G.; Dominguez, H.; Parajo, J.C. (1999): Hydrothermal processing of lignocellulosic materials. *Holz als Roh- und Werkstoff* 57: 191-202
- Giebeler, E. (1983): Dimensionsstabilisierung von Holz durch eine Feuchte/Wärme/Druck-Behandlung. *Holz Roh- Werkst*, **41**, 87–94
- Goroyias, G.J.; Hale, M.D. (2002a): Heat treatment of wood strands for OSB production: Effect on the mechanical properties, water absorption and dimensional stability. International Research Group on Wood Preservation, Document no. IRG/WP 02-40238
- Goroyias, G.J.; Hale, M.D. (2002b): The Effect of High Temperature and Long Pressing Time on the Dimensional Stability and Decay Resistance of OSB. Paper prepared for the 33rd Annual Meeting of the International Research Group on Wood Preservation in Cardiff, Wales
- Hadi, Y.S. (1992): Acetylated flakeboard properties. In Chemical modification of lignocellulosics, Rotorua, New Zealand, 7-8 November 1992 (compiled by Plackett D.V. & Dunningham E.A.). Forestry Research Institute, Ministry of Forestry FRI Bulletin, **176**, 9-15
- Heebink, B.G.; Hefty, F.V. (1969): Treatment to reduce thickness swelling of phenolic bonded particleboard. *Forest Products Journal* **19**(11), 17-29
- Hillis, W.E. (1984): High temperature and chemical effects on wood stability. *Wood Science and Technology*, **18**, 281-293
- Hsu, W.; Schwald, W.; Shields, J.A. (1988): Chemical and physical changes required for producing dimensionally stable wood-based composites. Part 1. Steam pre-treatment. *Wood Sci Tech* **22**, 281–289
- Klinga, L.; Tarkow, H. (1966): Dimensional stabilization of hardboard by acetylation. *Tappi*, **49**(1), 23–27
- Kollmann F, Schneider A (1963): Über das Sorptionsverhalten wärmebehandelter Hölzer. *Holz Roh- Werkst*, **41**, 87–94

- Kollmann, F.; Fengel, D. (1965): Änderungen der chemischen Zusammensetzung von Holz durch thermische Behandlung. Holz Roh-Werkst, **21**(3), 77–85
- Lehmann, W.F. (1964): Retarding dimensional changes in particleboards. Information Circular 20 Oregon State University, Corvallis
- Lukowsky, D.; Böttcher, P. (2001): Beschichtung von hitzevergütetem Holz. (Technischer Bericht 2323/2001. In: Burk, R. (2002): Evaluierung technischer Eigenschaften von hitzevergütetem Holz unter besonderer Berücksichtigung der Entwicklung hochwärmegeämmter Holzfenster, Abschlussbericht des FuE-Vorhabens Kap. 0810, Titel 682 01-04. FH Kaiserslautern/ Pirmasens). 31 Seiten
- Maku, T.; Sasaki, H. (1956): Some factors which affect swelling properties of chipboard. Composite Wood, **3**, 135-139
- McDonald, A.; Fernandez, M.; Kreber, B. (1997): Chemical and UV-VIS spectroscopic study on kiln brown stain formation in Radiata pine. In: 9th International Symposium of Wood and Pulping Chemistry, Montreal, Canada 70, 1-5
- Murphy, R.J.; Turner, P. (1989): A vapour phase preservative treatment of manufactured wood based board materials. Wood Science Technology, **23**(3), 273-279
- Niemz, P. (2002): Thermisch vergütetes Fichtenholz. Holzforschung Schweiz 1: 28-29
- Noack, D. (1969): Über die Heisswasserbehandlung von Rotbuchenholz im Temperaturbereich von 100 bis 180°C. Holzforsch Holzverwert, **21**(5), 118–124
- Ohlmeyer, M. (2002): Untersuchung über die Eigenschaftsentwicklung von Holzwerkstoffen nach dem Heißpressen. Dissertation Universität Hamburg, 203 p.
- Ohlmeyer, M.; Lukowsky, D. (2004) Wood-based panels produced from thermal treated wood – Properties and perspectives. In: Wood-frame housing durability and disaster issues conference. October 4–6 2004, Las Vegas, USA
- Paul, W.; Ohlmeyer, M. (2005): Optimisation of wood based panel properties by heat pre-treatment. In: Proceedings of the Ninth European Panel Product Symposium, October 5-7 2005, Llandudno, UK

- Paul, W.; Ohlmeyer, M.; Leithoff, H.; Boonstra, M.J.; Pizzi, A. (2006): Optimising the properties of OSB by a one-step heat pre-treatment process. Holz als Roh- und Werkstoff, **64**(3), 227-234
- Papadopoulos, A.N.; Traboulay, E. (2002): Dimensional stability of OSB made from acetylated fir strands. Holz Roh- Werkstoff, **60**, 84–87
- Papadopoulos, A.N.; Gkaraveli, A. (2003): Dimensional stabilization and strength of particleboard by chemical modification with propionic anhydride. Holz Roh- Werkst., **61**(2), 142–144
- Rapp, A.O.; Sailer, M.; Peek, R.-D. (2000): Innovative Holzvergütung zur Erhöhung der Dauerhaftigkeit. Mitteilungen der Bundesforschungsanstalt fuer Forst- und Holzwirtschaft Nr. 200, 27-34
- Roll, H. (1997): Distribution of EMDI on particles and particleboard. Proceedings of the 1st European Panel Products Symposium. Llandudno, Wales, UK, p 235
- Rowell, R.M. (1975): Chemical modification of wood: Advantages and Disadvantages. In: Proceedings of the 71st Annual Meeting of the AWWA, San Francisco, **71**, 41-51
- Rowell, R.; Tillman, A.; Simonson, R. (1986a): A simplified procedure for the acetylation of hardwood and softwood flakes for flakeboard production. Wood Chemistry and Technology. **6**(3), 427–448
- Rowell, R.; Simonson, R.; Tillman, A. (1986b): Dimensional stability of particleboard made from vapor phase acetylated pine wood chips. Nordic Pulp & Paper Research Journal, **2**(1), 11–17
- Rowell, R.; Tillman, A.; Liu, Z. (1986c): Dimensional stabilization of flakeboard by chemical modification. Wood Science and Technology, **20**(1), 83–95
- Rowell, R.; Wang, H.; Hyatt, J. (1986d): Flakeboards made from aspen and southern pine wood flakes reacted with gaseous ketene. Wood Chemistry and Technology. **6**(3), 449–471
- Rowell, R.; Youngquist JA; Sachs, I.B. (1987): Adhesive bonding of acetylated aspen flakes. I: Surface changes, hydrophobicity, adhesive penetration and strength. International Journal of Adhesion and Adhesives, **7**(4), 183-188
- Rowell, R.; Youngquist, J.; Imamura, Y. (1988): Strength tests on acetylated aspen flakeboards exposed to a brown-rot fungus. Wood and Fiber Science, **20**(2), 266–271

- Rowell, R.; Tillman, A.; Simonson, R.. (1989): Acetylation of lignocellulosic materials. U.S. Patent 4,804,384.
- Rowell, R.; Youngquist, J.; Rowell, J.; Hyatt, J. (1991): Dimensional stability of aspen fiberboard made from acetylated fiber. *Wood and Fiber Science*, **3**(4), 558–566
- Seborg RM, Tarkow H, Stamm AJ (1953): Effect of heat upon the dimensional stabilisation of wood. *J For Prod Res Soc*, **3**(9), 59–67
- Sekino, N.; Inoue, M.; Irle, M.A. (1997): Thickness swelling and internal bond strength of particles made of steam-pretreated particles. *Mokuzai Gak-kaishi* **43**(12), 1009–1015
- Sekino, N.; Inoue, M.; Irle, M. (1998) The bond quality of steam pretreated particles. In: *The 2nd European Panel Products Symposium*, 30–38
- Sehlstedt-Persson, M. (2003) Colour responses to heat treatment of extractives and sap from pine and spruce. 8th International IUFRO Wodd Drying Conference, Brasov, Romania, 459-464
- Sheen, A.D. (1992): The preparation of acetylated wood fibre on a commercial scale. In: *Chemical modification of lignocellulosics*, Rotorua, New Zealand, 7-8 November 1992 (compiled by Plackett D.V. & Dunningham E.A.). Forestry Research Institute, Ministry of Forestry FRI Bulletin, 176, 1-8
- Shen, K.C. (1973): Steam-press process for curing phenolic-bonded particleboard. *Forest Prod J*, **23**(3), 21–29
- Stamm, A.J.; Burr, H.K.; Kline, A.A. (1946): Heat Stabilized Wood (Staybwood). *Forest Products Laboratory Madison (USA)*, Rep. No. R. 1621
- Stamm, A.J. (1964): *Wood and Cellulose Science*. The Ronald Press Company, USA. Chapter 19, pp 312–342
- Sudo, K. (1979): Character of hardboards from acetylated Asplund pulp. *Japan Wood Research Society Journal*, **25**(3), 203–208
- Subyanto, B.; Takino, S.; Kawai, S.; Sasaki, H. (1991) Production of thick low-density particleboard with a semi-continuous steam-injection press. *Mokuzai Gakkaishi* **37**(1):24–30
- Sundqvist, B.; Morén, T. (2002) The influence of wood polymers and extractives on wood colour induced by hydrothermal treatment. *Holz als Roh- und Werkstoff*, **60**, 375-376

- Tillman, A.; Simonson, R.; Rowell, R. (1987): Dimensional stability and resistance to biological degradation of wood products by a simplified acetylation procedure. In: *Proceedings, 4th International symposium of wood and pulping chemistry*, April 27–30; Paris, France. Wood and Pulping Chemistry Association.
- Tarkow, H.; Turner, H.D. (1958): The Swelling Pressure of Wood. *Forest Products Journal* **8**(7):193-197.
- Tjeerdsma, B.F.; Boonstra, M. ;Militz, H. (1998): Thermal modification of non-durable wood species. Part 2. Improved wood properties of thermally treated wood. *International Research Group on Wood Preservation*, Document No. IRG/WP 98-40124
- Tomek, A. (1966): Die Heißvergütung von Holzspänen, ein neues Verfahren zum Hydrophobieren von Spanplatten. *Holztechnologie*, **7**(3), 157-160
- Tomimura, Y.; Matsuda, T. (1986): Particleboard made of steamed flakes. *Mokuzai Gakkaishi* **32**(3), 170–175
- Vick, C.; Krzysik, A.; Wood, J. (1991): Acetylated isocyanate-bonded flakeboards after accelerated aging. *Holz als Roh- und Werkstoff*, **49**, 221–228.
- Youngquist, J.A.; Rowell, R.M.; Krzysik, A. (1986): Mechanical properties and dimensional stability of acetylated aspen flake-boards. *Holz als Roh- und Werkstoff*, **44**, 453–457
- Youngquist, J.A.; Rowell, R.M. (1990): Adhesive bonding of acetylated aspen flakes. Part III. Adhesion with isocyanates. *International Journal of Adhesion and Adhesives*, **10**(4), 273-276
- Youngquist, J.A.; Rowell, R.M.; Ross, N.; Krzysik, A. M; Chow, P. (1990): In: *Proceedings of the 1990 Joint International Forest Products Conference*, Taipei, Republic of China, 159-162
- Youngquist J.A., Krzysik A.M., Muehl J.H. et al (1992): Mechanical and physical properties of air formed wood fiber/polymer fiber composites. *Forest Products Journal*, **42**(6), 42-48

COST

COST- the acronym for European Cooperation in Science and Technology- is the oldest and widest European intergovernmental network for cooperation in research. Established by the Ministerial Conference in November 1971, COST is presently used by the scientific communities of 36 European countries to cooperate in common research projects supported by national funds.

The funds provided by COST - less than 1% of the total value of the projects - support the COST cooperation networks (COST Actions) through which, with EUR 30 million per year, more than 30 000 European scientists are involved in research having a total value which exceeds EUR 2 billion per year. This is the financial worth of the European added value which COST achieves.

A "bottom up approach" (the initiative of launching a COST Action comes from the European scientists themselves), "à la carte participation" (only countries interested in the Action participate), "equality of access" (participation is open also to the scientific communities of countries not belonging to the European Union) and "flexible structure" (easy implementation and light management of the research initiatives) are the main characteristics of COST.

As precursor of advanced multidisciplinary research COST has a very important role for the realisation of the European Research Area (ERA) anticipating and complementing the activities of the Framework Programmes, constituting a "bridge" towards the scientific communities of emerging countries, increasing the mobility of researchers across Europe and fostering the establishment of "Networks of Excellence" in many key scientific domains such as: Biomedicine and Molecular Biosciences; Food and Agriculture; Forests, their Products and Services; Materials, Physical and Nanosciences; Chemistry and Molecular Sciences and Technologies; Earth System Science and Environmental Management; Information and Communication Technologies; Transport and Urban Development; Individuals, Societies, Cultures and Health. It covers basic and more applied research and also addresses issues of prenormative nature or of societal importance.

Web:<http://www.cost.esf.org>

Formal publisher: Brunel University Press

Book title: Wood-Based Panels: An Introduction for Specialists

Year of publication: 2010

ISBN: 978-1-902316-82-6



ESF provides the COST Office
through an EC contract



COST is supported by the EU RTD
Framework programme



Bern University of Applied Sciences
Architecture, Wood and Civil Engineering

ISBN 978-1-902316-82-6